Palaeotsunami imprints in the near-coast sedimentary records of the Gulfs of Lakonia and Argolis (Peloponnese, Greece)

Dissertation

zur Erlangung des Grades

„Doktor der Naturwissenschaften“

im Promotionsfach Geographie

am Fachbereich Chemie, Pharmazie und Geowissenschaften

der Johannes Gutenberg-Universität Mainz

vorgelegt von

Konstantin Ntageretzis

geboren in Attendorn

Mainz, 2014

Dekan:

1. Berichterstatter:

2. Berichterstatter:

Tag der mündlichen Prüfung: 25. Juli 2014

Αφιερωμένο στην μητέρα και στον πατέρα μου.

Acknowledgements

Abstract

From historical accounts it is well-known that the coasts of the Gulfs of Lakonia and Argolis (southern and eastern Peloponnese, Greece) have been repeatedly affected by tsunamis during historical times. It is assumed that these palaeotsunamis left sedimentological and geomorphological traces in the geological record which are still detectable these days. As both gulfs are located within one of the seismically most active regions in whole western Eurasia in particular the nearby Hellenic Trench is regarded as the main trigger for tsunami generation.

Against this background, selected near-coast sedimentary archives were studied by means of sedimentological, geomorphological, geophysical, geochemical and microfaunal investigations in order to detect signatures of Holocene palaeotsunamigenic activity.

The investigations revealed allochthonous sediment layers featuring distinctive sedimentary characteristics of marine high-energy event deposits in most of the investigated study areas. In order to differentiate between the geomorphodynamic driving mechanisms for the deposition of the associated marine high-energy event layers, a multi-method approach was used.

The detected high-energy marine deposits are suggested to be of tsunamigenic origin. Radiocarbon dating results allowed establishing local event geo-chronostratigraphies and correlations on a local and regional scale as well as correlations with already described palaeotsunami findings on a supra-regional scale. The geochronological dataset attests repeated tsunamigenic activity at least since the 5th millennium BC up to the 17th century AD. For the studied areas in southeastern Lakonia up to four palaeotsunami event generations were identified, for central Lakonia three and for the investigated areas around the Argolis Gulf also up to four. Comparing the findings with literature data, chronological correlations were found with palaeotsunami deposits detected in near-coast geological archives of Akarnania, of the southwestern, the western and northwestern Peloponnese, with event deposits found on Crete and on the Ionian Islands of Cefalonia and Lefkada as well as with findings from southeastern Sicily (Italy) and Cesarea (Israel).

By the identification of multiple palaeotsunami event layers, disturbing autochthonous near-coast sedimentary records of the Gulfs of Lakonia and Argolis during the last seven millennia, a significant tsunami frequency is attested for these regions.

Kurzzusammenfassung

Aus überlieferten Aufzeichnungen ist bekannt, dass die Küsten entlang des Lakonischen und Argolischen Golfes (südliche und östliche Peloponnes, Griechenland) während historischer Zeiten wiederholt von Tsunamis beeinträchtigt wurden. Es ist davon auszugehen, dass diese Paläotsunamis sedimentologische und geomorphologische Spuren innerhalb der geologischen Archive hinterlassen haben, die auch heute noch nachweisbar sind. Da sich beide Golfe innerhalb einer der seismisch aktivsten Regionen des gesamten westlichen Eurasiens befinden, wird vor allem der nahegelegene Hellenische Graben als Hauptauslöser für Tsunamis angesehen.

Vor diesem Hintergrund wurden ausgewählte küstennahe Archive mittels sedimentologischer, geomorphologischer, geophysikalischer, geochemischer und mikrofaunistischer Methoden untersucht, um Spuren holozäner Paläotsunami-Aktivität nachzuweisen.

Die Untersuchungen ergaben, dass sich in den meisten der untersuchten Gebiete allochthone Sedimentlagen finden, die charakteristische Merkmale mariner hochenergetischer Ereignisablagerungen aufweisen. Ein multimethodaler Ansatz wurde genutzt, um zwischen den geomorphodynamischen Auslösemechanismen zu unterscheiden, die für die Ablagerungen der marinen hochenergetischen Ereignislagen verantwortlich gewesen sein müssen.

Die nachgewiesenen Hochenergie-Ablagerungen deuten demnach auf tsunamigene Entstehung hin. Ergebnisse von Radiokarbon-Datierungen ermöglichten es, Geochronologien für lokale Ereignisse zu erstellen, wodurch auch Zusammenhänge auf lokaler und regionaler Ebene ermittelt werden konnten sowie Korrelationen mit bereits beschriebenen Paläotsunami-Befunden auf supra-regionaler Ebene.

Die geochronologischen Datensätze belegen wiederholte tsunamigene Aktivität mindestens seit dem fünften Jahrtausend BC bis ins 17. Jahrhundert AD. Für die untersuchten Gebiete in Südost-Lakonien konnten bis zu vier Generationen von Paläotsunami-Ereignissen identifiziert werden, für Zentral-Lakonien drei und für die untersuchten Gebiete entlang des Argolischen Golfes ebenfalls bis zu vier.

Bei einem Vergleich der Belege mit Literaturdaten zeigen sich zeitliche Korrelationen mit Paläotsunami-Ablagerungen, welche in küstennahen geologischen Archiven Akarnaniens, der südwestlichen, westlichen und nordwestlichen Peloponnes, mit Ereignis-Lagen, die auf Kreta und den Ionischen Inseln Kephallonia und Lefkada gefunden wurden sowie mit Befunden von Südost-Sizilien (Italien) und Cesarea (Israel).

Durch die Identifizierung multipler Paläotsunami-Ereignislagen, welche die küstennahen autochthonen Sedimentarchive des Lakonischen und Argolischen Golfes während der letzten sieben Jahrtausende beeinflussten, ist eine signifikante Tsunami-Frequenz für diese Regionen belegt.

Table of contents

List of Figures

List of Tables

List of Abbreviations

a = year

AD = Anno Domini

BC = before Christ

BP = before present (= 1950)

c. = circa

cm = centimeter

EC meter = electrical conductivity meter

ERT = earth resistivity tomography

HAT = Homogenite Augias Turbidite

ICG/NEAMTWS = Intergovernmental Coordination Group for the Tsunami Early Warning and Mitigation System in the North-eastern Atlantic, the Mediterranean and connected seas

IOT = Indian Ocean Tsunami on December 26th, 2004

ITC - inner tropical convergence zone

km = kilometer

m = meter

m a.s.l. = meter above sea level

m b.s.l. = meter below sea level

m b.s. = meter below ground surface

NOA = National Observatory Athens

NTWC = National Tsunami Warning Centre

OTH = Olympia Tsunami Hypothesis

PTHA = Probabilistic Tsunami Hazard Analysis

TLS = terrestrial laser scanning

TWP = Tsunami Watch Providers

Ωm = Ohm-meter

Chapter 1 – Introduction & Objectives

The devastating Indian Ocean Tsunami (IOT) on Boxing Day 2004 as well as the fatal tsunami triggered by the 2011 Tōhoku-oki earthquake have drawn public awareness on this kind of natural disaster. Both mentioned events took place in seismic active regions, well known for tsunamigenic activity. The fact that this type of natural phenomenon is characterized worldwide by the Japanese word *tsunami* (津波), meaning "harbor wave", constrains that tsunamis have been incorporated in Asians daily grind for a long time. The destructive dimension of both events has spread all over the world in its most terrible way. As a consequence of this, nowadays all the world knows about the vulnerability of SE-Asia in consequence of tsunamigenic activity.

Since 1850 tsunamis were responsible for the death of over 420.000 lives and billions of dollars of damage to coastal infrastructures all over the world – astonishingly thereby most fatalities were triggered by local events, occurring about once per year somewhere in the world (BERNARD et al. 2009).

What most people do not know is that also the Mediterranean bears a very high tsunamigenic potential, as one of the tectonically most complex and active regions of the world. Modern calculations of the Mediterranean tsunami triggered by the 365 AD Crete earthquake indicate an open ocean amplitude of the tsunami wave within the eastern Mediterranean compatible with the modeled and observed Indian Ocean Tsunami from 2004 (POLONIA et al. 2013).

Although Greek scientists have published tsunami studies already in the 1950s and 1960s giving evidence about historic and modern tsunamis in the Mediterranean, this remained widely unnoticed by the public. Worth to mention here are the works from ANGELOS GEORGIOU GALANOPOULOS (1957) and NICHOLAS NEOCLIS AMBRASEYS (1960) who deal with the Cyclades tsunami from July 9th, 1956. In Greece, a multitude of historical sources exist, especially from Classical and Hellenistic times, giving detailed description of exceptional events of the sea, often associated to earthquakes – nowadays known as tsunamis. The Greek historian and Athenian general *Thucydides/Θουκυδίδης* (460 - c. 395 BC) for instance gives specific descriptions about the effects of the 426 BC tsunami at Orobiae (Maliakos Gulf – Greece) in his *"History of the Peloponnesian War* (3.89.2) (SMID 1970, ANTONOPOULOS 1992, PAPAIOANNOU et al. 2004).

However, modern geoscientists became aware of palaeo-tsunami events basically by the studies of ATWATER (1987) and DAWSON et al. (1988). Since then, numerous disciplines have been successfully established worldwide, exploring modern as well as palaeo-tsunami events and their implications. As a positive consequence of this, plenty locations all over the world were identified featuring traces of (palaeo) tsunami activity.

Against the background that the Mediterranean, especially Greece, offers numerous hints on palaeo-tsunamigenic activity by historic accounts, there is reason to believe that those events must have left tracks within the geological and stratigraphical record of near-coast archives. Accordingly, tsunami characteristics were successfully detected by different research groups along several coastal areas around Greece during the last two decades. Furthermore, modern numerical simulations clearly document the spatial extension of palaeo-tsunamis respectively the extent of possible future events along numerous Greek coasts (e.g. TINTI et al. 2005a, SHAW et al. 2008, OKAL et al. 2009, TSELENTIS et al. 2010, MITSOUDIS et al. 2012, EBELING et al. 2012, RÖBKE et al. 2012, RÖBKE et al. 2013). Within this context, the investigation of (pre-)historic tsunami events is considered to be the most suitable geoscientific method for the assessment of present and future tsunami hazards of an area (VÖTT et al. 2011a, 2011c).

The present study is integrated in the project of the DFG (Deutsche Forschungsgemeinschaft – German Research Foundation) "Quaternary tsunami events in the eastern Ionian Sea – reconstructing and modeling extreme events based on interdisciplinary geo-scientific investigations" (DFG Gz. 938/3-1).

The objective of this work is to provide geoscientific information on historical tsunami landfall in selected coastal areas along the Lakonian Gulf and the Gulf of the Argolis (Peloponnese – Greece) by a multidisciplinary approach based on sedimentological, geophysical, geochemical and microfaunal analyses.

Based on literary evidence, the coasts of the Peloponnese are known to have been repeatedly hit by tsunamis during historical times. However, so far no sedimentological and geomorphological investigations have been carried out within this context in Lakonia and the Argolis, except by SCHEFFERS et al. (2008) and FEDERICI et al. (2002) as well as FEDERICI & RODOLFI (2008) who mainly focused on mega clasts dislocated by extreme wave activity. At least with regard to Lakonia, this is because profound coastal archives of the Holocene sedimentary record, offering the potential to preserve marine borne inputs, are scarce or non-existent.

The multidisciplinary approach of this study is based on 33 vibracorings conducted by an engine-driven coring device. Geophysical earth resistivity tomography measurements (ERT) were locally accomplished in order to identify subsurface structures, such as the bedrock topography, and the general stratigraphical pattern within the Holocene sedimentary record. The encountered sedimentary units were subjected to laboratory analyses (e.g. grain size distribution, XRF analyses, magnetic susceptibility, spectroscopic color measurements). Furthermore, macro- and microfaunal studies of selected vibracore samples were carried out in order to differentiate between autochthonous and allochthonous sedimentary environments. Selected organic samples were radiometrically dated using the ^{14}C-AMS dating technique.

The general objectives of this study can be summarized as follows:

i) to detect palaeotsunami imprints in adequate near-coast geological archives,

ii) to identify event deposits by means of sedimentological, geochemical as well as micro- and macrofossil methods,

iii) to describe the spatial extent of event layers and to decipher the role of extreme wave impacts on overall geomorphological changes of coastal palaeogeographies,

iv) to establish a geochronology of palaeotsunami events based on radiocarbon dating,

v) to compare the palaeotsunami imprint of Lakonia and Argolis with each other as well as to search for potential (supra-)regional patterns compared to palaeotsunami events already described in literature

vi) and to show how palaeotsunami research may be helpful within the framework of modern tsunami risk assessment.

Chapter 2 – Extreme wave events in the course of modern geosciences

2.1 Current state of research

The development of modern tsunami research

Scientific reports about tsunamis are already available from the 19th century, for instance the descriptions by SYMONDS et al. (1888) about the tsunami triggered by the 1883 Krakatoa volcano eruption (Indonesia) or those by CHARLES DARWIN about the Valdivia tsunami that hit Chile in February 1835 (DAWSON & STEWART 2007). Yet in the late 1940s, detailed geoscientific data about tsunamigenic deposits were published by SHEPARD et al. (1949) who reported on the April 1st, 1946 Hawaiian Island tsunami. WRIGHT & MELLA (1963) gave descriptions about modifications of the soil pattern of south-central Chile due to the 1960 earthquake and tsunami. And REIMNITZ & MARSHALL (1965) reported on the effects of the Alaska earthquake and tsunami on recent deltaic sediments.

With regard to the Mediterranean, the Greek geologists A. G. GALANOPOULOS (1957) and N. N. AMBRASEYS (1960) were the first to report on the Cyclades tsunami from July 9th, 1956, the most recent large Mediterranean tsunami (PAPADOPOULOS & PAPAGEORGIOU 2014). Moreover, already in the 1960s and 1970s, scientists discussed controversially about historic sea wave events (palaeotsunamis) and associated implications (GALANOPOULOS & BACON 1969, FINLEY 1969, GALANOPOULOS 1970). Historical accounts turned out to be helpful for the reconstruction and analysis of historical seismic and tsunamigenic activities in the Mediterranean during ancient times, such as with regard to the 373 BC tsunami which is assumed to have destroyed ancient Helike at the southern shores of the Gulf of Corinth (GALANOPOULOS 1960, ANTONOPOULOS 1979, PAPADOPOULOS & CHALKIS 1984).

However, first with the publications on prehistoric tsunami signatures, detected at the western coast of the United States by ATWATER (1987) and at the Scottish coast by DAWSON et al. (1988), modern geosciences started to intensify the research of palaeotsunami events. These studies combined local coastal stratigraphies and seismic or landslide-induced tsunamis of the recent geological past and thereby helped to develop systematic concepts and principles of tsunami-laid sediments or tsunami deposits (ENGEL & BRÜCKNER 2011). Especially for the estimation of tsunami hazard in a distinct area, as well as for effective coastal protection measures comprehensive knowledge about comparable past tsunami events is required (MAY 2010).

Since that time, several interdisciplinary research disciplines have been established in order to explore the role of tsunamis within the overall context of coastal changes. So far, a huge number of papers have been published, giving evidence of recent and historic tsunamigenic activity in large

parts of the world. The amount of tsunami-related publications increased considerably after the IOT in 2004 (see ENGEL & BRÜCKNER 2010, fig. 1, p. 66). The research status of tsunami science before and beyond Boxing Day 2004 is presented in detail by SYNOLAKIS & BERNARD (2006). Also, SCHEFFERS et al. (2009) discussed the development of tsunami research after the 2004 IOT. And MARRINER et al. (2010) explain when, where and why (neo-)catastrophism has gained new currency since 1950 amongst the earth and planetary sciences.

As a result of the intensive multidisciplinary investigations during the last two decades, numerous tsunami signatures, both sedimentological and geomorphological, have been identified. Sedimentary characteristics of tsunami deposits detected along numerous coastal regions of the world are described for instance by CLAGUE & BOBROWSKY (1993, 1994), DAWSON (1999, 2005), DAWSON & SHI (2000), BRYANT & NOTT (2000), SCHEFFERS & KELLETAT (2001, 2003), KELLETAT & SCHEFFERS (2003, 2004), KELLETAT et al. (2004, 2007), SCHEFFERS (2005), DOMINEY-HOWES et al. (2006) or HAWKES et al. (2007). Whether modern tsunami tracks (allochthonous fine grained and/or coarse grained deposits besides erosional features – will be explained in more detail in the next subchapter) differ from historical and if there are any significant regional differences by global comparison are crucial questions within this young research area (DOMINEY-HOWES et al. 2006). Selections and compilations of typical (palaeo-) tsunami signatures sorted by locations and authors were presented by DOMINEY-HOWES et al. (2006), by MAMO et al. (2009) as well as by ENGEL & BRÜCKNER (2011). A book about tsunamiites as an overview about the state-of-the-art in tsunamiite sedimentology with contributions of 37 tsunami experts was published by SHIKI et al. (2008). And a guideline for the identification of fossil tsunami deposits was presented by PETERS & JAFFE (2010a, 2010b).

The role of field surveys and post-event surveys within tsunami-geosciences

The identification of (palaeo) tsunami signatures within the sedimentary record and the understanding of the related geomorphodynamic driving mechanisms and processes were contributed by post-event surveys that were undertaken in numerous near-coast geological and biological archives all over the world.

Especially the sedimentological and geomorphological effects of the 2004 IOT lay in the focus of interest, yielding in a variety of publications. Just to name a few as examples, SZUCZINSKI et al. (2005), BAHLBURG & WEISS (2006), JAFFE et al. (2006), MOORE et al. (2006), GOTO et al. (2007), HAWKES et al. (2007), KELLETAT et al. (2007), WASSMER et al. (2007), MORTON et al. (2008b), PARIS et al. (2007, 2009), among others. And with regard to past tsunamigenic activity in SE-Asia JANKEAW et al. (2008) were able to identify by sedimentary evidences probable historic precedents of the 2004 IOT at a grassy beach-ridge plain 125 km north of Phuket (Thailand). Historic tsunami references from Cape Pakarang (Thailand) were also delivered by NEUBAUER et al. (2011) on the basis of sediment analyses

from vibracorings and datings of displaced coral boulders. And BRILL et al. (2011, 2012a, 2012b) used optical stimulated luminescence techniques (OSL) in order to study historic tsunami deposits along selected coasts of Thailand.

Several post-event surveys were conducted also after the February 27th, 2010 Chile tsunami. FRITZ et al. (2011) collected data on tsunami flow depth, run-up and coastal uplift measurements, MORTON et al. (2011) and SPISKE & BAHLBURG (2011) report both on erosional and depositional effects such as the accumulation of sheets of sand and gravel. Moreover, SPISKE & BAHLBURG (2011) calculated flow speed and transport setting with regard to coarse clasts.

The geological aftermaths of the Tōhoku-oki tsunami from March 11th, 2011 were investigated in detail, for instance by CHAGUÉ-GOFF et al. (2012), PILARCZYK et al. (2012), RICHMOND et al. (2012) and SZCZUCIŃSKI et al. (2012). GOTO et al. (2012) described dislocated boulders and SUGAWARA & GOTO (2012) presented a numerical model of the 2011 Tōhoku-oki tsunami in the offshore and onshore of Sendai Plain (Japan). Previous tsunami studies in Japan have been carried out, for instance, by MINOURA & NAKATA (1994), NISHIMURA et al. (1995), SATO et al. (1995) and NANAYAMA et al. (2000, 2007).

Also the deposits and sedimentary characteristics of the 1998 Papua New Guinea tsunami were studied, for instance, by GELFENBAUM & JAFFE (2003). And within the Caribbean and along numerous coasts of the Pacific characteristics of palaeotsunami deposits were described, for instance, by SCHEFFERS et al. 2005, ENGEL & MAY 2012, RIXHON et al. 2012, GOFF et al. 2001, PINEGINA & BOURGEOIS 2001, HIGMAN & BOURGEOIS (2008), BOURGEOIS et al. (2006) and SWITZER et al. 2005, just to name a few.

Tsunami tracks along the European Atlantic coasts

With regard to Europe palaeotsunami impacts were also detected along the Atlantic coasts of Spain (e.g. DABRIO et al. 1998, LUQUE et al. 2002, REICHERTER et al. 2009, 2010a) and Portugal (e.g. by ANDRADE 1992, DAWSON et al. 1995, DA SILVA et al. 1996, HINDSON & ANDRADE 1999, KORTEKAAS & DAWSON 2007, COSTA et al. 2008 and FONT et al. 2010). RODRÍGUEZ-VIDAL et al. (2011) presented evidence of the 1755 AD Atlantic tsunami on the Gibraltar coast. And REGNAULD et al. (2010) report on boulders along the west coast of France which were displaced by extreme waves. Evidence for North Sea tsunamis was given by BONDEVIK et al. (2005). Based on literature and newspaper research NEWIG & KELLETAT (2011) and NEWIG (2013) were able to reconstruct a tsunami that occurred in the North Sea in 1858.

Tsunami tracks along the coasts of the (eastern) Mediterranean

During the last two decades, numerous tsunami sediments were also identified in the eastern Mediterranean (VÖTT et al. 2008, VÖTT & MAY 2009, Vött 2011). Along wide parts of the Italian coasts,

sedimentary and geomorphological traces document repeated past tsunamigenic activity (e.g. GIANFREDA et al. 2001, DE MARTINI et al. 2003, MARAMAI et al. 2005, MASTRONUZZI et al. 2006, SCICCHITANO et al. 2007, 2008, 2012, ARMIGLIATO et al. 2008, PANTOSTI et al. 2008, SMEDILE et al. 2011). After GRAZIANI et al. (2008) the Messina tsunami from December 28th, 1908 represents the most important event for Italy.

Investigations of tsunami deposits in Greece were long time limited on the Aegean Sea and associated coastal regions (DOMINEY-HOWES 2002). Sedimentary signatures of the Cyclades tsunami from July 9th, 1956 were studied by DOMINEY-HOWES (1996), DOMINEY-HOWES et al. (2000b), PAPADOPOULOS et al. (2005) and OKAL et al. (2009). Detailed descriptions on the effects of the palaeotsunami generated by the late Minoan eruption of the Santorini volcano were published by DOMINEY-HOWES et al. (2000), MCCOY & HEIKEN (2000), MINOURA et al. (2000) and BRUINS et al. (2008). A model of the associated tsunami was applied by NOVIKOVA et al. (2011). And already in 1991 PAPAZACHOS & DIMITRIU studied tsunami indicators in Greece and the surrounded areas in order to show their relations to the earthquake focal mechanisms.

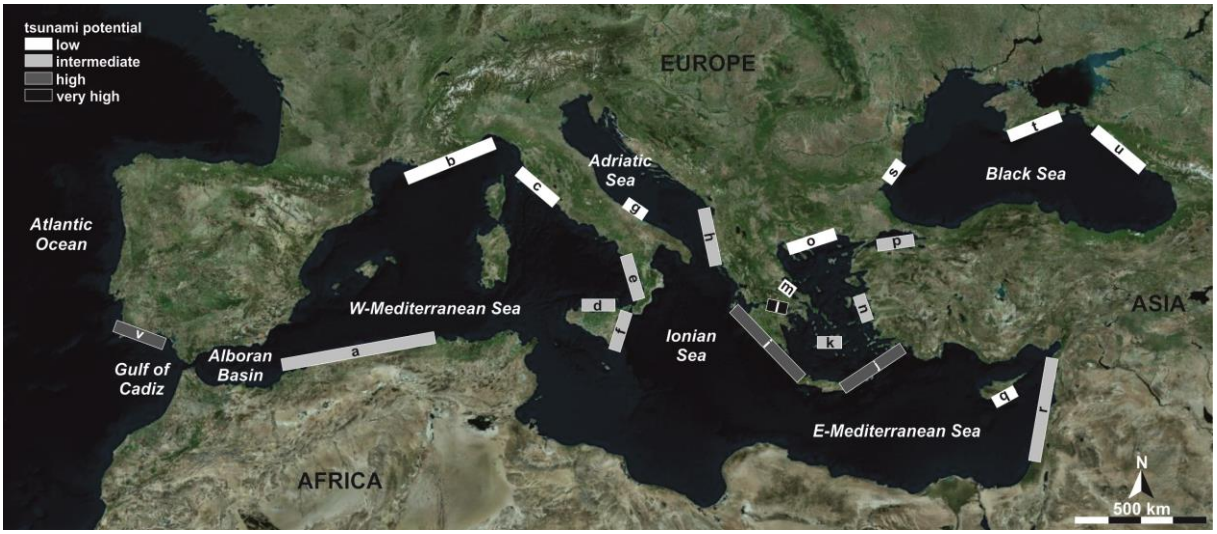

Figure 1: The map shows the tsunamigenic zones defined from documentary sources and their relative tsunami potential classification after PAPADOPOULOS & PAPAGEORGIOU (2014): a = Alboran Sea, b = Côte d'Azur & Liguria, c = Tuscany, d = Aeolian Islands, e = Tyrrhenian Calabria, f = Eastern Sicily & Messina Straits, g = Gargano, h = East Adriatic Sea, i = West Hellenic Arc, j = East Hellenic Arc, k = Cyclades, l = Gulf of Corinth, m = Maliakos Bay, n = East Aegean Sea, o = North Aegean Sea, p = Sea of Marmara, q = Cyprus, r = Levantine Sea, s = Bulgaria, t = Crimea, u = East Black Sea, v = SW Iberia (source: own illustration, modified after PAPADOPOULOS & PAPAGEORGIOU 2014, map based on Bing Aerial images/data, access June 2014).

Along the shores of northern Greece palaeotsunami traces were identified for instance in the Thermaikos Gulf by RÖSSLER et al. (2008) and REICHERTER et al. (2010b) and along the coast of the Thracian Sea by MATHES-SCHMIDT (2013). And in the country`s southeastern part tsunami hints were detected by PIRAZZOLI et al. (1999), CUNDY et al. (2000) and GAKI-PAPANASTASSIOU et al. (2008) around Euboea. Along the coasts of the Corinthian Gulf, separating the Peloponnesian peninsula from the Greek mainland, tsunami deposits were described by KONTOPOULOS & AVRAMIDIS (2003), ALVAREZ-ZARIKIAN et al. (2008), KORTEKAAS et al. (2011), SAKELLARIOU et al. (2011) and within a geoarchaeological

context by HADLER et al. (2011b, 2012b, 2013). Boulders displaced by extreme wave events were identified by FEDERICI et al. (2002) and FEDERICI & RODOLFI (2008) in Lakonia, the southeastern part of the Peloponnese. Similar boulders were described also by SCHEFFERS (2006a) for Crete and by KELLETAT & SCHELLMANN (2001, 2002) and WHELAN & KELLETAT (2002) for Cyprus.

Multiple extreme wave activity during (pre-)historical times was found in sedimentary archives of coastal Akarnania, the western Peloponnese and the Ionian Islands by VÖTT et al. (2006, 2007, 2008b, 2008c, 2009a, 2011c, 2013), HADLER et al. (2011a), WILLERSHÄUSER et al. (2011a, 2011b, 2012a, 2012b, 2013), MAY et al. (2012). And within this study context, RÖBKE et al. (2012, 2013) found good accordance between numeric simulations and palaeotsunami field data.

Palaeoevent compilations

The increased research on palaeotsunamis as well as on palaeoseismicity during the last few decades yielded also in the publication of several event catalogs (e.g. GUIDOBONI et al. 1994, SOLOVIEV et al. 2000, TINTI et al. 2001, PAPADOPOULOS 2002, TINTI et al. 2004, GUIDOBONI & COMASTRI 2005, PAPADOPOULOS & FOKAEFS 2005, PAPADOPOULOS et al. 2007, SCHIELEIN et al. 2007, AMBRASEYS 2009, AMBRASEYS & SYNOLAKIS 2010 or NGDC/NOAA). According to BASILI et al. (2013) the most accurate and complete historical earthquake catalogs, covering a timespan of several centuries, are those from the Mediterranean. Historical accounts, for example, document that the 365 AD Crete earthquake and tsunami destroyed cities and drowned thousands of people in coastal regions from the Nile to modern-day Dubrovnik (SHAW et al. 2008). Similar to the 365 AD event, also the 8th, August 1303 AD tsunamigenic earthquake, which ruptured between Crete and Rhodes, was one of the largest reported historical events in the Mediterranean according to PAPADOPOULOS & PAPAGEORGIOU (2014) (see also GUIDOBONI & COMASTRI 1997, AMBRASEYS 2009 and PAPADOPOULOS 2011). In recent times, tsunamis occurred, for instance, in 1908 in the strait of Messina (Italy), causing at least 60.000 deaths (BILLI et al. 2008). Also, the tsunami at Izmit (Turkey) on August 17th, 1999 caused many casualties and severe damages (ALTINOK et al. 2001), referring to the general vulnerability of the eastern Mediterranean because of tsunamigenic activity.

Modern modelling approaches

The understanding of tsunami hydraulics, wave propagation and the dimensions of tsunami landfalls was considerably improved by modeling (pre-) historic tsunami events (VÖTT et al. 2011c), for example by TINTI et al. (2005a), LORITO et al. (2008), SHAW et al. (2008), OKAL et al. (2009), FLOTH et al. (2010), TSELENTIS et al. (2010), NOVIKOVA et al. (2011), EBELING et al. (2012), MITSOUDIS et al. (2012) or RÖBKE et al. (2012, 2013), i.a. And recently BASILI et al. (2013) presented a new approach by integrating seismic fault-source data into tsunami hazard studies.

2.2 Physical characteristics of extreme wave events and their related deposits

Physical characteristics of tsunamis

Today it is well known that several mechanisms of tsunami generation exist (Fig. 2). Tsunamis can be generated, for instance, by offshore earthquakes, by submarine slides and coastal landslides into the ocean, by volcanic flank collapses, pyroclastic flows and explosive volcanism as well as by meteorite/cosmic impacts (MILLER 1960, NOMANBHOY & SATAKE 1995, TINTI et al. 2005b, DAWSON & STEWART 2007, MATTIOLI et al. 2007 and SUGAWARA et al. 2008).

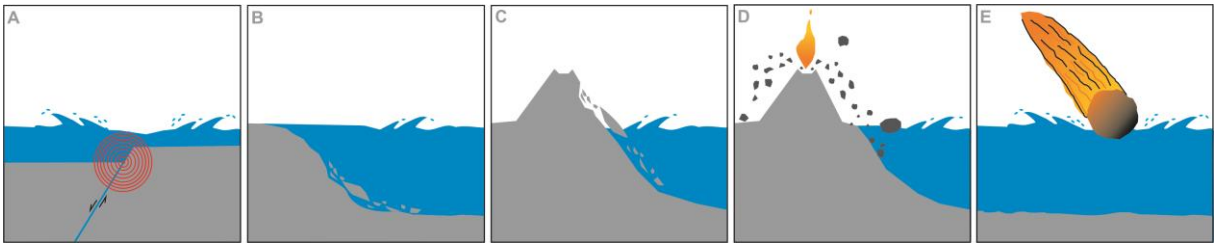

Figure 2: The graphics illustrate the different mechanisms for the generation of tsunamis. A: offshore earthquakes, B: submarine slides, C: volcanic flank collapses respectively coastal landslides, D: explosive volcanism and/or pyroclastic flows and E: meteorite/cosmic impacts (source: own illustration 2014).

In contrast to wind induced waves, tsunamis generated by earthquakes consist of long wavelength (long period water waves), produced by an impulsive vertical displacement of the water column, directly due to the seismic event or indirectly due to submarine mass movements respectively slides (POLONIA et al. 2013). The wavelength can reach several hundreds of kilometers and the time passing between two wave crests can last between 10 to 120 minutes (DAS GUPTA 2006, VÖTT 2011). Tsunami waves travel at a velocity proportional to the square root of the water depth (BERNARD et al. 2006). While traveling across the ocean the waves are thus able to reach velocities up to several hundred kilometers per hour in the open sea; when water depths become shallower, these kinematic waves decrease in velocity (DAWSON & STEWART 2007) while wave height is increasing. Major tsunamis are composed out of 6 to 12 large waves that may hit the coastline at intervals between 30 to 90 minutes (BERNARD et al. 2006). While inundating the landmass, the body of water is capable to erode and to deposit collected material. Thereby, sediment deposition can occur either during inflow or backflow (BAHLBURG & SPISKE 2012).

Geomorphological and sedimentological tsunami signatures

Onshore tsunami deposits feature a variety of distinct sedimentary characteristics. Within the eastern Mediterranean geomorphological and sedimentological depositional traces of tsunamis can be categorized into four main groups (VÖTT & MAY 2009) (Fig. 3).

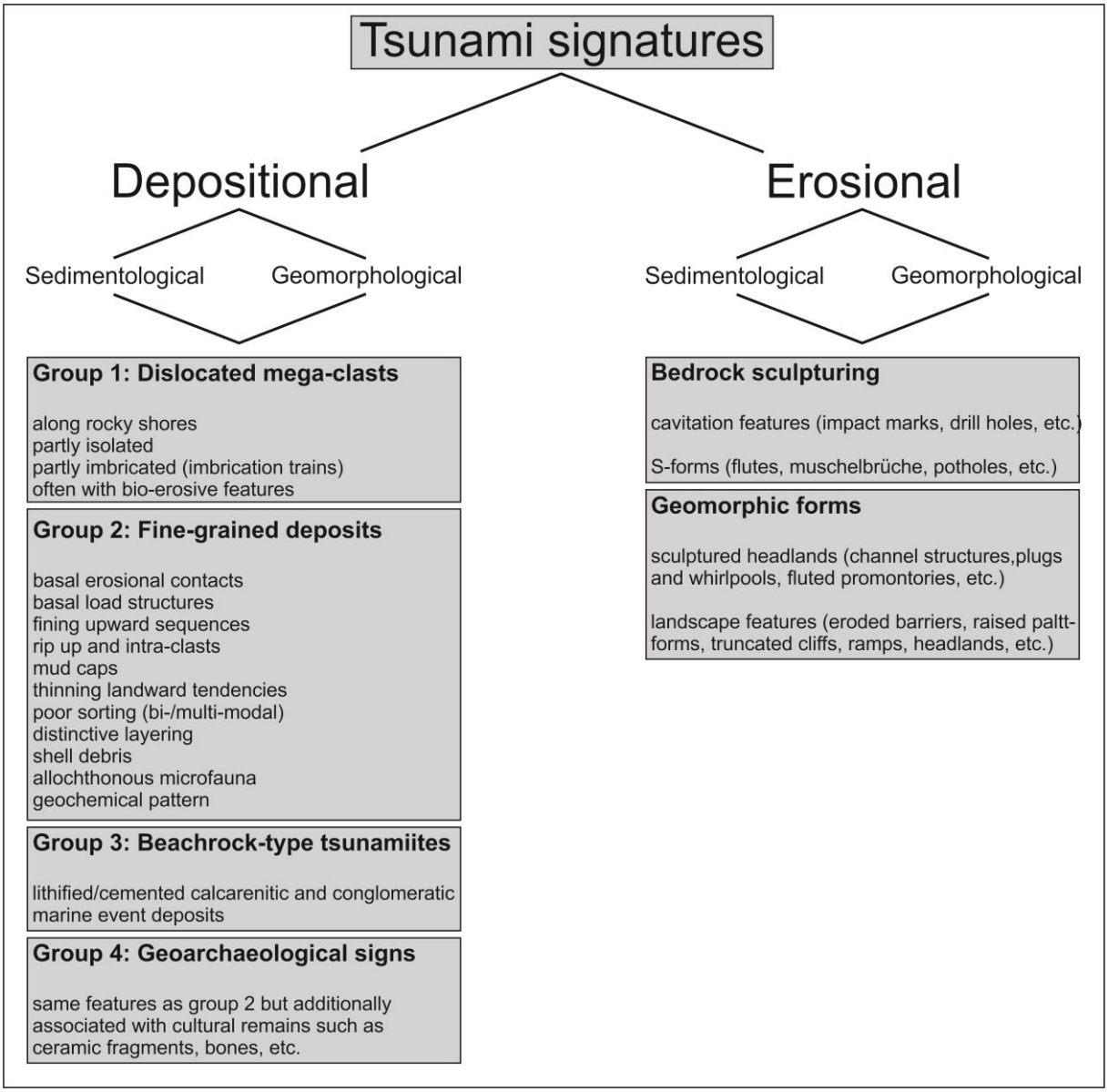

Figure 3: The figure summarizes the tsunami signatures that are discussed in literature. From the sedimentological and geomorphological point of view these signatures are generally divided into two main categories – erosional and depositional ones. Thereby, each category can be divided into sub-groups (source: own illustration compiled and adapted from BRYANT & NOTT 2001, GELFENBAUM & JAFFE 2003, DOMINEY-HOWES et al. 2006, MORTON et al. 2007, VÖTT & MAY 2009 and ENGEL & BRÜCKNER 2011).

Group 1: Dislocated mega-clasts/boulders

The first group comprises wave-emplaced boulders, respectively block deposits, which can be found along many rocky shorelines. Their origin is located within the littoral zone (or beyond), often attestable by the presence of bio-erosive features such as rock-pools and/or notches. Commonly, several boulders are imbricated and arranged in the form of imbrication trains. Such high-energy wave displaced mega clasts or boulders are reported from numerous coasts all over the world (e.g. NOTT 1997, 2003a, 2003, BRYANT & NOTT 2000, SCHEFFERS & KELLETAT 2003, NOORMETS et al. 2004, VÖTT et al. 2006, IMAMURA et al. 2008, SPISKE et al. 2008, FROHLICH et al. 2009, GOTO et al. 2009, 2010,

BOURGEOIS & MACINNES 2010, PARIS et al. 2010, SWITZER & BURSTON 2010 or ENGEL & MAY 2012). Moreover, dislocated mega clasts were also described offshore of Lefkada Island (W-Greece) in water depths between 2 and 5 meters by VÖTT et al. (2008).

Figure 4: Dislocated and partly imbricated boulders at the western rocky shoreline of the Paliki Peninsula (Cefalonia Island, W-Greece) (source: own photos taken in September 2009, detail picture A taken with automatic release).

In general, dislocated boulders are subject to a controversial debate whether their origin is related to storm or tsunami influence (e.g. NOTT 2003, SCHEFFERS & KELLETAT 2003, GOTO et al. 2007, KELLETAT 2008, SPISKE et al. 2008). NOTT (2003) introduced a mathematical approach to make statements on the transport source of a boulders movement (tsunami versus storm). Until now NOTT's equation (2003) is widely used, even though it was revised by several authors (e.g. PIGNATELLI et al. 2009, BENNER et al. 2010 and NANDASENA et al. 2011). However, within this context HOFFMEISTER et al. (2013a) concluded – by using the before mentioned equations combined with high resolution data of displaced boulders delivered by the precise TLS-method – that the estimated wave heights for tsunami events are mostly significantly exaggerated. A modeling approach regarding the boulder transport setting was elaborated by IMAMURA et al. (2008) based on experiments in an open water channel with cubic and rectangular shaped boulders. Anyway the assessment, whether block deposition was caused by storm or by tsunami, must be based on the evaluation of the local geomorphological and geological setting.

With regard to the Mediterranean, boulders displaced by extreme wave events, were described for several coasts, for instance by MASTRONUZZI & SANSÒ (2000, 2004), MASTRONUZZI et al. (2006, 2007), SCICCHITANO et al. (2007, 2012), PANTOSTI et al. (2008), PIGNATELLI et al. (2009) and MASTRONUZZI & PIGNATELLI (2012) for Italy, by KELLETAT (2005) for southern Turkey, by KELLETAT & SCHELLMANN (2002) for Cyprus and by MORHANGE et al. (2006), MAOUCHE et al. (2009) and MAY et al. (2009) for the Levantine and the north African coast. Examples for mainland Greece are given by SCHEFFERS et al. (2008) and VÖTT et al. (2006, 2008a, 2009a, 2010), MAY et al. (2011, 2012) and for Crete by SCHEFFERS & SCHEFFERS (2007).

Group 2: Fine-grained allochthonous sediment layers in near-coast geo-archives

The second type of tsunami sediment signatures is represented by mostly fine-grained layers of allochthonous marine sediments found in sub- and supra-littoral or near-shore geological archives – embedded in the local autochthonous sedimentary record intersecting autochthonous deposits – sometimes being associated to cultural debris (VÖTT et al. 2010).

During the last years sets of distinctive features and typical sedimentary characteristics of such onshore tsunami deposits were described and listed by several authors, for instance by TUTTLE et al. (2004), DOMINEY-HOWES et al. (2006), FUJIWARA (2008), SWITZER & JONES (2008a), MAMO et al. (2009) or ENGEL & BRÜCKNER (2011).

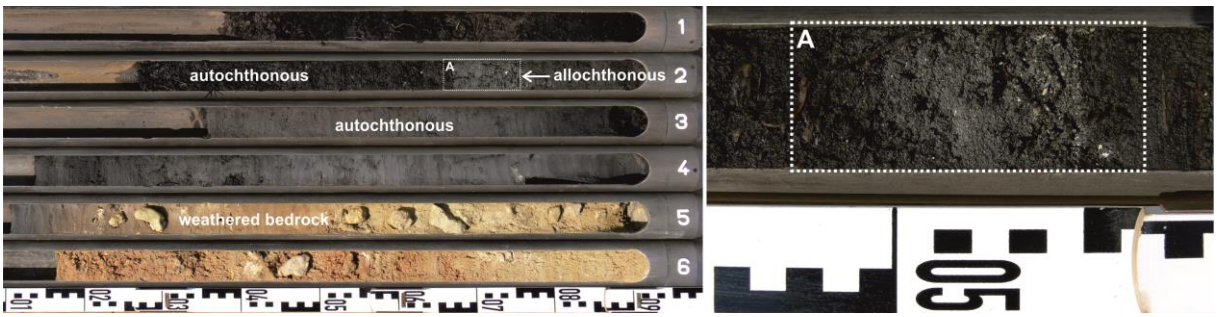

Figure 5: Example for an allochthonous marine fine-grained layer intersecting an autochthonous low-energetic swampy environment located in back-beach position (source: own pictures 2010 and illustration 2014).

With regard to the sedimentary characteristics of tsunami deposits, sand sheets are a common feature in tsunami-devastated lowlands (lagoons and marshes) – even though many other coastal processes are also able to leave sand sheets such as long-term sea-level changes, storm surges and river floods or liquefaction (NANAYAMA 2008). However, the author refers that common characteristics of onshore tsunami deposits generally are associated with sandy or gravelly layers intersecting peat successions or lacustrine sediments, featuring fining upwards sequences or graded structures and often the wedge-shaped sediments sheets are thinning landwards (see also DAWSON et al. 1988). Similar description about fining upward and thinning landward characteristics of the event related sediment body can be found also in the works from NANAYAMA et al. (2000), GELFENBAUM & JAFFE (2003), TUTTLE et al. (2004) or DOMINEY-HOWES et al. (2006), among others. Typical for tsunami deposits are erosional discordances between the event deposit itself and the underlying pre-event deposit as well as load structures in the lower-basal tsunami units (DOMINEY-HOWES et al. 2006). Based on literature review, DONATO et al. (2009) list sharp erosive bases, graded beds, hummocky crossstratifactions and mud drapes as diagnostic features of shallow water tsunami deposits. After FUJIWARA (2008) a tsunami comes along as a chain of high-energy flows resulting in the deposition of three units – a run-up unit, a backwash flow and a stagnation unit – whereas the run-up and the backwash units generally leave an erosional basis, exhibiting reversed and normal grading, which are covered by a mud drape or a layer with gyttja or plant debris from suspension

fallout while stagnation. About rip-up or intra-clasts in tsunami deposits, representing incorporated reworked material of the underlying sediments, report GELFENBAUM & JAFFE (2003) as well as DOMINEY-HOWES et al. (2006). With regard to the varying regional setting (topography, bathymetry, sediment supply, etc.) and different characteristics of each tsunami, its imprint in the geological record can differ, which has to be considered when comparing deposits from different locations (MAY 2010). Moreover, tsunamigenic deposits alter with time due to several processes such as erosion, compaction, diagenesis and/or bioturbation (MATHES-SCHMIDT 2013), thus complicating their identification.

Group 3: Beachrock-type tsunamiites

In 2010 VÖTT et al. introduced another type of tsunami deposits, the so called beachrock-type tsunamiites. According to VÖTT et al. (2010) these deposits are concerned to be lithified/cemented calcarenitic and conglomeratic event deposits, which were calcified above the local sea level by post event pedogenetic processes. Within these deposits sedimentary characteristics were identified such as basal erosional unconformities, rip-up clasts, large intraclasts, multiple fining upward sequences as well as bi- to multimodal grain size distribution – all of which are reported as typical of tsunami deposits (for further details see VÖTT et al. 2010).

Figure 6: Beachrock formations at Pheia, the harbor of ancient Olympia in Elis (NW-Peloponnese – Greece). A: Outcrop of the beachrock formations at the beach of Aghios Andreas. B: Ceramic fragments incorporated in the beachrock formations. C: By beachrock covered and enwrapped ancient wall remains. According to VÖTT et al. (2011c) the Aghios Andreas beachrock does not represent a lithified *in situ* beach deposit but a post-depositionally cemented tsunamite (source: own pictures taken in September 2008 and own illustration 2014).

Group 4: Geoarchaeological palaeotsunami features

Within the context of geoarchaeological investigations in Greece, a fourth group of tsunami signatures – mixed with cultural remains – is gaining more attention in younger times (BRUINS et al. 2008, VÖTT et al. 2011a, 2011b, HADLER et al. 2011, 2012, HADLER 2014, WILLERSHÄUSER 2014). These mainly badly sorted sediments feature characteristics such as erosional discordances, a multi-modal grain size distribution, marine macro fauna besides ceramic fragments and bone remains (VÖTT & MAY 2009).

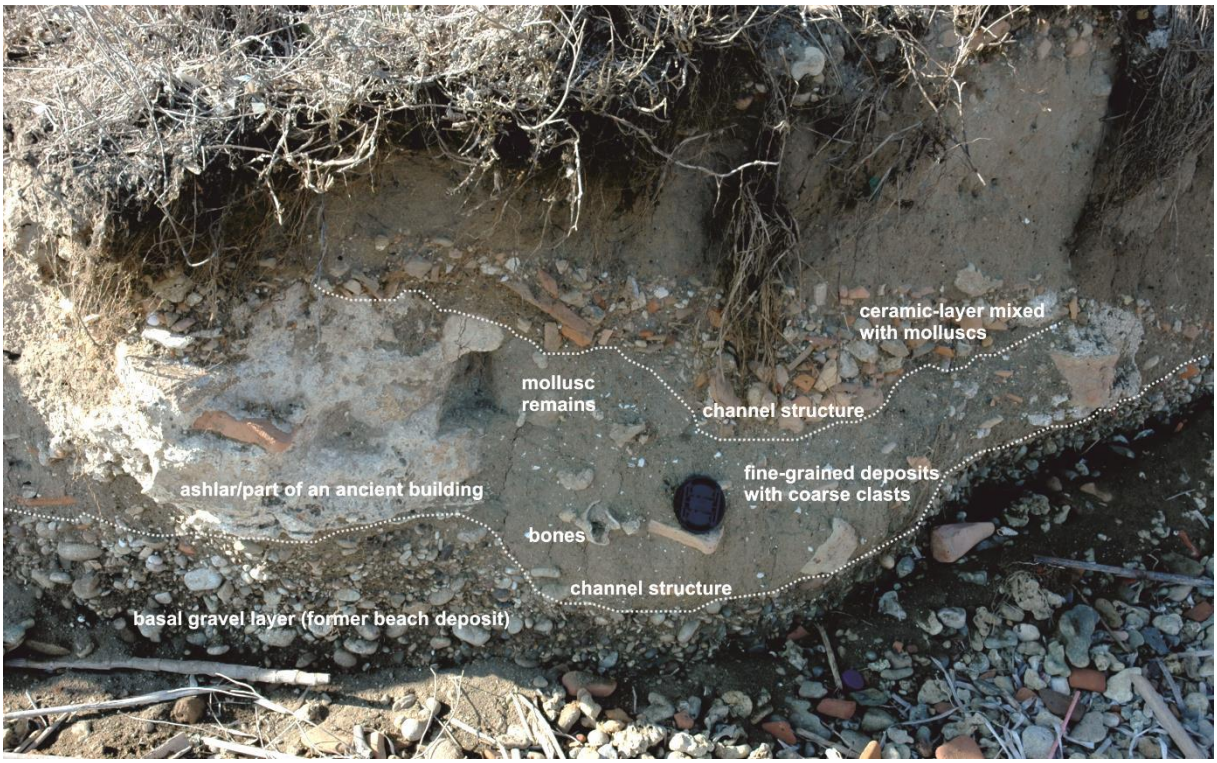

Figure 7: Along the cliff in the area of the ancient harbor of Kyllini (NW-Peloponnese – Greece), geoarchaeological destruction layers are disclosed. According to HADLER (2014) these destruction layers represent tsunami event deposits, that feature sedimentary characteristics such as channel structures, lamination, fining upwards sequences and a heterogeneous mixture of terrestrial and marine deposits (fine-grained sediments besides gravels, ceramic fragments, bone remains and marine molluscs) (source: own photo taken in September 2010 and own illustration 2014).

Offshore tsunami deposits

Already in 2007 DAWSON & STEWART stated that scientists should pay more attention on offshore submarine tsunami deposits within the framework of (palaeo) tsunami research. Due to backwash flows, from the coast towards the open sea, the sea ground can be draped by the associated backwash deposits. Simultaneously turbidites can be triggered as a consequence of the backwash flows and/or the event itself. Fortunately nowadays more attention is drawn on these kinds of event deposits. As a result of this, several interesting studies were carried out during the last years focusing on such deposits, e.g. for Israel by REINHARDT et al. (2006) and GOODMAN-TCHERNOV (2009), for the Sirte and Ionian abyssal plain by SHIKI & CITA (2008), for the Gulf of Corinth by NOMIKOU et al. (2011)

and by SAKELLARIOU et al. (2011) and for Italy by SMEDILE et al. (2011), i.a. Already in 2000 HIEKE & WERNER were concerned in studying the Augias megaturbidite located in the Ionian and Sirte abyssal plains. Concerning to the authors this turbidite was probably mobilized by the tsunami following the Minoan Santorini collapse around 3500 BP (see HIEKE & WERNER 2000). Within this context VÖTT et al. (2006) draw parallels between the Augias Turbidite and onshore event deposits found in Akarnania (W-Greece). However, recently POLONIA et al. (2013) identified the so called HAT – Homogenite Augias Turbidite to be triggered by the tsunami following the 21st, July 365 AD Cretan Earthquake. Furthermore, POLONIA et al. (2013) refer to that 93-95 % of the volume of the Holocene and late Pleistocene sediment cover in the Ionian Sea was deposited by turbidity currents basically triggered by seismic activity. On the basis of hydrodynamic simulations the associated tsunamis from the 6th, October 1947 earthquake in the Peloponnese and the 9th, February 1948 earthquake near Karpathos are believed to be caused by submarine landslides induced by these earthquakes rather than by the earthquakes themselves (EBELING et al. 2012). Hence, co-seismically induced submarine mass movements must be considered a substantial hazard source, so that residents and decision-makers have to be educated about them (EBELING et al. 2012).

Geo-scientific methods to identify fine-grained tsunami deposits

Nowadays modern geosciences operate with a wide range of methods in order to identify (palaeo-) tsunami signatures within the geological record. A model to calculate tsunami flow speed from tsunami deposits (TsuSedMod) was introduced by JAFFE & GELFENBAUM (2007). This model was applied for instance by SPISKE et al. (2010) for the deposits of the 2004 Sumatra and 2006 Java tsunami, thus being able to make implications for the estimation of flow parameters of past tsunamis. Chemical signatures of palaeo-tsunamis are discussed for instance by CHAGUÉ-GOFF (2010) and SZCZUCINSKI et al. (2006) used geochemical patterns to study the sediments of the 2004 IOT. Rock magnetism techniques were applied by FONT et al. (2010) for the identification of tsunami-induced deposits. The impact of the 2004 IOT on the texture and mineralogy of associated sediments in SW-India was analyzed by BABU et al. (2007). Lately the identification and analysis of microfossil assemblages within tsunami layers has moved to the fore, resulting in numerous publications. For instance MAMO et al. (2009) published an article about tsunami sediments and their microfossil assemblages, by reviewing the gaps in understanding and making recommendations in order to assist researchers to enhance the use of microfossils within tsunami geology. Their review of the available literature suggests that at best, displaced assemblages and/or deeper water species being transported and deposited into shallow water, lagoonal and marsh settings reinforce the tsunami origin of the deposit. Accordingly, a deep water assemblage sitting within a high marsh environment should be extremely obvious (MAMO et al. 2009). However, according to VÖTT (2014) tsunamis usually erode and transport material which

is to be found *in situ*. Especially along the continental slopes and shelves this includes the deposition of open water and/or deep sea foraminiferal species. Nevertheless, the absence of deep sea species in onshore event deposits does not preclude tsunamigenic activity. On the contrary a mixture of species associations from different habitats can indicate tsunamigenic influences. Predominantly those species are transported while tsunami inundation which are to be found in immediate vicinity of the depositional area (VÖTT 2014, personal communication).

Within the context of microfossil analyses also shell taphonomy and statistical methods are used. The potential of foraminiferal taphonomy as a tsunami indicator in a shallow arid system lagoon at Sur (Sultanante of Oman) was tested by PILARCZYK & REINHARDT (2012). And DONATO et al. (2008) for instance identified tsunami deposits by using bivalve shell taphonomy. Ostracods from a Marmara Sea lagoon (Turkey) as tsunami indicators were analyzed by MISCHKE et al. (2012). Paleontological and sedimentological studies of tsunami deposits accompanying the great Chilean earthquake of February 2010 were carried out by HORTON et al. (2011). And benthic foraminiferal and its environmental degradation studies of tsunamigenic sediments from coasts of southeast India were applied by SURESH GANDHI et al. (2007). Besides analyses on foraminifers or ostracods also diatom biostratigraphy is applied in this regard, as undertaken by DAWSON (2007) on deposits from the 1998 Papua New Guinea tsunami. Thereby, the research on microfossils is in no way limited only to onshore tsunami deposits. GOODMAN-TCHERNOV (2009), for example, studied the micropaleontology and sedimentology of offshore tsunami deposits detected in the ancient harbor of Caesarea. And multivariate analyses on benthic foraminiferal assemblages from offshore sediment samples pointing on tsunamigenic activity from the Augusta Bay (Eastern Sicily-Italy) were undertaken by SMEDILE et al. (2011).

Tsunami versus storm

In some regions of the world severe storms or hurricanes can reach the potential of tsunamis with regard to the associated wave regime, e.g. in the Caribbean, in SE-Asia or partly in the North Sea. Consequently in those regions both event types can leave similar sedimentary features and characteristics within the geological record, thus appropriate distinguishability is exacerbated. Therefore, the differentiation between storm and tsunami deposits has been an embarrassing problem for researchers from the beginning of tsunami geology (FUJIWARA 2008).

Important factors in the distinction between tempestites and tsunamiites are due to differences in the hydrodynamic characteristics between tsunamis and storms (SUGAWARA et al. 2008). According to SWITZER & JONES (2008a) storm surges are the result of a large number of inundation pulses that release less energy. Thus, the extremely large wavelength and period in contrast to those of storm waves are responsible for the distinctive features of tsunami deposits (FUJIWARA 2008).

Although it is difficult to differentiate between storm and tsunami deposits, possible criteria for the identification are offered by the characteristics of tsunamis (SUGAWARA et al. 2008). Facies models and compilations about the sedimentological differentiation criteria between tsunami and storm deposits (compiled from numerous different studied sites all over the globe) are given respectively are listed for example by DAWSON & STEWART (2007), KORTEKAAS & DAWSON (2007), MORTON et al. (2007) or SUGAWARA et al. (2008), ENGEL & BRÜCKNER (2011), among others.

Accordingly, in regions where storms can reach tsunami qualities it is necessary to compare and combine different detected sedimentary features and characteristics of a supposed event deposit, before attributing the deposits to a specific event type. And within this context it does not suffice merely to compile sedimentary differentiation criteria without regarding relevant regional and local geographical circumstances. Therefore, the geomorphological and topographical setting, the tectonic constellation, the regional climate and especially the local wind and wave regime have to be considered when interpreting the data.

More precisely this means that the problem, whether event deposits are to be associated to storm or to tsunami activity, has to be discussed against the background of the regional climate and on the basis of local and regional storm climatologies (for wind generated waves). Additionally storm event compilations, summarizing past events, have to be studied within this context. However, with regard to the Mediterranean – for which indeed several palaeotsunami event catalogs exist – equivalent compilations, summarizing past extraordinary storm events (centenary or millennia events), apparently do not exist.

Chapter 3 – Study regions & the physical and geotectonic setting

In search of tsunami fingerprints within the Holocene geological record three coastal regions in the Gulfs of Lakonia and Argolis (southern and eastern Peloponnese – Greece) were investigated. The specific study sites in the Lakonian Gulf are the area around Neapolis (southeast Lakonia) and the Evrotas River delta (central Lakonia). In the Argolis, palaeotsunami studies were carried out around Limnothalassa Moustou, in the eastern part of the Argive Plain around ancient Tiryns as well as in the Bay of Drepano at Asinis Beach.

3.1 The physical and geotectonic setting of Greece

In whole western Eurasia, Greece exhibits the highest seismic activity (KARAKAISIS & PAPAZACHOS 2002). From the tectonic point of view, the region is located within a complex zone of plate boundaries, containing the Anatolian, Arabian and Nubian plates and the Aegean microplates (EBELING et al. 2012). According to HOLLENSTEIN et al. (2008), the dominating tectonic regimes of the eastern Mediterranean are characterized by (i) the right-lateral strike-slip motion of the North Anatolian fault zone (NAFZ) into the North Aegean trough (NAT), (ii) the right-lateral strike-slip along the Cefalonia fault zone (CFZ), (iii) the plate convergence along the Hellenic Arc and (iv) extensional dynamics in northern and central Greece as well as in the Peloponnese. Along the Hellenic Arc/Trench system, the oceanic lithosphere of the Nubian Neo-Tethys is being subducted northward underneath the southern Aegean plate (EBELING et al. 2012).

A Benioff zone was first identified in S-Greece based on investigations by PAPAZACHOS & COMNINAKIS (1970, 1971) on earthquake foci and by PAPAZACHOS & DELIBASIS (1969) on fault plane solutions, giving first evidence of a subduction zone in the eastern Mediterranean (see also KARAKISIS & PAPAZACHOS 2002). This subduction system expands along the 1000 km long Hellenic Arc which stretches NW-SE from Cefalonia to Crete (West Hellenic Arc) and SW-NE from eastern Crete to Rhodes (East Hellenic Arc) (BASILI et al. 2013). The velocity of the southwestward crustal movement of the overriding Aegean microplate is about 30 mm/yr in southern Peloponnese and about 40 mm/yr in Crete (KAHLE et al. 1998, 2000, COCARD et al. 1999, MCCLUSKY et al. 2000).

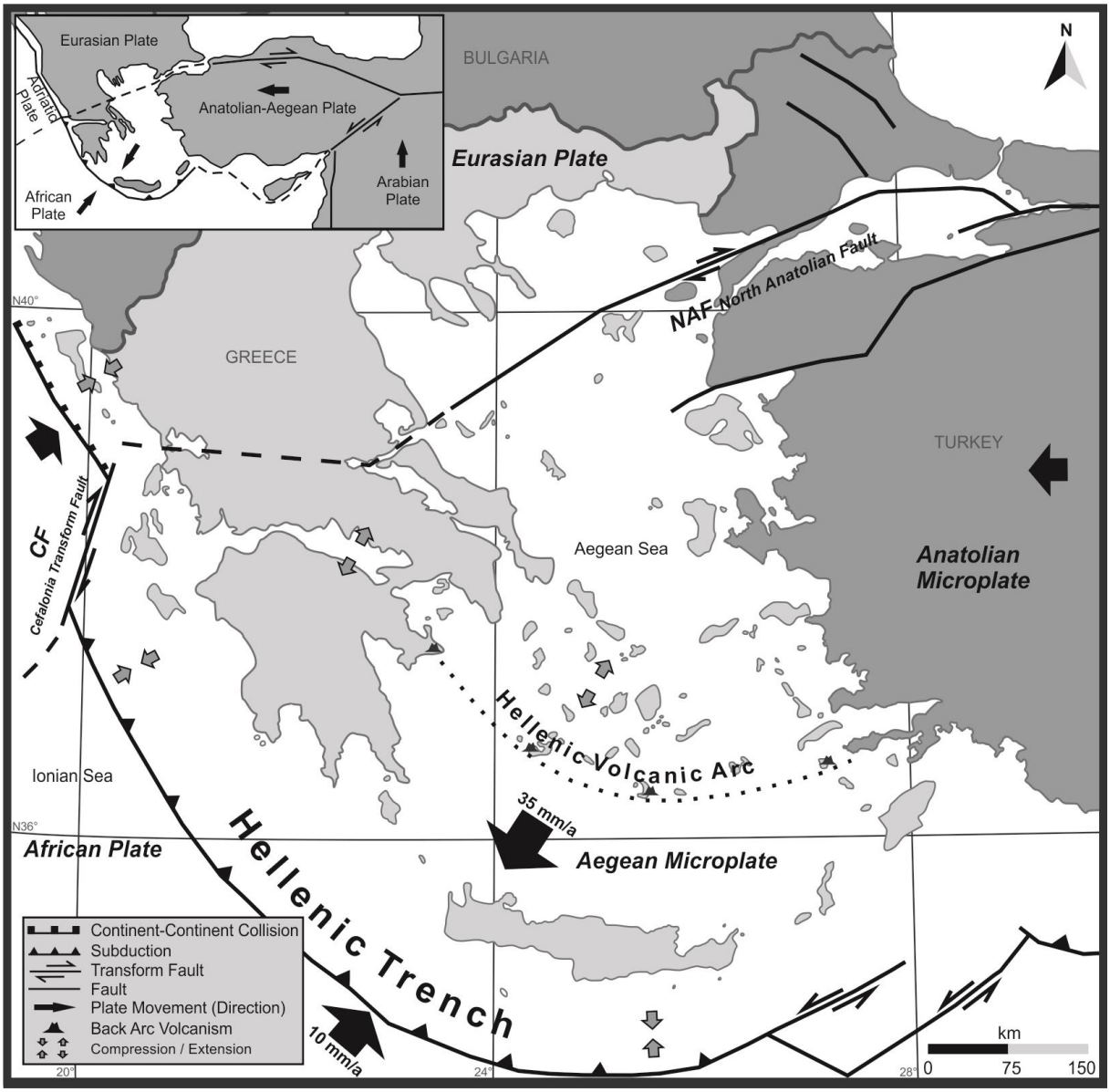

Figure 8: Overview of the tectonic constellation of the eastern Mediterranean (source: own illustration based on data from CLEWS 1989, HASLINGER et al. 1999 and DOUTSOS & KOKKALAS 2001).

The tectonic evolution of the Aegean is mainly characterized by back-arc spreading and stretching (JACKSON & MCKENZIE 1984). Thus, the back-arc area is dominated by normal faulting along a dominant zone of north-south extensions and a secondary zone following the Hellenides mountain chains with east-west extensions (KARAKAISIS & PAPAZACHOS 2002). In contrast to the adjacent mainland, the Aegean Sea is therefore affected by crustal thinning and high thermal fluxes (JACOBSHAGEN 1986).

According to PAPAZACHOS & PAPAZACHOU (1997) the western Hellenic Arc represents Europe's most seismically active region. And in general, the high seismicity is mainly related to the subduction zone of the Hellenic Trench which crosses the eastern Mediterranean (SCHÖNENBERG & NEUGEBAUER 1997). More than 4500 intermediate-size earthquakes (M > 49) that were recorded within a time span of about 30 years reflect this high seismicity (HOLLENSTEIN et al. 2008). For more than 40 years, it is known that the high shallow seismicity along the subduction zone comes along with magnitudes up

to M_s = 8.2 (PAPAZACHOS & COMNINAKIS 1969, PAPAZACHOS 1990, PAPAZACHOS & KIRATZI 1991). PAPAZACHOS & PAPAZACHOU (1997) divided Greece and the surrounding areas into 67 hazard zones with similar homogeneous shallow seismicity.

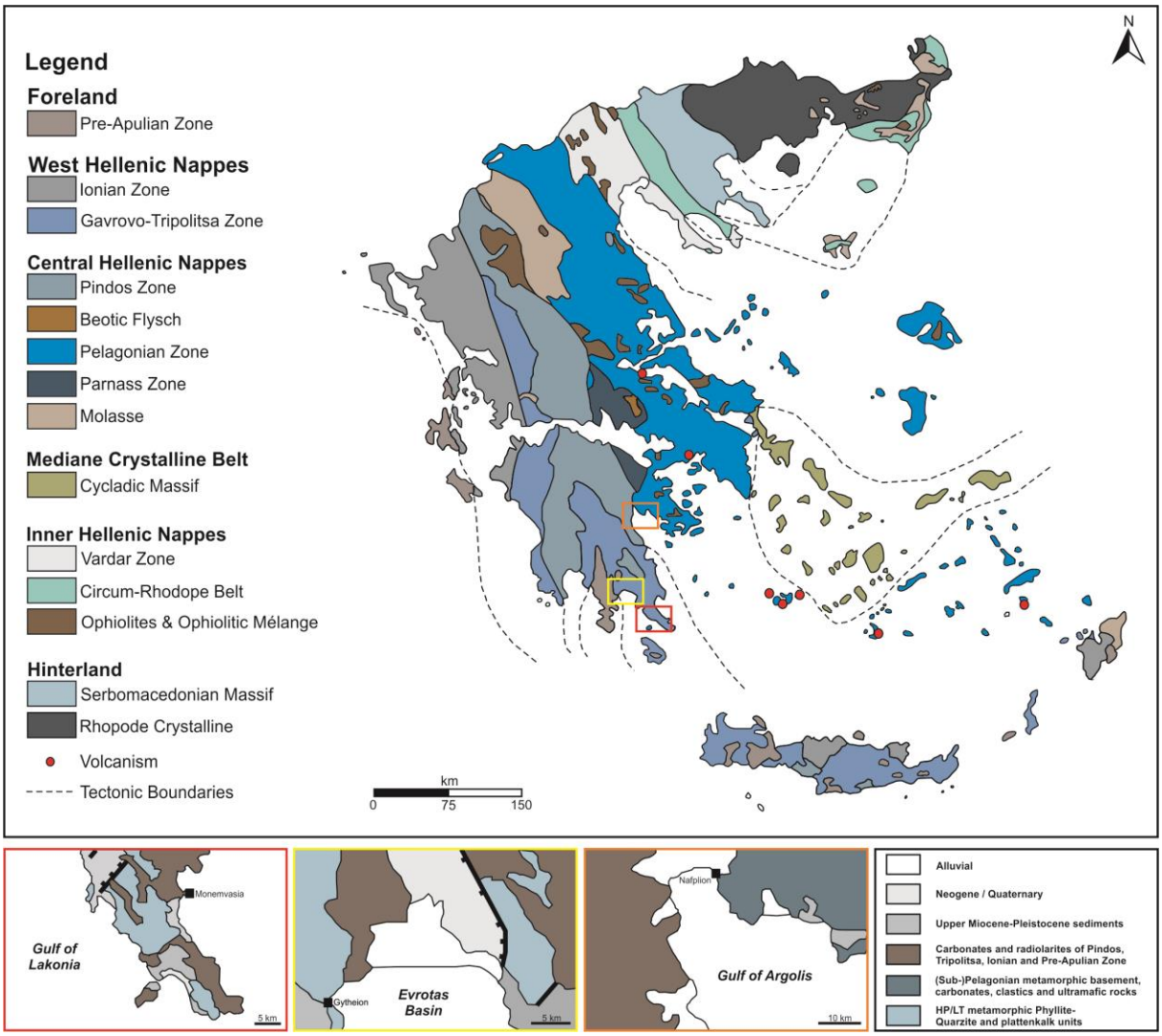

Figure 9: Overview of the geological constellation of Greece (upper big map) and the simplified geological constellation of the study regions (lower detail maps) (source: own illustration based on data from BORNOVAS & RONDOGIANNI-TSIAMBAOU 1983, JACOBSHAGEN 1986 and TOUGIANNIDIS 2009).

Generally, earthquakes can be seen as the most likely source of tsunamis worldwide (BASILI et al. 2013). And with regard to the focal depth, as one crucial factor in tsunami formation, PAPAZACHOS & DIMITRIU (1991) published a map marking the tsunamigenic zones in and near Greece. Thereby, the southeastern Peloponnese is exposed to a high tsunami hazard (PAPAZACHOS & DIMITRIU 1991). On the basis of numerical simulated earthquake-generated tsunami scenarios for the SE-Aegean Sea, MITSOUDIS et al. (2012) note, that a re-evaluation of the seismic potential of the Hellenic Arc is necessary, so that earthquakes of magnitudes > 9.0 have to be included. In general, around Greece 30 % of all earthquakes generate a measurable seismic wave (BRYANT 2008, see also KURAN & YALÇINER 1993, TINTI & MARAMAI 1999).

Modern studies indicate that especially submarine slides pose substantial danger in triggering tsunamis. Therefore, much attention has been given to tsunami induced submarine landslides (AMBRASEYS & SYNOLAKIS 2010). EBELING et al. (2012) concluded that observed historical tsunamis in the Greek seas were most likely triggered by submarine landslides induced by earthquakes. This hazardous potential increases against the background that over 90 % of the volume of the Holocene and late Pleistocene sediment cover were deposited by turbidity currents induced by seismic activity; in turn, earthquake induced tsunamis can trigger big submarine mass movements, respectively megaturbidites (POLONIA et al. 2013).

3.2 Climatic conditions of Greece

Greece's climate is a typical Mediterranean climate with relatively warm and dry summers and mild and rainy winters with extended periods of sunshine throughout most of the year (HNMS 2012) (see climate diagram Fig. 10). After KÖPPEN (1931) the Mediterranean *Cs-climate* is also known as "Etesian climate" (*Ετήσιος/Etêsios* = Greek for annual), due to the northern winds which blow throughout the summer months between May and September.

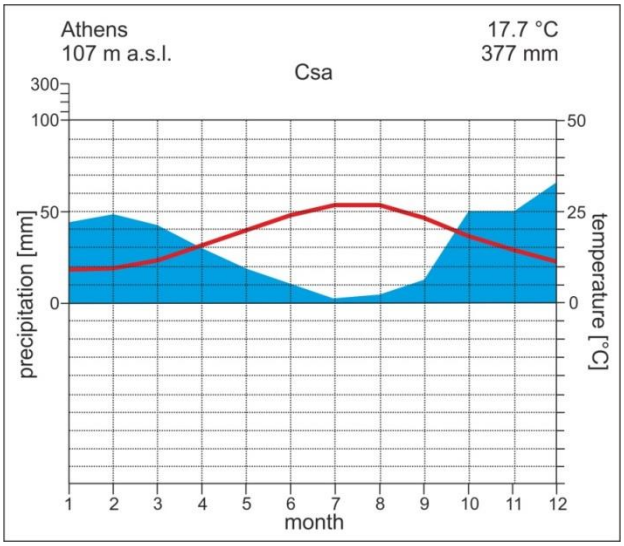

Figure 10: As an example, the climate diagram after *Walter* for Athens should depict the mean climatic conditions in Greece during the year (source: own illustration modified after MUHR 2007).

The term "Etesian" was used since antiquity, describing these dry northern winds which were the dominant meteorological feature for the ancient Greek navy – however, in modern times it was replaced by the Turkish term "Meltemi" (SAUERWEIN 1996, TOLLNER 1976). Estival pressure differences between the anti-cyclone over the Azores and the Near East monsoon cyclone of the lower troposphere result in the development of these geostrophic winds in the northeastern part of the Mediterranean basin (WEISCHET & ENDLICHER 2000). Normally, the Etesians begin to blow during mornings, by clear sky and high temperatures, until the early afternoon they increase up to 9

Beaufort, while weakening in the evenings and abating during the night (SAUERWEIN 1996). During wintertime, when the inner tropical convergence zone (ITC) and the "horse latitude belt" have moved southwards, cyclones of the west wind zone can stream over the Mediterranean region, resulting in rain and snow showers with intermediate fair weather phases (SAUERWEIN 1996).

The regions of Greece are characterized by a variety of climate subtypes within the Mediterranean climate frame due to the country's topography and geomorphology, the extension over 7 latitudes (34°48' N to 41°45' N) as well as the meridional extent from 19°22' E to 29°38' E (SAUERWEIN 1996, HNMS 2012). These regional climatic aspects in combination with the country's geographic position and its complicated horizontal and vertical dismemberment, makes Greece to be one of Europe's windiest areas (CHRONOPOULOU et al. 2010). Thereby, the seasonal prevailing barometric systems (anticyclones and depressions) are to be the main factors that configure the wind tracks, besides local winds (NASTOS et al. 2002). During the year, the dominant wind direction over Greece is from north, north-east and north-west for 78 % of the 59 meteorological stations, whereas at the remaining stations the different wind directions are due to local winds (CHRONOPOULOU et al. 2010). Thereby, the northern and central continental parts of Greece are characterized by low mean annual wind speed between 1.5-2-5 m/sec., whereas the southern regions and the Peloponnese reach mean annual wind speed between 3.5-4.0 m/sec. In the central Aegean Sea, maxima of 5.5-6.0 m/sec. appear during winter, which is considered to be the windiest season of the year, whereas in southern Lakonia wind speed measures 4.0-4.5 m/sec. and in the Argive Plain 2.0-3.0 m/sec. Nevertheless, for the region of southeastern Lakonia offshore winds are predominant within the annual overview, thus resulting in wind-generated waves from northeastern directions (MEDATLAS GROUP 2004, CHRONOPOULOU et al. 2010, fig. 3). For the southern Peloponnese northeastern and northwestern winds create waves of equal directions. In the Argolis Gulf prevailing winds and thus wind-generated waves show northern directions (MEDATLAS GROUP 2004, p. A.25 & A.26), however CHRONOPOULOU et al. (2010, fig. 3) specifies that the entrance of the Argolis Gulf is dominated by winds from southeastern directions.

Regions	Mean wind directions	Mean wind speeds	Mean wave heights
S-Lakonia	↘ ↓ ↙	4.0-4.5 m/sec.	< 1.0 m
C-Lakonia	↘ ↓ ↙	3.5-4.0 m/sec.	< 0.8 m
Gulf of Argolis	↖ ↓	2.0-3.0 m/sec.	< 0.8 m

Table 1: The table summarizes the mean wind and wave parameters for the three study regions (source: data based on MEDATLAS GROUP 2004 and CHRONOPOULOU et al. 2010).

For the development of storm surges, onshore winds are necessary in order to push the water directly toward the coast. According to GAKI-PAPANASTASSIOU (2010: p.111) the shelf offshore the Argive plain is with 3-5 km very wide, measuring water depths less than 100 m in wide parts. The bathymetric map indicates maximum water depths off the investigated area at Nafplion of 22 m

(MITROPOULOS & ZANANIRI 2010). Along a flat shelf mainly long and shallow waves can be generated. When approaching the shallow water, the orbital movement within the wave is reaching the ground, thus wave velocity is slowed down. Along gradually ascending shores, like the Argolis Gulf, waves break mainly in the form of spilling breakers in sufficient distance to the shoreline while dissipating their energy slowly (KALLENRODE 2003). Therefore the velocity and height of the waves is moderate when approaching the shore itself. Similar conditions apply to the northern part of the Lakonian Gulf (see STATE AGENCY FOR GEODESY AND CARTOGRAPHY AT THE COUNCIL OF MINISTERS OF THE USSR 1988). For the Ionian Sea off the southern Peloponnese, the annual mean significant wave height is lower than 1.0 m and in the northern part of the Lakonian Gulf as well as in the Argolis Gulf lower than 0.8 m and the probability that significant wave heights exceed > 4.0 m in areas close to the shores tend to zero (see MEDATLAS GROUP 2004, p. A.26 & A.27).

TSIMPLIS & SHAW (2010) analyzed an extensive dataset of hourly sea level values from tide gauges and the output of a barotropic model in respect of seasonal extreme values within the Mediterranean Sea and the Atlantic coasts of Iberia. Their results indicate that the Atlantic stations show larger extreme values than the Mediterranean Sea, primarily due to the tide signal. Seasonal sea level extremes occur during the autumn and winter months showing less than 40 cm for the eastern Mediterranean and around 200 cm in the Adriatic Sea, the latter partly due to the direct atmospheric forcing, showing significant increases at the northern Adriatic stations, as well as due to the locally increasing tidal signal (TSIMPLIS & SHAW 2010).

According to PETTERSSEN (1956) and MOSCATELLO et al. (2008) it is well known that the Mediterranean Sea may experience cyclonic storms, but the occurrence of tropical-type vortices over the Mediterranean was first discussed in the early 1980s. These hurricane-like Mediterranean cyclones, also called “medicanes”, feature characteristics such as a rounded cloud area with a free cloud center (“eye”), strong cyclonic winds and intense convection (FITA et al. 2007). PYTHAROULIS et al. (2000) list at least nine events which were documented between 1960 and 2000. For the timespan between 1982 and 1996, LAGOUVARDOS et al. (1999) list four reported cases. However, complex atmospheric processes, the complex orography, the small dimensions of the Mediterranean basin and the continental influences from the African and European mainland limit and modify the evolution of tropical-like systems in the Mediterranean (FITA et al. 2007). Nevertheless, it is assumed that such events may leave more or less regular low- to mid-energy signatures in appropriate local geological archives (VÖTT et al. 2011c). However, with regard to historical tradition dealing with extreme wave events caused by such storms intense literature research was unsatisfactory. Than in contrast to tsunami catalogs comparable compilations for severe storm wave activity do seemingly not exist for the Mediterranean – probably reflecting the tangential respectively insignificant influences of such “medicanes”.

3.3 Relative sea level evolution

When interpreting sedimentological signatures of past extreme wave events from near-coast geological archives/stratigraphies, the results have to be evaluated against the background of the local sea level evolution and changing palaeogeographical coastal constellations.

The local sea level history is subject to temporal and spatial changes/fluctuations which in turn are caused by different factors (FAHRBACH 2002). Short-term sea level variations, generally on a local or regional scale, can be due to tides, extreme waves, wind setup, atmospheric pressure fluctuations, and varying water supply by fluvial systems or due to the geostrophic current. However, the major causes for global long-term sea level changes are eustatic effects. On the one hand, these effects are due to changes in the volume of the ocean basins (marine sedimentation, plate tectonics and seafloor spreading); on the other hand, they are due to changes in the mass of the ocean water body as a consequence of climate changes and a changing water balance (melting or accumulation of continental ice during interglacials or glacials) (KELLETAT 1999, 2002a, 2002b, FAHRBACH 2002).

Another determining factor for regional long-term sea level changes is the isostasy, an equalizing motion of the earth's crust as a reaction of load/compression or load removal/decompression. Eustatic and isostatic sea level changes as well as tectonic processes overlap, thus sea level rise or sea level fall will result from the combination of the different factors (BRÜCKNER & RADTKE 1990). Accordingly, each coastal area features an individual historical evolution with regard to a changing local sea level. Therefore, local data is essential when reconstructing the local sea level evolution of a coastal area (LOY 1967, KRAFT et al. 1985).

In Greece, enormous differences with regard to the local sea level evolution exist even in close proximity (BESONEN 1997). Thus, tectonic processes should not be underestimated when studying the local and/or regional sea level evolution of coastal areas in Greece.

By comparing seven neighboring coastal regions in northwestern Greece, VÖTT (2007a) showed that significant intraregional differences of the relative sea level evolution are due to tectonic processes. Until the end of the Last Glacial Maximum (LGM) of Marine Isotope Stage 2 (MIS 2) (~18.000 years BP), the seal level was ~120-125 m below the present one (FAIRBANKS 1989, KELLETAT 1990, BRÜCKNER 1997, PERISSORATIS & CONISPOLIATIS 2003). At that time, wide shelf regions were exposed to subaerial conditions, numerous islands were bounded to the mainland and lakes have been developed in the deeper areas of several Greek gulfs (PERISSORATIS & CONISPOLIATIS 2003). During late and post glacial times, the global sea level rose during the Flandrian Transgression due to the melting of continental polar and mountain piedmont glaciers (KELLETAT 1999, USGS 2013). However, the associated sea level rise was not constant through time but it was subject to fluctuations during warmer or colder periods of the Late Pleistocene and Holocene. Dependent to varying values of melting water, the global sea

level rise occurred during two major intervals, which were separated from each other by the Younger Dryas stadial (FAIRBANKS 1989). During the two major intervals, the sea level rose by around 1.5-2 cm/a (LAMBECK 1996). At the beginning of the Holocene, the volume of the Weichselian ice sheets was reduced to half, thus the sea level was around -60 m at ~11,500 years BP (BLOOM 1983). Around 8,000 BP, the sea level was about -15 m and the rate decreased to an average of 2 mm/a, therefore the tectonic influence as well as sedimentation processes increased significantly, initiating also the formation of Holocene river deltas (PERISSORATIS & CONISPOLIATIS 2003).

The development of alluvial plains in low-lying coastal areas due to fluvial sedimentation and delta progradation caused the seaward shifting of local shorelines. As a result of the Late Holocene regression, several ancient coastal settlements and harbors can be found nowadays in several kilometers distance to the recent shoreline (examples within the geoarchaeological context are given for instance by KRAFT et al. 1977, VÖTT et al. 2002, BRÜCKNER 2003, PERISSORATIS & CONISPOLIATIS 2003, VÖTT 2007b).

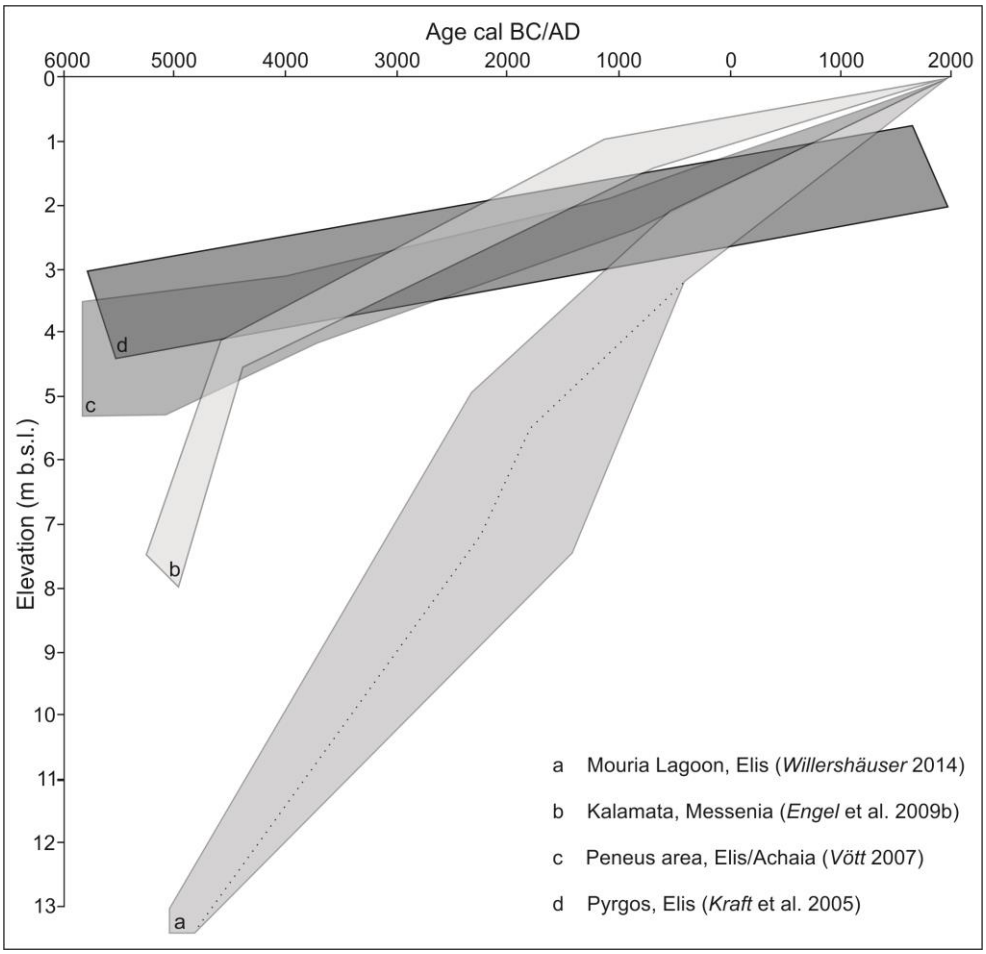

Figure 11: Relative local sea level curves for the western and southwestern Peloponnese published by different authors. The sea level bands were reconstructed by radiocarbon datings of material that acts as an sea level indicator (peat and molluscs) that were encountered in vibracores (source: own illustration, amalgamated data from KRAFT et al. 2005, VÖTT 2007, ENGEL et al. 2009 and WILLERSHÄUSER 2014).

Investigations from VÖTT et al. (2003) and VÖTT (2007a) on basis of vibracorings and radiocarbon dated material indicate that the relative sea level was never higher than the present one since the mid-Holocene in coastal Akarnania, coastal Elis and neighboring Achaia (northwestern Peloponnese). Similar results are presented also by KRAFT et al. (2005) for the region around Pyrgos (Elis, northwestern Peloponnese), by ENGEL et al. (2009b) for coastal Kalamata (Messinian Gulf, southwestern Peloponnese) and recently by WILLERSHÄUSER (2014) for the Mouria Lagoon (Elis, northwestern Peloponnese). By comparing the sea level curves from KRAFT et al. (2005), VÖTT (2007a) and ENGEL et al. (2009b), as done by VÖTT et al. (2011c), no essential differences are noticeable in the relative sea level evolution of the western and southwestern Peloponnese. Rather a more or less constant sea level rise is visible of 0.5-0.7 mm/a, with one exception of several meters of relative tectonic subsidence for Messinia for the time before 4,500 cal BC (ENGEL et al. 2009b).

With regard to the investigation sites in southeastern Lakonia, the Bronze Age building foundations and pottery found at Pavlopetri, which lie submerged at a water depth of 4 – 5 m (HENDERSON et al. 2011), must have undergone subsiding movements due to tectonic activity beside the eustatic sea level rise. According to HENDERSON et al. (2011), it is not yet possible to attribute the subsidence to a particular event, while a frequent occurrence of seismicity is well documented for the region (see also ANGELIER et al. 1982, PIRAZZOLI et al. 1982, STIROS 2009). A similar situation can be assumed for the partly submerged archaeological site of Plitra close to Boza Bay. In addition the island of Antikythera, situated about 80 km southwards, must have been uplifted in the geologic past due to intermittent seismic movements (FLEMMING 1973, PIRAZZOLI et al. 1982, see also HENDERSON et al. 2011). Therefore, it might be expected that there are some tectonic correlations between uplift in the south (Antikythera) and subsidence in the north (southeastern Lakonia). It seems probable, according to HENDERSON et al. (2011), that the Bronze Age town of Pavlopetri was inundated by the time of the Roman Empire, because younger constructions and archaeological findings are absent, whereas other settlements in Lakonia were also occupied during Roman and Byzantine times.

Concerning the Evrotas River delta, the progradation of the river and the associated evolution of the coastal plain caused a seaward shifting of the local coastline (KRAFT et al. 1972, 1977).

3.4 The bays of Vatika and Boza (SE-Lakonia)

The Lakonian Gulf is exposed to the Hellenic Arc (see Fig. 8) and forms a huge asymmetric graben between the Parnon Mountains (1935 m above present sea level (m a.s.l.)) in the east and the mountains of the Taygetos (2407 m a.s.l.) in the West (FEDERICI et al. 2002, CUNDY et al. 2006). The most conspicuous feature of the graben, the huge Taygetos fault, is located in the central part of the Lakonian Gulf. Normal faults lie between the city of Gythio and Cape Menaro in the west and between Cape Xili and Elafonisos Island in the east (FEDERICI et al. 2002).

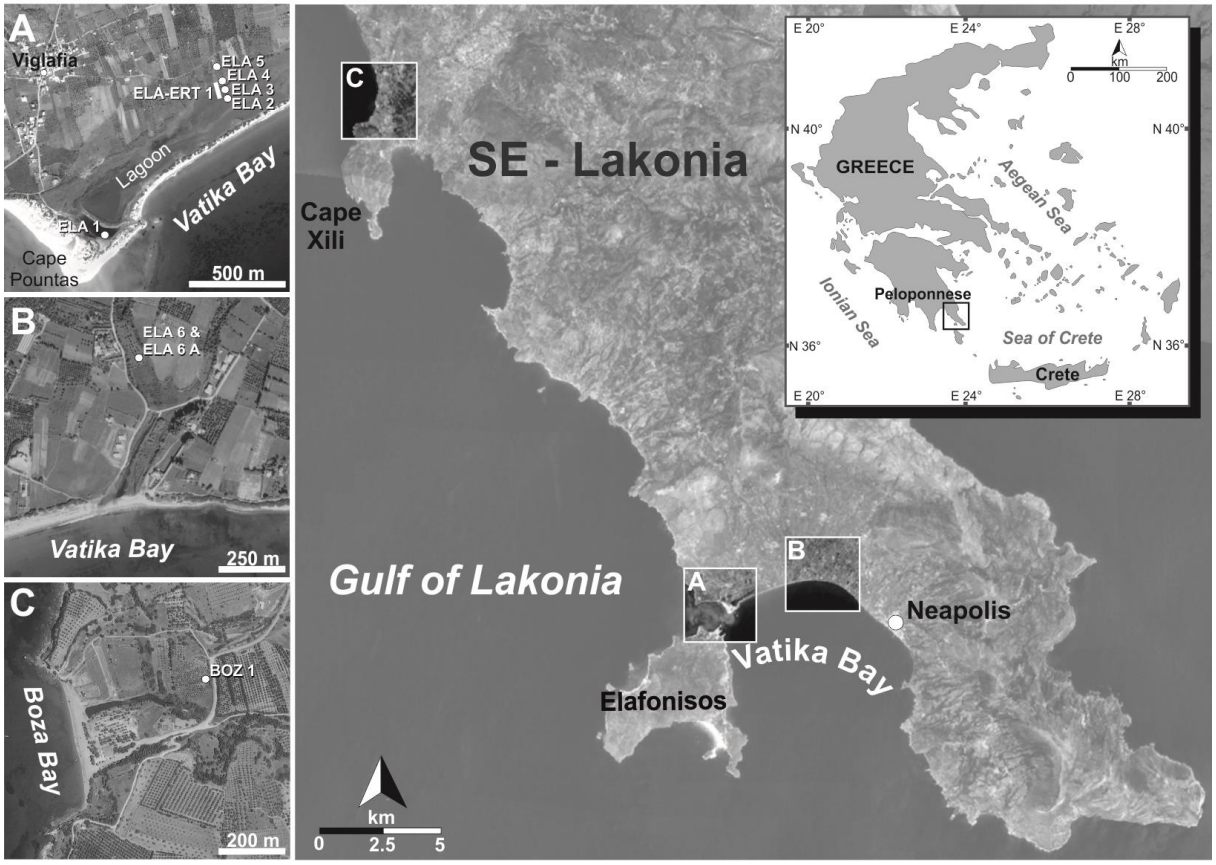

Figure 12: Overview of study areas in southeast Lakonia. The study area of Viglafia is situated opposite to Elafonisos Island near the village of Viglafia and the Viglafia Lagoon (A). The study area of Vatika is located to the northwest of Neapolis in the central part of Vatika Bay within a dry valley (B). The study area of Boza lies in another dry valley in the north of the Xili peninsula running towards the Bay of Boza (C) (source: own illustration 2012, maps based on NASA World Wind and Google Earth images/data, access January 2012).

Geologically, the Lakonian peninsula belongs to the West Hellenic Nappe which was incorporated into the Hellenic orogenetic complex during the Miocene (JACOBSHAGEN 1986). In many places, parts of the West Hellenic nappe are disclosed, showing quartz-sericit schists, glimmer schists, quartzites and evaporites as main rock types (FEDERICI 2002). In other places, the nappe is covered by Jurassic-Eocene carbonatic rocks of the Gavrovo-Tripolitsa zone and by Eocene-Miocene flysch units (JACOBSHAGEN 1986).

Geoscientific investigations were carried out close to the small village of Viglafia, located in the westernmost part of the Neapolis Basin bordering Vatika Bay (Fig. 12). The western edge of Vatika Bay is prolonged by Elafonisos Island which is separated from the mainland only by a narrow and flat natural water channel. More specifically, the study area of Viglafia is situated at the northern margin of a swampy lagoon, about 600 m eastward from Viglafia and 900 m northeastward from Cape Pounta. In the study area of Viglafia vibracorings ELA 2, 3, 4 and 5 complementing earth resistivity measurements were carried out.

The Lagoon of Viglafia is protected from the open sea by a dune ridge. Several washover fans extend from the dune ridge into the lagoon in a northern direction (see Fig. 12, A). The mountain ranges framing the Neogene basin of Neapolis are mainly made out of Triassic to Eocene carbonates of the Tripolitsa series, a subzone of the Gavrovo-Tripolitsa Zone (JACOBSHAGEN 1986, ZEEH 1989). After IGME (2002) the bedrock around Viglafia is mainly built out of marine sediments of Pliocene to Pleistocene age, partly covered by unconsolidated Holocene dune sands and alluvial deposits. In large parts, the scenery is affected by marine terraces. Beside eustatic and coastal dynamic processes, the marine terraces are basically controlled by young Pleistocene tectonic uplift (KOWALCZYK et al. 1992) thus reflecting the regional tectonic activity (see Fig. 13).

Figure 13: Displaced and partly imbricated boulders along the rocky coast west of Cape Pounta in southern Lakonia. Rock pools attest the littoral origin of these blocks. In the background, different generations of Pleistocene marine terraces are visible (source: own photo taken in September 2008 and own illustration 2014).

Cape Pounta is well known for the Mycenaean settlement of Pavlopetri the remains of which lie in up to 5 m water depth. Graves belonging to this settlement are cut into the calcarenitic aeolianite which forms the local bedrock. Submerged undated cart tracks near Cape Pounta also indicate that the relative sea level has undergone considerable rise since the mid-Holocene and has never been higher

than at present (SCHEFFERS et al. 2008). According to HENDERSON et al. (2011) and classical references (STRABO: iii. 5.1, PTOL: iii. 16.9 and PAUSANIAS: iii. 22.10) Elafonisos must has been connected by an isthmus to the mainland. To the west of Cape Skala, many large boulders were found dislocated and partly imbricated by high-energy impact (SCHEFFERS et al. 2008). Results from high-resolution terrestrial laserscanning (TLS) in combination with DGPS and lab-borne density measurements of a block-train near Cape Pounta constrain a maximum boulder-weight of more than 4.6 t (NTAGERETZIS 2009, NTAGERETZIS et al. 2011, HOFFMEISTER et al. 2013a) (see Fig. 14).

Figure 14: Photo and 3D model of a block train near Cape Skala (southeastern Lakonia) modeled by the software RiScanPro. The biggest measured block has a maximum weight of about 4.6 t. In the background Elafonisos Island with its marine terraces is visible (source: own photo taken in September 2008, model by D. Hoffmeister 2009).

Although we do not definitely know the transportation source for the boulders near Cape Pounta, a tsunamigenic origin seems probable due to historical accounts which clearly testify tsunamis in the area of Lakonia. During historical times, the southern Peloponnese was repeatedly affected by strong earthquakes such as in 365 AD, 1303 AD, 1750 AD, 1789/1795 AD, 1842 AD, 1866 AD, 1867 AD, 1927 AD as well as 1944 AD (SOLOVIEV et al. 2000, AMBRASEYS & SYNOLAKIS 2010, PAPADOPOULOS et al. 2013). Associated to the earthquakes in 365 AD, 1303 AD (PAPADOPOULOS et al. 2013, PAPADOPOULOS & PAPAGEORGIOU 2014) as well as 1866 AD and 1867 AD tsunamis were observed (PAPAZACHOS & PAPAZACHOU 1997). Also DOMINEY-HOWES (2002) points to a high tsunami hazard especially for the southeastern part of Lakonia (Fig. 15). Furthermore, datings of vermitide rims, attached to some of the dislocated boulders, indicate a transportation age of around 1300 cal AD, thus possibly referring to the tsunami and earthquake which affected large parts of the eastern Mediterranean in 1303 AD (SCHEFFERS et al. 2008).

The study area of Vatika is located at half distance between Viglafia and Neapolis in the central part of the Vatika Bay (Fig. 12, B). Vibracoring site ELA 6 lies in the middle of a small and flat dry valley. The fact that an olive grove covers the valley floor underlines that at least in younger times no appreciable river water runoff, neither perennial nor torrential, happened. The distance to the present coastline is about 430 m.

The study area of Boza is located about 30 km to the northwest of Neapolis at the northernmost part of the Xili peninsula (see Fig. 12, C). Vibracoring BOZ 1 was drilled approximately 300 m inland in the midst of an orange plantation situated in a small dry valley. Incised in upper Pliocene to lower

Pleistocene rocks (marine to lacustrine, clastic to biogenic sediments), the valley runs into the small Bay of Boza. The valley infill is made out of alluvial deposits (IGME 2002). In the southern embayment of Cape Xili (about 1.5 km to the south of vibracoring site BOZ 1), the partly submerged site of Plitra is situated which is considered to be either the ancient town of Asopos (s. PAUSANIAS: 3.22.9) or Cyparissia (s. STRABO: 8.360, HADJIDAKI & LIANOS 1985). In antiquity, Plitra – covering a flat peninsula, more than 1 km long – is believed to have had an elevation of at least 4 m above the sea level at that time (HADJIDAKI & LIANOS 1985).

Figure 15: Overview of the tsunamigenic zones in the Ionian and Aegean Sea after DOMINEY-HOWES (2002) (see also PAPADOPOULOS & CHALKIS 1984, PAPAZACHOS et al. 1986 and SOLOVIEV 1990). The larger the ellipse is, the greater is the tsunami intensity. Study region in SE-Lakonia is marked by an arrow (source: own modified and adjusted figure based on DOMINEY-HOWES 2002).

3.5 The Elos Plain and its surroundings (Central Lakonia)

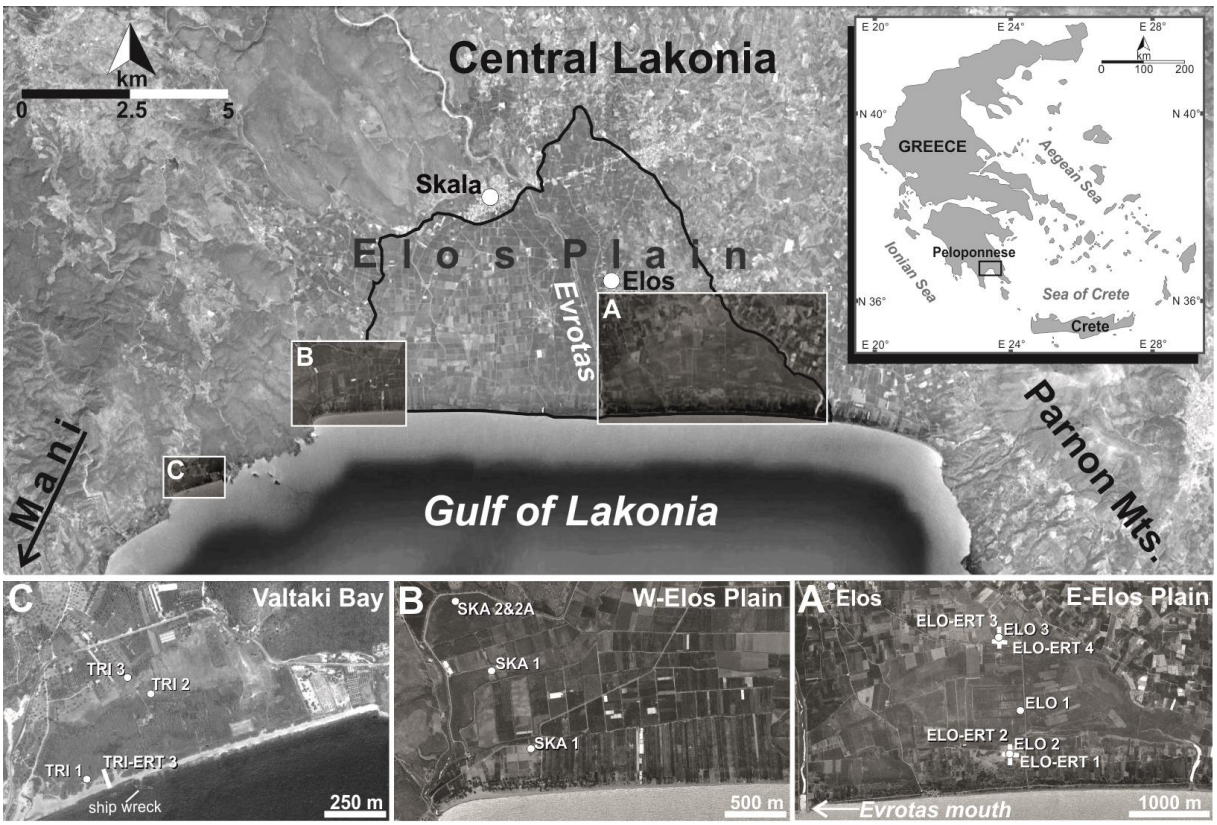

Figure 16: Overview of central Lakonia with the Evrotas River delta and its surroundings. The study area in the eastern Evrotas River delta is situated in the vicinity of the village Elos (A). The study area in the western Evrotas River delta is located close to the village of Skala (B). The study area of Trinisia is to be found in back-beach position of the small Vatika Bay in the northwestern part of the Lakonian Gulf close to the three islands of Trinisia (C) (source: own illustration 2013, maps based on Google Earth images/data, access May 2013).

Within the Evrotas River delta and its surroundings three selected areas were investigated in search of tsunami-fingerprints within the sedimentological record. Framed by the Taygetos Mountains in the west and the Parnon Mountains in the east, the Elos plain is located in the central part of the Lakonian graben structure, where the 82 km long Evrotas River discharges into the sea. The river is following a NNW to SSE trending tectonic depression (POPE et al. 2003). With a watershed of about 1.700 km^2 (KARAGIOZI et al. 2011), the River Evrotas represents one of the main fluvial systems of the Peloponnese. The karstic spring of the Evrotas River is situated south of Skortsinos in Arkadia. On the fertile riverbanks, in the middle part of the Evrotas River within the Sparta basin, ancient Sparta was founded. The basin itself is shaped by the ~64 km long Sparta Fault system that is bounded to the eastern flank of the Taygetos mountains front (2407 m) and the activation of which in 464 BC caused an earthquake devastating ancient Sparta (PAPANIKOLAOU et al. 2013). Modern seismic hazard mapping suggests that a similar destructive event may hit the town every 1792 ± 458 years; since no mayor event has so far been generated by the Sparta Fault system since 464 BC, it is highly probable that the area will experience a strong seismic shock in the near future (PAPANIKOLAOU et al. 2013).

During the Trojan War it was considered, that "Elos, the Castle by the Sea" (HOMER, Iliad) was a tributary to Sparta and Mycenae (KRAFT et al. 1997). In Greek the word Elos means swamp. Interestingly, the Greek word for malaria, *elonosia*, stems from the same word (*elos + nosos*, thus the disease from the marsh) (KOUSOULIS et al. 2013). And according to historical sources, malaria spread apparently in Greece around the 5th century BC (KOUSOULIS et al. 2013).

In former times, the Evrotas River delta was much reduced in size (KRAFT 1972 and KRAFT et al. 1977), and the Lakonian Gulf extended farther north. Toward the present, delta progradation caused a seaward shifting of the shoreline and led to the development of a floodplain up to the recent shoreline (KRAFT et al. 1977). Nowadays, the plain is limited by an almost linear c. 15 km long dune spit, bordering the Lakonian Gulf to the north (KELLETAT & GRASSERT 1975). The width of the dune spit, anthropogenically strongly modified, varies between several tens and hundreds of meters. Recently the plain is widely drained so that the light grey sediments (KELLETAT 1974) are cultivated intensively (e.g. oranges and other citrus fruits, vegetables, olives as well as cotton). Satellite images document that the plain is widely crossed by drainage channels and the Evrotas River is canalized and regulated in wide parts. After IGME (1989) the Evrotas River delta is framed by Pliocene formations (marine, coastal and lacustrine sediments) towards the east and northeast, whereas the western and northwestern sections are characterized by alternating units of the Tripolis zone, containing Jurassic limestones and Triasssic dolomites, as well as the Permian Tyros beds. From a geomorphological point of view, several screes and talus cones are detectable, rising from the mountain flanks into the plain (IGME 1989).

Along a south-north trending transect, between the small village of Asteri and the coast, three vibracorings (ELO 1, 2 and 3) were drilled and four earth resistivity tomography transects (ERT) were conducted in the eastern Evrotas River delta (Fig. 16, A). Vibracoring ELO 1 was carried out in a swampy environment on top of a man-made infill, about 1.5 m thick and 1 km distant from the present coastline. On half distance between vibracoring site ELO 1 and the coast, vibracoring ELO 2 was drilled at the northern extension of the dune spit. By regarding satellite images, this section of the dune spit seems to expand further northwards in contrast to the narrower areas in the east and west. From a geomorphological point of view, the shape resembles more a washover fan rather than a linear dune spit. Vibracoring site ELO 3 is located about 2 km inland. In the central part of the plain, approximately 2.5 km northwestwards from the vibracoring transect, the modern village of Elos is situated. For the village of Elos, KRAFT et al. (1977) detected subsurface floodplain conditions to the north and marine conditions to the south, thus indicating the above mentioned seaward shifting of the shoreline.

In the western Evrotas River delta, vibracores SKA 1, 2, 2A and 3 were drilled (Fig. 16, B). Vibracoring site SKA 3 is located some 350 m distant from the sea at the northern extensions of the complex

beach ridge and dune system. Vibracore SKA 1 was drilled some 800 m distant from the coast in the midst of a marsh-type area covered with *Juncus* sp. Vibracoring site SKA 2 (and parallel core SKA 2A) lies in the northernmost part of the alluvial plain close to the mountain foothills, some 1.7 km inland.
The study area of Valtaki with its ridge out of beach and dune sand, its adjacent back-beach marsh and alluvial plain (IGME 1989, CUNDY et al. 2006) is located close to the Trinisa island group (Fig. 16, C). Valtaki Bay lies about 4 km to the southwest of the Evrotas River delta and about 5 km to the northeast of the city of Gythion, known to be an important harbor of Sparta during Classical and Hellenistic times. In general, the relief is dominated by a series of NW-SE trending and NE dipping normal faults, creating several promontories as well as low-lying and barrier protected indentations (KELLETAT & GASSERT 1975, CUNDY et al. 2006). To the west, Valtaki Bay is framed by platy limestones of Upper Cretaceous to Eocene age, by volcanosedimentary series of the Tyros Beds, as well as by a small zone of Pliocene marine sediments. The eastern flank is built out of Triassic dolomite series and by Pliocene marine sediments (IGME 1989). Beachrock is present in the subtidal beach face. Late Roman - Early Byzantine wall remains, partly submerged, can be followed from the beach into the dune. KELLETAT & GASSERT (1976) refer to that the buildings must have been founded when the sea-level was lower, thus indicating a local sea-level rise (similar to the situations of the submerged sites of Pavlopetri and Plitra in southeastern Lakonia). The beach scenery is characterized by the ship wreck of Aghios Dimitrios, stranded on beachrock formations. Several decades before, the ship was badly anchored in Gythion, thus swept away by the sea current and brought to its present position.
In order to check coastal stratigraphies for extreme wave event deposits, three vibracores (TRI 1, 2 and 3) were retrieved from the marshy back-beach area of Valtaki Bay. Vibracore TRI 1 was drilled directly behind the beach ridge in the marsh, some 60 m distant to the sea. Vibracore TIR 2 was drilled in the transition zone between the marsh and the adjacent cultivated area some 300 m inland. Vibracoring site TRI 3 lies some tens of meters to the north of site TIR 2 in the midst of an olive grove.

3.6 Limnothalassa Moustou, Asinis Beach & Argive Plain (Gulf of Argolis)

From a geographical point of view, the Gulf of Argolis is situated off the east coast of the Peloponnese, opening into the Aegean Sea (MITROPOULOS & ZANANIRI 2010). The Argolis Gulf and the Argive Plain represent a 75 km long and 30 km wide fault-bounded tectonic depression of Plio-Pleistocene age, exhibiting an elongated shape of NW-SE direction with a maximum water depth of 800 m (GAKI-PAPANASTASSIOU 2010). The gulf is characterized by a regular seafloor morphology featuring an amphitheatric pattern (MITROPOULOS & ZANANIRI 2010). The linear NNW-SSE trending western flank of the gulf represents the marginal eastern foothills of the Parnon mountain chain. The

shelf zone is extremely narrow and only a few tens or hundred meters wide (GAKI-PAPANASTASSIOU et al. 2010). On the opposite side, the Argolis Peninsula forms an outcrop of the southern prolongation of the Pelagonian zone of the internal Hellenides (SENOWBARI-DARYAN et al. 1996, see also JACOBSHAGEN et al. 1976, BACHMANN & RISCH 1979, VRIELYNCK 1981/82, ROBERTSON et al. 1991). The greatest part of the peninsula is covered by the Pantokrator facies, part of the Upper Triassic – Lower Jurassic carbonate series (POMONI-PAPAIOANNOU 2008). In contrast, the morphology of the eastern side of the bay shows a broader shelf.

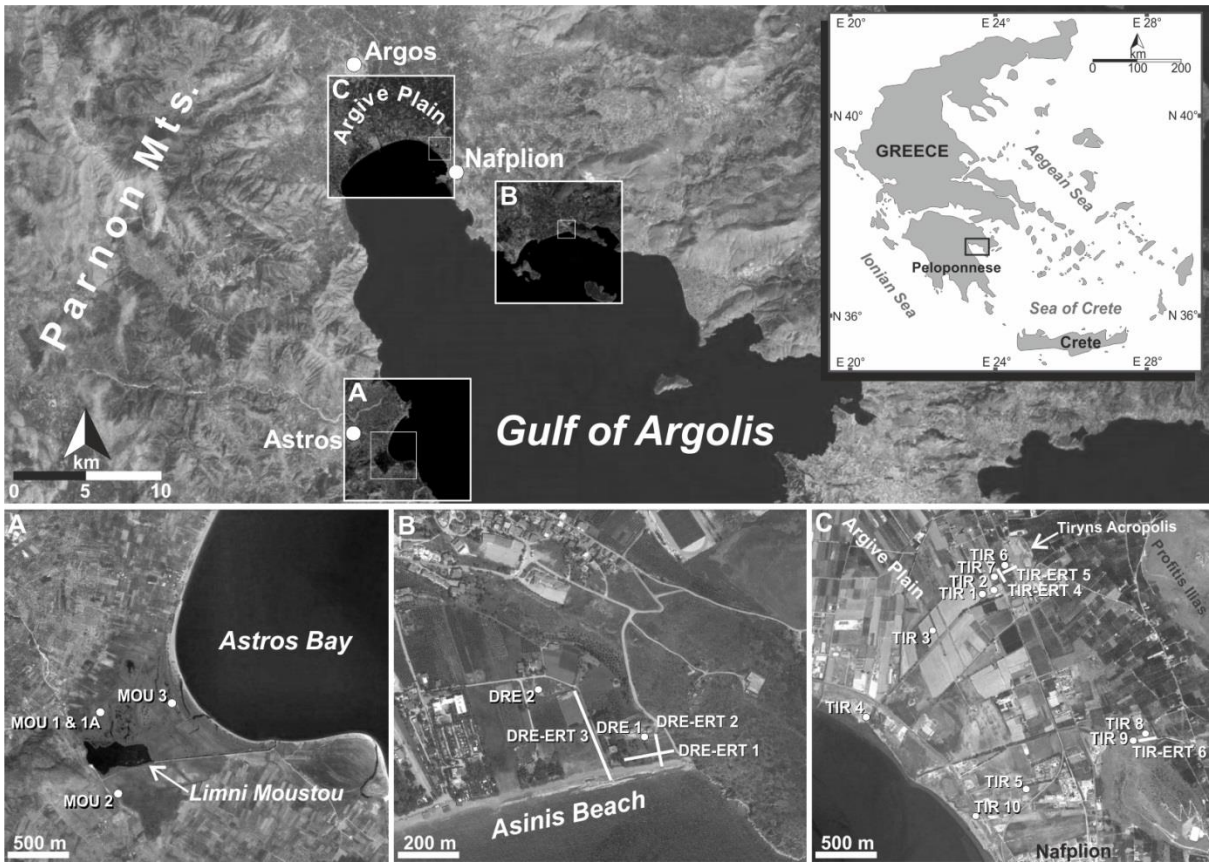

Figure 17: Overview of the Golf of Argolis and the three study areas (of Limnothalassa Moustou, Argive Plain and Asinis Beach. Limnothalassa Moustou (A) is situated in the outer western part of the gulf, at the Parnon Mountain foothills in the southern part of Astros Bay. Further study areas are the Bay of Drepano at Asinis Beach (B), as well as the Argive Plain close to ancient Tiryns and modern Nafplion (C) in the inner Gulf of Argolis (source: own illustration, maps based on Bing and Google Earth images/data, access May 2013).

Hence, the lobed coastline is characterized by several embayment's of different size and shape with sandy beaches, by steep promontories, capes and cliffs, as well as by a couple of small islands close to the mainland. In its northern central part, in between the Parnon Mountain foothills and the Argolis Peninsula, the gulf finds its continental continuation in the fertile Argive Plain. The plain itself has been developed by rivers, draining the surrounding ranges, and their progradation resulted in the evolution of a wide shelf (3-5 km) (PAPANIKOLAOU et al. 1988). Important prehistoric and Mycenaean settlements such as Argos and Tiryns, the latter well known for its cyclopean walls, are situated within this alluvial plain. The seasonal Inachos River is flowing through the plain, discharging in its

central part into the Argolis Gulf. KRAFT et al. (1977) suggest that during Early to Middle Helladic times the shoreline was much closer to the lower town of Tiryns and its fortification, nowadays situated in about 1.5 km distance to the present coastline. Due to regression dynamics, the formerly infertile swampy land of Argos had become arable at the time of Aristotle's (384 – 322 BC) (KRAFT et al. 1977). Furthermore, KRAFT et al. (1977) point on the influence of the Helladic people in altering the landscape, e.g. by the anthropogenic interference with the fluvial system in the form of dams, channels and stream bypasses.

The Argive Plain itself was built due to Holocene delta progradation and sedimentation processes of the Inachos River and smaller local creeks causing also local regression processes as well as the formation of a 3-5 km wide shelf (KRAFT et al. 1977, ZANGGER 1993, GAKI-PAPANASTASSIOU et al. 2010). On the basis of subsurface stratigraphy data ZANGGER (1993) reconstructed the late Pleistocene and Holocene evolution of the Argive Plain.

BY historical accounts, it is well known that the area experienced tsunami events (e.g. April 22nd, 1928 Aegean Sea, see: SOLOVIEV et al. (2000), p. 140: Tsunamis in the Mediterranean Sea – 2000 B.C.-2000 A.D.).

Figure 18: Configuration of the coast in the eastern part of the Argive Plain between Nafplion and the village of Nea Kios. The coast of the plains eastern part, eastward from the Inachos embouchure at Nea Kios, is mainly dominated by sandy beach with marshy characteristics (source: own photos taken in March 2010).

In the eastern part of the Argive Plain, close to modern Nafplion and ancient Tiryns, 10 vibracores (TIR 1 – TIR 10) were drilled (Fig. 17, C). These drillings were arranged in two transects starting at the present coastline heading towards inland. Being the starting point of the first vibracoring transect, vibracoring site TIR 4 is located about 3 km to the northwest of Nafplion at the coast. Vibracoring site TIR 3 is located within an agricultural area approximately 850 m distant to the present shoreline. Vibracores TIR 1 and TIR 2 were drilled about 500 m and 650 m, further to the northeast, respectively. Vibracoring sites TIR 6 and TIR 7 lie on private property in the midst of an orange plant some 1.6 km distant from the sea and close to the walls of ancient Tiryns.

The second vibracoring transect starts with vibracoring site TIR 10, located at the coast close to the city of Nafplion. Vibracore TIR 5 was drilled some 500 m further inland; vibracoring sites TIR 8 and TIR 9 are located some 1.65 km distant from the coast.

Figure 19: Configuration of the coast in the western part of the Argive Plain between the villages of Nea Kios and Mili. The coast of the plains western part, westward from the Inachos embouchure at Nea Kios, is mainly dominated by gravels. The photos were taken in March 2010 by calm weather after several rainy and stormy days (source: own photos taken in March 2010).

The Argive Plain finds its continuation in southeastern direction, reaching the Argolis Gulf on its eastern flank at Paralia Asinis, opposite to the Island of Plateia (FINKE 1988: Fig. 9, see also VAN ANDEL et al. 1990: Fig. 4). The study site at Asinis Beach is located to the east of the town of Tolo in the Bay of Drepano (Fig. 17, B). The beach itself is separated from the Bay of Tolo only by the small promontory of Cape Kastraki. To the west the beach is limited by an appendix-like rocky structure out of Upper Triassic – Lias and Dogger carbonate deposits (IGSR 1970d). This peninsula is bonded to the mainland only at its western part, at Drepano village. To the east and north the peninsula is separated from the mainland by a narrow branch of the Argolis Gulf, the Bay of Vivari. The bay is finding its continuation eastwards in a lagoon. The sediments at Asinis Beach are mainly dominated by gravel and coarse sand. Further, significant beachrock complexes are attending the coastline. Vibracoring site DRE 1 lies some hundred meters south of Drepano close to the beach face. Vibracore DRE 2 was drilled ca. 250 m distant from the coastline.

About 20 km southwards from the central Argive Plain, the study area of Limnothalassa Moustou (*Limnothalassa/Λιμνοθάλασσα* = Greek for lagoon) is situated on the western flank of the Gulf of Argolis within a low lying coastal plain at the foothills of the Parnon Mountains (Fig. 17, A). From a geomorphological point of view, Limnothalassa Moustou is lying in between two river deltas forming the recent coastal plain. To the north, Tanos Potamos (*Potamos/Ποταμός* = Greek for river), has formed a delta, ca. 3 km wide. In the south Rema Vrasiatis (*Rema/Ρέμα* = Greek for creek) flows into the Aegean Sea next to the small harbor of Aghiou Andreas. After IGSR (1970b, 1970c), the low-lying coastal plain around Limnothalassa Moustou is made out of recent coastal and alluvial deposits.
From the northern and western foothills, made out of Upper Cretaceous limestones, several recent and older talus cones of debris are running into the plain (IGSR 1970b). Aerial photos further indicate that a torrential creek has formed a fan-delta to the south of Astros close to Limnothalassa Moustou.

The village of Astros itself is built on a small isolated rocky hill out of Upper Cretaceous limestones, surrounded by alluvial deposits (IGSR 1970b). To the south, in between the village of Aghiou Andreas and the correspondent harbour, the plain is limited by Middle – Lower Jurassic limestones and dolomites (IGSR 1970c). In the south, Rema Vrasiatis marks the transition between the plain and the mountain foothills which are built out of Middle – Lower Jurassic limestones and dolomites (IGSR 1970c).

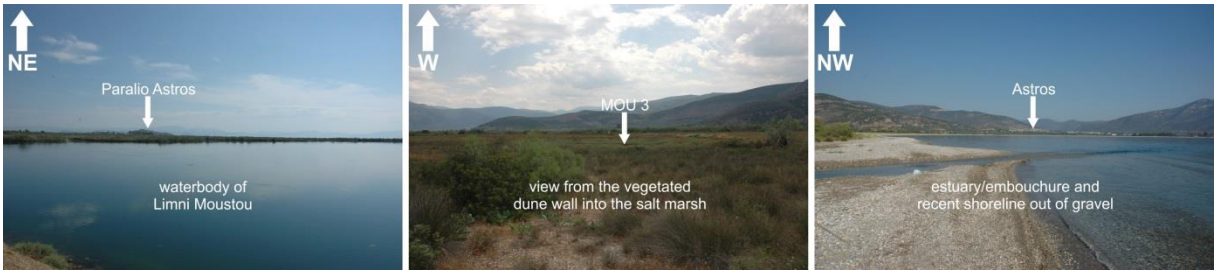

Figure 20: Physical setting of the study area Limnothalassa Moustou. The left photo shows the relatively small water body of the wetland area. The middle photo depicts the southernmost vibracoring site MOU 3 situated behind the recent dune wall and about 200 m inland. The right photo illustrates the recent coastline configuration at a small embouchure. It is visible that the coast is dominated by coarse material, in this case gravel and coarse sand (source: own photos taken in March 2010).

Limnothalassa Moustou is a NATURA 2000 site (site code: GR2520003). 43.5 % of the area is covered by salt marshes and the total inland water body amounts only 1.6 % (see NATURA 2000). The maximum water depth reaches 5 m and its salt content varies between 11 to 15 % (after PARNONAS.org). The beach barrier, protecting the lagoon from the open Aegean Sea, is mainly made out of gravel and coarse sand (Fig. 20).

Vibracore MOU 1, and parallel core MOU 1A, were drilled in the northern part of the study area on dry salt marsh some 800 m distant from the coastline and some 350 m away from the lagoonal shore. Vibracoring site MOU 3 was drilled within a system of former beach ridges some 200 m distant from the present shoreline. Vibracoring site MOU 2 is located on the opposite side of the lagoon at the foot of the Parnon spurs.

Chapter 4 – Methods

The multidisciplinary approach applied in this study comprised several fieldwork and laboratory methods. Therefore, at first the used fieldwork methods are presented and afterwards the methods in laboratory.

4.1 Fieldwork methods

Vibracorings

Sedimentological and geomorphological studies in Lakonia and the Argolis (Peloponnese – Greece) were carried out in March and June 2010. Altogether 33 vibracores were drilled at selected locations by means of an Atlas Copco mk1 corer using core diameters of 6 and 5 centimeters. At specific locations parallel cores were retrieved as a whole within inliners for the purpose of detailed laboratory studies. The encountered sediment cores were cleaned, photographed and documented for sedimentological and pedological criteria (e.g. sediment color, grain size distribution, grain rounding, texture, carbonate content and other features as recommended by Ad-hoc ARBEITSGRUPPE BODEN (2005)). Afterwards the sediment cores were sampled for continuative geochemical analyses in the laboratory. Sample intervals were chosen inconsistently depending on relevant changes in the stratigraphic record.

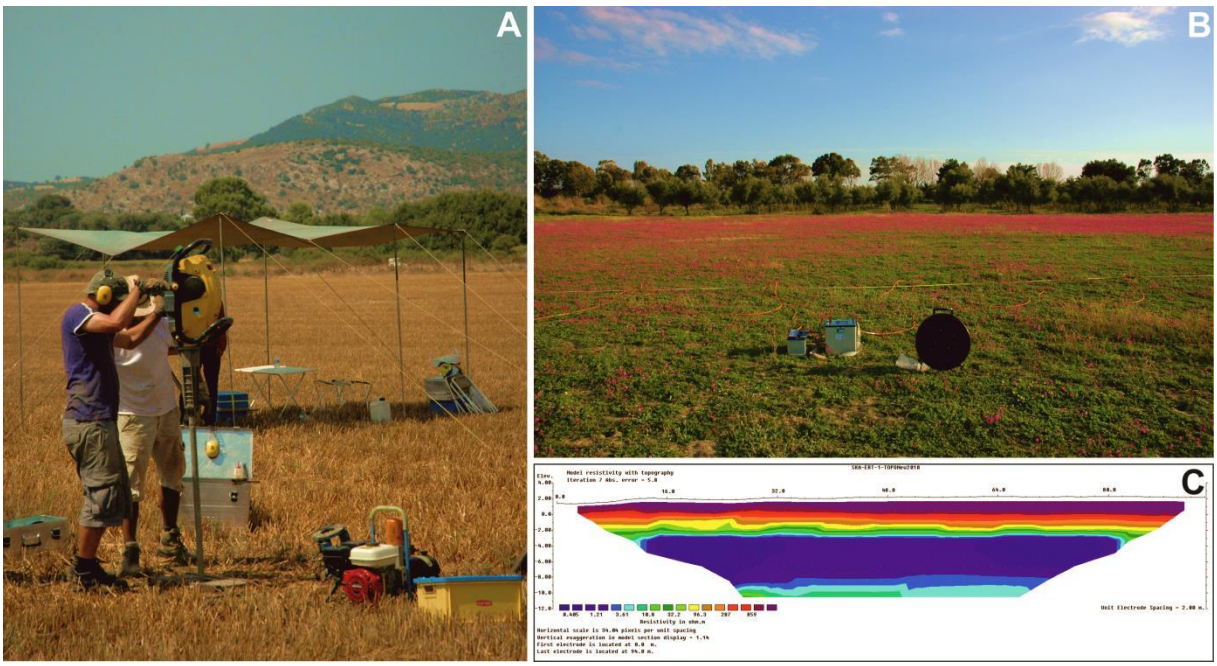

Figure 21: Fieldwork methods used within this study. Photo A shows the manually drilling with an engine driven Atlas Copco mk1 corer in the coastal plain of Palairos-Pogonia (Akarnania – Greece) (source: photo taken by A. Vött in September 2008). And picture B illustrates exemplarily an ERT-measurement configuration applied in the eastern part of the Elos Plain (Lakonia – Greece) (source: own photo taken in March 2010). The outcome of the ERT-measurement is presented in picture

C in the form of a calculated inverse resistivity model. Thereby, the different colors represent subsurface zones with different resistivity values, possibly referring to facies changes.

Earth resistivity tomography

In addition to the drilled vibracoring transects, earth resistivity tomography measurements (ERT) were carried out in order to study subsurface stratigraphy's and to detect the depth of the local bedrock by using a multi-electrode geoelectrical instrument (IRIS Instruments, type Syscal R1+ Switch 48). With regard to geoscientific and geoarchaeological questions, such geophysical methods can help to provide meaningful results (PERRONE et al. 2004, KNEISEL 2003, 2006, JORDAN 2009, GAFFNEY & GARTNER 2011, VÖTT et al. 2011a). To gain high vertical as well as high horizontal resolutions a Wenner-Schlumberger array was applied (KNEISEL 2006). Relative to these geophysical measurements it is important to mind, that several parameters have an influence on the electrical conductivity of the measured subsurface material. Hence, the chemical composition as well as the mineral configuration and structure but also void space, interstitial water and permeability, temperature, the materials age as well as the ion content influence the electrical conductivity of the measured subsurface material (BERCKHEIMER 1997, GREINWALD & THIERBACH 1997, REYNOLDS 1997, KEAREY et al. 2006, SCHROTT & SASS 2008, FAZZITO et al. 2009). Therefore, the mentioned factors have to be considered when interpreting geophysical data. To better construe ERT data it is necessary to combine the method with other geoscientific methods (HECHT 2007). In this case the ERT data was calibrated by sediment cores encountered parallel to or on an ERT transect. Data processing was carried out by means of the RES2Dinv software, adopting the least-square inversions by a quasi-Newton method (LOKE & BAKER 1996, LOKE & DAHLIN 2002, LOKE et al. 2003).

DGPS measurements

To determine precise elevation data and the exact geographical position, vibracoring sites and ERT transects were measured by means of a high resolution differential GPS, using a Topcon HiPer Pro FC-200 instrument with a vertical and horizontal accuracy of ± 2 cm.

4.2 Laboratory methods

Sedimentological laboratory methods

Laboratory studies comprised the analysis of the organic and calcium carbonate content as well as the measurement of electrical conductivity.

The electrical conductivity represents an indicator for the content of all dissolved and dissociated compounds within a soil suspension. A sediments electrical conductivity can thus be a supportive parameter to better understand and interpret the facies distribution. The electrical conductivity of

the samples (1:5 soil:water suspension) were determined by using an EC meter (electrical conductivity meter) whose sensor consists of two metal electrodes. The physical unit is specified by milli Siemens (mS) respectively micro Siemens (µS) (SCHLICHTING et al. 1995). High values of the electric conductivity mostly point to marine environments or eutrophic peat layers and due to their extensive offer on exchangeable ions also clayey sediments come along with increased values (MÜLLENHOFF 2005, BARSCH et al. 2000).

Organic content was determined by loss on ignition (LOI), at which the samples were oven-dried at 105 °C for 12 hours and ignited at 550 °C for 4 hours in a muffle furnace (BECK et al. 1995). By defining the organic matter with the combustion loss determination method, conclusions can be drawn about the sedimentary environment because organic matter is preferably deposited in still water environments such as lagoons, lakes or back waters (MÜLLENHOFF 2005).

The content of calcium carbonate was detected after the specifications of the Scheibler-method based on DIN ISO 10693 (SCHLICHTING et al. 1995, BARSCH et al. 2000, BLUME et al. 2011).

In order to better characterize the sedimentary units and to better report on the geomorphodynamic depositional mechanisms grain size distributions (in %) were conducted for samples out of selected vibracores by the method after KÖHN (1928). Based on these data grain size ratios were calculated (ratio of sand in relation to the sum of clay and silt). Thereby, a low ratio refers to quiescent low-energetic conditions relating to the deposition of fine grain size fractions such as clay and silt whereas a high ratio testifies a higher-energetic potential of the associated geomorphodynamic process.

XRF-measurements

Different sedimentary facies feature characteristic geochemical profiles due to different environmental factors that relate to specific chemical components (HADLER 2014). Sediment samples were thus scanned for their total contents of Ca, Fe, Ti, K and 25 other elements, using a field portable, handheld Thermo instrument X-ray fluorescence spectrometer (XRF), type Niton XL3t 900s GOLDD. By utilizing calibration mode SOIL, every sample was measured once for 30 sec. through three different filters what resulted in mean relative concentrations per measured elements (THERMO FISHER SCIENTIFIC 2010). To standardize and to eliminate potential influences, such as moisture content or grain size, primarily calculated elemental rations were employed for data interpretation (VÖTT et al. 2011c).

Photospectrometric measurements

For the detection of changes and boundaries within the geological record, color values can be supportive. Therefore, exact color features and brightness values of air-dried sediment samples were

calculated by means of a Konica-Minolta Spectrophotometer (CM-600D), equipped with a fixed aperture setting of 8 mm. Within this colorimeter a silicon photodiode array detector and a light source of a pulsed xenon lamp with an UV cut filter are installed. In combination with the SpectraMagic NX software data evaluation was carried out simultaneously to the measurement procedure. Calibration was accomplished after 10 measurements by measuring a black and white standard plate. In this study, the SCI-method (Specular Component Included-method) was applied. This type of color evaluation measures the materials total appearance independent of the surface conditions (KONICA MINOLTA SENSING, INC. 2003).

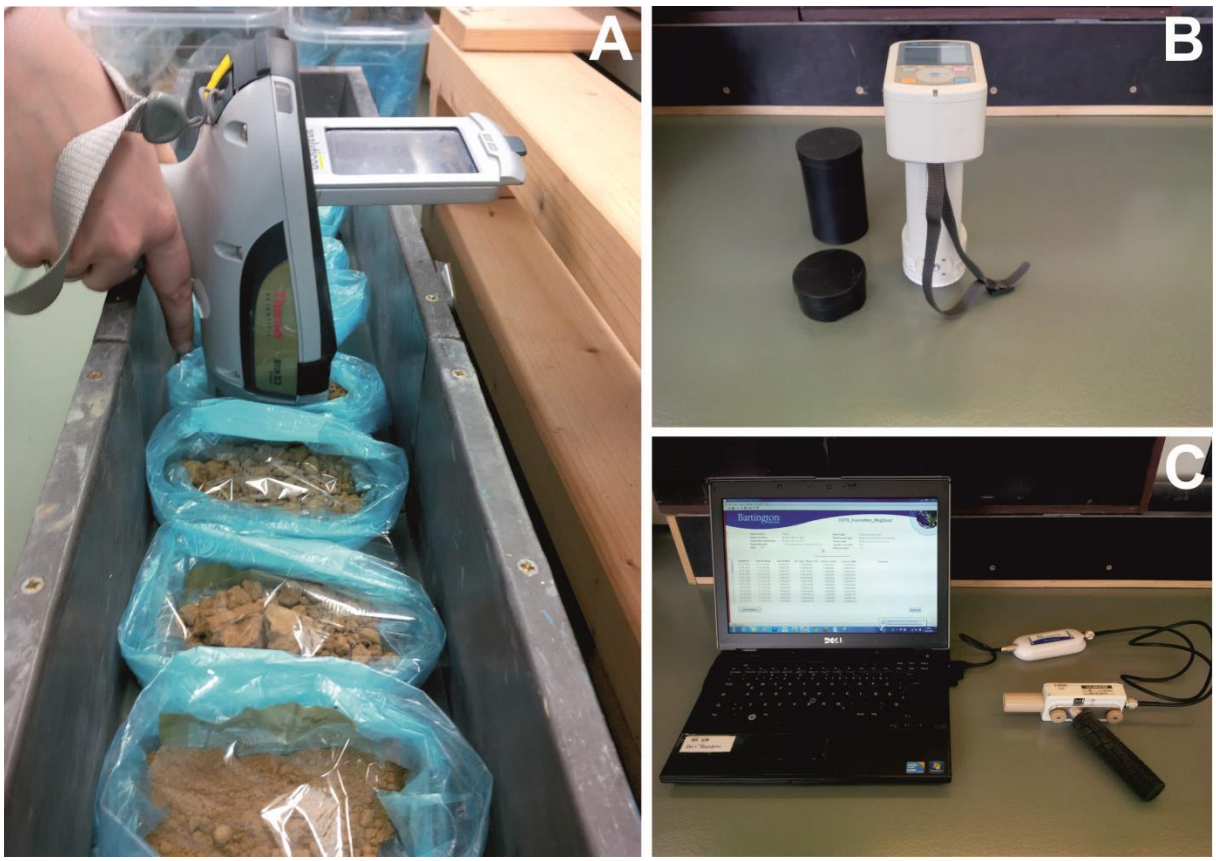

Figure 22: Photo A shows the measurement of air-dried sediment samples (placed in a lead box) with the handheld X-ray fluorescence spectrometer (type Niton XL3t 900s GOLDD). On photo B the Konica-Minolta Spectrophotometer (CM-600D) with the two reference samples for calibration purposes (black and white standard plates) are pictured. And photo C illustrates the Bartington MS2K device for the purpose of measuring the magnetic susceptibility of air-dried sediment samples (source: own photos taken in May 2014).

Magnetic susceptibility

Furthermore, magnetic susceptibility of air-dried samples was measured using the Bartington MS2K device (24.5 mm response area, 8 mm response depth), in order to better understand environmental fingerprints and to identify formation and transport processes within the geological record (DEARING 1999). The magnetic susceptibility, a dimensionless factor, specifies how magnetisable a material is. Detailed descriptions about the method and features of different magnetisable materials can be found e.g. in THOMPSON & OLDFIELD 1986, DEARING 1999 and EVANS & HELLER 2003. Each sample was

measured for 1 sec. and after 10 measurements a calibration was applied as well as the measurement of a standard sample in order to control deviations. The dimensionless values are expressed in whole numbers without units (MATHES-SCHMIDT 2013).

Microfaunal analyses

For facies determination and to confirm the origin of distinct sedimentary units macro- and microfaunal investigations were carried out on 157 samples out of 11 selected vibracores. For dispersion the sample material (c. 10 cm^3) was preprocessed with H_2O_2 (30%) and afterwards wet sieved to segregate the fractions of < 400 µm, 200-400 µm, 125-200 µm and < 125 µm. Finally, the separated grain fractions were put into glass cylinders, which were filled with ethanol for conservation. For their content of foraminifera, ostracods, bivalves and gastropods the samples were first regarded under a Nikon SMZ-74St stereoscope (binocular) using a 10x - 40x magnification. Detected specimens were isolated, selected and finally put into Krantz-cells for documentation.

Figure 23: The left bigger photo shows the Nikon SMZ-74St stereoscope (binocular) combined with the NIS Elements software (Basic Research) for the purpose of detailed microfaunal analyses. The smaller pictures in the middle and right show exemplarily species of foraminifers, ostracods and gastropods that were detected in sediment samples and that were photographed with the high resolution DS-Fi2 Nikon camera mounted on the stereoscope (source: own photos and data 2013).

Afterwards the found specimen and/or specimen assemblages were photographed under polarized light using a high resolution DS-Fi2 Nikon camera in combination with the NIS Elements software (Basic Research). To photograph macrofossils > 400 µm the camera was mounted on the stereoscope, with varying magnifications between 10 to 40 times. The 200-400 µm-fractions and 125-200 µm-fractions were inspected in detail with an Eclipse 50-POL polarization microscope. These fractions were photographed with the same camera mentioned above. To cope with the depth of focus problem 10 to 50 pictures of one sample were taken, everyone with another depth of focus ranging between 1-100 µm. Finally, all pictures were framed to one sharp and clear image by means

of the software. Fractions < 125 µm were not investigated. Accordingly, a total of 471 samples (Σ = 157 individual samples from 11 cores x 3 fractions) were investigated for that purpose.
The microfossil content was recorded semi-quantitatively using a scale from 0 to 6 [0 = none; 1 = very rare/singular (1 sp.); 2 = rare (2-3 spp.); 3 = few (up to 6 spp.); 4 = fairly many (up to 9 spp.); 5 = many (up to 12 spp.); 6 = a great many (more than 12 spp.)]. Species identification was carried out using special literature (see particular chapters).

Dating approach

Besides the identification of tsunami and palaeotsunami deposits the dating of such sediments is a vital element in understanding the late-Holocene tsunami hazard and risk (DOMINEY-HOWES et al. 2006). Thus, where possible, organic material and mollusc remains were taken out of distinctive areas within the sediment cores to obtain geochronological information by the ^{14}C-AMS technique. ^{14}C-AMS analyses were kindly conducted by Dr. M. Hüls (Leibniz Labor für Altersbestimmung und Isotopenforschung – Christian-Albrechts-Universität Kiel, Germany), Dr. Tom Rockwell (KECK CARBON CYCLE AMS FACILITY – Department of Earth System Science, University of California, Irvine, USA) and Beta Analytic Radiocarbon Dating Laboratory Miami (USA). Calibration of radiocarbon ages into calendar ages was carried out using the CALIB 6.0 software and the Intcal09 dataset of REIMER et al. (2009). ^{14}C-AMS ages of marine material were corrected for a marine reservoir effect for the eastern Mediterranean of ~408 years (REIMER & MCCORMAC 2002, REIMER et al. 2009). Marine calibration was also used for plant remains which were identified as sea grass when δ^{13}C-values were determined to 15 ‰ ± 3 ‰ (see e.g. WALKER 2005). Thereby, it was possible to successfully date 24 samples in order to better understand the chronological evolution of the investigated areas. Where possible, in this study the sampled material was chosen after the so called “sandwich dating approach” (see e.g. VÖTT et al. 2009b. 2012). Thereafter, autochthonous organic material or mollusc shells right above or below the layer of interest were chosen and dated. Preferably land plant remains were chosen to avoid marine reservoir effects. Moreover, radiocarbon ages derived from autochthonous C_3 land plants deliver the most promising and reliable results. By using that dating strategy the derived ages from samples out of allochthonous high-energy deposits yield only maximum ages for the event (*termini ad* or *post quos*) due to reworking effects that cannot be excluded. Whereas, the material out of post-event sedimentary units represent *termini ante quos* for the suggested event.

Chapter 5 – Results from southeast Lakonia

Abstract: Historical accounts indicate that the coasts of the Lakonian Gulf (southeastern Peloponnese) have been repeatedly affected by tsunamis during historical times. However, for southeastern Lakonia only few data have been published which give information on palaeo-tsunami imprints in the region dealing with sedimentary and geomorphological features in near-coast environments.
The small number of publications is certainly related to the fact that promising geological archives do not exist in the study area. In search of palaeotsunami traces we focused on different geo-archives along the southeastern coast of the Peloponnese.
On the basis of sedimentological, geomorphological, geophysical, geochemical and microfaunal investigations we detected different sediment layers related to high-energy event deposits. By presented analyses it was possible to prove repeated tsunamigenic inundation in the study area. Based on analogical conclusions and radiocarbon dating one of the detected events most likely correlates to the well-known 365 AD tsunami and another younger event must have affected the coasts of southeastern Lakonia in the Early Modern Age.

5.1 Palaeotsunami record in near-coast sedimentary archives of the Bays of Vatika and Boza

The Lakonian Gulf is directly exposed to the Hellenic Trench and thus characterized by an extremely high seismicity and tsunami hazard (PAPAZACHOS & DIMITRIU 1991). Strong earthquakes along this subduction zone are often accompanied by high vertical displacements of the ocean floor (SCHIELEIN et al. 2007). During historical times, the southern Peloponnese was repeatedly affected by strong earthquakes such as in 365 AD, 1303 AD, 1750 AD, 1789/1795 AD, 1842 AD, 1866 AD, 1867 AD, 1927 AD and 1944 AD (SOLOVIEV et al. 2000, AMBRASEYS & SYNOLAKIS 2010, PAPADOPOULOS et al. 2013). Associated to the earthquakes in 365 AD, 1303 AD (PAPADOPOULOS et al. 2013, PAPADOPOULOS & PAPAGEORGIOU 2014) as well as in 1866 AD and 1867 AD tsunamis were observed (PAPAZACHOS & PAPAZACHOU 1997). PARARAS-CARAYANNIS (2011) for instance reports that large parts of Alexandria (Egypt) were repeatedly destroyed by earthquakes and associated tsunamis. These events are correlated to the 365 AD earthquake on Crete and the 1303 AD earthquake generated in the area south of Rhodes Island (DEGG 1990, SHAW et al. 2008). The 1303 AD event has been one of the most devastating historical events within the Mediterranean which propagated through an extensive part of the eastern Mediterranean Sea causing abrupt changes of the coastline configuration (VÖTT et al. 2006, SCHEFFERS et al. 2008) as well as damages and fatalities in Heraklion (northern Crete), Acre (Israel) and Alexandria (Egypt) (AMBRASEYS 2009, PAPADOPOULOS 2011, PAPADOPOULOS & PAPAGEORGIOU 2014). In addition to the 365 AD and 1303 AD events, the region around the Hellenic Trench experienced at least 13 further tsunami-generating earthquakes reaching Magnitudes of 7.0 (*Ms*) and partly higher during the last 2 ka (SCHIELEIN et al. 2007).

*A paper based on this chapter will be submitted for publication in the international journal *Zeitschrift für Geomorphologie N.F., Supplementary Issues* (authors: Konstantin Ntageretzis, Andreas Vött, Peter Fischer, Hanna Hadler, Kurt Emde, Björn Roman Röbke, Timo Willershäuser).

In this context DOMINEY-HOWES (2002) points to a high tsunami hazard especially for the southeastern part of Lakonia where sedimentological and geomorphological traces of these extreme events in near-coast environments are to be expected.

SCHEFFERS et al. (2008) found sedimentological and geomorphological evidence of tsunami impact in the Bay of Viglafia (southeastern Lakonia) in the form of allochthonous sand layers in a near-coast mud environment, dislocated and partly imbricated boulders as well as washover fans. Dislocated boulders in southern Lakonia indicating extreme wave activity were also mapped by FEDERICI et al. (2002) and FEDERICI & RODOLFI (2008).

However, promising near-coast geological archives yielding thick Holocene sedimentary sequences are rare in southern Lakonia, because the bedrock is widely striking out close to the surface so that the accommodation space for Holocene deposits is extremely small. Thus, in search of palaeotsunami traces we focused on available archives near the remains of a submerged Mycenaean town called Pavlopetri and two small valleys near Neapolis and Cape Xili, respectively.

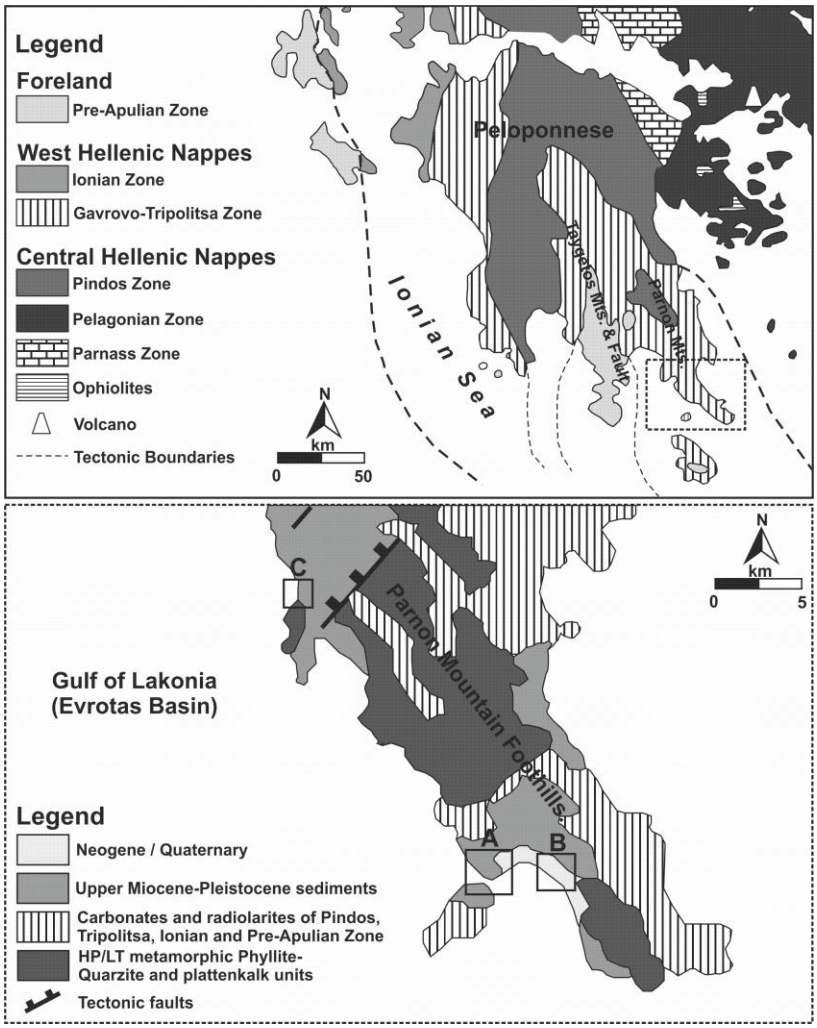

Figure 24: 0verview of the geological constellation of the Peloponnese (upper big map) and the simplified geological constellation of the study region in southeastern Lakonia (lower detail map). The three studied regions are marked by boxes A: Viglafia Lagoon, B: the Vatika dry valley and C: the Boza dry valley (source: own illustration based on data from BORNOVAS & RONDOGIANNI-TSIAMBAOU 1983, JACOBSHAGEN 1986 and TOUGIANNIDIS 2009).

5.2 Regional setting

The Lakonian Gulf is exposed to the Hellenic Arc and forms a huge asymmetric graben between the Parnon Mountains (1935 m above present sea level (m a.s.l.)) in the east and the mountains of the Taygetos (2407 m a.s.l.) in the west (FEDERICI et al. 2002, CUNDY et al. 2006). The most conspicuous feature of the graben, the huge Taygetos fault, is located in the central part of the Lakonian Gulf while distinctive normal faults are located between the city of Gythio and Cape Menaro in the west and between Cape Xili and Elafonisos Island in the east (FEDERICI et al. 2002).

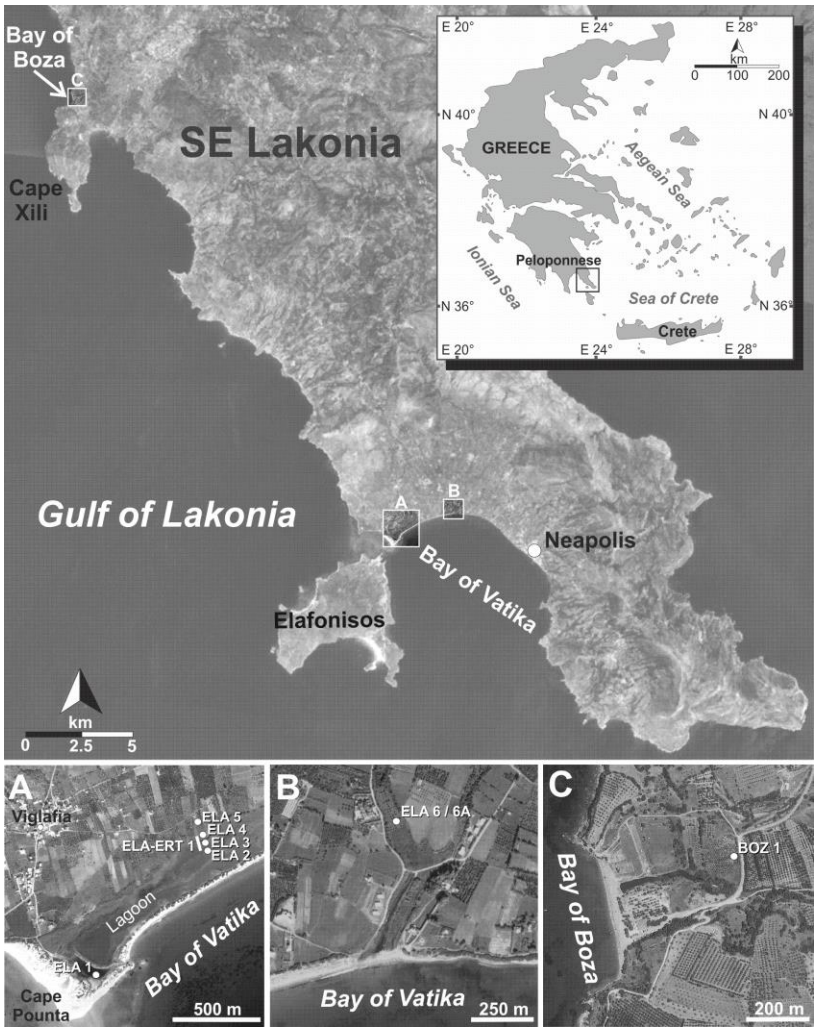

Figure 25: Overview of study areas in southeast Lakonia. The study area of Viglafia is situated opposite to Elafonisos Island near the village of Viglafia and the Viglafia Lagoon (A). The study area of Vatika is located to the northwest of Neapolis in the central part of Vatika Bay within a dry valley (B). The study area of Boza lies in another dry valley in the north of the Xili peninsula running towards the Bay of Boza (C) (source: own illustration 2013, maps based on NASA World Wind and Google Earth mages/data, access May 2012).

Geologically, the Lakonian peninsula is part of the West Hellenic Nappe which was incorporated into the Hellenic orogenetic complex during the Miocene (JACOBSHAGEN 1986). It is dominated by quartz-sericit and glimmer schists, quartzites and evaporites (FEDERICI 2002) which are partially covered by Jurassic to Eocene carbonatic rocks of the Gavrovo-Tripolitsa zone and by Eocene to Miocene flysch units (JACOBSHAGEN 1986) (Fig. 24).

Study site Viglafia Lagoon

Geoscientific investigations were carried out close to the small village of Viglafia located in the westernmost part of the Neapolis Basin bordering Vatika Bay (Fig. 25 A). The western edge of Vatika Bay is prolonged by Elafonisos Island which is separated from the mainland by a narrow and flat natural water channel. Vibracoring and Earth Resistivity Tomography (ERT) were carried out at the northern margin of the Viglafia lagoon, about 600 m eastward from Viglafia and 900 m northeastward from Cape Pounta.

The Lagoon is shielded from the open sea by a dune ridge. Several washover fans extend from the dune ridge into the lagoon in a northern direction. After IGME (2002) the bedrock around Viglafia is mainly consisting of marine sediments of Pliocene to Pleistocene age, partly covered by unconsolidated Holocene dune sands and alluvial deposits. In large parts marine terraces are developed which are mainly controlled by young Pleistocene tectonic uplift (KOWALCZYK et al. 1992).

Cape Pounta, the southern spit of Vatika Bay, is well known for the submerged Mycenaean settlement of Pavlopetri. Graves belonging to this settlement were cut into the calcarenitic aeolianite which forms the local bedrock. Submerged undated cart tracks near Cape Pounta also indicate that the relative sea level has undergone considerable rise since the mid-Holocene and has never been higher than at present (SCHEFFERS et al. 2008). According to HENDERSON et al. (2011) and classical references (Strabo: iii. 5.1, Ptol: iii. 16.9 and Pausanias: iii. 22.10) Elafonisos was connected by an isthmus to the mainland. About 1.5 km westward of Cape Pounta the Cape Skala is located. Along the rocky shoreline west of Cape Skala many large dislocated boulders were found partly imbricated by high-energy wave impact (SCHEFFERS et al. 2008). Results from high-resolution terrestrial laserscanning (TLS) in combination with DGPS and lab-borne density measurements of a block-train near Cape Pounta constrain a maximum boulder-weight of more than 4.6 t (NTAGERETZIS 2009, NTAGERETZIS et al. 2011, HOFFMEISTER et al. 2013).

Radiocarbon ages of vermitide rims, attached to some of the dislocated boulders, indicate a transportation age around 1300 cal AD, which implies a correlation to the tsunami affecting large parts of the eastern Mediterranean in 1303 AD (SCHEFFERS et al. 2008).

Study sites Vatika and Boza dry valleys

The study site of Vatika is located between Viglafia and Neapolis in the central part of the Vatika Bay (Fig. 25 B). Vibracoring site ELA 6 is situated in the bottom of a small dry valley in approximately 430 m distance to the recent shoreline.

The study site of Boza is located about 30 km to the northwest of Neapolis at the northernmost part of the Xili peninsula (Fig. 25 C). Vibracore BOZ 1 was drilled approximately 300 m inland in the midst of an orange plantation situated in a small dry valley draining towards the Bay of Boza. Following

IGME (2002) the valley has incised into upper Pliocene to lower Pleistocene rocks (marine to lacustrine, clastic to biogenic sediments). The valley infill is dominated by alluvial deposits. About 1.5 km to the south of vibracoring site BOZ 1, the partly submerged site of Plitra is situated which is considered to be either the ancient town of Asopos (s. Pausanias: 3.22.9) or Cyparissia (s. Strabo: 8.360, HADJIDAKI & LIANOS 1985). It is assumed that Plitra had an elevation of at least 4 m above the sea level in Antiquity (HADJIDAKI & LIANOS 1985).

5.3 Methods

A multi-proxy approach was applied to detect and characterize sedimentary fingerprints of palaeotsunami impacts within the near-coast stratigraphical records of the investigation sites.

A total of six vibracores using steel augers of 60 and 50 mm in diameter (ELA 1-6, BOZ 1) and one vibracore using closed auger heads with polypropylene liners of 50 mm in diameter (ELA 6A) were drilled in southeastern Lakonia using a hand-operated Atlas Copco mk1 corer. After cleaning sediment cores were photo-documented and recorded by sedimentological and geomorphological methods with the requirements of the AD-HOC-ARBEITSGRUPPE BODEN (2005). Finally, sediment cores were sampled for further sedimentological, geochemical and microfaunal studies in the laboratory.

Laboratory studies included the determination of organic contents by loss on ignition (550°C), measurements of pH-values and electric conductivity and the determination of calcium carbonate contents following the *Scheibler-method*. Element concentrations were measured by means of X-ray fluorescence (XRF) using a portable energy-dispersive analyser (type Thermo Niton XL3t 900S GOLDD, calibration mode SOIL). Magnetic susceptibility measurements were conducted using a Bartington MS2K magnetic susceptibility meter to complete the lithostratigraphical characterisation of the cores.

Microfaunal studies were carried out using 15 ml of sediment extracted from selected stratigraphical units. Samples were wet-sieved in fractions of > 400 µm, 400-200 µm, 200-125 µm and < 125 µm and subsequently analysed using a stereo microscope (type Nikon SMZ 745T). Z-Series photos of different foraminiferal specimen were taken using a light-polarizing microscope (type Nikon Eclipse 50i POL with Digital Sight DS-FI2 digital camera). Fractions < 125 µm were not investigated. The microfossil content was recorded semi-quantitatively using a scale from 0 to 6 [0 = none; 1 = very rare/singular (1 sp.); 2 = rare (2-3 spp.); 3 = few (up to 6 spp.); 4 = fairly many (up to 9 spp.); 5 = many (up to 12 spp.); 6 = a great many (more than 12 spp.)]. Species identification followed the literature of LOEBLICH & TAPPAN (1988), CIMERMANN & LANGER (1991), MURRAY (1991), GROSS (2001) and HAYWARD & GROSS (2011).

Electrical resistivity measurements (ERT) were carried out in order to detect stratigraphical differences within the near-surface quaternary deposits and underlying bedrock structures using a multi-electrode geoelectrical device (*IRIS Instruments*, type Syscal R1+ Switch 48). A Wenner-Schlumberger electrode array and a spacing of 2 m were chosen. To invert the measured data RES2Dinv (Geotomo Software) was used. Inversion models are based on 7 iterations wherein the topography has been included. To determine the exact geographical position and elevation of vibracoring sites and ERT transects differential GPS measurements were accomplished using a *Topcon HiPerPro* device.

Geochronological data is based on the ^{14}C-AMS dating technique of organic material. To calibrate the ages Calib. 6.0 after REIMER et al. (2009) was used.

5.4 Results

5.4.1 Viglafia Lagoon

5.4.1.1 Vibracore stratigraphies

Four vibracores (ELA 2-5) were conducted along a south-north trending transect (Fig. 25 A). The transect is located approximately 1 km in distance to vibracoring site ELA 1 (SCHEFFERS et al. 2008) which is situated at the southern fringe of the Viglafia Lagoon.

In core ELA 1 sedimentological evidence of tsunami imprint was found for the first time in the southeastern Peloponnese. A sand-dominated sequence overlying autochthonous lagoonal mud on top of a sharp erosional unconformity is interpreted as a tsunamigenic deposit. Obviously, the lagoonal environment has not been re-established documenting an abrupt change of sedimentary and ecological conditions. Radiocarbon dating of a wood fragment indicates that the lagoon was hit by an event at or after 134; 380 cal AD (2σ max; min cal AD; using InterCalib04) (for further details see SCHEFFERS et al. 2008).

Vibracoring site ELA 2 (N 36°31’30.41’’, E 22°59’42.84’’) is located at the northern fringe of the lagoon about 240 m inland at approximately 0.62 m a.s.l. (Figs. 25 A and 26). The basal unit is composed of limestone covered by clayey silt (1.23-0.42 m b.s.l.) which is again covered by a rust-colored brownish sequence (0.42 m b.s.l. - 0.46 m a.s.l.) consisting of clayey fine and middle sand containing calcareous concretions and gravel up to 1.5 cm in diameter. The top of the core consists of clayey silt containing fragments of *Cerastoderma glaucum* (0.46-0.62 m a.s.l.). Vibracore ELA 3 (N 36°31’30.76’’, E 22°59’42.67’’) was drilled in the marshy fringe of the lagoon at an elevation of 0.66 m a.s.l. (Figs. 25 A and 26) showing a comparable stratigraphy compared to vibracore ELA 2. On top of the bedrock a sequence of clayey to partly sandy silt and a layer of brown to rust-colored silty to middle sandy fine sand (0.55 m b.s.l - 0.53 m a.s.l.) is developed. The fine sand layer also contains

pieces of gravel. The top of the profile is characterized by marshy sediments showing alternating layers of silty fine sand and clayey silt with hydromorphic features. Vibracore ELA 4 (N 36°31'32.93'', E 22°59'42.09'') was drilled some 70 m to the north of site ELA 3 at 1.47 m a.s.l. in the midst of an olive grove (Figs. 25 A and 26). The base of the sequence shows a dark rust-colored palaeosol out of clayey to silty sand covered by middle-sandy to clayey fine sand (0.30- 1.17 m a.s.l.). This unit partly contains gravel up to 1 cm in diameter and plant remains. At 0.55 m a.s.l. a non-diagnostic ceramic fragment was found indicating a Holocene age of this layer. The top of vibracore ELA 4 is characterized by dark brown sandy silt including gravel and another ceramic fragment at 1.25 m a.s.l. Vibracore ELA 5 (N 36°31'36.50'', E 22°59'41.64'') is situated some 400 m inland and approximately 110 m to the north of site ELA 4 in the midst of the same olive grove at 2.49 m a.s.l. (Figs. 25 A and 26). A dark rust-colored clayey to sandy silt, including numerous stones and gravels, as well as a thin sand layer between 2.07 m and 1.93 m a.s.l. was encountered. The top of the core is made out of dark-brown silty fine-sand.

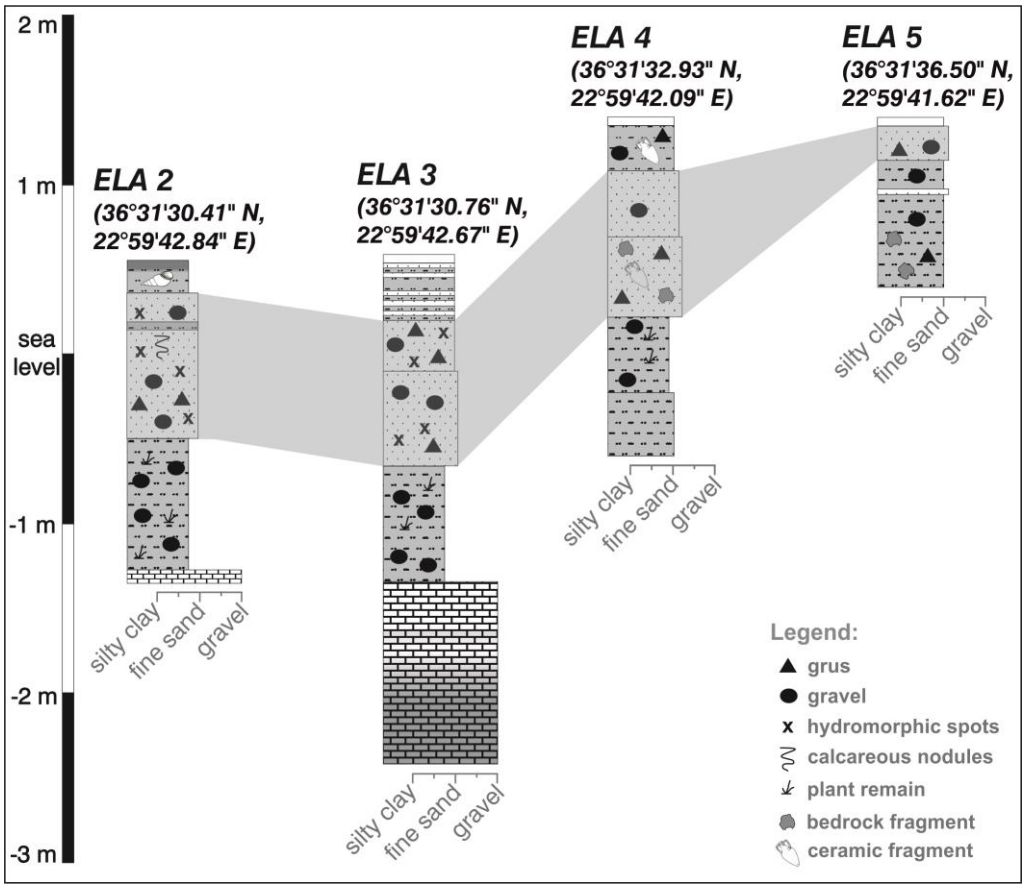

Figure 26: Simplified facies profiles of vibracores ELA 2-5. The vibracores were drilled along a south-north trending transect in continuation to vibracore ELA 1 studied by Scheffers et al. (2008). A sandy stratum is clearly visible in each vibracore (source: own data and illustration 2013).

Additional stratigraphic information can be deduced from earth resistivity tomography transect ELA ERT 1 which was applied parallel to vibracores ELA 2, ELA 3 and ELA 4 on a flat to slightly sloping

ground (Fig. 25 A and 27). Starting in the marshy margin of Viglafia Lagoon the 94 m long transect crosses a densely vegetated wall and continues on grazing land partly covered with olive trees.

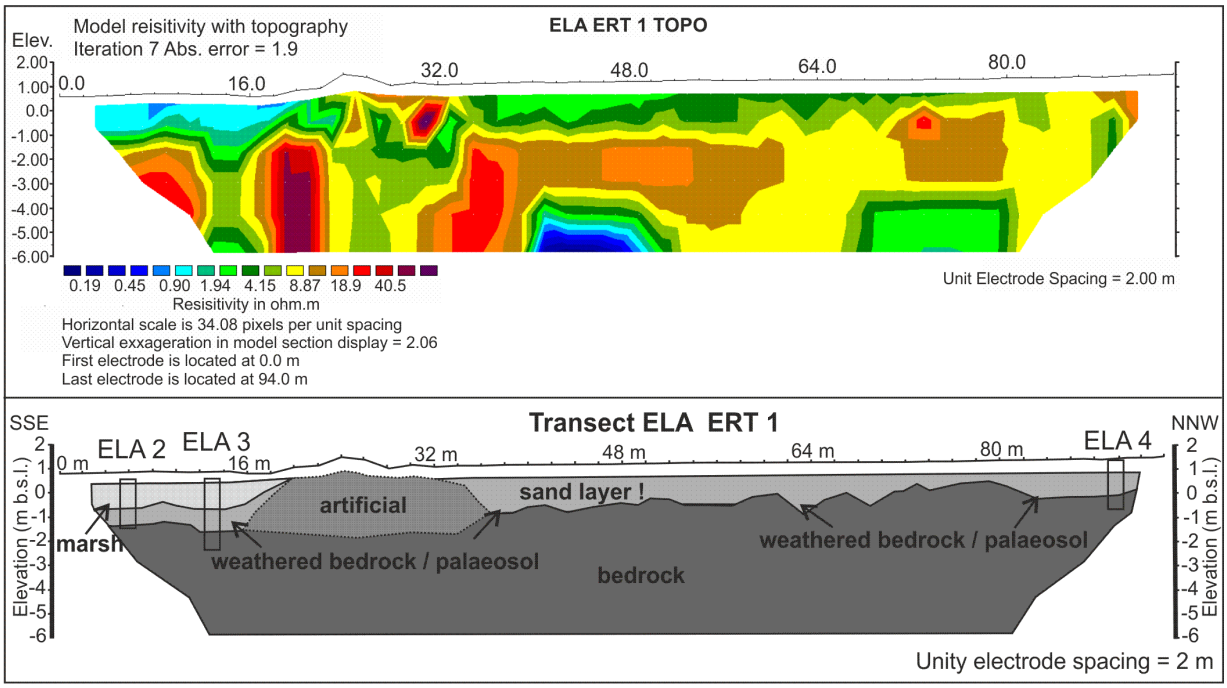

Figure 27: Results and interpretation of the earth resistivity tomography measurement of transect ELO ERT 1 accomplished at the northern margin of the Viglafia lagoon parallel to vibracores ELA 2, 3 and 4 (source: own pictures, data and illustration 2013).

The results and the interpretation of the inverse resistivity model for ERT transect ELA ERT 1 are illustrated in Figure 4. Three subsurface units can be differentiated. Based on vibracore stratigraphies low resistivity values in the transects southern part are correlated to fine grained lagoonal deposits. Furthermore, a high ground water level has to be considered when interpreting the data, which can also result in low resistivity values. The following unit is characterized by resistivity values varying between 2 and 8 Ωm. This unit represents the sandy deposit as well as the palaeosol and weathered bedrock material which cannot be differentiated in more detail. Highest resistivity values most likely represent the bedrock material. The ridge-like structure between 16 and 32 m is most likely due to anthropogenic influences. Overall, the ERT-transect shows that the bedrock is striking out close to the surface and that the thin Holocene sedimentary sequence is well covered by the vibracores.

5.4.2 Bay of Vatika

5.4.2.1 Vibracore stratigraphy

Vibracores ELA 6 and ELA 6A (N 36°31’56.24’’, E 23°01’13.20’’) were drilled in a small dry valley, incised into local limestone bedrock, draining towards the central part of Vatika Bay (Fig. 25 B) approximately 415 m inland at an elevation of 1.47 m a.s.l. Both cores show an almost identical stratigraphical record. Here, the results of vibracore ELA 6A are presented.

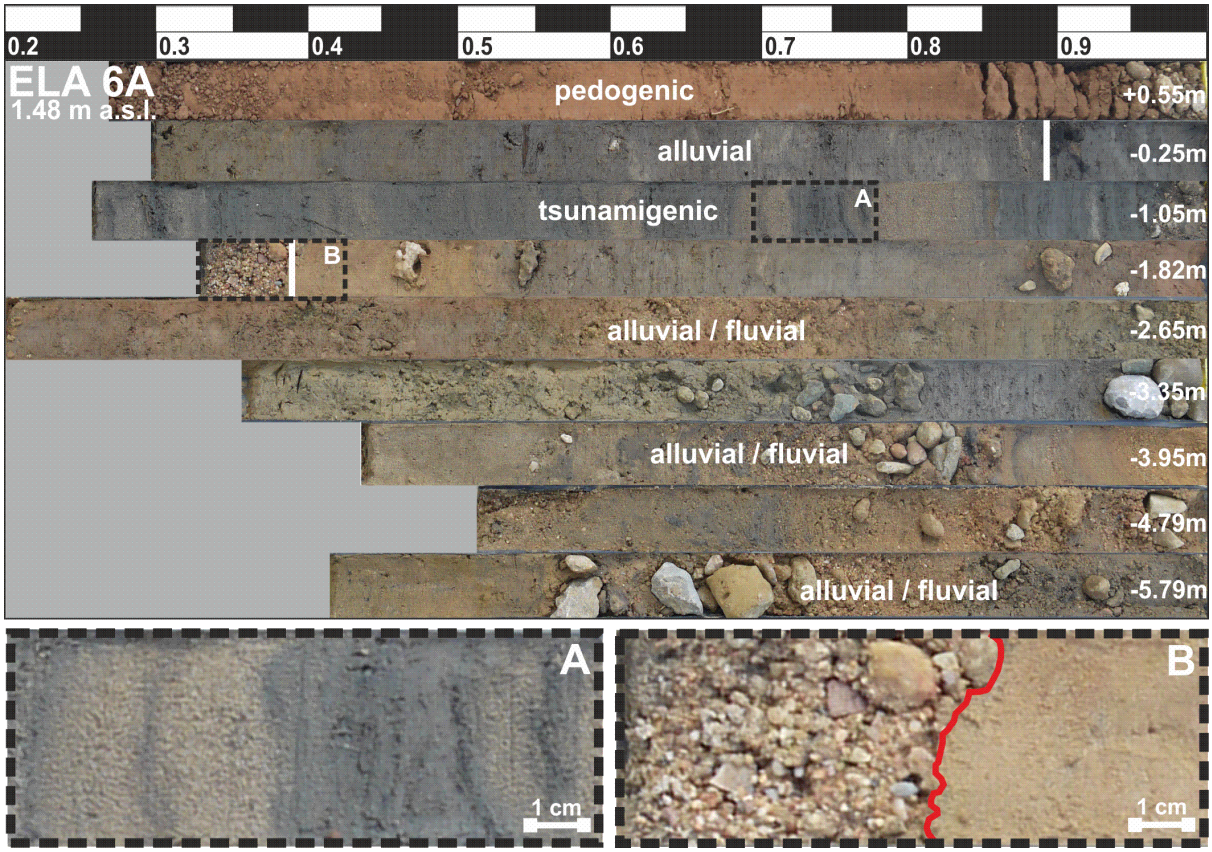

Figure 28: Photography of vibracore ELA 6A encountered in the midst of an olive grove within a dry valley that bottoms out in the Vatika Bay close to Neapolis and detailed views of the event layer encountered between 2.67 and 1.60 m b.s.l. Picture A illustrates the lamination in the form of alternating sandy and clayey laminas. Picture B shows the sharp erosional unconformity indicating the strong erosional behavior of the associated event (source: own pictures and illustration 2013).

The base and the lower part of the core (Fig. 28) are characterized by alternating silty fine sands and gravel layers in a silty respectively sandy matrix. The gravels within this heterogeneous sequence are well rounded. In the upper part of these deposits (between1.35 and 1.27 m b.s.l.) mollusc and gastropod fragments as well as coral fragments were found. Brown, rusty and ferruginous colors of several layers within this unit indicate weathering processes and partly soil formation under oxygenic conditions. These weathering processes may be of pre- or post-depositional origin. A well rounded ceramic fragment found at 2.42 m b.s.l. points to a Holocene age of this unit. At 1.19 m b.s.l. a distinctive erosional unconformity marks a transition from silty fine sand to a layer consisting of coarse sand and gravels initiating the following sedimentary unit (1.19-0.12 m b.s.l.). This gravel layer is covered by clayey silt with fine sandy intersections followed by fine sandy to clayey silt (1.19-0.12 m b.s.l.). In addition, this unit is characterized by a fining upward trend and lamination, a multi-modal grain size distribution. Marine mollusc fragments, plant and charcoal particles as well as ceramic fragments are incorporated between 0.62 and 0.52 m b.s.l. The sharp erosional contact indicates an abrupt change of the depositional environment and associated energetic potential. On top of the coarse grained layer alternating laminae out of greyish clayey silt and fine sand indicate marine

inundation. Sediments on top of another gravel layer in a depth of 0.55 m a.s.l. show pedogenetic superimposition.

5.4.2.2 Sedimentological and geochemical analyses

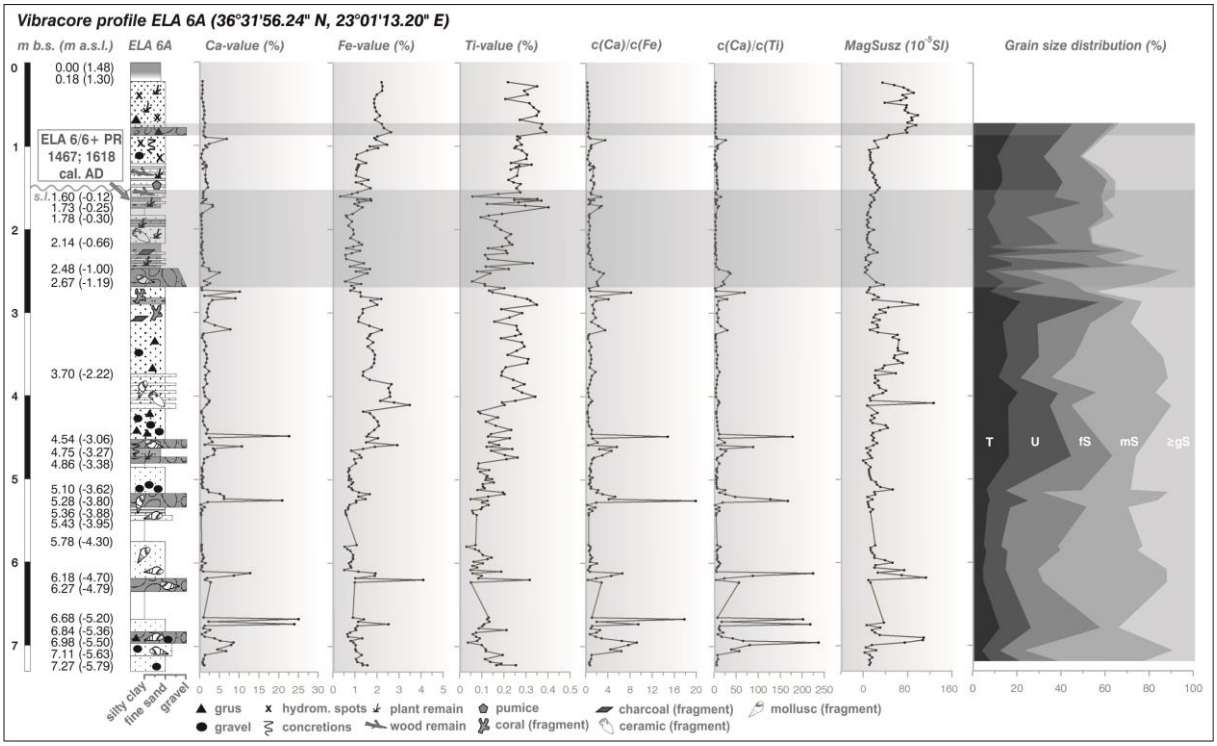

Figure 29: Stratigraphy, facies distribution and geochemical analyses of vibracore ELA 6A drilled in a dry valley in the Vatika Bay (source: own data and illustration 2013).

Results of sedimentological and geochemical analyses are summarized in Figure 29. The lower part of the profile is dominated by middle and fine sand in the grain size distribution of the fraction < 2 mm. Distinct maximum peaks of the susceptibility values can be observed below the lowest gravel layer (5.36-5.50 m b.s.l.) and on top of the second gravel layer (4.70-4.79 m b.s.l.) indicating an enrichment of magnetizable minerals. Especially the second maximum peak is accompanied by increasing Fe- and Ti-values. On top of these coarse grained layers Calcium values show distinct maxima also indicating enrichment due to leaching and relocating. In between these maximum peaks calcium content is very low pointing to weathering which is also supported by the Ca/Fe- and Ca/Ti-ratios. It has to be discussed if weathering processes are of post-depositional origin or if pre-weathered material was relocated in the course of sedimentation. The distinct maximum peaks in calcium contents also controlling curve progression of the Ca/Fe- and Ca/Ti-ratios in the gravel layers between 3.80-3.88 m b.s.l. and 3.06-3.38 m b.s.l. are most likely due to incorporated limestones from reworked bedrock material. In general, clay and silt contents show an increase above 3.62 m b.s.l. towards 1.19 m b.s.l. accompanied by increasing Ti and susceptibility values indicating decreasing depositional energy and

increasing weathering. The alternating sequence of silt, sand and gravel between 1.19 and 0.66 m b.s.l. is well reflected in grain size distributions. In contrast, geochemical proxies and magnetic susceptibility show low variations for the unit between 1.19 b.s.l. and 0.55 m a.s.l. including the laminated unit between 0.25 m b.s.l. and 0.18 m a.s.l. The uppermost part of the profile is characterized by high Fe and Ti values and high values of the magnetic susceptibility reflecting soil formation processes. In a summary view, the proxies indicate high contents of weathered material in the entire sequence. Based on sedimentary features and grain size distribution it seems likely that pre-weathered material was incorporated during relocation processes in high amounts.

5.4.2.3 Microfaunal analyses and chronostratigraphy

Results of microfaunal analyses of selected sedimentary units of vibracore ELA 6A are summarized in Figure 30.

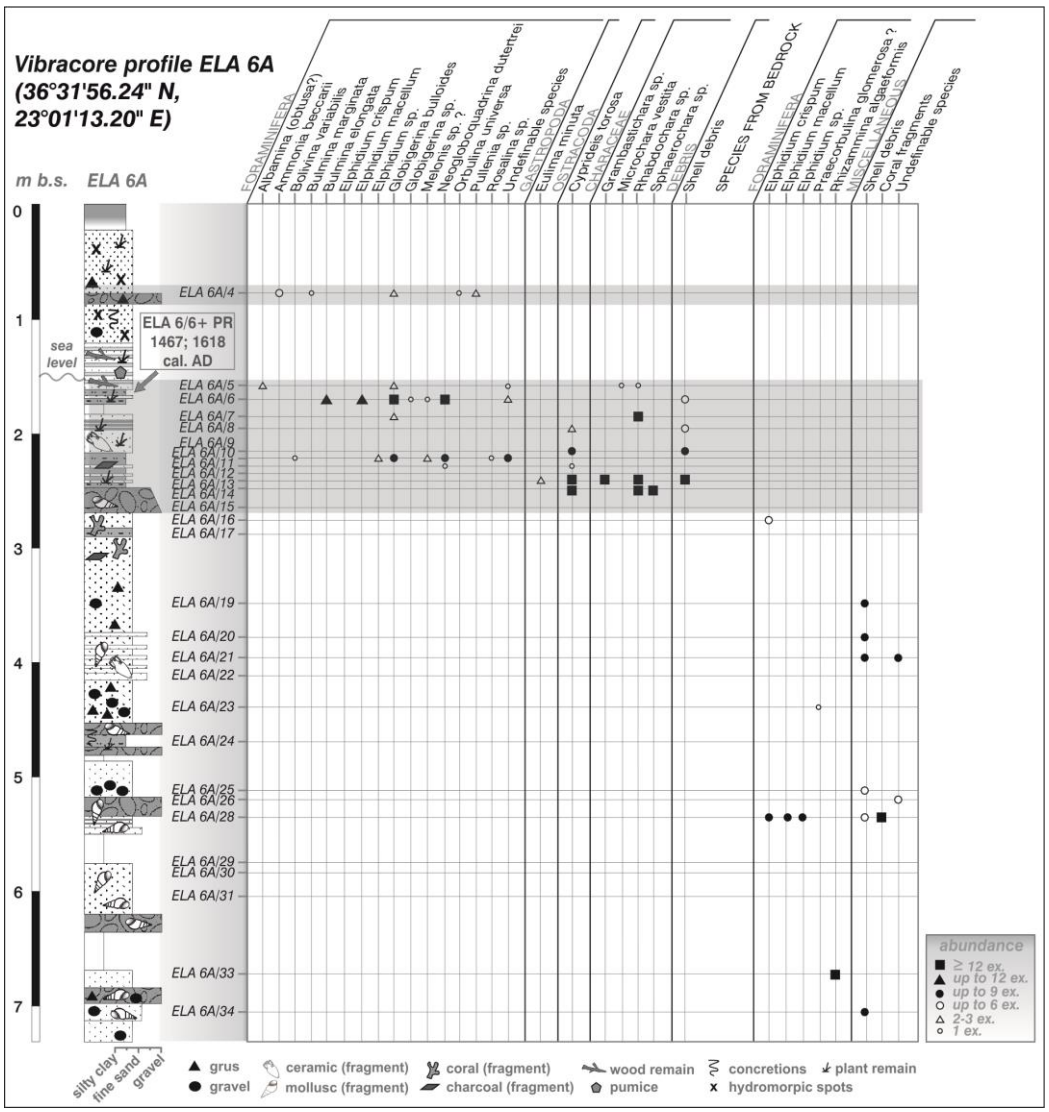

Figure 30: Stratigraphical record, facies distribution and microfossil analyses of vibracore ELA 6A drilled in a dry valley in the Vatika Bay (source: on data and illustration 2013).

The lower sedimentary units (5.79-1.19 m b.s.l.) contain no younger microfossils beside some rare reworked microfossils (e.g. foraminifera species: *Elphidium crispum, Elphidium macellum, Elphidium sp.* and *Praecorbulina glomerosa*?) originating from the local bedrock and some Plio-Pleistocene mollusc and coral fragments as well as specimens of *Rhizammina algaeformis* (Fig. 31 E and F).

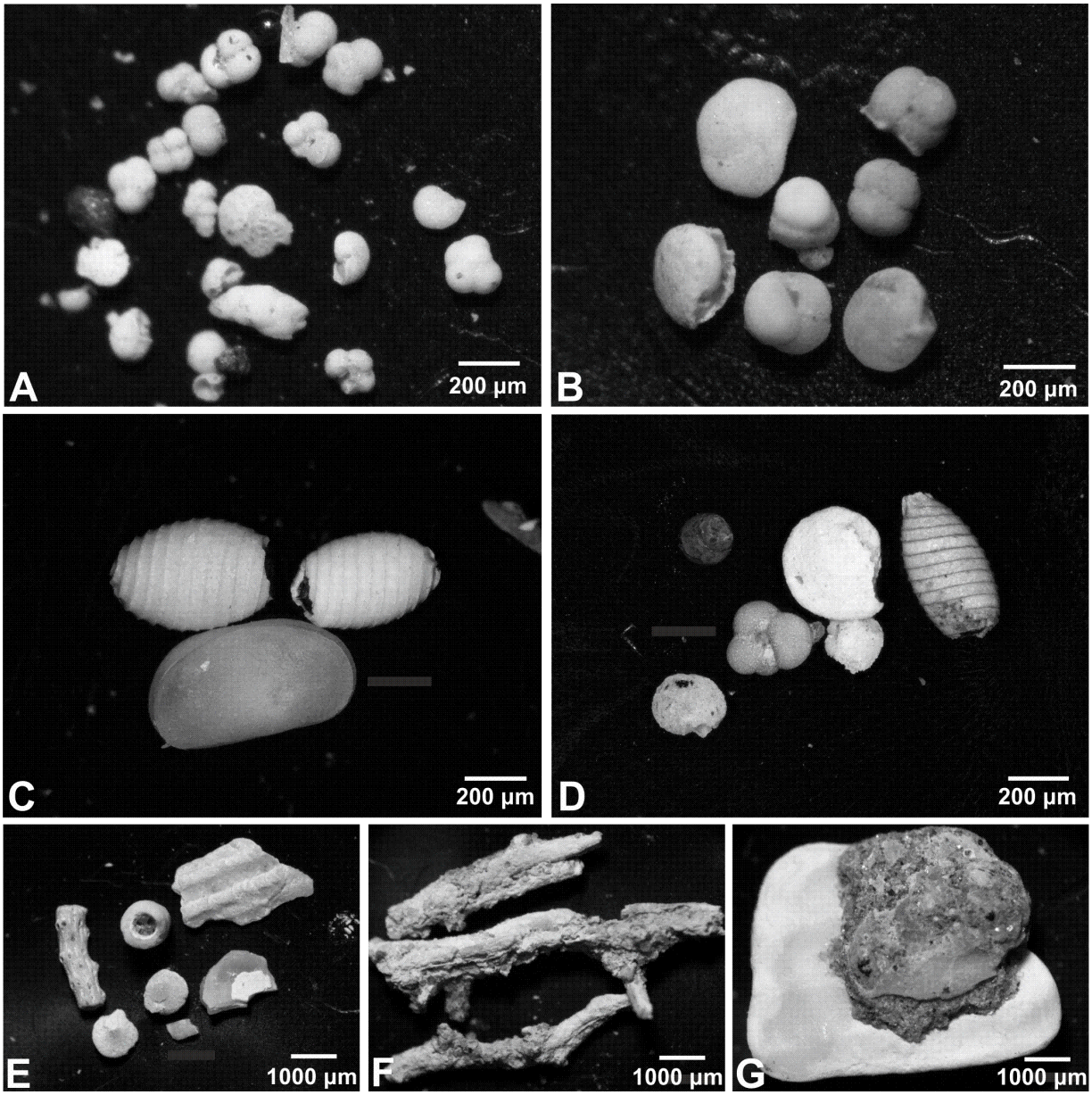

Figure 31: Selection of detected microfossils from vibracore ELA 6A. Pictures A-D display the species found in the allochtonous marine layer. The lower pictures E-G show the pre-Holocene species found in the fluvial and terrestrial dominated lower part of the vibracore. Bedrock attachments and recrystallization traces are clearly visible (source: own pictures and illustration 2013).

These microfossils often show traces of recrystallization (Figs. 31 E and G). In contrast, the unit between 1.19 and 0.12 m b.s.l. is characterized by well-preserved microfossils (foraminifera, ostracods, gastropods and characeae) showing no recrystallization indicating marine inundation into the valley (Figs. 31 A-D). With regard to the preferred habitat of each species the microfossil content of the allochtonous marine gravel and sand layers with alternating laminae represent a widespread

spectrum of brackish (e.g. foraminifera: *Ammonia beccarii,* ostracod: *Cyprideis torosa* and algae: *Grambastichara* sp., *Microchara vestita, Rhabdochara* sp., *Sphaerochara* sp.) and shallow-marine species as well as taxa from the inner shelf (e.g. *Ammonia beccarii, Elphidium crispum, Elphidium macellum, Elphidium* sp. i.a.) and open-marine species (benthic foraminifera e.g. *Bulimina marginata, Bulimina elongata, Bolivina variabilis, Pullenia* sp., *Melonis* sp. as well as planktonic foraminifera e.g. *Globigerina bulloides, Globigerina* sp., *Neogloboquadrina dutertrei* or *Orbulina universa*). Generally, all samples from this event layer contained microfossils in varying abundance and preservation stages. The subsequent and uppermost sedimentary unit is intersected by a 6 cm thick gravel and grus layer embedded in a fine sandy matrix starting at 0.55 m a.s.l. Microfaunal analyses yielded few entire and broken foraminifera species – both benthic (*Ammonia beccarii* and *Bulmina marginata*) and planktonic (*Globigerina bulloides*, *Orbulina univer*sa and *Pullenia sp.*) indicating marine influence for this layer as well.

Chronological information for the allochthonous marine layer intersecting the fluvial to terrestrial dominated environment in the dry valley near Neapolis is based on radiocarbon dating of plant remains found in the uppermost part of the event deposit at 0.15 m b.s.l. yielding an age interval of 1467; 1618 cal AD (Tab. 2). Reworking cannot be excluded because the dating material was extracted from the event deposit itself. Therefore, the age interval represents a *terminus ad* or *post quem* for the marine inundation event.

Sample name (Lab. No.)	Depth (m b.s.)	Depth (m b.s.l.)	Sample description	$\delta^{13}C$ (in ‰)	^{14}C age (BP)	1σ max; min (cal BC/AD)
ELA 6/6+ PR (KIA 45979)	1.63	0.15	plant remains	-25.88±0.35	365±20	1467; 1618 cal AD

Table 2: Radiocarbon data for the sampled plant remains from vibracore ELA 6 drilled in a dry valley near Neapolis (Peloponnese – Greece). Note: Sample name – sample name chosen while field work; (Lab. No.) – laboratory number given by the Leibniz Laboratory for Radiometric Dating and Isotope Research, Christian-Albrechts-Universität zu Kiel (Germany); m b.s. – meter below surface; m b.s.l. – meter below sea level; (a) $\delta^{13}C$-value – shows incorporation of C4 plants or aquatic material and indicates a potential reservoir effect; (b) $\delta^{13}C$-value – indicates purely atmospheric C3 photosynthesis without contamination by old carbon; 1σ max; min (cal BC/AD) – calibrated ages, 1σ-range; ";" – semicolon is used in cases where several age intervals because of multiple intersections with the calibration curve are possible; oldest and youngest age depicted; Calibration is based on the software Calib 6.0 (REIMER et al. 2009).

5.4.3 Bay of Boza

5.4.3.1 Vibracore stratigraphy

A comparable geographical constellation as described for site ELA 6A was found in a small valley to the north of the Xili peninsula near the small housing estate of Boza. Vibracore BOZ 1 was drilled within a dry valley located to the north of the Xili Peninsula some 290 m inland at an elevation of 1.32 m a.s.l. (Fig. 25 C)

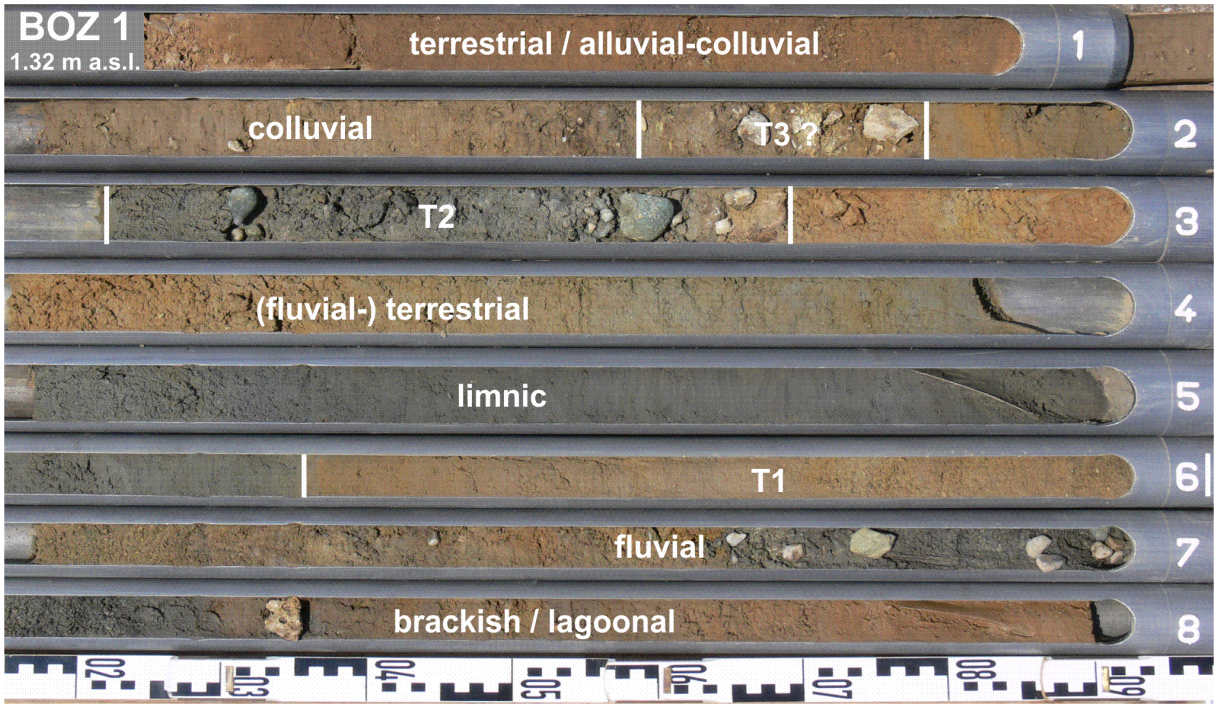

Figure 32: Photo and simplified facies profile of sediment core BOZ 1 encountered in a dry valley bottoming out at Boza Bay in the northern margin of Cape Xili in southern Lakonia (source: own photography 2010 and illustration 2014).

The base of the core (Fig. 32) consists of relatively homogeneous silt dominated clayey sediments of brownish color. From 5.92 m b.s.l. the color changes towards greenish-grey accompanied by a clear coarsening upward trend (5.92-5.43 m b.s.l.). On top (5.43 and 4.68 m b.s.l.) gravel and grus within a greyish to greenish sandy to silty matrix were accumulated. Alternating sediment colors indicate sediment mixing. The Holocene age of this unit is proved by a weathered ceramic fragment. Further upcore a bright brown fining upward sequence (4.68-4.03 m b.s.l.) from gravel and grus to coarse and middle sand and finally to clayey silt is developed. In the upper part rip up clast were detected. Numerous marine mollusc fragments point to a marine origin of the deposit. This allochthonous sedimentary unit is followed by autochthonous limnic sediments consisting of homogeneous grey clayey silt. From 2.97 m b.s.l. upwards coarse, middle and fine sand was deposited in a silty matrix showing a slight fining upward trend and color changes from grey over rusty grey to rusty brown. The color change towards more brownish and rusty colors together with the presence of calcareous concretions and hydromorphic features suggest a gradual silting up of the limnic environment in back-beach position and thus increasing terrigenous influences. Between 1.37 and 0.90 m b.s.l. badly sorted gravel and grus embedded in a sandy matrix was found, containing bedrock and ceramic fragments as well as plant remains deposited under high-energetic conditions. The uppermost unit of vibracore BOZ 1 (from 0.68 m b.s.l. upwards) is characterized by grey to brownish clayey silt indicating increasing terrigenous influence due to weathering and soil formation processes or relocation of pre-weathered soil sediments in the course of alluvial to colluvial deposition. An

imbedded gravel layer at 1.50 m b.s.l. points to a short phase of high-energetic depositional conditions.

5.4.3.2. Sedimentological and geochemical analyses

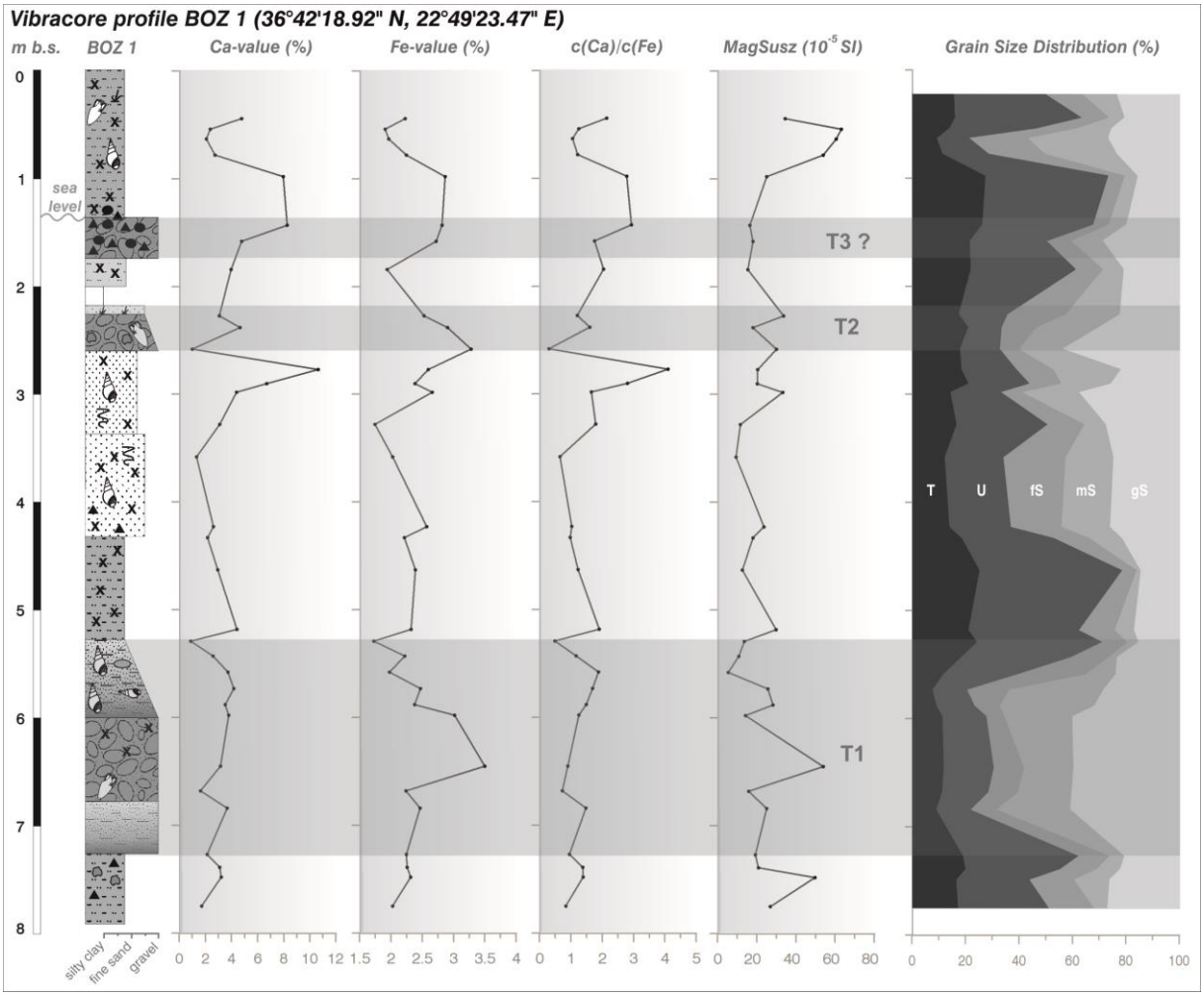

Figure 33: Stratigraphy, grain size distribution and selected geochemical parameters of vibracore BOZ 1 drilled in a dry valley at the northern margin of Xili peninsula. For stratigraphical legend see figure 11 (source: own data and illustration 2013).

Results of sedimentological and geochemical analyses are summarized in Figure 33. The base of the profile (6.58-5.92 m b.s.l.) is characterized by relatively high susceptibility values and increasing clay and silt contents towards the top. Above this unit a clear coarsening upward trend is visible in the grain size distribution accompanied by decreasing susceptibility values. Calcium and iron values as well as the Ca/Fe-ratio show only minor variation. From 5.43 to 4.68 m b.s.l. sand content as well as iron and susceptibility values increase significantly indicating changing depositional conditions and the input of coarse grained, pre-weathered material. The fining upward from 4.68 to 4.03 m b.s.l. as already described during field documentation is clearly visible in grain size distributions. The Ca/Fe-ratio shows increasing values in this part of the profile. Sediments on top (4.03-1.68 m b.s.l.) show only minor fluctuations of selected elements and within the susceptibility values whereas a distinct

shift in grain size distribution from clay and silt dominated sediments towards significant sand input is visible at 2.97 m b.s.l. Distinct increase of the Ca/Fe-ratio and decreasing susceptibility values indicate the input of unweathered material between 1.68 and 0.98 m b.s.l. The laminated sediments on top of the uppermost gravel layer (0.46-0.18 m b.s.l.) again show increasing values of the Ca/Fe-ratio and increasing clay and silt contents. Pedogenic superimposition in the first meter of the sequence is indicated by low Ca and high susceptibility values.

5.4.3.3 Microfaunal studies

Detailed microfaunal analyses were carried out for 17 samples from vibracore BOZ 1. The results are summarized in Figure 34.

The basal unit of vibracore BOZ 1 is characterized by the broadest spectrum of species and greatest abundance within the whole stratigraphical sequence. The foraminiferal assemblage is composed of lagoonal and (shallow) marine, most probably (sub-) littoral species such as *Ammonia beccarii, Ammonia tepida, Elphidium advenum, Elphidium crispum* or *Elphidium macellum*. In addition, species were found that occur in both, shallow and open marine environments as well as on continental shelfs, such as *Rosalina* sp*., Orbulina* sp*., Globigerina* sp*., Bulimina aculeata, Bolivina robusta* or *Asterigerinata mamilla*. From 5.92 (sample BOZ 1/30) m b.s.l. upcore, open marine taxa strongly recede whereas brackish and limnic species like the algae *Rhabdochara* sp. and *Sphaerochara* sp. emerge as well as sea urchin spines pointing to (sub-)littoral conditions.

The coarse deposit encountered between 5.43 and 4.68 m b.s.l. shows no microfossil record with the exception of an old recrystallized species of *Elphidium crispum* which originates from the local bedrock (sample BOZ 1/28). In the following fining upward sequence, beside numerous gastropod fragments and shell debris, benthic foraminiferal species typical of littoral and shallow marine environments, such as *Ammonia beccarii, Ammonia tepida, Elphidium advenum, Elphidium crispum, Haynesina depressula* or *Lobatula lobatula* and planktonic open water specimens of *Globigerina* sp. were found. Thus, the microfaunal record proves a marine origin of the sediments between 4.68-4.03 m b.s.l. The investigated samples between 4.03 and 1.37 m b.s.l. yielded only few microfaunal remains, covering mainly species from the local bedrock. In contrast, the fining upward sequence between 1.37 and 0.90 m b.s.l. yielded few younger microfaunal species. These are species of *Ammonia beccarii, Elphidium crispum, Rosalina densitiva,* remains of sea urchin spines as well as scores of gastropod remains. The encountered foraminifera are not well preserved, which may indicate weathering processes possibly due to temporal sub-aerial exposition or reworking effects. Towards the top of the core, the microfaunal data show that marine species from the beach zone,

such as *Elphidium* sp., *Haynesina* sp. and few species of algae *Rhabdochara* sp. as well as sea urchin spines were deposited under high-energetic conditions during prevailing limnic sedimentation.

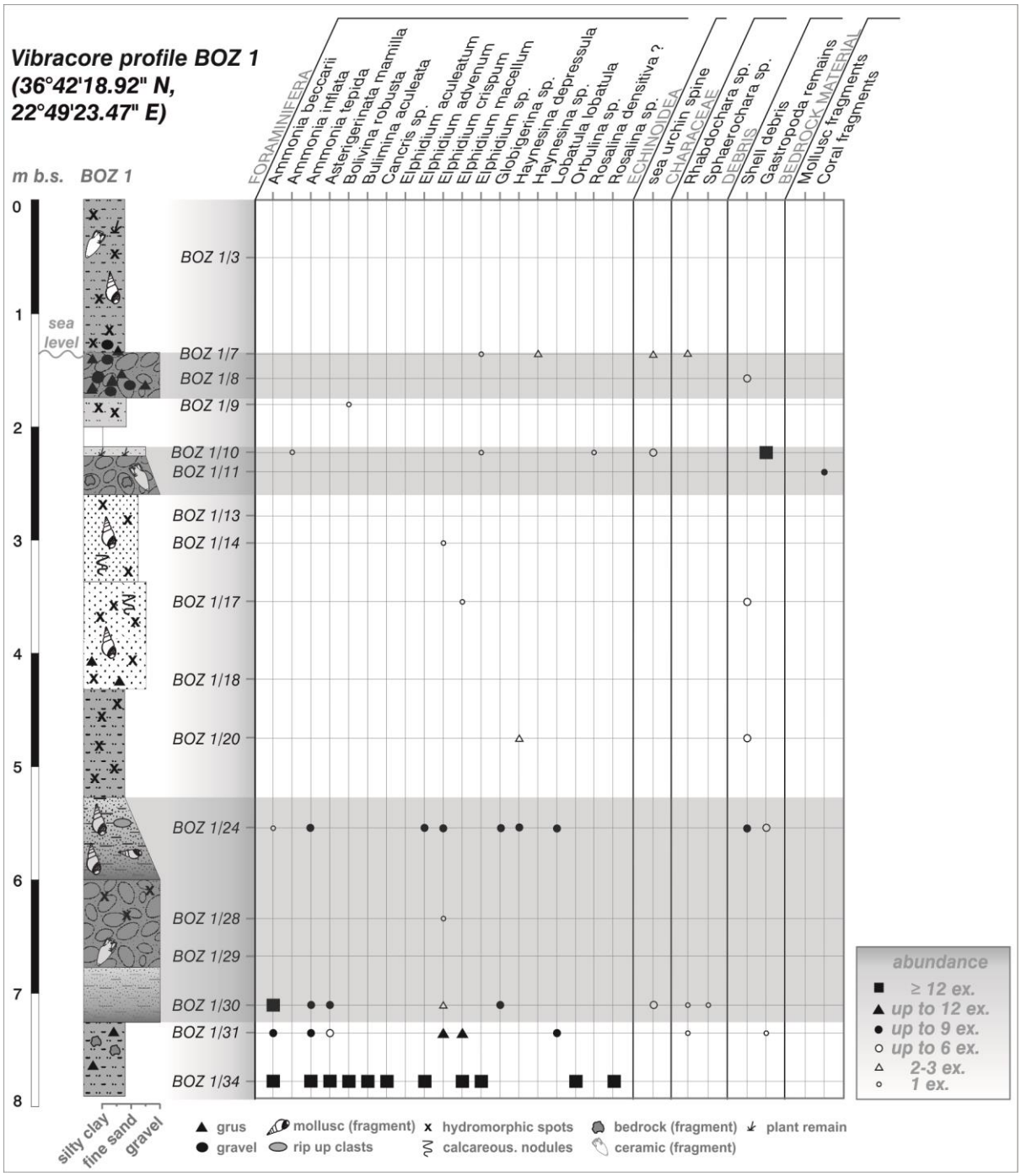

Figure 34: Stratigraphy and microfossil analyses of vibracore BOZ 1 drilled in a dry valley bottoming out at Boza Bay at Cape Xili (source: own data and illustration 2013).

5.5 Discussion

From written sources it is well known that the coasts of the Lakonian Gulf (southeastern Peloponnese, Greece) have been repeatedly affected by tsunamis during historical times. In contrast, for southeastern Lakonia only few data have been published on palaeotsunami imprints dealing with sedimentary and geomorphological features, related to such events. The small number of publications is certainly related to the fact that promising geological archives are rare in the study area. In southeastern Lakonia, the bedrock strikes out close to the surface so that the accommodation space for Holocene deposits is very small to almost non-existing. On the basis of our sedimentological, geomorphological, geochemical and microfaunal investigations sediment layers were detected featuring distinctive sedimentary characteristics of high-energy event deposits related to palaeotsunami inundation.

At the northern fringe of the Viglafia Lagoon, a layer of sand was encountered up to 400 m inland showing a clear thinning landward trend. Marine macrofaunal remains as well as well-rounded pebbles were transported far inland and deposited associated with the sand sheet (Fig. 26). From a stratigraphical point of view this sandy layer corresponds to the sandy sequence encountered at coring site ELA 1 ascribed to tsunami impact by SCHEFFERS et al. (2008). Apart from the sedimentary features of this sand layer its landward thinning trend also points to the tsunamigenic influence which is a common feature observed for both recent as well as historical tsunami deposits (MORTON et al. 2007, SUGAWARA et al. 2008, VÖTT et al. 2011a). The palaeogeographical constellation and prevailing system conditions underwent an abrupt change which have never been re-established after the high-energy impact. According to the radiocarbon dating results from SCHEFFERS et al. (2008) the lagoon was hit by an event at or after 134-380 cal AD, thus most probably pointing on the well-known 365 AD event. A correlation of the tsunamigenic deposits described by SCHEFFERS et al. (2008) and the findings in the vibracore transect ELA 2-5 presented here is most likely. Moreover, satellite images document that fan-like structures are running from the beach-ridge in northern direction into the Viglafia Lagoon (Fig. 35).

The satellite image of Figure 35 thus indicates that the low-lying lagoonal back-beach area shows a lob-like contour line at its northern margin. Such geomorphological structures are assumed to result from marine inundation during extreme wave events and the accompanied accumulation of sediments (MAY 2010 see also ANDRADE 1992, KRAUS 2003, DONELLY et al. 2006, YULIANTO et al. 2007, GOFF et al. 2009). This together with the presence of dislocated and partly imbricated boulders, situated some hundreds of meters westward from the Viglafia Lagoon along the rocky shoreline west of Cape Skala, are suggested to represent geomorphological signatures of past tsunamigenic activity.

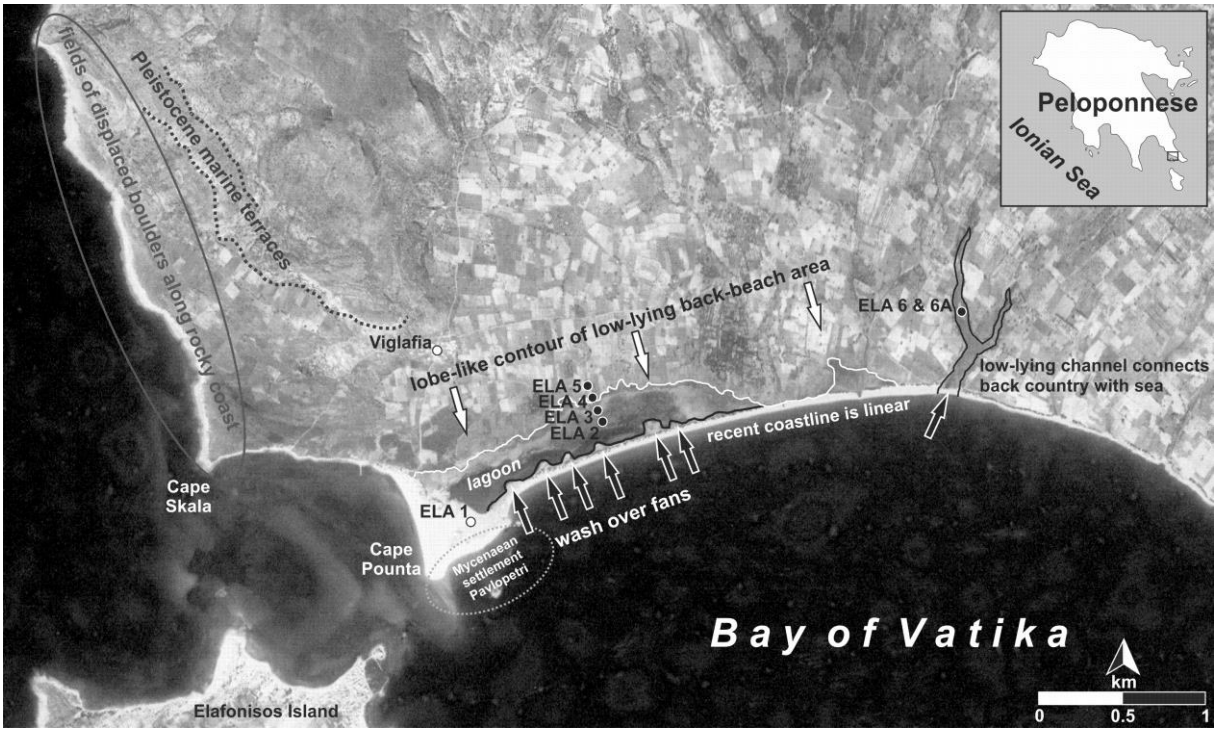

Figure 35: Geomorphological and sedimentological hints for palaeo-tsunamigenic activity in the Bay of Vatika (source: own illustration 2014, map based on Corona satellite images (USGS)).

Marine high-energy signals were detected also in the stratigraphical record retrieved from the dry valley within a fluvio-terrestrial environment in back-beach position situated in the central part of the Vatika Bay, some kilometers east of Viglafia. Sedimentological and geochemical analyses of the lower and middle parts of vibracore ELA 6A, which are characterized by alternating thick layers of fine sand and gravel, clearly trace the predominance of fluvial processes within the back-beach environment. Fine grained layers represent fluvial respectively alluvial deposits accumulated under low to mid-energetic conditions whereas the coarser intersections represent phases of stronger torrential runoff. Reworking of sediments and bedrock material is also indicated by geochemical proxies and microfaunal analyses.

Above a sharp erosional unconformity fluvial deposits are abruptly disturbed by an allochthonous coarse gravel layer of marine origin. Sedimentological, geochemical and especially microfaunal results prove that this deposit represents a high-energy impact from the sea side. The sedimentological characteristics are typical for sub-recent and recent tsunami events (SATO et al. 1995, HINDSON & ANDRADE 1999, GELFENBAUM & JAFFE 2003, PARIS et al. 2007, BILLI et al. 2008, RICHMOND et al. 2012, OKAL et al. 2010, VÖTT et al. 2009b, 2011a, 2011b, among others). The set of sedimentary features as described between 1.19 and 0.12 m b.s.l. comprises (i) a sharp erosional unconformity accompanied by the transition from silty fine sand to thick gravel, (ii) a clear fining upward within the grain size distribution, (iii) a distinctive lamination of alternating sandy and clayey laminas, (iv) a multi-modal grain size distribution as well as (v) a heterogeneous composition including marine

mollusc fragments, plant remains, charcoal particles as well as ceramic fragments. Lamination for instance (Fig. 28, detailed images) is described as a typical feature of tsunami sediments due to backwash effects and waning phases (PARIS et al. 2007, CHOOWONG et al. 2008, MORTON et al. 2007, MORTON et al. 2008, MAY 2010).

In addition, the marine origin of the sedimentary unit is attested by marine microfossils appearing for the first time in vibracore ELA 6A at 1.19 m b.s.l. The microfaunal assemblage proves the input of species from different habitats – brackish, shallow- and open-marine besides deep-sea species. The simultaneous deposition of various microfaunal species is considered to be another striking feature for tsunamiites (DAWSON et al. 1995, HINDSON & ANDRADE 1999, KORTEKAAS & DAWSON 2007, MAMO et al. 2009, VÖTT et al. 2009b). Especially, the presence of open-water and deep-sea planktonic foraminifera refers to extreme wave activity.

As the local wind regime is dominated by offshore winds (MEDATLAS GROUP 2004) storm wave activity can be excluded as another cause for marine inundation. In addition, the distance of about 500 m to the present coastline seems too far for wind induced inundation, as sandy storm related deposits extend less than 300 m from the beach towards the hinterland (MORTON et al. 2007). Moreover, wind induced inundations exhibit no significant backwash flows (MORTON et al. 2007), to which the lamination can be attributed to.

After the marine inundation and the deposition of the associated sediments fluvial and terrigenous conditions have been re-established. However, a 6 cm thick gravel intersection in the upper part of the sequence possibly refers to a second marine disturbance. The grain-size data indicate that the coarse layer was deposited under higher energetic conditions in contrast to the under- and overlying sediments. The coarse grain size distribution and fining upward tendency (Fig. 29) as well as the presence of foraminifera out of different habitats (Figs. 30 and 31) support the idea that the coarse intersection represents a second marine influence also caused by tsunami inundation.

Environmental interferences referring to repeated marine high-energy activity, as described for core ELA 6A drilled in the Vatika dry valley, are also documented by the stratigraphical record of vibracore BOZ 1, encountered in a comparable environment in about 30 km northwards of the Vatika Bay. Thereafter, the base of vibracore BOZ 1 is mainly characterized by brackish-lagoonal conditions which were proven by microfaunal analyses (Fig. 34). On top a coarse grained layer indicates rising energetic depositional conditions. An erosional discordance introduces the following marine fining upward sequence which contains several rip up clasts respectively intra-clasts as well as numerous mollusc fragments. The Ca/Fe-ratio points to the input of weakly weathered material. In addition, the presence of numerous gastropod fragments, shell debris as well as benthic littoral and planktonic open water foraminiferal species testify the marine origin and refers to extreme wave activity. Moreover, the described sedimentary characteristics of the high-energy deposit seem to be typical

for recent and historic tsunami events (CISTERNAS et al. 2005, MORTON et al. 2007, VÖTT et al. 2006, 2009a, 2009b, 2010, 2011a, 2011b, CHAGUÉ-GOFF et al. 2011, BAHLBURG & SPISKE 2012), similar as already described for the tsunami deposit found in core ELA 6A.

Between 1.37 and 0.90 m b.s.l. an allochthonous coarse-grained layer refers to a second marine inundation, showing sedimentary features of a tsunami deposit, which stratigraphically correlates to the lower tsunami layer detected in vibracore ELA 6A between 1.19 and 0.12 m b.s.l. This is obvious by regarding the changing values of the geochemical parameters at the height of the erosional discordance and upwards, pointing on a mixed signal out of limnic, terrestrial and most possibly marine components. Beside the sedimentary features, the marine origin is supported by the presence of marine microfossils, sea urchin spines and scores of gastropod fragments which appear first again in the allochthonous layer. Similar to vibracore ELA 6A, where a 6 cm thick intersection in the cores uppermost part most probably refers to another younger tsunami event, also core BOZ 1 shows in comparable stratigraphical position indications for a further later event. Thereafter, the Boza valley archive exhibits up to three tsunami event layers, whereby the two younger event layers can stratigraphically be compared over a distance of more than 30 km with the tsunami event layers found in the Vatika valley archive in core ELA 6A.

Regarding the radiocarbon age, our results indicate that the older tsunami deposit of core ELA 6A represents an event that must have hit Vatika Bay at or after 1467; 1618 cal AD. Accordingly, this event layer, which correlates to the second event found in core BOZ 1, does not represent the event layer encountered in the ELA 2-5 vibracore transect, which in turn correlates to the event layer described by SCHEFFERS et al. (2008) for vibracore ELA 1 that most probably refers to the well-known 365 AD event. Hence, the allochthonous and heterogeneous layer, which must have been deposited at or after 1467; 1618 cal. AD represent a further later event that hit the region around Vatika and Boza during historical times. Furthermore, this also implies that the youngest corresponding event deposits of vibracores ELA 6A and BOZ 1 characterize a tsunami event that affected the region after 1618 cal. AD.

In a summary view, this means that our results, together with those of SCHEFFERS et al. (2008), refer to up to four tsunami event generations affecting the coasts of southeastern Lakonia during the younger geological past. These are (i) the sandy event deposits encountered in core ELA 1 and in the vibracore transect ELA 2-5 ascribed most probably to the 365 AD event, (ii) the displaced boulders that refer to a transportation age around 1300 cal. AD, thus most probably pointing to the 1303 AD event, (iii) the tsunami event layers found in cores ELA 6A and BOZ 1 that refer to an event that happened at or after 1467; 1618 cal AD and (iv) a probable later and thus youngest event that must have affected the area after 1618 cal AD, whose deposits are to be found in cores ELA 6A and BOZ 1. Probably the oldest event generation, encountered in the basal section of vibracore BOZ 1,

corresponds to the sandy event layer found in the Viglafia archive which in turn points on the 365 AD event. However, further datings are required to prove this assumption.

Generally, the results indicate that the investigated near coast areas of southeastern Lakonia underwent long-term geomorphological changes during the younger geological past. However, the environments were repeatedly influenced during historical times by short-term extreme wave impact of tsunamigenic origin. Moreover, the here presented results show analogies with already described tsunami events which were detected along the coasts of the western Peloponnese, coastal Akarnania and the Ionian Islands of Cefalonia and Lefkada (VÖTT et al. 2006, 2009b, 2011b, HADLER 2014, WILLERSHÄUSER 2014).

5.6 Conclusions

Based on vibracorings in combination with sedimentological, geophysical, geochemical as well as microfaunal investigations in different near-coast geological archives in southeastern coastal Lakonia, the following conclusions can be drawn.

i. All stratigraphical records indicate an interruption of autochthonous depositional conditions by allochthonous sediments caused by tsunami impact. Storm induced extreme wave events are excluded as the local wind and associated wave regime of SE Lakonia is dominated by offshore winds and sedimentary marker horizons were found more than 300 m inland – a distance that is too far to be overcome for wind induced extreme waves.
ii. In addition, historical accounts clearly document that the region was repeatedly affected by tsunami activity during the past and recent tsunami catalogues point to a high tsunami hazard for the region of SE-Lakonia due to the direct exposure and close distance to the seismogenically active Hellenic Trench.
iii. Geomorphological structures such as the lobe-like shaped margin of the Viglafia Lagoon, wash-over fans and dislocated boulders, situated westward of Cape Skala, confirm the assumption of past tsunamigenic activity at Vatika Bay.
iv. At the Viglafia Lagoon, an event layer was detected extending more than 400 m inland with a clear thinning landward tendency correlating to an event deposit described by SCHEFFERS et al. (2008) caused by a tsunami at or after 134 – 380 cal AD. Based on these findings it seems likely that the event correlates to the well-known 365 AD tsunami that affected large parts of the eastern Mediterranean and whose deposits were detected along several coastal areas around Greece.

v. In the bays of Viglafia and Boza, high-energy deposits in corresponding stratigraphic positions were found with sedimentary characteristics typical of recent and sub-recent tsunamites such as basal erosional unconformities, fining upward sequences, rip up and intra-clasts, multi-modal grain size distribution and allochthonous microfaunal assemblages of shallow marine and deep sea species. Based on microfaunal evidence, it was possible to differentiate between torrential and marine high-energy deposits.

vi. A tsunami layer encountered at site ELA 6A, stratigraphically corresponding to the second tsunami layer of core BOZ 1, was deposited by an event at or after 1467; 1618 cal AD. A correlation to the 1303 AD tsunami detected by SCHEFFERS et al. (2008) near Vatika remains questionable. Hence, the Viglafia tsunami deposit most likely represents another younger event that affected Vatika Bay during or after the Renaissance period.

vii. In the uppermost parts of vibracorings ELA 6A and BOZ 1 always a further allochthonous sediment layer were to detect in stratigraphically corresponding positions, showing indications of a tsuanmi deposits. Based on our sedimentological, geochemical and microfaunal findings it can be argued that these layers probably refer to another and thus youngest high-energy wave event, although the signal is weak.

viii. Altogether, the presented results contribute to recent tsunami research in the area and broaden state of knowledge compared to previous studies. Although, archives of Holocene coastal changes in high resolution are scarce our studies in selected near-coast environs clearly show that the southeastern Peloponnese was repeatedly affected by tsunami events. The results fit well with studies conducted along the western coasts of the Peloponnese and the Ionian Sea.

Chapter 6 – Results from central Lakonia

Abstract: Central Lakonia is directly exposed to the Hellenic Trough, one of Europe's most seismically active and tsunamigenic regions. Aside from historical accounts on past tsunami events; the aim of this study was to search for geomorphological and sedimentological traces of palaeotsunamis in near-coast geological archives. Based on geophysical surveys, systematic stratigraphical studies were carried out in the Elos Plain in the Evrotas River delta using a multi-proxy approach.
Palaeotsunami signatures were searched along two south-north running vibracoring transects. Our methodological approach comprised sedimentological, geomorphological, geochemical, geochronological, microfaunal and geophysical investigations.
We identified three allochtonous marine-borne sediment layers intersecting autochthonous limnic-lagoonal deposits over a distance of up to two kilometers. These intersecting sheets out of allochthonous marine sand document repeated tsunami landfall in the Elos Plain.
The oldest tsunami signature encountered in the Elos Plain (T1) was radiocarbon dated to the time shortly after approximately 4400 cal BC. A second event occurred between approximately 1300 cal BC and 850 cal BC (T2), and a third one was dated to the time shortly before approximately 1450 cal AD (T3). The youngest event (T3) deciphered from the Elos Plain sedimentary record is a reasonable candidate for the historically known tsunami that occurred in 1303 AD associated to a strong earthquake. Events T1 and T2 occurred during prehistoric times; comparable findings in terms of sedimentary, geochemical and geochronological fingerprints are known from the Ionian Islands, northwestern Akarnania and the northwestern Peloponnese which allows to conclude that these events were of supra-regional nature.

6.1 Palaeotsunami history of the Elos Plain (Evrotas River delta, Peloponnese, Greece)

Lakonia is directly exposed to the seismogenically active Hellenic Trench. Historical accounts attest several strong earthquakes affecting the southern Peloponnese from which some of them were accompanied by tsunamis (e.g. 365 AD, 1303 AD, 1866 AD and 1867 AD (PAPAZACHOS & PAPAZACHOU 1997, PAPADOPOULOS et al. 2013,). Numerical simulations, for instance of the 365 AD Crete tsunami (SHAW et al. 2008), indicate that the coasts of the Lakonian Gulf are sensitive towards such seismic sea waves. In search of tsunami fingerprints within the geological record of the southern coastal Peloponnese, the alluvial Elos plain represents an ideal near-coast geological archive in back-beach position. The Elos Plain exhibits a thick Holocene sedimentary sequence in which geo-scientific fingerprints of past extreme wave activity were expected to be preserved. The main objectives of this study therefore were to (i) search for palaeotsunami signatures in the Elos Plain sedimentary record, (ii) to characterize palaeotsunami deposits based on a multi-proxy approach and (iii) to establish a local event-geochronostratigraphy to be compared with tsunami imprints of the wider region and beyond.

*A paper based on this chapter will be submitted for publication in the international journal *Zeitschrift für Geomorphologie N.F., Supplementary Issues* (authors: Konstantin Ntageretzis, Andreas Vött, Peter Fischer, Hanna Hadler, Kurt Emde, Björn Roman Röbke, Timo Willershäuser).

6.2 Geotectonic and natural settings

The vast Elos Plain was formed by the Holocene progradation of the Evrotas River delta within the Lakonian graben structure. The river is following a NNW to SSE trending tectonic depression (POPE et al. 2003). With a watershed of about 1.700 km^2 (KARAGIOZI et al. 2011), the Evrotas River represents one of the main fluvial systems of the Peloponnese. The karstic spring of the Evrotas River is situated south of Skortsinos in Arkadia. It is framed by the Taygetos Mountains in the west and the Parnon Mountains in the east. The Lakonia basin is dominated by the Sparta Fault system that is bound to the eastern flank of the Taygetos mountains front (2407 m above sea level). Based on seismic hazard mapping the Sparta fault zone is believed to produce destructive events every 1792 ± 458 years; since no mayor event has occurred since 464 BC, it is highly probable that the area will experience a strong seismic shock in the near future (PAPANIKOLAOU et al. 2013).

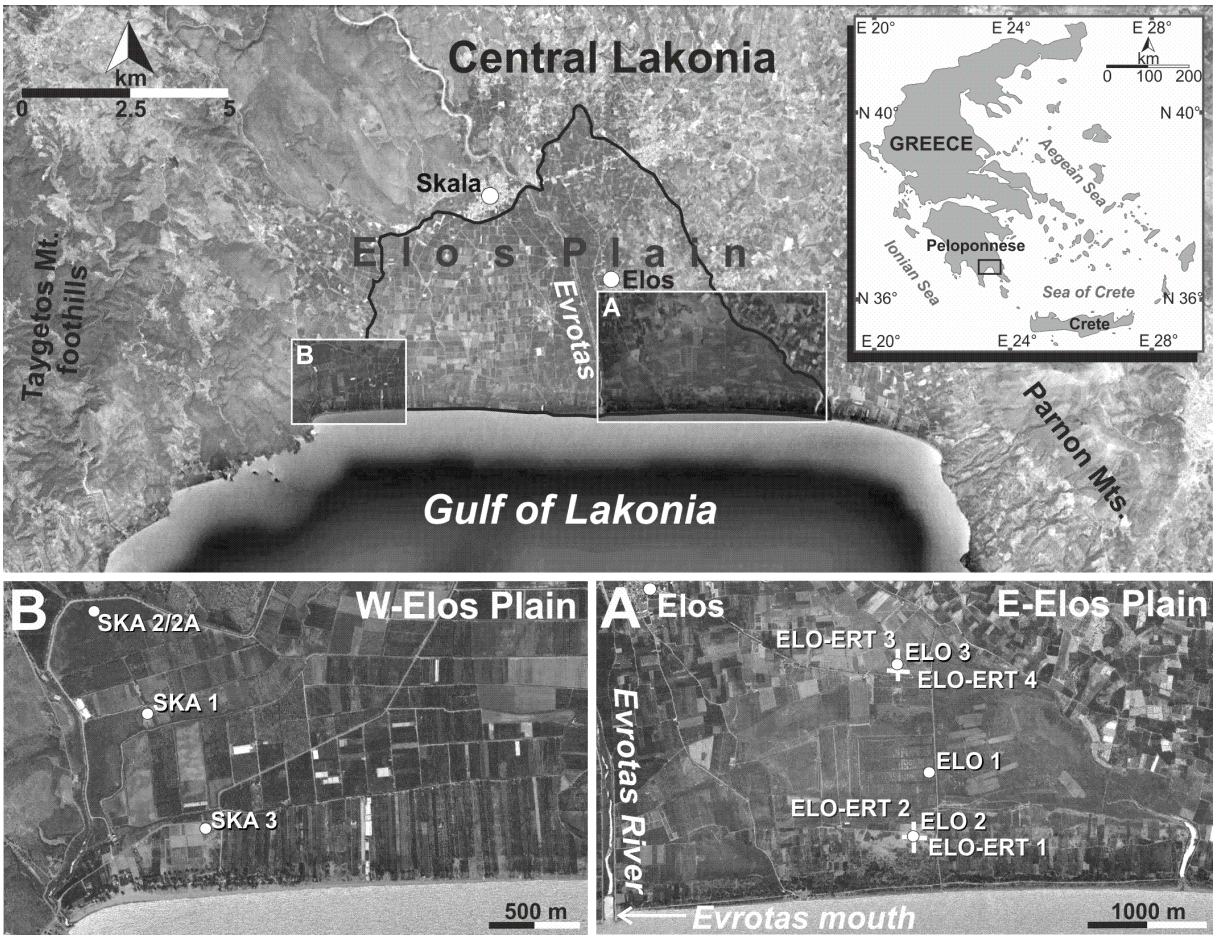

Figure 36: Overview of central Lakonia with the Evrotas River delta and its surroundings. The study area in the eastern Evrotas River delta is situated in the vicinity of the village Elos (A). The study area in the western Evrotas River delta is located close to the village of Skala (B) (source: own data and illustration 2014, maps based on Google Earth images/data, access May 2013).

In former times, the Evrotas River delta was much reduced in size and the Lakonian Gulf extended further north (KRAFT 1972). Toward the present, delta progradation caused a seaward shifting of the shoreline and formed a vast floodplain (KRAFT et al. 1977). Nowadays, the plain is limited by an

almost linear dune spit bordering the Lakonian Gulf to the north (KELLETAT 1974, KELLETAT & GRASSERT 1975). The width of the dune spit, anthropogenically strongly modified, varies between several tens and hundreds of meters. The Evrotas River is framed by Pliocene formations (marine, coastal and lacustrine sediments) towards the east and northeast, whereas the western and northwestern sections are characterized by alternating units of the Tripolis zone, containing Jurassic limestones and Triasssic dolomites, as well as the Permian Tyros beds (IGME 1989).

For this study, we selected two target areas which were investigated in search of tsunami-fingerprints. In the eastern part of the Elos Plain, three vibracores (ELO 1, 2 and 3) were drilled along a N-S trending transect (Fig. 36 A). In the western Evrotas River delta, vibracores SKA 1, 2, 2A and 3 were also drilled along a N-S running transect (Fig. 36 B).

6.3 Methods

We used a multidisciplinary approach in order to detect sedimentary palaeotsunami fingerprints within the near-coast stratigraphical record of the investigation sites.

Vibracores (6 open cores and 1 plastic inliner core) were retrieved from the eastern and western parts of the alluvial Elos Plain by means of an Atlas Copco mk1 corer using core diameters of 6 and 5 cm. The sediment cores were cleaned, photographed and described based on geomorphological and sedimentological criteria, such as sediment color, grain size distribution, texture, carbonate content and pedogenetic features (AD-HOC-ARBEITSGRUPPE BODEN 2005). Geochemical studies in the laboratory were realized using sediment material sampled in field.

Laboratory studies included the analysis of the organic content by loss on ignition (550°C), the measurement of pH-value, electric conductivity and the content of calcium carbonate using the *Scheibler-method* (BLUME et al. 2011). X-ray fluorescence analyses of sediment samples yielded concentrations of 30 different elements using a *Thermo Niton instrument (type Xl3t 900S GOLDD*, calibration mode SOIL).

Moreover, macro- and microfaunal analyses of selected sediment samples were carried out for facies determination. Species identification and information about the related habitats were established on the basis of the literature of VESPER (1972), HEIP (1976), HERMAN & HEIP (1982), LOEBLICH & TAPPAN (1988), CIMERMANN & LANGER (1991), MURRAY (1991), DELAMOTTE & VARDALA-THEODOROU (2001), GOFAS et al. (2001), GROSS (2001), RÖNNFELD (2008), HAYWARD & GROSS 2011, BRANDÃO & HORNE (2013) and HAYWARD (2013) The material (approximately 15 cm^3) was preprocessed with H_2O_2 (30%) and afterwards wet sieved to segregate fractions of < 400 µm, 200-400 µm, 125-200 µm and < 125 µm. Foraminifera, ostracods, bivalves and gastropods were collected from the samples using a Nikon SMZ-74St stereoscope (binocular) with an optional tenfold to fortyfold magnification. For

documentation the discovered specimens were isolated, selected and finally put into Krantz-cells. Individual specimens and/or specimen assemblages were photographed using a light-polarized DS-Fi2 Nikon camera mounted on a Nikon Eclipse 50-POL polarization microscope. The microfossil content was recorded semi-quantitatively using a scale from 0 to 6 [0 = none; 1 = very rare/singular (1 sp.); 2 = rare (2-3 spp.); 3 = few (up to 6 spp.); 4 = fairly many (up to 9 spp.); 5 = many (up to 12 spp.); 6 = a great many (more than 12 spp.)].

Electrical resistivity tomography (ERT) measurements were carried out in order to detect local subsurface conditions such as stratigraphical aspects and the depth of the bedrock using a multi-electrode geoelectrical instrument (*IRIS Instruments*, type Syscal R1+ Switch 48). We used a Wenner-Schlumberger array with 48 electrodes and an electrode spacing of 2 m and 1.5 m. Depth sections were calculated using the RES2Dinv software.

A *Topcon HiperPro FC-200* differential GPS (accuracy ± 2 cm) was used to measure positions of vibracoring sites and ERT transects.

A local event-geochronostratigraphy was established based on ^{14}C-AMS dating of organic material and biogenic calcium carbonate. We used the calibration software Calib. 6.0 to calculate calendar ages (REIMER et al. 2009). ^{14}C-AMS dating was conducted by the Leibniz Laboratory for Radiometric Dating and Isotope Research, Christian-Albrechts-Universität zu Kiel (Kia, Germany) and by the Beta Analytic Radiocarbon Dating Laboratory Miami (Beta, USA).

6.4 Results

6.4.1 Sedimentological traces of extreme wave impact on the eastern Elos Plain

6.4.1.1 The Elos vibracore transect

Vibracores ELO 2 (36°48’34.77’’ N, 22°43’29.42’’ E), ELO 1 (36°48’52.16’’ N, 22°43’40.90’’ E) and ELO 3 (36°49’22.86’’ N, 22°43’28.05’’ E) were drilled along a N-S running transect to the east of the Evrotas River (Fig. 36, A).

The sedimentary sequence of vibracore ELO 1 begins with alternating clayey and sandy deposits (Figs. 37 and 38). At 7.96 m b.s.l., an erosional contact leads over to a fining upward sequence, starting with sand and gravel (7.96-6.94 m b.s.l.), including numerous marine mollusc fragments. Subsequently, several coarse sand layers were found that pass over into limnic-lagoonal clay deposits. At 5.17 m b.s.l., another erosional unconformity marks the abrupt input of allochthonous sand showing a heterogeneous composition. At 4.35 m b.s.l. limnic-lagoonal sediments re-appear but were again interrupted at 3.08 m b.s.l. by two fining upward sequences out of coarse-grained material of marine origin. An erosional contact and several rip up-clasts from the underlying material

refer to high-energy inundation. Towards the top, limnic-lagoonal conditions were re-established after the impact. The top of the core is made out of anthropogenic infill.

Figure 37 summarizes the results of grain size analyses and geochemical analyses conducted for samples from core ELO 1. High-energy deposits come along with a significant peak in the S/(U+T)-ratio indicating an interruption of autochthonous low-energy conditions. Also, they show a multimodal grain size distribution and fining-upward tendencies. Coarse-grained intersections are further characterized by decreased potassium concentrations indicating a temporary interruption of the prevailing eutrophic conditions in the autochthonous low-energy quiescent environment.

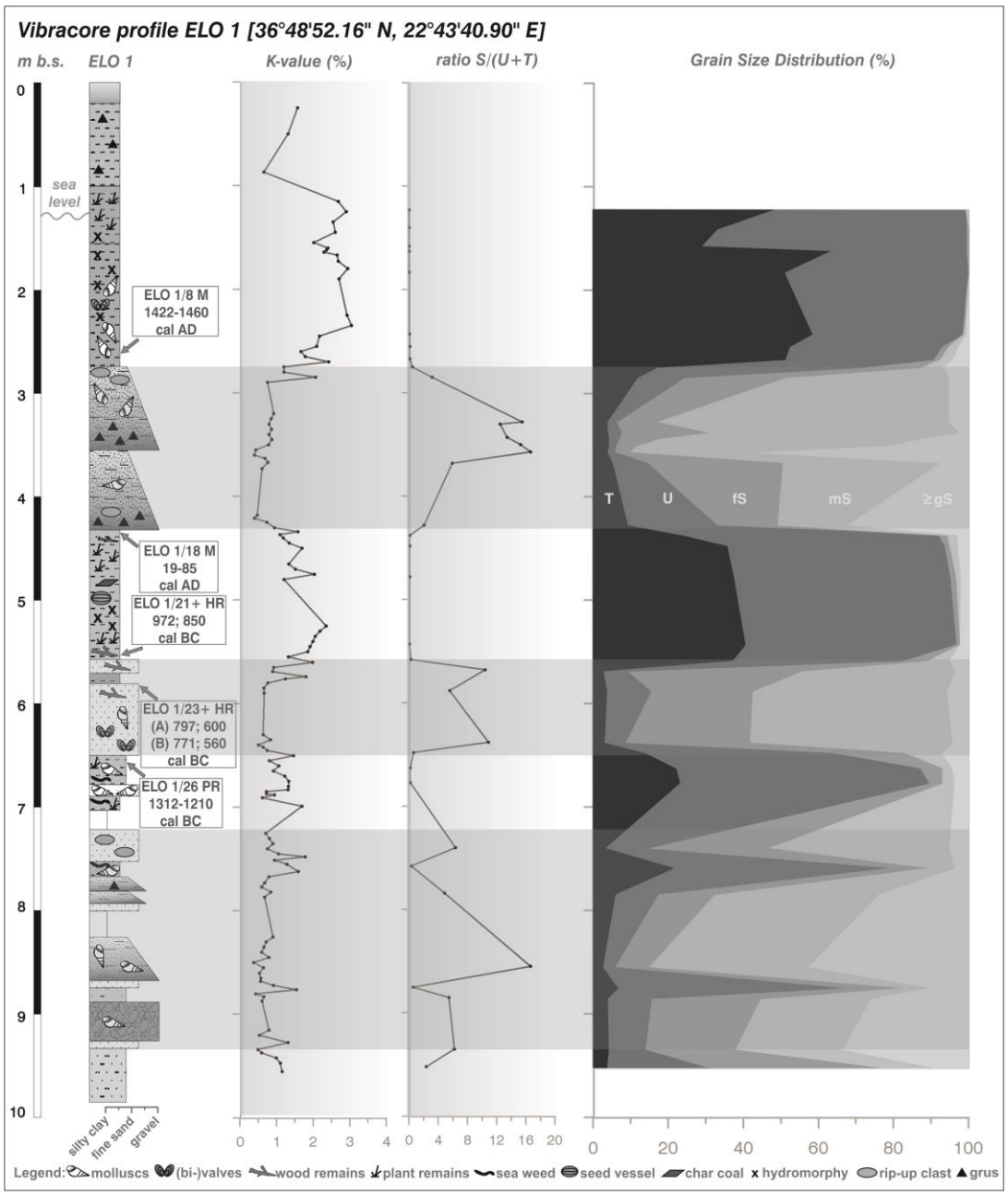

Figure 37: Stratigraphy, geochronological data, potassium values and grain size data of vibracore ELO 1 drilled in the eastern Elos Plain (source: own data and illustration 2013).

The stratigraphical record of vibracore ELO 2 starts with fine sand that partly contains marine mollusc fragments (Fig. 38). From 3.13 m b.s.l. upwards, the sand becomes coarser, and from 2.38 m b.s.l. it is covered by heterogeneous sand containing laminae out of coarse sand and fine gravel. Furthermore, grus and mollusc fragments were detected. The following thick sand layer (0.78 m b.s.l. - 1.13 m a.s.l.) is made out of medium sand partly containing coarser laminae as well as gravel and agglutinated sand grains. Towards the top, we found well-sorted fine sand presumably of aeolian origin.

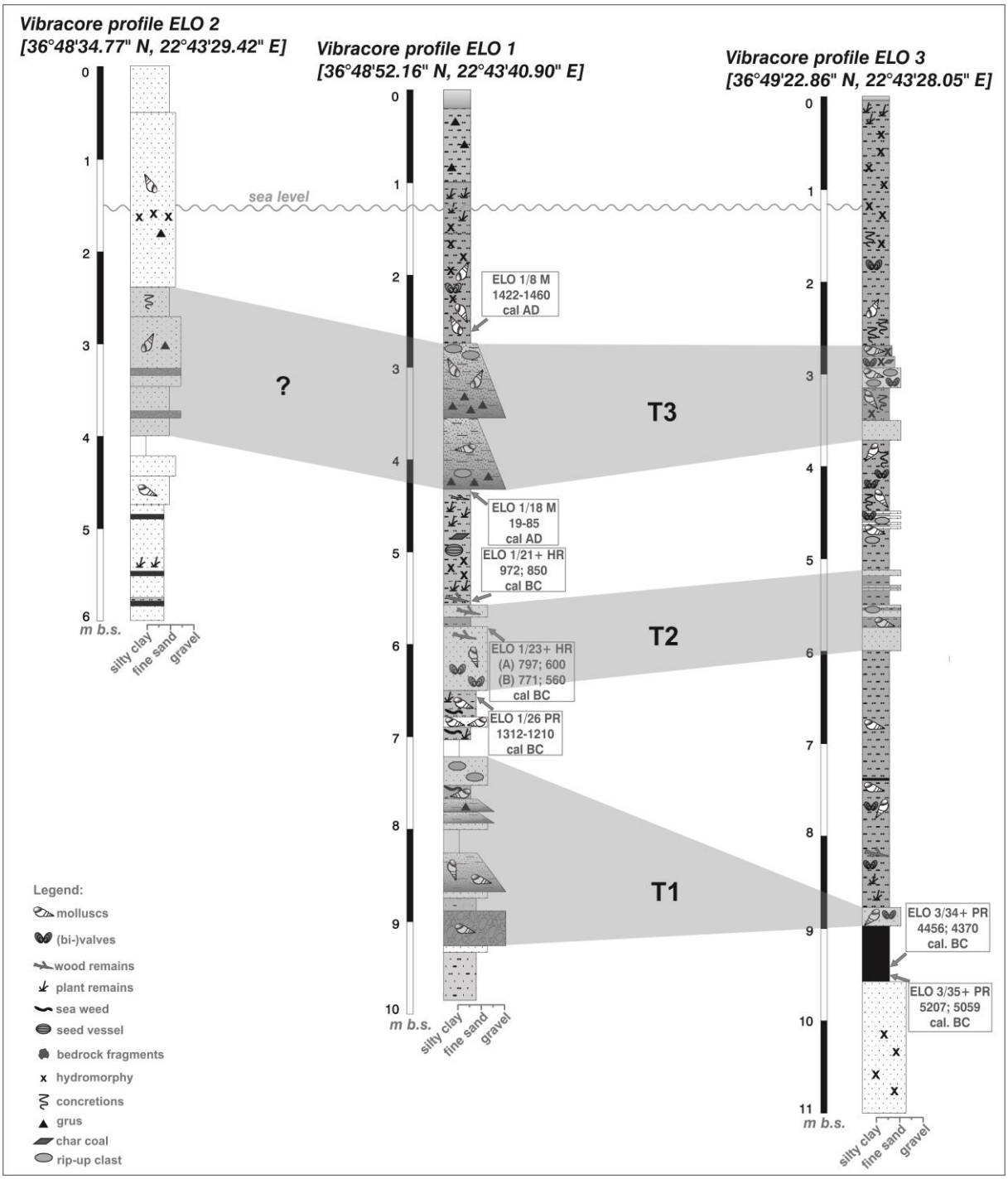

Figure 38: Results of the ELO vibracore transect drilled from southern to northern direction eastward from river Elos. The event layers can be correlated over a distance of nearly 2 km (source: own data and illustration 2013).

At the base of vibracore ELO 3, we found well sorted fine sand (9.88-8.46 m b.s.l., Fig. 38), followed by a black peat layer (8.46-7.87 m b.s.l.). The latter is abruptly covered by a sand layer, 20 cm thick, containing marine bivalve fragments (7.87-7.67 m b.s.l.). Subsequently, we found a thick section out of grey clay which was deposited in a lagoonal low-energy near-coast environment. This unit shows two sandy intersections at 4.83-4.40 m b.s.l. and 2.55-1.72 m b.s.l. marked by erosional unconformities and associated with rip up-clasts out of underlying material.

In a summary view, the ELO vibracore transect (Fig. 38) shows the following stratigraphical and sedimentary characteristics:

(i) Vibracores ELO 1 and ELO 3 are mainly characterized by autochthonous silty to fine sandy sediments deposited in a quiescent limnic to lagoonal environment in back-beach position.

(ii) This low-energy environment was repeatedly affected by the input of heterogeneous, unsorted coarse-grained high-energy deposits which include fragments of marine macrofauna and are characterized by fining upward cycles, rip up clasts out of underlying material and sharp erosional unconformities which are typical of sea-borne high-energy wave events.

(iii) Distinct high-energy layers were found in consistent stratigraphical positions over a distance of more than 2 km documenting a thinning landward tendency.

6.4.1.2 Microfossil analyses

Altogether 25 sediment samples were selected from core ELO 1 and studied for their content of foraminifera, ostracods, bivalves and gastropods. Thereby, it was possible to identify 58 different species. The results are summarized in Figure 39.

At the base of the core (samples ELO 1/36 and ELO 1/35), a numerous miliolida were found such as *Adelosina* sp., *Cycloforina* sp., *Miliolinella* sp., *Pseudotriloculina* sp., *Quinqueloculina* sp. and *Spiroloculina* sp. Furthermore, many benthic specimens of the order of rotaliida were encountered such as *Ammonia beccarii*, *Ammonia tepida*, *Ammonia sp.*, *Elphidium acculeatum*, *Elphidium crispum.* Also, we found abundant shell debris, some specimens of the bivalve *Yoldiella messanensis* and the gastropod *Pirenella* sp., a spine of a sea urchin and few specimens of the ostracod *Cyprideis torosa.* These micro-and macrofossil data document quiescent shallow marine near-coast conditions for the basal part of the core.

The microfossil record of the following fining upward unit (sample ELO 1/34) is clearly enriched by additional marine species such as *Cibicides* sp., *Haynesina* sp., *Lobatula lobatula* as well as

Asterigerinata sp. In its upper part (sample ELO 1/32) abundance of species is reduced but additional planktonic foraminifera (Globigerinidae) such as *Orbulina universa* were found. This sedimentary unit thus comprises a distinct mixture of species that occur in different environments, namely open marine, shallow marine to littoral as well as lagoonal or brackish environments.

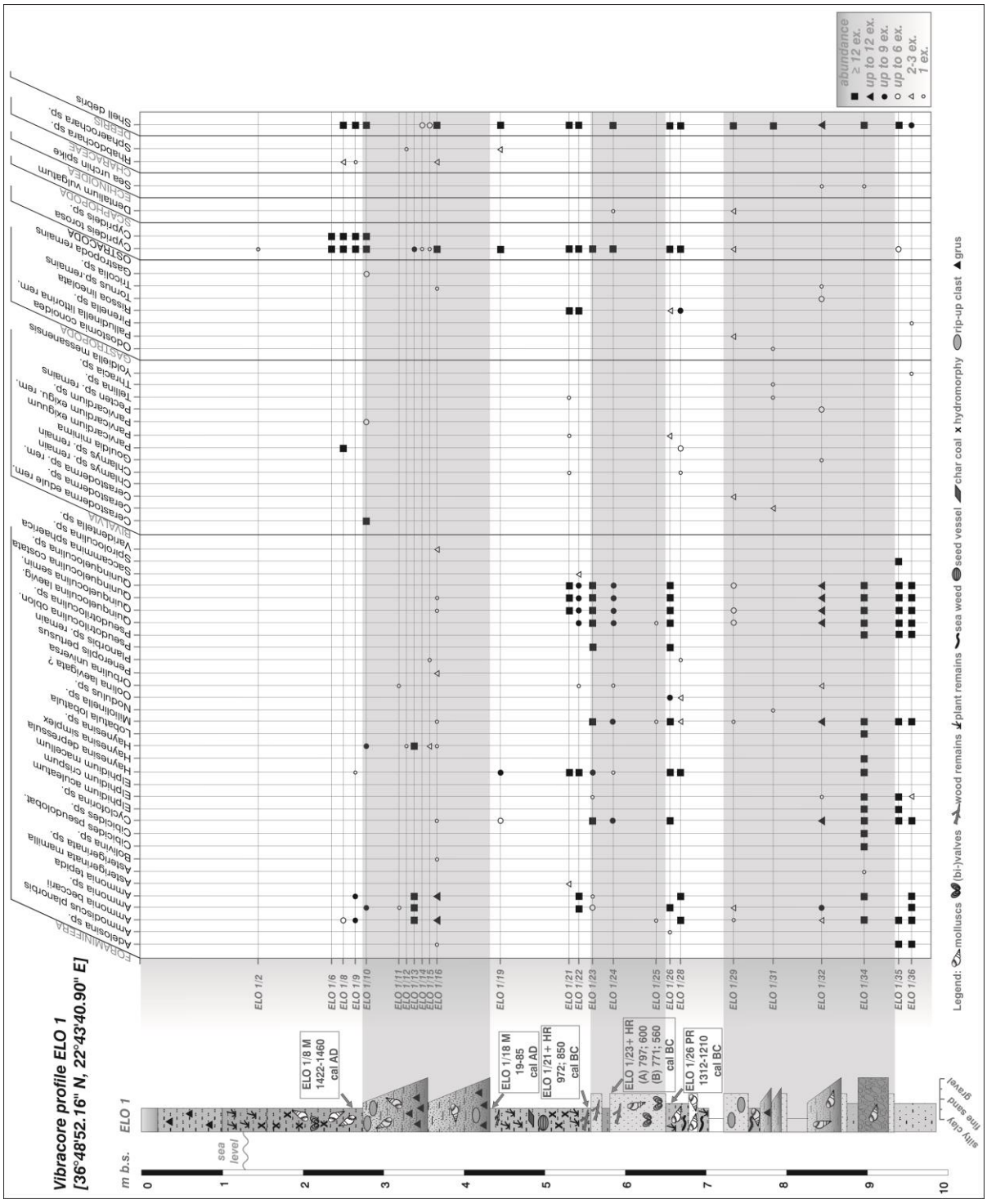

Figure 39: Results of the conducted micro- and macrofossil analyses of key core ELO 1 encountered in the eastern Elos Plain (source: own data and illustration 2013).

The subsequent samples ELO 1/31 and ELO 1/29 mirror a clear change towards quiescent lagoonal conditions characterized by a strongly reduced biodiversity of species and low abundances.

Samples ELO 1/28, ELO 1/26 and ELO 1/23, retrieved from intersecting high-energy sand layers, however, again show strongly mixed fully marine and lagoonal species such as *Haynesina* sp., *Quinqueloculina* sp. and *Cyprideis torosa,* respectively. Samples ELO 1/25 and ELO 1/24 show a reduced spectrum of foraminifera and ostracods compared to the underlying and overlying strata. However, a single specimen of the planktonic foraminifera *Orbulina universa* (Globigerinidae) was found.

Samples ELO 1/22 and ELO 1/21 document quiescent lagoonal conditions although some distinct open marine species such as *Quinqueloculina* sp. are present. Sample ELO 1/19 shows almost no more foraminifera, with the exception of only rare respectively few species of *Cycloforina sp.* and *Haynesina depressula*, but simultaneously a great many ostracod species of *Cyprideis torosa* indicating quiescent brackish conditions. However, the two following fining upward sequences again show 14 different foraminiferal species of fully marine indication in varying abundances (samples ELO 1/16 to ELO 1/10). Remains of *Cerastoderma edule* and abundant shell debris were found besides few specimens of *Parvicardium exiguum* and two algae species (Characeae). Also, a specimen of the planktonic foraminifera *Orbulina universa* was found within this sandy deposit. Samples from the overlying silty clay (samples ELO 1/9 and ELO 1/8) are dominated by the ostracod *Cyprideis torosa* indicating freshwater to brackish conditions. Only few foraminifera species such as *Ammonia* sp. were found altogether documenting quiescent brackish to limnic conditions.

Detailed micro- and macrofaunal studies thus showed that autochthonous quiescent lagoonal deposits were repeatedly interrupted by high-energy sand and gravel from the seaside associated with a distinct mixture of foraminifera species originating from deep sea open marine to shallow water lagoonal environments.

6.4.1.3 Radiocarbon dating results

Altogether 7 samples were dated by means of the ^{14}C-AMS dating technique in order to establish a local event-geochronostratigraphy. Plant material or wood remains were preferably sampled instead of marine material in order to avoid marine reservoir effects, the fluctuations of which in time and space (sedimentary environments) are still unknown (VÖTT et al. 2011b). Radiocarbon dates obtained for cores ELO 1 and ELO 3 are summarized in Table 3 and depicted in Figures 37 and 38. All radiocarbon dates were measured in the Leibniz Laboratory for Radiometric Dating and Isotope Research, Christian-Albrechts-Universität zu Kiel (Germany).

Sample name (Lab. No.)	Depth (m b.s.)	Depth (m b.s.l.)	Sample description	$\delta^{13}C$ (in ‰)	^{14}C age (BP)	1σ max; min (cal BC/AD)
ELO 1/8 M (KIA 45980)	2.66	1.41	mollusc* (marine shell)	-0.38±0.11	900±25*	1422 - 1460 cal AD
ELO 1/18 PR (KIA 45981)	4.38	3.13	plant remains	-26.15±0.15	1945±30	19 - 85 cal AD
ELO 1/21+ HR (KIA 45982)	5.47	4.22	wood remains	-23.62±0.11	2770±25	972; 850 cal BC
(A) ELO 1/23+ HR (KIA 45983)	5.76	4.51	wood remains	-25.76±0.29	2555±25	797; 600 cal BC
(B) ELO 1/23+ HR (KIA 45983)	5.76	4.51	wood remains	-26.37±0.18	2515±25	771; 560 cal BC
ELO 1/26 PR (KIA 45983)	6.48	5.23	plant remains* (sea weed)	-13.25±0.27	3346±27*	1313 - 1210 cal BC
ELO 3/34+ PR (KIA 45985)	9.32	8.20	plant remains	-27.38±0.25	5595±30	4456; 4370 cal BC
ELO 3/35+ PR (KIA 45986)	9.57	8.45	plant remains	-28.30±0.17	6165±30	5207; 5059 cal BC
SKA 1/4+ PR (Beta 231496) [b]	1.29	2.10	plant remains	-26.8	1370 ± 40	632 - 681 cal AD
SKA 1/6+ PR (Beta 231497) [b]	1.76	2.44	plant remains	-26.0	1240 ± 50	689 - 860 cal AD
SKA 1/14+ PR (Beta 23149) [b]	3.97	4.78	plant remains	-26.9	4880 ± 40	3695 - 3641 cal BC
SKA 2/5+ PR (KIA 46018) [a]	1.66	1.49	plant remains	-23.78 ± 0.26	950 ± 20	1030; 1150 cal AD
SKA 2/8+ PR (KIA 46019) [a]	1.82	1.65	plant remains	-23.40 ± 0.32	>1954 AD	>1954 AD

Table 3: Radiocarbon dates of samples from vibracores ELO 1 and ELO 3 drilled in the eastern part of the Evrotas River delta, and of samples from vibracores SKA 1 and SKA 2 drilled in the western part of the Evrotas River delta, in in the central Lakonian Gulf (Peloponnese – Greece). (Lab. No.) – laboratory number Leibniz Laboratory for Radiometric Dating and Isotope Research, Christian-Albrechts-Universität zu Kiel (Germany); m b.s. – meter below surface; m b.s.l – meter below sea level; (a) $\delta^{13}C$-value – shows incorporation of C4 plants or aquatic material and indicates a potential reservoir effect; (b) $\delta^{13}C$-value – indicates purely atmospheric C3 photosynthesis without contamination by old carbon; * – marine reservoir correction with 400 years of reservoir age; 1σ max; min (cal BC/AD) – calibrated ages, 1σ-range; ";" – semicolon is used in cases where several age intervals because of multiple intersections with the calibration curve are possible; oldest and youngest age depicted; Calibration is based o6n the software Calib 6.0 (REIMER et al. 2009).

The wood fragment of sample ELO 1/23+ HR was extracted with 1 % HCl, 1 % NaOH at 60 °C and then again with 1 % HCl (lye residue). As a control always two portions of the treated sample material, in this case the lye residue, were burned to CO_2 and finally measured. Thereafter, two age intervals (A and B) were calculated yielding two similar age intervals of 797; 600 cal BC (A) and 771; 560 cal BC (B), respectively. Ages obtained for samples ELO 1/8 M and ELO 1/26 PR, an articulated specimen of *Cerastoderma glaucum* and seaweed remains, respectively, were calibrated using the marine dataset. In this study, 1σ intervals (confidence interval 68.3%) instead of 2σ -intervals (confidence interval 95.4 %) are given in order to make aware that the physical dating accuracy must not be

overestimated to the disadvantage of the sedimentological and geomorphological dating accuracy (VÖTT et al. 2011c).

6.4.1.4 Electrical resistivity measurements

At vibracoring site ELO 2, two ERT transects were applied on flat to slightly sloping sandy ground close behind a dune ridge. Transect ELO ERT 1 runs from E to W parallel to the coastline (Fig. 36 A). Three subsurface units can be identified (Fig. 40). The first unit between 1 m and 0 m above present sea level (a.s.l.) shows resistivity values between 80 to 400 Ωm and seems to represent the upper part of the local dune made out of fine sands. The second unit exhibits values between 20 to 80 Ωm between 0 m a.s.l. and 4 m b.s.l. The third unit with values between 20 and 1 Ωm most probably represents shallow marine fine sand encountered below 4 m (b.s.l.). However, also the influence of (salty) groundwater must be taken into account. Transect ELO ERT 2, running from N to S, shows similar results (Fig. 40) both of them clearly reflecting the stratigraphical units found in vibracore ELO 2 (Fig. 38).

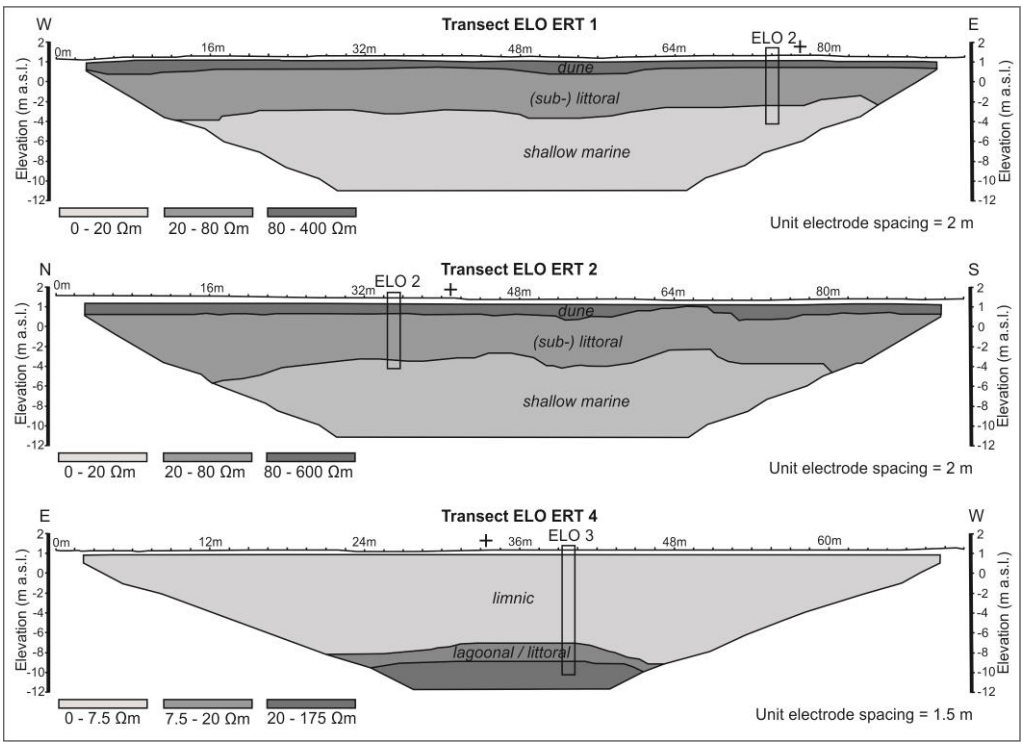

Figure 40: Interpreted and simplified diagrams of west-east running ERT transect ELO ERT 1, of north-south running ERT transect ELO ERT 2, both measured at vibracoring position ELO 2 on sandy ground behind the recent dune wall of the eastern Elos Plain, and of east-west running ERT transect ELO ERT 4, measured at vibracoring position ELO 3 and crossing transect ELO ERT 3 at c. meter 30. The crosses "+" mark the crossing points with other ERT transects. In each case a Wenner-Schlumberger array with 48 electrodes was applied. Electrode spacings were of 2 m and 1.5 m. All computed pseudosection models were based on the 7th iteration creating absolute errors of 1.3 % for ELO ERT 1, of 2.6 % for ELO ERT 2 and of 1.2 % for ELO ERT 4 (source: own data and illustration 2013).

Transect ELO ERT 3 trends from S to N and transect ELO ERT 4 from E to W in the environs of coring site ELO 3. The ERT data clearly depicts basal marine sand encountered in core ELO 3 and overlying peat with resistivity values > 7.5 Ωm whereas the subsequent thick sequence of lagoonal mud is

characterized by strongly reduced resistivity values (Fig. 40). However, the resolution of the ERT depth sections does not allow detecting intersecting thin high-energy sand and gravel layers.

6.4.2 Sedimentological traces of extreme wave impact on the western Elos Plain

6.4.2.1 The Skala vibracore transect

In the southwestern part of the Elos Plain near Skala, vibracores SKA 3 (36°48'29.99'' N, 22°37'37.98'' E, ground surface at 1.91 m a.s.l.), SKA 1 (36°48'53.20'' N, 22°37'27.06'' E, ground surface at 0.89 m b.s.l.) as well as SKA 2 and SKA 2A (open core and closed inliner core; 36°49'11.77'' N, 22°37'13.06'' E, ground surface at 0.17 m a.s.l) were drilled along a S-N running transect between the present coastline and the adjacent mountain foothills (Fig. 36 B).

The base of vibracore SKA 3 shows a sequence of fine to coarse sand including marine mollusc fragments and fine gravel (Fig. 41). From 3.99 m upwards, the sediment becomes finer and the number of mollusc fragments decreases in favor of plant and wood remains. At 1.95 m b.s.l., a distinct erosional discontinuity was detected leading over to fining upward sequences out of gravel and coarse to medium sand between 1.95 m and 0.74 m b.s.l. that intersect well sorted homogenous fine sand. Within these sequences, we found many mollusc fragments, pieces of grus as well as sand lenses. The top of the profile is characterized by a thick unit of homogeneous fine sand with hydromorphic features.

Vibracore SKA 1 starts with fine sand that contains organic layers and marine mollusc fragments (Fig. 41). Between 4.81 and 4.76 m b.s.l. a peat layer, containing fruit capsules and remains of freshwater gastropods, documents an environmental change towards semi-terrestrial conditions. Between 4.76 m and 3.24 m b.s.l., we found again fine sand including hydromorphic features, calcareous nodules and traces of root penetration. Between 3.24 m and 2.20 m b.s.l., clayey silt was encountered containing numerous marine shell fragments and a ceramic fragment. The top of this unit shows a layer of organic silt, 10 cm thick, which is unconformably covered by medium and fine sand. Numerous marine mollusc fragments document the marine origin of this sand. At 1.50 m b.s.l., a peat layer was found including freshwater gastropods, showing that low-energy swampy conditions were re-established in back-beach position. From 1.32 m b.s.l. to the top (0.89 m b.s.l.), a man-made infill layer was detected.

At the base of vibracore SKA 2 (5.83-3.97 m b.s.l.), we encountered weathered bedrock covered by clayey silt including thin peat layers (Fig. 41). At 1.83 m b.s.l., clayey silt rich in organic material indicates that environmental conditions changed towards (semi-)terrestrial. This low-energetic swampy environment was disturbed by the input of a layer of marine medium and fine sand, 13 cm thick, showing a clear fining upward tendency. A distinct erosional discordance at 1.63 m b.s.l.

documents the strong erosional dynamics and the high-energy characteristics of this process. This allochthonous sediment layer is located in consistent stratigraphical position compared to high-energy marine deposits found at vibracoring sites SKA 3 and SKA 1. From 1.50 m b.s.l. towards the top, low-energy peat deposits were encountered partly containing silt laminae.

In a summary view, our results show that along the SKA vibracore transect (Fig. 41) there are significant discrepancies between autochthonous mud or fine sand deposits and intercalating allochthonous medium to coarse sand of marine origin. The latter refer to abrupt short-term high-energy geomorphodynamic interferences of low-energy near-coast or littoral environments.

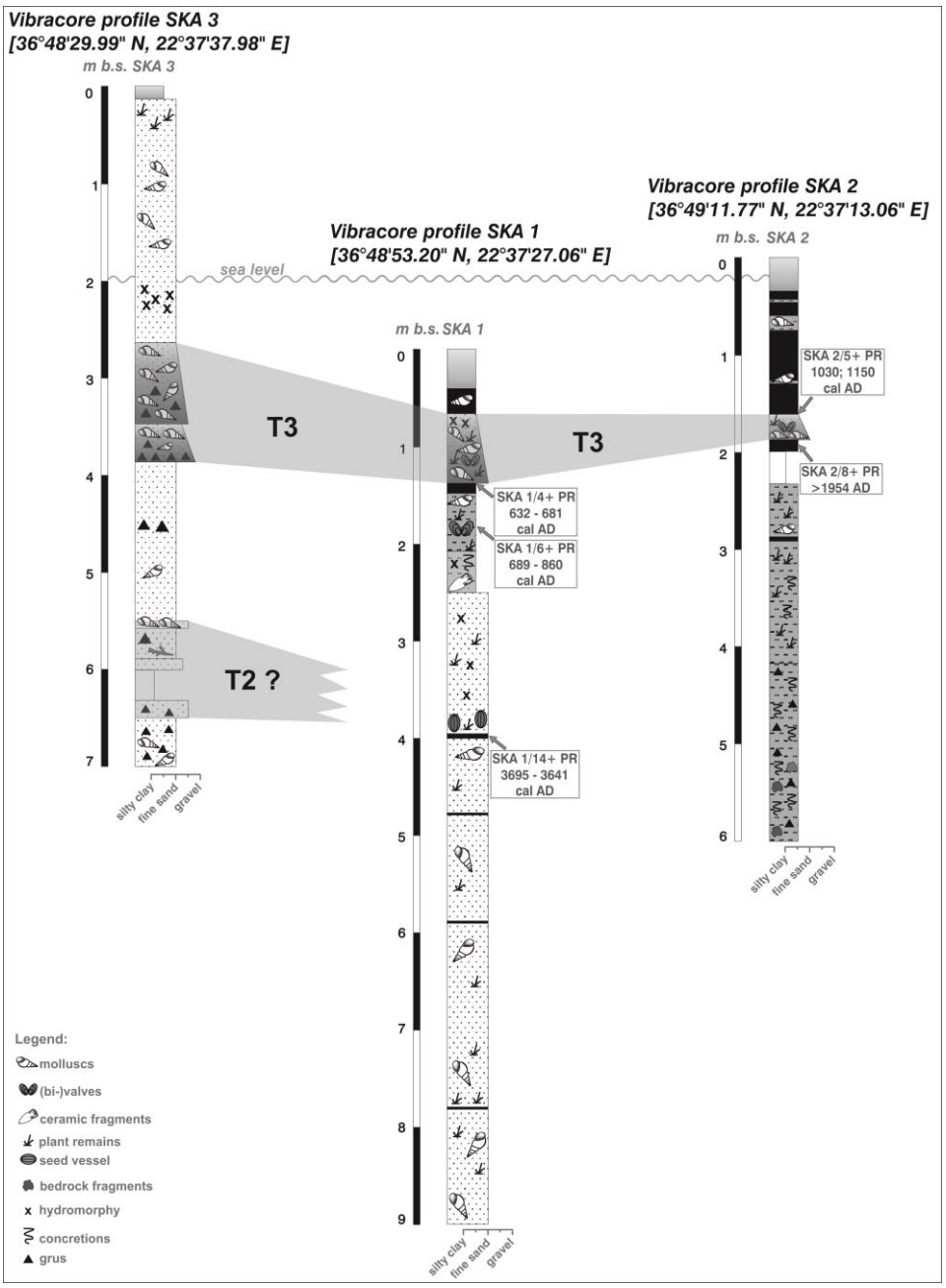

Figure 41: Results of the SKA vibracore transect drilled from southern to northern direction westward from river Elos. The event layer can be correlated over a distance of more than 1.7 km (source: own data and illustration 2014).

6.4.2.2 Microfossil analyses

We studied 13 samples from vibracores SKA 2 and SKA 2A for their micro- and macrofossil contents. The results are summarized in Figure 42.

The basal units of vibracore SKA 2 (sample SKA 2/17) show few specimens of *Ammonia* sp., *Elphidium* sp., and spines of sea urchins which, according to recrystallization and weathering features, seem to originate from the local bedrock. In the peat layer between 1.66 and 1.73 m b.s.l. (sample SKA 2/9), we found many remains of the freshwater snail *Planorbis planorbis,* typical of ponds, swamps or lakes with slow moving or stagnant waters (CONCHOLOGICAL SOCIETY OF GREAT BRITAIN AND IRELAND 2010, SEDDON & VAN DAMME 2012), as well as few specimens of *Cyprideis torosa* which is an extremely common and widespread species typical of shallow, quiescent brackish to even freshwater conditions where large amounts of organic detritus is present (HERMAN & HEIP 1982, VESPER 1972, HEIP 1976).

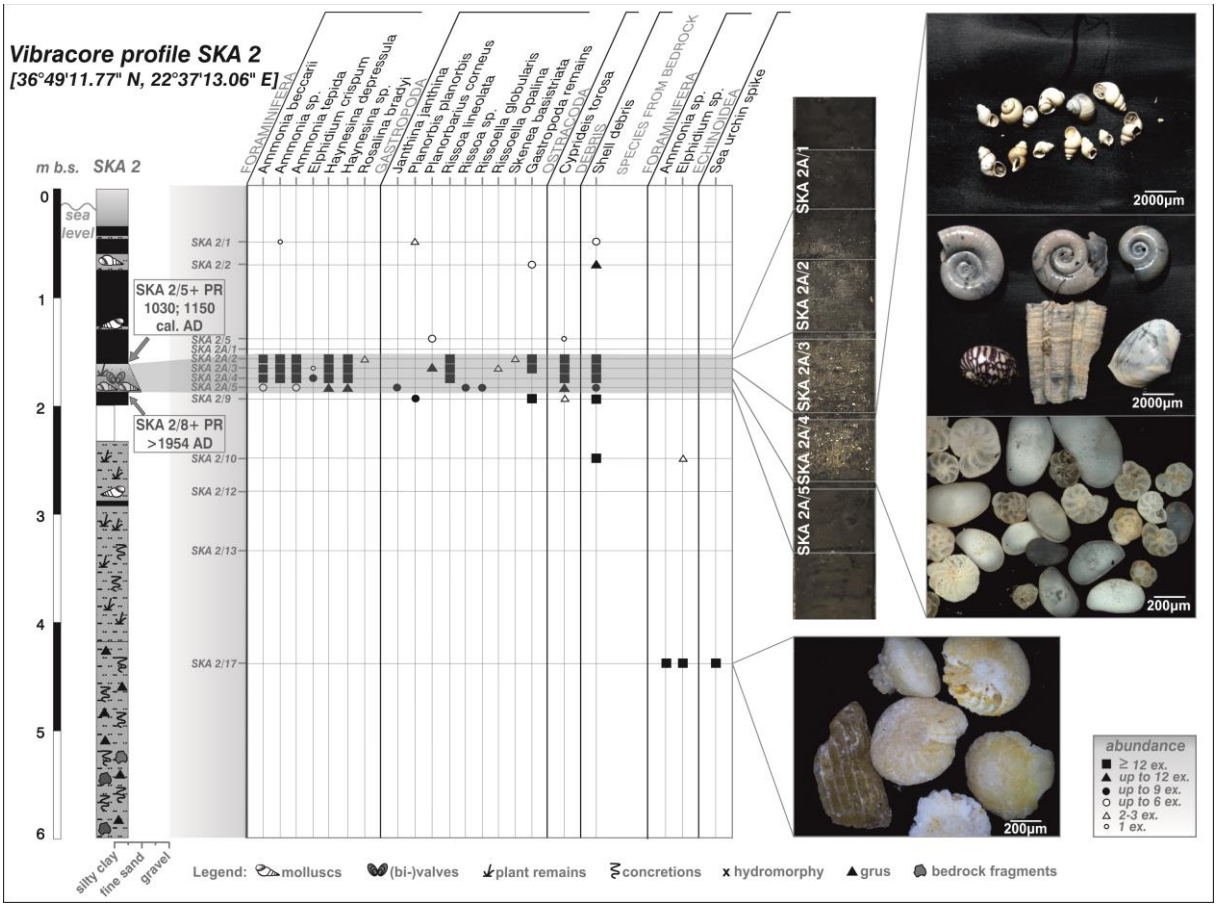

Figure 42: Results of the conducted micro- and macrofossil analyses of key core SKA 2 respectively 2A. The species found in the cores lower part clearly indicate recrystallization features and thus considerably differ from the species found in the layer between 1.63 and 1.50 m b.s.l. (source: own data, pictures and illustration 2013).

On the contrary, the high-energy sand layer intersecting quiescent mud deposits between 1.63 m and 1.50 m b.s.l. is characterized by many different foraminifera species such as *Ammonia* sp., *Elphidium* sp., *Haynesina* sp. and *Rosalina* sp. all of them without recrystallization features and thus of Holocene age (samples SKA 2A/5 to SKA 2A/2, Fig. 42). Furthermore, the samples contained a

many specimens of *Cyprideis torosa* and different marine gastropod species. The ecological spectrum of foraminifera species thus comprises a wide range from brackish to shallow marine and inner shelf environments. Furthermore, many specimens of the holopelagic gastropod *Janthina janthina* from the pleuston and adapted to surface dwelling (VAN DER SPOEL et al. 1997) were found.

Micro- and macrofossil data from the sand layer document the marine origin of the sediment; strong mixing of species from different environments proves that the material was accumulated within the course of a high-energy event.

Sample SKA 2A/1, taken from the top-core peat unit was void of micro- or macrofossils. Further towards the top (samples SKA 2/2 and SKA 2/1, Fig. 42), the presence of *Planorbarius corneus* and *Cyprideis torosa* reflect that the quiescent environment was re-established after the extreme event.

6.4.2.3 Geochronostratigraphical results of the SKA vibracore transect

Three samples from vibracore SKA 1 and two samples from core SKA 2 were dated using the ^{14}C-AMS technique. Only plant remains were used in order to avoid marine reservoir effects. The radiocarbon dates are listed in Table 3.

6.4.3 Excursus: Sedimentological and geophysical investigations in the marshy back-beach area of Valtaki Bay near the Trinisa Island Group

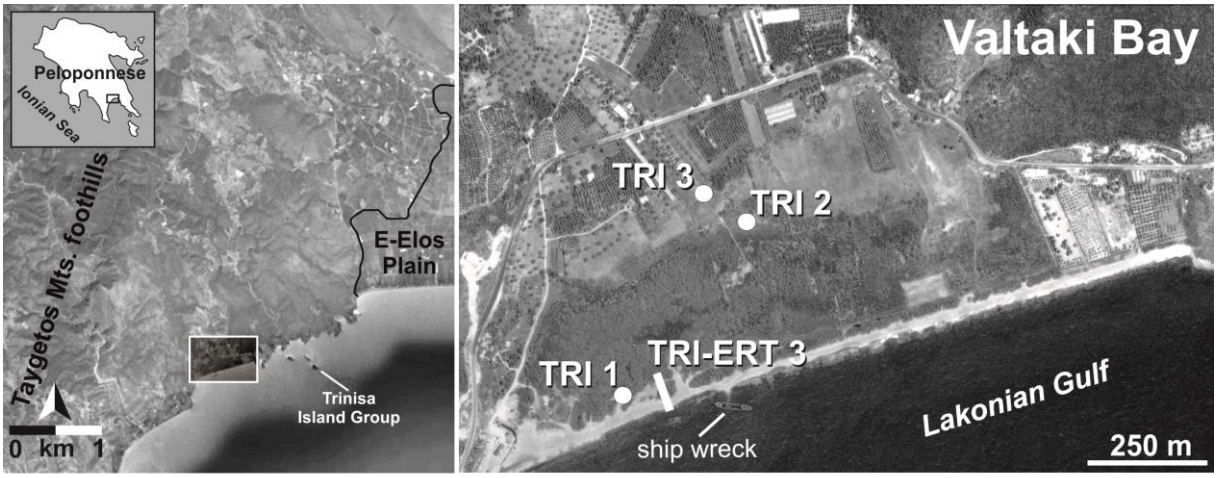

Figure 43: In the back-beach area of the small Valtaki Bay, located westward of the Elos Plain close to the Trinisa Island Group, altogether 3 vibracorings were drilled along a south-north trending transect starting behind the recent dune ridge (source: own illustration, maps based on NASA World Wind and Google Earth images/data, access June 2013).

6.4.3.1 The Trinisa vibracore transect

Valtaki or Trinisa Bay lies about 4 km to the southwest of the Skala vibracore transect (Fig. 43). Subsurface stratigraphical data were collected along a south-north running vibracoring transect. Coring site TRI 1 (36°47'21.76'' N, 22°35'01.31'' E) is situated on marshy ground behind the beach

ridge some 60 m distant to the sea. Vibracore TRI 2 (36°47'30.53'' N, 22°35'09.10'' E) was drilled some 300 m inland in the transition zone between the marsh and the cultivated area. Vibracoring site TRI 3 (36°47'32.17'' N, 22°35'06.95'' E) is located further north in the midst of an olive grove.

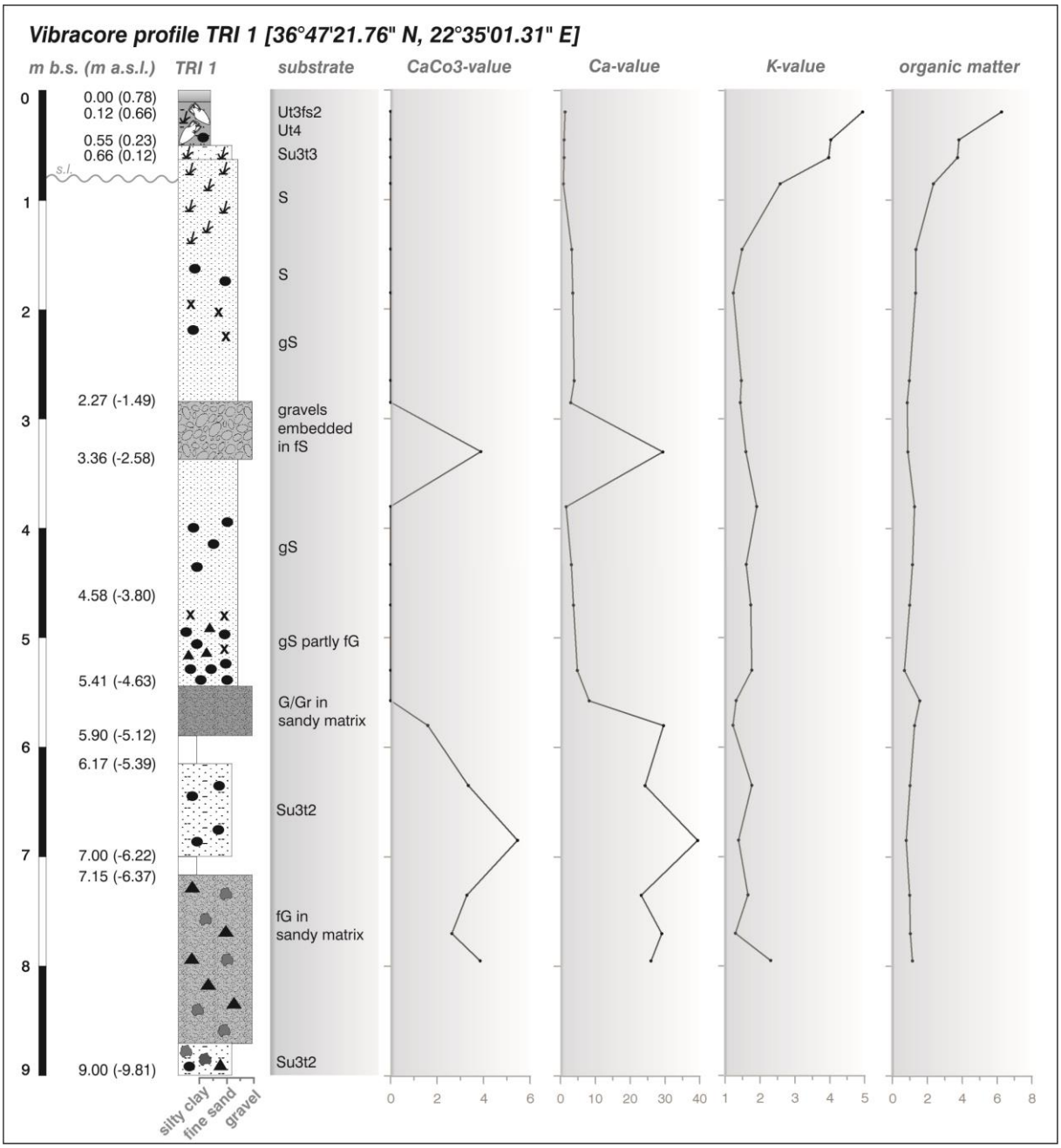

Figure 44: Geochemical data and stratigraphy of vibracore TRI 1 drilled in the Valtaki Bay back-beach area (source: own data and illustration 2013).

The sedimentary sequence of core TRI 1 begins with a heterogeneous unit out of alternating sand and gravel layers (Fig. 44). Furthermore, grus and weathered bedrock fragments were found. At 3.80 m b.s.l. these deposits are covered by well sorted sand (3.80 m b.s.l. and 0.12 m a.s.l.) intersected by heterogeneous and badly sorted fine to medium sand containing coarse clasts and grus between 2.58 m and 1.49 m b.s.l. At 0.12 m a.s.l., silty to clayey sand follows which turns into clayey silt from

0.23 m a.s.l. upwards featuring hydromorphic remarks and including ceramic fragments, indicating human presence.

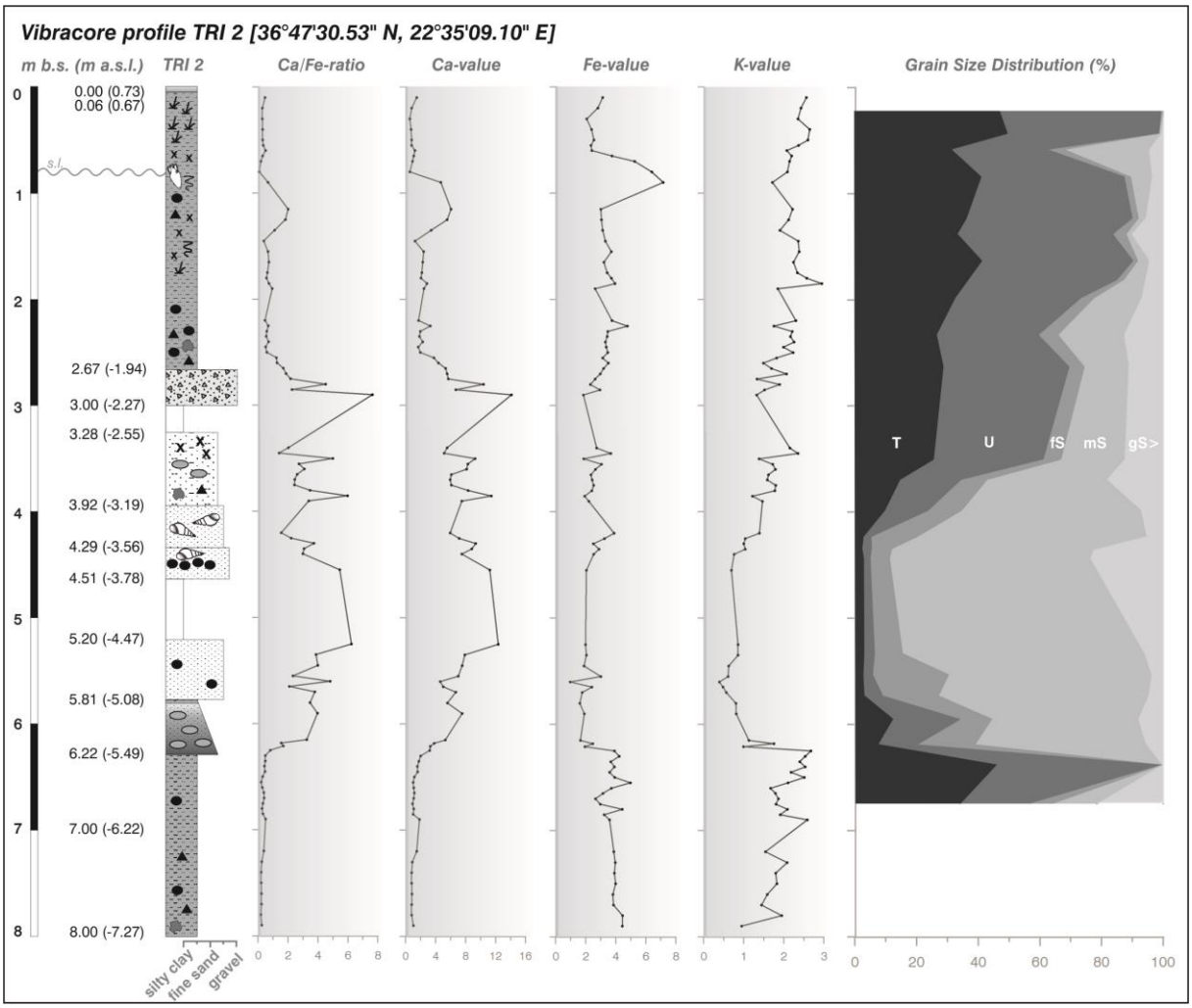

Figure 45: Stratigraphy, geochemical data and grain size distribution of vibracore TRI 2 (source: own data and illustration 2013).

Vibracore TRI 2 starts with compact clayey silt (7.27-5.49 m b.s.l.) that contains grus, gravels as well as bedrock fragments (Fig. 45). At 5.49 m b.s.l., a sharp erosional unconformity leads over to fining upward sand and a mud cap. Additionally, numerous clasts out of clayey silt were found within this fining upward sequence. The subsequent unit (5.08-3.19 m b.s.l.) is predominantly made out of medium sand but also contains gravels and coarse sand. Also undeterminable mollusc fragments were detected within this unit. Between 3.19 and 2.55 m b.s.l., silty sand was found covered by a layer of grus, 33 cm thick (2.27-1.94 m b.s.l.). The uppermost stratigraphical unit of vibracore TRI 2 is characterized by grus and gravel at its base and subsequent clayey silt and peat that contain numerous roots and plant remains.

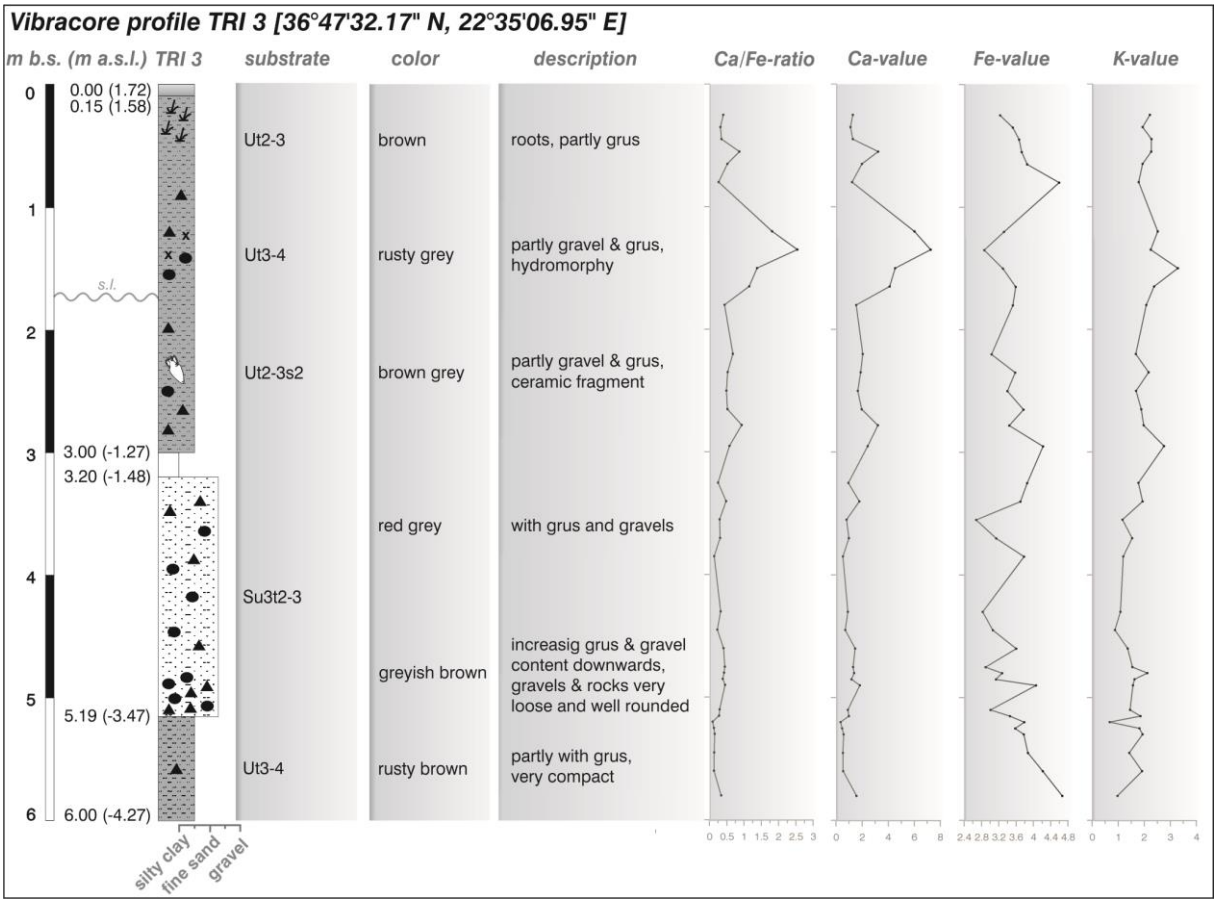

Figure 46: Stratigraphy and results of the geochemical analyses of core TRI 3 drilled in the back-beach are of Valtaki Bay (source: own data and illustration 2013).

At the base (4.27-3.47 m b.s.l.) of vibracore TRI 3 compact clayey silt with grus was encountered, the latter most probably originating from the local bedrock material (Fig. 46). From 3.47 m b.s.l. upwards, silty sand follows that shows an increased content of gravel, grus and bedrock particles. From 1.48 m b.s.l. towards the top clayey silt is predominant partly containing gravels and grus. Furthermore, hydromorphic features and ceramic fragments were found.

The stratigraphic and sedimentary findings along TRI vibracore transect are as follows:

i. At site TRI 1, basal alluvial sediments were covered by a thick sequence of coastal sand and finally by limnic to marshy mud. Several intercalating layers of coarse material such as grus and gravel including marine macrofossils were found.

ii. At vibracoring site TRI 2, weathered bedrock is covered by sediments of a quiescent marsh environment. A sharp erosional contact with a sandy fining upward sequence on top and ending with a mud cap, documents abrupt high-energy influence. This allochthonous unit is followed by littoral sand documenting that marshy to limnic conditions were not re-establish after the high-energy event and considerable changes of the coastal configuration have to be assumed.

iii. Sedimentological characteristics of the allochthonous deposit such as a sharp erosional discordance, a fining upward of the sediment body, clayey intraclasts as well as a mud cap speak for a sudden inundation from the marine side. Coarse deposits that were found in stratigraphically consistent positions in the upper parts of vibracores TRI 1 and TRI 2 possibly reflect a second allochthonous disturbance of the Valtaki back-beach area. Furthermore, these deposits were found in similar stratigraphical positions compared to the high-energy marine deposits encountered in the Skala vibracore transect, situated only 4 km northeastwards from Valtaki Bay.

6.4.3.2 Geochemical analyses and XRF measurements

Geochemical data of vibracore TRI 1 show that $CaCO_3$- and Ca-concentrations are generally low (Fig. 44). Higher concentrations were only found in the basal coarse unit as well as between 2.58 m and 1.49 m b.s.l. where gravels, partly made out of limestone material, are intersecting the well sorted sand. Furthermore, the data support the assumption that marshy to limnic conditions were predominant in younger geological times. This is shown by high K-values and increasing contents of organic matter from c. 0.80 m b.s.l. upwards.

The geochemical data of vibracore TRI 2 shows that the basal clay is widely decalcified and iron concentrations are relatively high (Fig. 45). Especially from 5.87 m b.s.l. upwards the K-value significantly increases. The sharp erosional discontinuity at 5.49 m b.s.l comes along with a strong increase of the Ca/Fe-ratio due to abruptly decreasing iron values and coevally ascending Ca-values. Moreover, a strong decrease of the K-value is noticeable. Within the subsequent sandy sequence (5.08-2.65 m b.s.l.) Ca-values remain high and the Fe-values low in contrast to the clayey units in the upper and lower parts of the core. This underlines the coastal character of the sediments. The highest Ca-concentration of the profile was found in the stratum out of coarse carbonatic material embedded in a loamy matrix (2.37-1.94 m b.s.l.), overlying the coastal sediments. Uppermost clayey sediments are characterized by decreased Ca-values and increased Fe- and K-values thus marking a change towards more terrestrial conditions. Because iron (Fe) is a major product of soil formation and weathering thus representing a marker for terrestrial conditions and high potassium (K) values often refer to limnic environments (VÖTT et al. 2002, 2011c). The highest iron concentration with 7.15 % was found at 0.17 m b.s.l. Here the sediments also show a clear orange to rusty coloring. This is possibly related to ground water influences, as the rusty shades were found in stratigraphical position consistent with the present sea level.

Concerning vibracore TRI 3, the Ca-concentration remains low (Fig. 46). However, a weak peak with a Ca-concentration of 5.99 % was detected at 0.52 m a.s.l. Moreover, the geochemical data document

beside the sedimentological features changing environmental conditions at the transition between weathered bedrock material and sandy alluvial deposits at 3.47 m b.s.l. There a drop-off of the potassium and iron values and simultaneously slightly increasing Ca-concentrations are identifiable.

6.4.3.3 Microfossil analyses

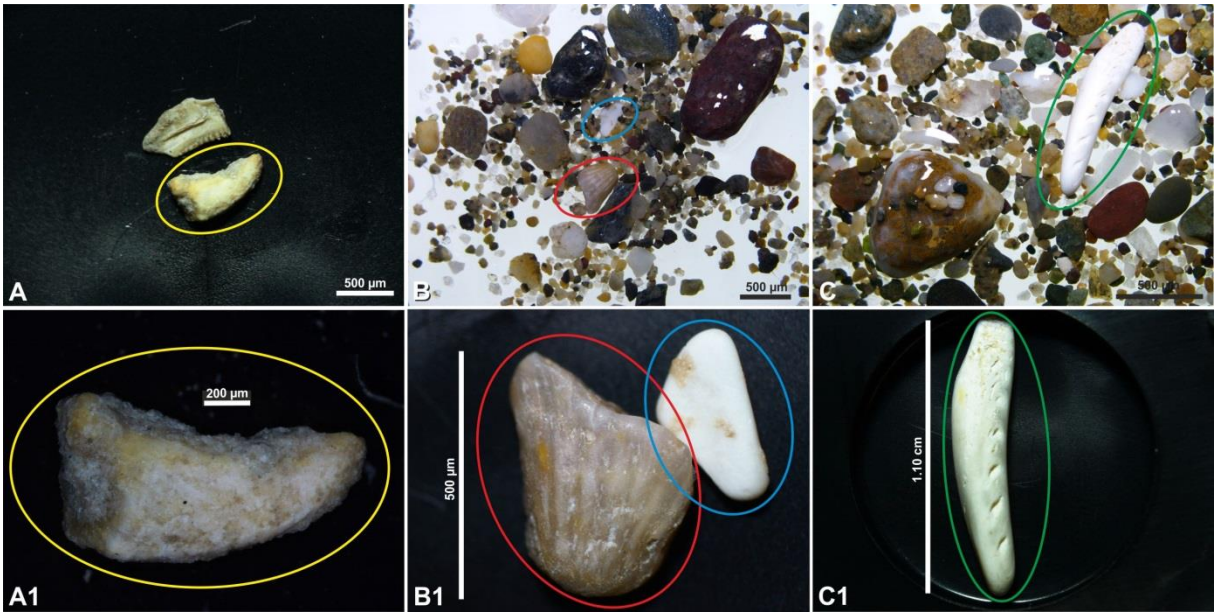

Figure 47: Photos of the studied grain fractions from selected samples of core TRI 2 for the purpose of microfossil analyses. Except some macrofossil remains no intact microfossils were detected in all studied fractions. Macrofossil remains show encrustations and traces of recrystallization and seem to be originated from the local bedrock (source: own data, pictures and illustration 2013).

For the purpose of macro- and microfaunal investigations altogether 15 samples were taken from vibracore TRI 2. Every sample was wet sieved for segregating the fractions < 400 µm, 200-400 µm, and 125-200 µm. Afterwards the samples were studied using a binocular. No intact microfossils or remains were detected except few undefinable shell fragments. Those were found in samples below 2.60 m b.s.l. and show recrystallization features, encrustations and rounded edges, indicating that they originate from the local bedrock (Fig. 47).

The lack of determinable microfossils may be due to the fact that the clayey sections in the core come along with very low Ca-concentrations thus pointing on probable post-sedimentary decalcification processes.

6.4.3.4 Earth resistivity tomography measurements (ERT) at Valtaki Bay

In the Valtaki Bay ERT-measurements were accomplished along three transects. Here, the results of transect TRI ERT 3 are presented. The 47 m long transect starts in the littoral zone on the beachrock outcrops and moves northwards in direction to the marshy back-beach area, while crossing the sandy beach and partly vegetated dune wall.

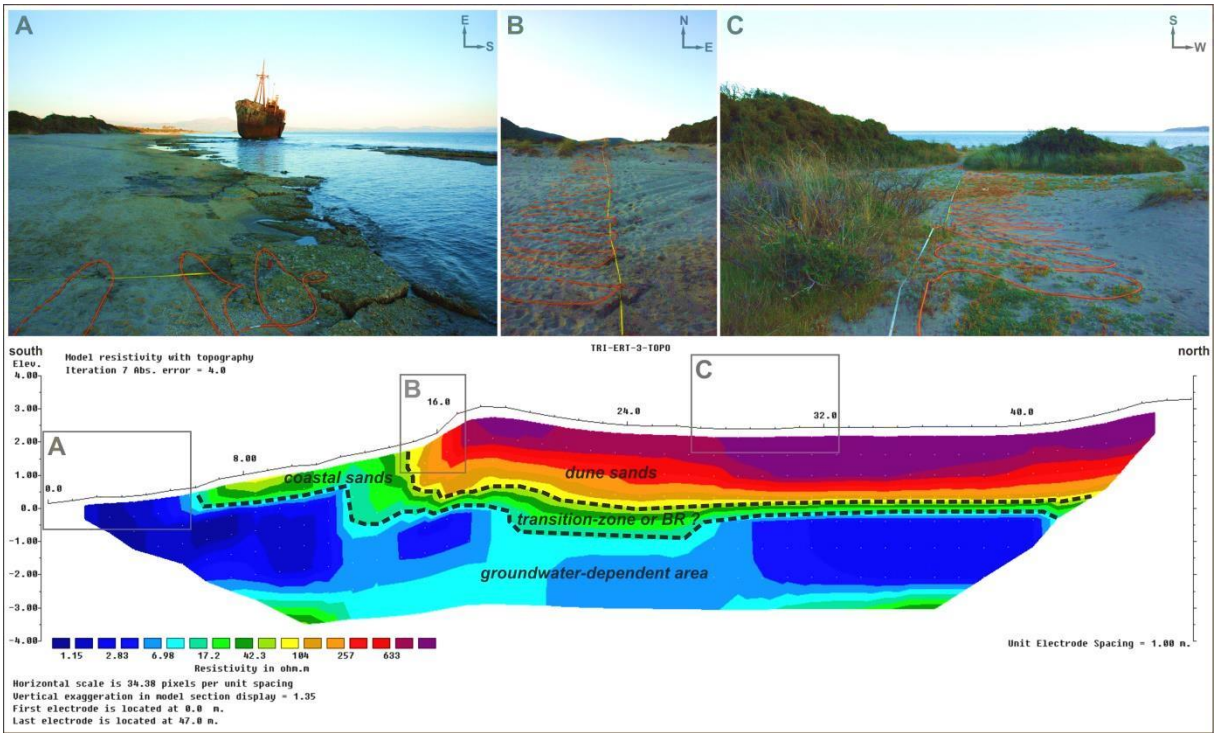

Figure 48: Setting and results of the earth resistivity tomography measurements of TRI ERT 3 accomplished at the coast of Valtaki Bay in Lakonia and interpretation approach (BR = beachrock) (source: own photos taken in March 2010 and own data and illustration 2014).

As visible in Fig. 48, the ERT pseudosection allows differentiating between three diverse units. Low resistivity values of less than 10 Ωm were found in the basal and southern sections. Resistivity values between 10 and 100 Ωm form a transition zone towards a third unit with resistivity values between 100 and 1000 Ωm.

The results of transect TRI ERT 3 can be interpreted as follows. Thereafter, the lowest resistivity values detected in the basal unit are most likely attributed to sea-and groundwater influences. Although the transect is starting on the solid beachrock formations, the materials water saturation can cause low resistivity values.

Resistivity values between 10 and 100 Ωm reflect the transition zone, most probably representing the area between the saturated and unsaturated conditions. Under circumstances this zone probably could also reflect a northward prolongation of the beachrock formations, which are covered in the splash-zone by loose sandy deposits, and possibly also continuing underneath the dune sands.

However, the upper high-resistant erythroid unit with resistivity values between 100 and 1000 Ωm reflects in all probability the sandy dune sediments, as the values are typical for earth-moist sandy material (GGU 2003).

6.4.3.5 The Holocene stratigraphical record in the Valtaki Bay

Based on stratigraphical and geochemical investigations the sedimentary record of the marshy back-beach area of Valtaki Bay attests that autochthonous sedimentary environments, mainly characterized by fine-grained sediments, were sporadically intersected by allochthonous coarse grained intercalations. From the sedimentological point of view these intercalations refer to higher-energetic geomorphodynamic processes.

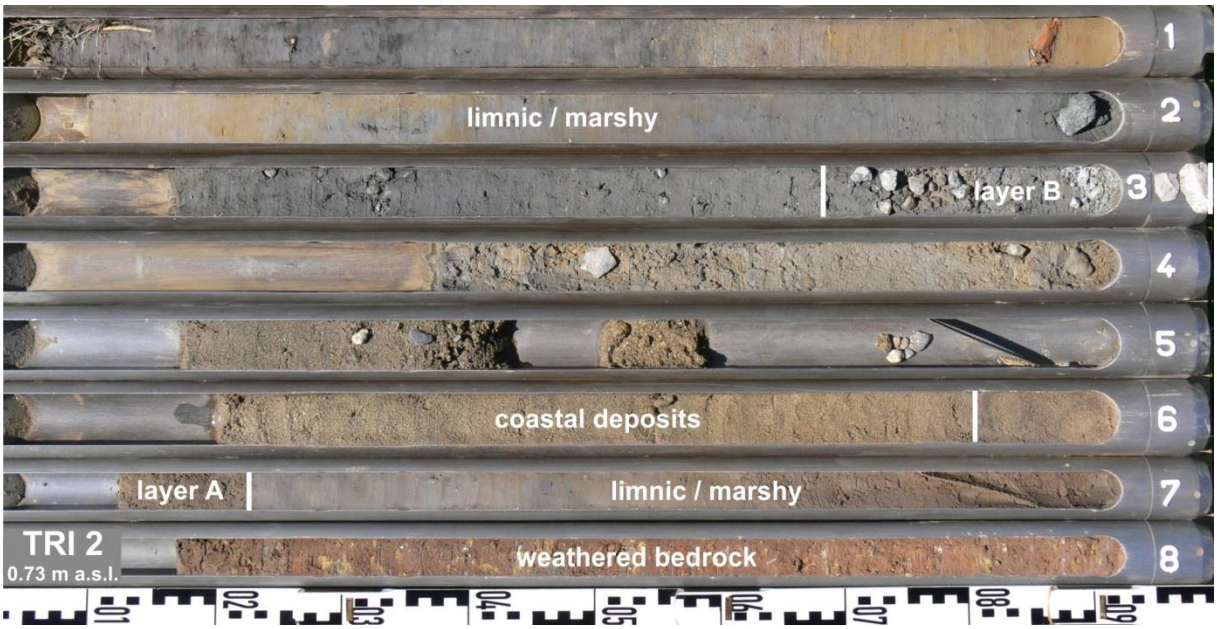

Figure 49: Photo and simplified facies profile of sediment core TRI 2 drilled in the marshy back-beach area of Valtaki Bay in central Lakonia (source: photo taken by T. Willershäuser in March 2010, own illustration 2014).

Hence, the here presented sedimentological and geochemical results indicate that the northern part of the Valtaki Bay (represented by core TRI 3) was dominated by terrestrial and limnic conditions. Thereafter, a limnic-marshy environment was established covering alluvial deposits found on top of weathered bedrock units. Most possibly this was linked to a rising ground water level in the course of the Holocene sea-level rise. This is likely because Late Roman/Early Byzantine remains of buildings along the shore of Valtaki Bay are partly submerged, thus a considerable local relative sea level rise is documented for the study area (KELLETAT & GASSERT 1975, CUNDY et al. 2006). And for Kamares Bay, situated c. 12 km to the southwest of Valtaki Bay, CUNDY et al. (2006) reconstructed a relative sea-level rise of 0.8-1 mm/a for the last 3500 years .

For the central part of the plain (represented by core TRI 2) the dataset also attests a limnic-marshy environment which developed over weathered bedrock. However, this limnic environment was disturbed by the sudden input of a sandy fining upward sequence (Fig. 49, layer A). From the sedimentological point of view this sequence shows features of marine-borne extreme events, such as i) a sharp erosional unconformity, ii) a fining upward trend, iii) intra and/or rip up clasts as well as iv) a mud cap. Moreover, the disturbance comes along with high Ca/Fe-ratio values and decreased

Fe- and K-values pointing to diminished terrestrial and limnic conditions. VÖTT et al. (2011a, 2011c) used the Ca/Fe-ratio as indicator for palaeotsunami reconstruction. Thereafter, a higher Ca/Fe-ratio within a stratigraphical sequence can refer to the input of marine material into a terrestrial environment. Accordingly, high Ca-concentrations can be related to marine sediments as they are attributed to an overload on ions from marine borne $CaCO_3$ and due to shell-forming organisms. On the contrary, simultaneously decreasing Fe-concentrations may reflect reduced terrestrial influences, as iron is a major product of weathering and soil formation (Vött et al. 2002, 2011c). Furthermore, the stratigraphy of core TRI 2 indicates that former limnic conditions did not continue to exist after the impact. It is assumed that the former beach ridge, whose sediments were encountered in the seaward core TIR 1, which separated the limnic environment from the influence of the open sea, was destroyed by the supposed marine event. It is thus supposed that this deposit refers to a sudden inundation from the marine side. And against the background that the geological record of the nearby Elos Plain bears at least three palaeotsunami layers this is rather likely. However, a clear classification of the sediment as a marine high-energy tsunami deposit is not possible due to the lack of identifiable microfossils. CUNDY et al. (2006) also do not report on intact microfossils found in their cores from the Valtaki Bay.

Due to the rising sea and ground water level the central and northern parts of the studied area have been dominated by quiescent limnic-marshy conditions during the younger geologic past. Towards the shoreline a dune ridge protects the adjacent marshy back-beach area against the influence of the open sea. And according to CUNDY et al. (2006), the back-barrier wetland of Valtaki Bay, that was present in pre-Roman times, was gradually filled with sediments. Nevertheless, the here detected coarse and heterogeneous deposit found in between the sandy and clayey sediments of core TRI 2 (Fig. 49, layer B) refers to a temporary allochthonous and higher-energetic sedimentation process, probably from the marine side. Moreover, it is striking that this allochthonous high-energy deposit stratigraphically corresponds to the layer out of gravel and grus intersecting dune sediments of core TRI 1. These intercalations are also documented in the geochemical datasets. Finally, these deposits are situated in consistent stratigraphical positions compared to the tsunami deposit encountered in the Skala vibracore transect, situated only 4 km to the northwest of Valtaki Bay.

6.5 Interpretation and discussion

Historical documents indicate repeated (palaeo-)tsunami activity for the southern Peloponnese (AMBRASEYS 2009). This seems not very surprising against the background that the area is directly exposed to the extremely active Hellenic Trench that comes along with frequent earthquakes and submarine slides which in turn can trigger devastating tsunamis. Accordingly, such palaeo-events should have left sedimentological traces within the geological record of near-coast archives along the central Lakonian Gulf – as described for several other Greek coasts. Our results, based on vibracore transects in the eastern and western parts of the Evrotas River delta, provided evidence of several palaeotsunami deposits.

In the eastern Elos Plain, we found traces of multiple allochthonous high-energy signals within the autochthonous low-energy back-beach sedimentary record. In the western part of the Elos Plain allochthonous marine sand deposits were found intersecting low-energy peat over a distance of more than 1.7 km inland from the present coast. Similar to the eastern part of the Elos Plain, the western part also shows a regressive tendency which resulted in a southward shifting of the shoreline.

The stratigraphical sequences along the ELO vibracore transect show that local autochthonous sedimentary environments are predominated by quiescent limnic-lagoonal conditions. We found these autochthonous deposits intersected by three units of allochthonous sediments. Grain size data as well as geochemical data document repeated high-energy interferences of low-energy quiescent conditions. Low potassium values, for example, found associated with the three allochthonous high-energy deposits at site ELO 1 (Fig. 37) represent repeated dilution effects of the local limnic-lagoonal eutrophic environment.

For the SKA vibracore transect (Fig. 41), a beach-barrier, encountered in the most seaward core SKA 3, promoted the development of a quiescent low-energetic environment. In situ deposits are mostly limnic-lagoonal mud deposits. However, autochthonous conditions were disturbed by the high-energy input of marine material best documented in cores SKA 2 and 2A where a sandy fining upward sequence intersects autochthonous peat.

Microfaunal data collected for key core ELO 1 (Fig. 39) reflect changing environmental conditions as well as interferences associated with the high-energy input of allochthonous marine deposits. Allochthonous high-energy sand deposits bear a fully marine foraminiferal signal mixed with species from a variety of different environments. For example, ELO 1 high-energy layers revealed specimens of the planktonic foraminifera *Orbulina universa* (Globigerinidae), proving an extraordinarily strong influence from the seaside.

Microfaunal analyses of samples from cores SKA 2 and SKA 2A (Fig. 42) prove the sudden input of allochthonous marine species in a non-marine sedimentary environment for which *Cyprideis torosa*

and *Planorbis planorbis* attest undisturbed limnic to lagoonal swampy conditions. Allochthonous sand deposits, however, come along with different marine gastropod species and a mixed foraminiferal record comprising species from shallow marine and inner shelf environments. MAMO et al. (2009) state, that tsunami influence leaves an abrupt rather than a gradual change in the foraminiferal record. Core SKA 1 thus clearly documents an abrupt tsunami-related flooding of the swampy back-beach.

With regard to the sedimentary characteristics, autochthonous event deposits in the Evrotas River delta are further characterized by (i) sharp erosional discordances, (ii) rip up clasts out of underlying material, (iii) fining upward sequences and (iv) thinning landward tendencies which clearly mirror high-energy influences to the local quiescent environments. The macro- and microfaunal record of these sediments finally proves that high-energy impact comes from the sea side. However, basal erosional contacts are often associated with tsunamigenic activity but were also described for extreme storm events (DOMINEY-HOWES et al. 2006, HAWKES et al. 2007, SUGAWARA et al. 2008, HORTON et al. 2009, WILLIAMS 2009). This is also true for fining upward sequences (GELFENBAUM & JAFFFE 2003, DOMINEY-HOWES et al. 2006, MORTON et al. 2007) as well as for rip up clasts (DOMINEY-HOWES et al. 2006, MORTON et al. 2007). Thinning landward tendencies of event layers are also described for both tsunamis and storms (GOFF et al. 2009, NOTT 2006, MORTON et al. 2007).

The southern Peloponnese is dominated by northeastern and northwestern winds and wind-generated waves (MEDATLAS GROUP 2004, p. A.25, A.26). The annual significant wave height for the northern central Lakonian Gulf is lower than 0.8 m and the probability that significant wave heights exceed > 4.0 m in near-shore areas tends to zero (MEDATLAS GROUP 2004, p. A.26, A.27). Aside from that, in the study area, showing a gradually ascending shelf and shore, storm waves are expected to break mainly as “spilling breakers” in sufficient distance to the shoreline (KALLENRODE 2003). Therefore, the Lakonian Gulf is characterized by a low to moderate wave climate so that the vulnerability for storm wave driven littoral dynamic processes is low.

Event deposits encountered in the ELO and SKA vibracore transects show stratigraphical consistencies over a distance of up to 2 km. Considering that the sea level in the wider area has never been higher than the present one (VÖTT 2007, ENGEL et al. 2009, BRÜCKNER et al. 2010), the spatial extent of the event deposits is – on the regional scale of the eastern Mediterranean – a crucial argument against the possibility that they were deposited by storm wave activity. In cores ELO 3 and ELO 1, the uppermost and thus youngest event deposit shows signs of subaerial weathering. Similar observations are reported by VÖTT et al. (2011b) and WILLERSHÄUSER (2013) for onshore tsunami sediments that were deposited above the local sea level and underwent post-sedimentary terrestrial weathering.

Against the background that several tsunami and earthquake catalogues and compilations attest that tsunami events occur frequently within the eastern Mediterranean (e.g. GUIDOBONI et al. 1994, SOLOVIEV et al. 2000, PAPADOPOULOS 2002, TINTI et al. 2001, 2004, GUIDOBONI & COMASTRI 2005, PAPADOPOULOS & FOKAEFS 2005, PAPADOPOULOS et al. 2007, SCHIELEIN et al. 2007, HADLER et al. 2012) and that there are no historical data on extraordinary storms, storm-related formation of the ELO and SKA high-energy layers is impossible and a tsunami-related formation has to be assumed.

Additionally, results from the adjacent Valtaki Bay demonstrate that the stratigraphical sequences show traces of sudden disturbances as well as coarse material intersecting autochthonous sediments (Fig. 49). Sedimentological features as well as the stratigraphical position of these layers give grounds to infer that the deposits possibly also correspond to the event layers found in the nearby Elos Plain.

Regarding the geochronological dating approach peat material from basal parts of core ELO 3 was dated to 4456 – 4370 cal BC representing a *terminus post quem* for the tsunami layer of event generation T1. Traces of an event that occurred at around 4200 cal BC were detected and described for the Bay of Palairos-Pogonia in coastal Akarnania by VÖTT et al. (2011a), for Pheia, the ancient harbor of Olympia, situated in the western part of the Peloponnese by VÖTT et al. (2011b), for the ancient harbor of Krane by VÖTT et al. (2013) and for the Bay of Lixouri by WILLERSHÄUSER et al. (2013). Against this background we assume that event generation I correlates to the before mentioned supra-regional event that seems to have affected large parts of the eastern Ionian Sea at around 4200 cal BC.

For tsunamiite T2 the geochronological data attests a *terminus post quem* of 1313 – 1210 cal BC and a *terminus ante quem* of 972 – 850 cal BC for the related event. This event is possibly correlated with tsunami traces of which were found in Akarnania and which were dated to around 1000 cal BC (VÖTT et al. 2006, 2009).

For the youngest tsunami impact T3 we found a *terminus ante quem* of 1422 – 1460 cal AD and *terminus post quem* of 19 – 85 cal AD. The time span includes the devastating 365 AD and 1303 AD tsunami events that effected large parts of the eastern Mediterranean. Because of the sharp basal erosional discordance we assume a considerable hiatus due to tsunami erosion and argue that event T3 most probably occurred not much before 1422 – 1460 cal AD. Event T3 is thus a reasonable candidate for the historically well-known 1303 AD event, traces of which were described by SCHEFFERS et al. (2008) for southern Lakonia. Also, VÖTT et al. (2006) report on a tsunami event that affected Lefkada Island between 1000 – 1400 cal AD which may speak for another supra-regional tsunami imprint at that time. The distinct tsunamiite recorded in the SKA vibracore transect stratigraphically corresponds well with tsunamiite T3 of the ELO vibracore transect. The SKA 1 age interval 632 – 681 cal AD represents a *terminus post quem* associated to a hiatus of unknown dimension. The SKA 2 age interval 1030 – 1150 cal AD yields a non-reliable *terminus ante quem* for the event because the $\delta^{13}C$

value of the dated sample (Table 1) is reduced, most possible due to post-sedimentary processes; the true age is assumed to be younger (GEYH 2005). The youngest tsunamiite encountered along the ELO and SKA transects thus represent traces of one and the same tsunami event (T3) which is a good candidate for the 1303 AD tsunami.

In general, the stratigraphical sequences together with the sedimentary characteristics show that the autochthonous environments were re-established after the interferences caused by high-energy tsunami events.

6.6 Conclusions

Combined sedimentological, geochemical, microfaunal, geophysical and geochronological studies in search of palaeotsunami signatures in near-coast sedimentary archives of the Evrotas River delta plain were conducted along two vibracore transects. The following conclusions can be made.

(i) Along the ELO vibracore transect, autochthonous mud deposits of a long-enduring palaeo-lagoon, were repeatedly intersected by the abrupt input of allochthonous marine high-energy sand and gravel over a distance of up to 2 km inland. Three marine inundation events (T1-T3) were identified. Also along the SKA vibracore transect, we found a distinct layer out of allochthonous marine deposits intersecting in situ low-energy mud in back-beach position around 1.7 km inland.

(ii) Allochthonous high-energy layers of the ELO and SKA vibracore transect were found in stratigraphical consistent positions over more than 9 km across the Evrotas River delta plain.

(iii) Detailed macro- and microfaunal analyses document the marine origin of the detected allochthonous event deposits.

(iv) Considering the spatial extent of the high-energy marine deposits, their sedimentary characteristics and the allochthonous microfossil assemblages as well as the fact that the local wind- and wave climate has to be considered weak to moderate, high-energy deposits encountered in the Evrotas River delta plain have to be regarded as palaeotsunamiites. Historical accounts document that the region is sensitive for tsunamis caused by the nearby tsunamigenic Hellenic Trench.

(v) Geochronological data suggest that the tsunamiites T1 and T2 are associated to supra-regional events which occurred around 4200 cal BC and around 1000 cal BC, respectively. The youngest event deposit T3 is a good candidate for the historically well-known tsunami which destroyed large parts of the eastern Mediterranean in 1303 AD.

Chapter 7 – Results from the outer Gulf of Argolis – Limnothalassa Moustou

Abstract: The Gulf of Argolis is located close to the Hellenic Volcanic Arc and the Hellenic Trench and thus faces a high risk to be affected by seismo-tectonically induced tsunami events. Historical accounts as well as modern tsunami catalogues document that the southern coasts of the Peloponnese were repeatedly affected by tsunamis. This is, however, the first study revealing geoscientific evidence on past extreme wave impact on the Gulf of Argolis. The low-lying near-coast limnic-lagoonal area around Limnothalassa Moustou, located in the central-western margin of the gulf, was investigated by means of sedimentological, geomorphological, geochemical and micropalaeontological methods in search of palaeo-tsunami fingerprints in the Holocene stratigraphical record. Our investigations have brought to light that the quiescent low-energy environments around Limnothalassa Moustou were affected by three tsunami impacts. The youngest event most possibly refers to the historically well-known tsunami from 1303 AD that affected wide parts of the eastern Mediterranean, especially the Peloponnese. Our stratigraphical data let us assume that tsunami inundations were accompanied by complex backwash flow dynamics resulting in the deposition of coarse-grained coastal and fluvial material. The sedimentary environments hit by the youngest tsunami landfall soon recovered after tsunami impact which is documented by homogeneous fine-grained sediments in the uppermost parts of all vibracores. These sediments are typical of quiescent low-energy marsh environments that existed in wide parts of the investigated back-beach area at least during the last 500 to 600 or so years.

7.1 Traces of repeated tsunami landfall in the vicinity of Limnothalassa Moustou (Gulf of Argolis – Peloponnese, Greece)

The Gulf of Argolis is exposed towards the Hellenic Volcanic Arc and the Hellenic Trench and is thus subject to a high risk of seismo-tectonically induced tsunamis. Historical accounts as well as modern catalogues document numerous tsunami events for the Peloponnese, for example the 365 AD, 1303 Ad and 1928 AD events (ANTONOPOULOS 1980, SOLOVIEV et al. 2000, GUIDOBONI & COMASTRI 2005, AMBRASEYS 2009, HADLER et al. 2012).

Against the background of recent geomorphological and sedimentological findings of past tsunami impacts along the coasts of the western and southern Peloponnese (HADLER et al. 2015, NTAGERETZIS et al. 2015a, 2015b, WILLERSHÄUSER et al. 2015a, 2015b), it was assumed that similar traces are also recorded in the stratigraphical archives of the Gulf of Argolis in the southeastern Peloponnese.

The main objectives of this study thus were (i) to search for palaeotsunami fingerprints in the local sedimentary record of Limnothalassa Moustou, situated at the western fringe of the Gulf of Argolis by means of sedimentological, geochemical and micropalaeontological methods, and (ii) to establish a local geochronostratigraphy for the study area using the ^{14}C-AMS radiocarbon technique.

7.2 Geotectonic and natural settings

The Gulf of Argolis is situated in the eastern Peloponnese opening to the Aegean Sea (MITROPOULOS & ZANANIRI 2010). The gulf and the adjacent Argive Plain to the north represent a NNW-SSE trending

*A paper based on this chapter will be submitted for publication in the international journal *Zeitschrift für Geomorphologie N.F., Supplementary Issues* (authors: Konstantin Ntageretzis, Andreas Vött, Peter Fischer, Hanna Hadler, Kurt Emde, Björn Roman Röbke, Timo Willershäuser).

tectonic graben-type depression of Plio-Pleistocene age, 75 km long and 30 km wide. The gulf is characterized by a regular seafloor morphology featuring an amphitheatric pattern (MITROPOULOS & ZANANIRI 2010) and a maximum water depth of 800 m (GAKI-PAPANASTASSIOU 2010). The western flank represents the marginal eastern foothills of the Parnon mountain chain. The shelf zone is extremely narrow and only a few tens or hundreds of meters wide (GAKI-PAPANASTASSIOU et al. 2010). On the eastern side, the Argolis Peninsula is made up of Pelagonian zone material of the internal Hellenides (JACOBSHAGEN 1986, BACHMANN & RISCH 1979), mostly of the Pantokrator facies, part of the Upper Triassic – Lower Jurassic carbonate series (POMONI-PAPAIOANNOU 2008). In contrast to the gulfs western side, the geomorphology of the eastern side is characterized by a broader shelf.

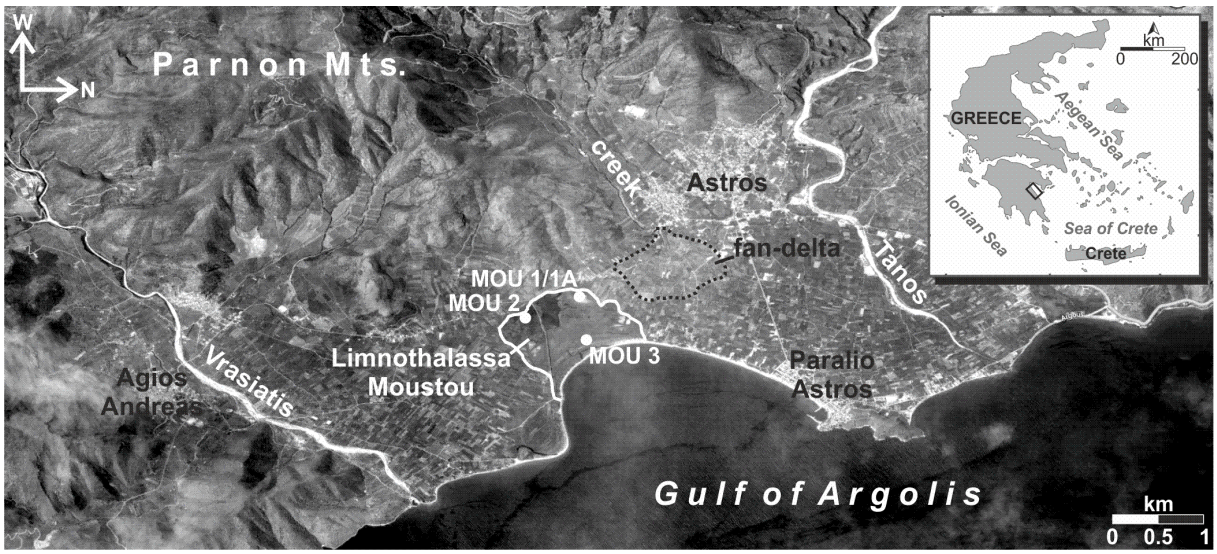

Figure 50: Oblique aerial photo showing the general geomorphological setting around Limnothalassa Moustou. The Tanos River and the Vrasiatis River directly flow eastwards into the Gulf of Argolis (source: own illustration, maps based on Bing and Google Earth images/data, access June 2014).

The Gulf of Argolis is characterized by a variety of different coastal forms such as embayment's with sandy beaches, steep promontories with capes and cliffs, as well as by a couple of small islands lying close to the mainland. Towards the north, the Argive Plain and the adjacent shelf, 3-5 km wide, have been formed by several rivers draining the surrounding mountain ranges (PAPANIKOLAOU et al. 1988), especially by the progradation of the non-perennial Inachos River since the mid-Holocene (KRAFT et al. 1977, ZANGGER 1993, GAKI-PAPANASTASSIOU et al. 2010). Important settlements such as Mycenaean Tiryns, well known for its cyclopean walls, are situated within the alluvial plain and at its fringes.

The study area of Limnothalassa Moustou (*Limnothalassa/Λιμνοθάλασσα* = Greek for lagoon) lies some 20 km to the south of the central Argive Plain at the western flank of the Parnon Mountains within a low-lying coastal plain (Fig. 50). Limnothalassa Moustou is right in between two river deltas, namely the delta of Tanos Potamos (*Potamos/Ποταμός* = Greek for river) in the north and the delta of Rema Vrasiatis (*Rema/Ρέμα* = Greek for creek) in the south (IGSR 1970a, 1970b, 1970c). The first

has formed a fan delta, approximately 3.6 km long, the fan delta of the latter is 4 km long and enters the gulf next to the small harbour of Agios Andreas.

The mountains to the north and to the west of the study area are made out of Upper Cretaceous limestones and their slopes show several Holocene to Pleistocene alluvial fans running towards the plain (IGSR 1970a, IGSR 1970b). Aerial photos show that a small fan-delta was formed by a creek to the south of the city of Astros with its distal parts representing the northern fringe of the lowland around Limnothalassa Moustou. Towards the south, in between the village of Agios Andreas and the homonymous harbour, there are outcrops of Middle to Lower Jurassic limestones and dolomites (IGSR 1970b, IGSR 1970c).

The environs of Limnothalassa Moustou represent a wetland of considerable ecological importance. Salt marshes cover most parts of the lowlands whereas the water body itself measured only 200 m from N to S, and 600 m from W to E. The maximum water depth reaches 5 m and its salt content varies between 11 to 15 % (after www.parnonas.org). The beach barrier, protecting the lagoon from the open Aegean Sea, is mainly made out of gravel and coarse sand.

Vibracore MOU 1 (drilled with open steel auger), and parallel core MOU 1A (drilled with closed steel auger and integrated plastic inliner), were performed in the northern part of the study area in a salt marsh some 800 m distant from the recent coastline and some 350 m to the north of the lagoonal shore. Vibracoring site MOU 2 is located on the opposite side of the lagoon at the foot of the Parnon spurs. Vibracoring site MOU 3 lies to the east of the water body within a system of palaeo beach ridges some 200 m distant from the present shoreline.

7.3 Methods

We used a multidisciplinary research approach comprising sedimentological, geomorphological, geochemical and microfaunal analyses. Additionally, geochronostratigraphical studies were carried out based on ^{14}C-AMS dating of selected samples.

Vibracorings were accomplished by means of an Atlas Copco mk1 coring device using core diameters of 6 and 5 cm. From the environs of Limnothalassa Moustou we retrieved altogether four vibracores three of which were drilled with open steel augers and one was drilled using plastic inliners. The sediment cores were cleaned, photographed, documented for geomorphological and sedimentological criteria such as sediment color, grain size distribution, grain characteristics, texture, carbonate content and pedogenetic features according to AD-HOC-ARBEITSGRUPPE BODEN (2005). Finally, sediment cores were sampled for further analyses in the laboratory.

Laboratory studies comprised the analyses of the grain size distribution applying the sieve and pipette method after KÖHN (BLUME et al. 2011) as well as element determination by means of XRF-

analyses using a portable, energy-dispersive device (type *Thermo Niton XL3t 900s GOLDD*, calibration mode SOIL). Moreover, we carried out macro- and microfaunal analyses of selected samples retrieved from vibracore MOU 1 as a base for facies determination and to get information on the origin of the sedimentary material. A sample volume of 15 cm^3 was dispersed using H_2O_2 (3 %) and afterwards sieved to the fractions of < 400 µm, 200-400 µm, 125-200 µm and < 125 µm. Fractions < 125 µm were not investigated. Grain fractions were stored in glass cylinders filled with ethanol for conservation. Identification of species of foraminifera, ostracods, bivalves and gastropods was accomplished using a Nikon SMZ-74St binocular with optional 10 x – 40 x magnifications. Selected specimens were isolated, picked out, put into Krantz-cells and photographed using a high-resolution DS-Fi2 Nikon camera mounted on a Nikon Eclipse 50-POL polarization microscope and the NIS Elements software (Basic Research). Species identifications and information about the detected species were based on the following literature: LOEBLICH & TAPPAN (1988), VESPER (1972), HEIP (1976), DANCE (1977), TARASCHEWSKI & PAPERNA (1981), HERMAN & HEIP (1982), CIMERMANN & LANGER (1991), MURRAY (1991), DELAMOTTE & VARDALA-THEODOROU (2001), GROSS (2001), HAYWARD & GROSS (2011), CRISCIONE & PONDER (2013) and HAYWARD (2013). The abundance of each determined species was documented in a semi-quantitative manner (0 = no specimens encountered; 1 = very rare/singular (1 specimen); 2 = rare (2-3 specimens); 3 = few (up to 6 specimens); 4 = fairly many (up to 9 specimens); 5 = many (up to 12 specimens); 6 = a great many (more than 12 specimens)).

The exact geographical positions of vibracoring sites were determined by means of a Topcon HiperPro FC-200 differential global positioning system (DGPS) instrument with a lateral measuring accuracy of ± 2 cm.

^{14}C-AMS dating of organic material allowed establishing a local event-geochronostratigraphy. Calendar ages were calculated using the calibration software Calib. 6.0 (see REIMER et al. 2009).

7.4 Results

7.4.1 The Moustou vibracore transect

Vibracores MOU 1 and MOU 1A (N 37°23'22.76'', E 22°44'41.42'', ground surface at 0.29 m a.s.l.) were drilled to the immediate north of the lagoon some 850 m inland in a marsh environment (Fig. 1). Vibracoring site MOU 2 (N 37°22'58.01'', E 22°44'47.53'', ground surface at 0.65 m a.s.l.) is located to the south of the lagoon about 1200 m inland at the foot of a hilly range. Vibracore MOU 3 (N 37°23'23.01'', E 22°45'07.81'', ground surface at 0.32 m a.s.l.) was drilled about 200 meters distant from the beach to the northeast of the lagoon.

At the base of vibracore MOU 1, we found grey clayey silt. At 7.45 m b.s.l., this unit is covered by a thick layer of sandy gravel (Fig. 51). Between 6.21 and 5.14 m b.s.l., we encountered silty fine-sand

containing marine mollusc fragments. This fine-grained unit is again covered by a coarse stratum out of well-rounded gravels embedded in a sandy matrix. Abundant marine mollusc fragments and pieces of gravel showing bio-erosional features document the marine origin of the material. At 2.58 m b.s.l., this heterogeneous unit is overlain by whitish grey clayey silt. On top, we found fine sandy silt including abundant mollusc and bivalve fragments, gastropods and plant remains covered by a black peat layer (0.17-0.35 m b.s.l.). The peat is again followed by homogenous clayey silt. The stratigraphy of core MOU 1A, drilled down to 4 m b.s. using plastic inliners, shows the same stratigraphy as core MOU 1.

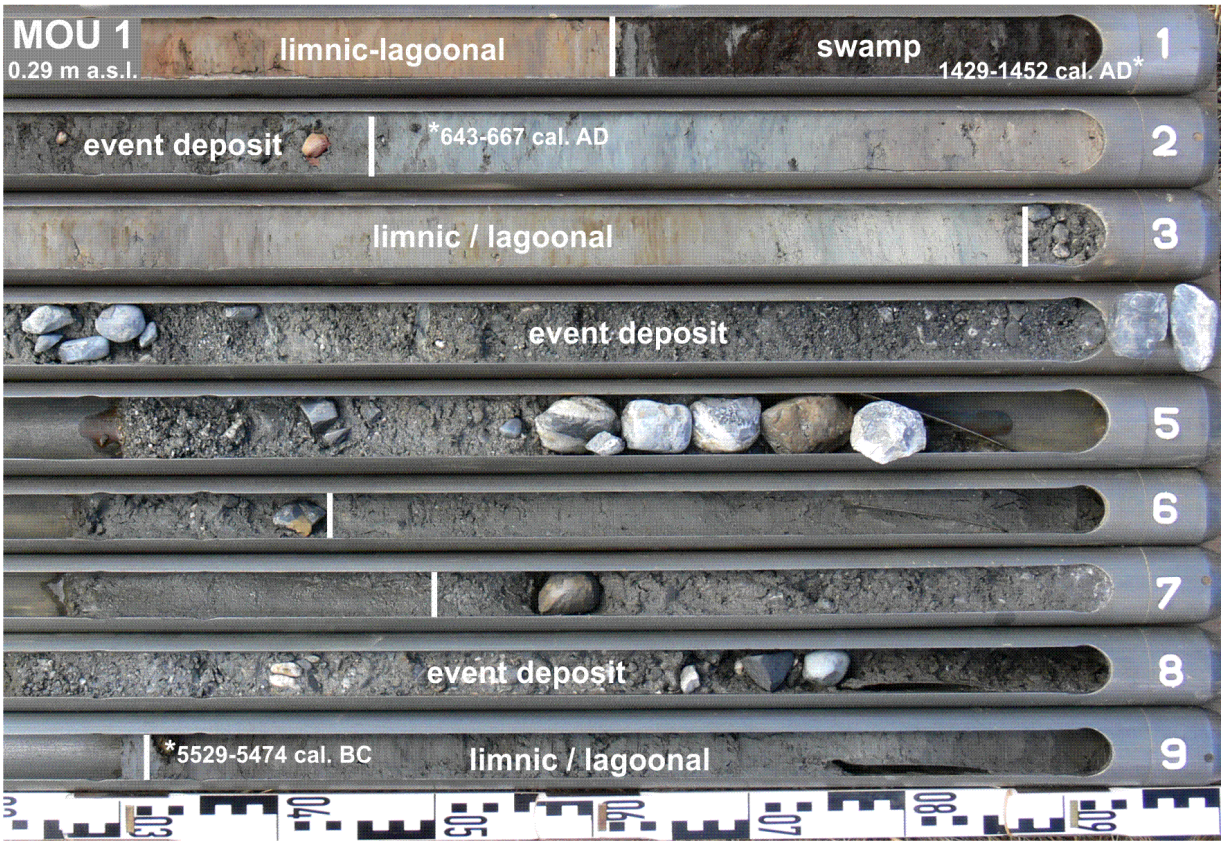

Figure 51: Simplified facies profile of sediment core MOU 1 showing three tsunami-related event layers (source: photo taken by P. Fischer in June 2010, own illustration 2014).

The base of vibracore MOU 2 consists of decalcified orange to yellow clayey silt. This palaeosol is covered by grey to brown silty fine sand including fine gravel (1.41 to 1.16 m b.s.l.). The following stratum (1.16-0.60 m b.s.l.) contains numerous calcareous nodules, plant remains and also fine gravel as well as incorporated palaeosol material. The subsequent layer is made out of clayey silt characterized by freshwater gastropods, calcareous nodules and hydromorphic features. Between 0.27 and 0.52 m a.s.l., we found a layer of fine sand intersecting this silt-dominated unit.

The sedimentary sequence of vibracore MOU 3 is mainly made out of homogenous grey silty fine sand including mollusc fragments and few laminae enriched with organic material. Between 2.94 and 2.18 m b.s.l., we detected several intersecting layers of sandy gravel. At 1.11 m b.s.l., another coarse-

grained layer shows a fining upward sequence of gravel, coarse, medium and fine sand. Towards the top, this unit shows rust-colored iron (hydr-) oxide spots documenting post-sedimentary subaerial weathering. The uppermost sedimentary unit (0.05-0.32 m a.s.l.) consists of clayey silt.

7.4.2 Geochemical analyses, grain size studies and microfossil investigations

Selected results of geochemical analyses of vibracore MOU 1 are depicted in Figure 52. Significant peaks of the Ca/Ti and the Ca/Fe ratios were identified associated to coarse-grained layers out of sand and gravel. At the same time, these layers show clearly decreased concentrations of potassium. K values are highest in fine-grained silt-dominated units of the core. Such discrepancies are also reflected in the grain size data. The calculated grain size ratio clearly illustrates the difference between predominating silt and intersecting sand and gravel units. The grain size ratio and the Ca/Fe- and Ca/Ti-ratios show comparable curve progressions.

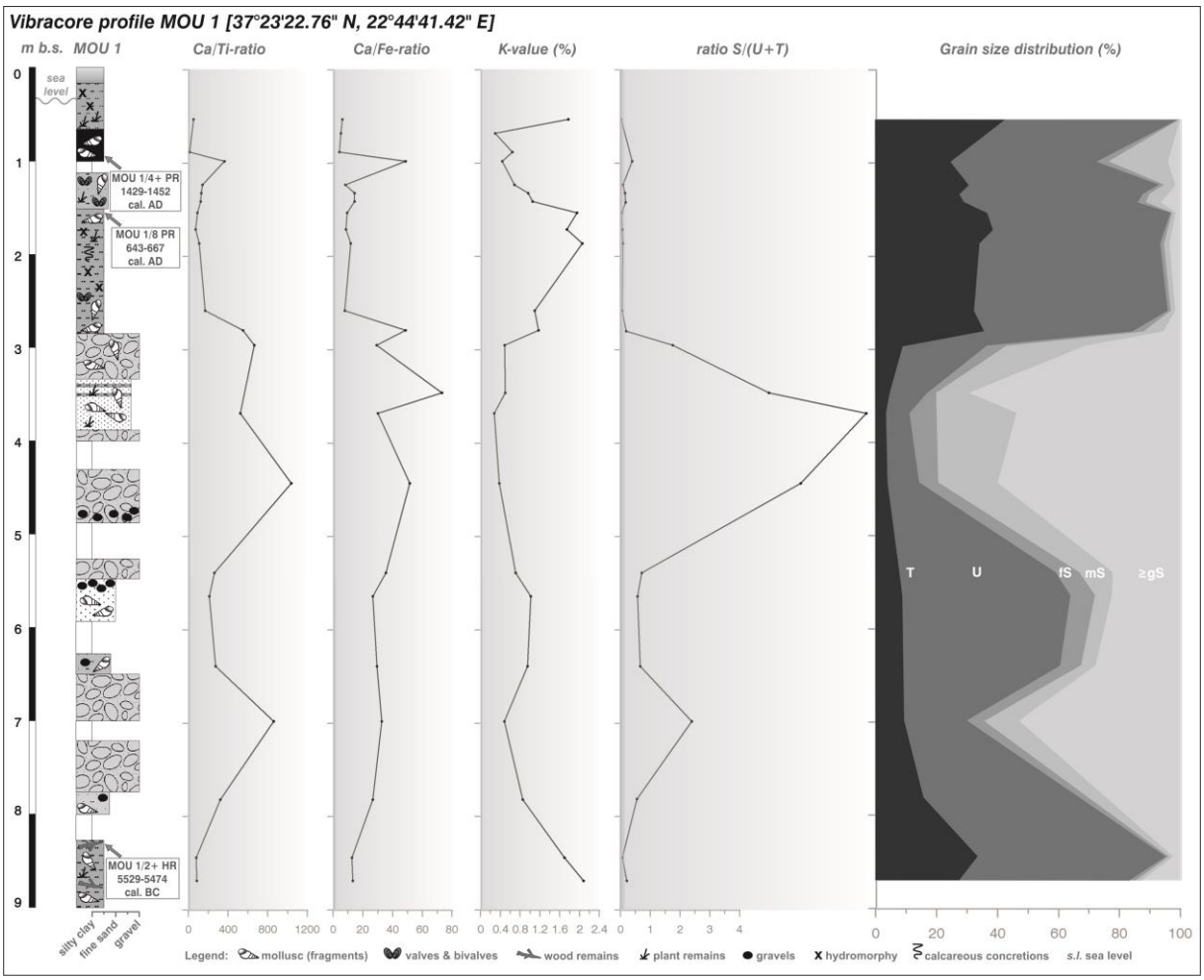

Figure 52: Stratigraphy of vibracore MOU 1 and results of grain size and geochemical analyses for selected sediment samples (source: own data and illustration 2013).

The results of the micropalaeontological analyses of selected samples from vibracore MOU 1 (foraminifera, gastropods, ostracods, bivalvia, among others) are illustrated in Figure 53.

Within the silt-dominated sediments at the base of the core, we identified species typical of brackish environments such as *Ammonia beccarii*, *Ammonia tepida, Haynesina depressula, Rosalina* sp. and *Adelosina mediterranensis* (samples MOU 1/23 and MOU 1/22). The spectrum of gastropods comprised *Gibbula* sp., *Cerithium* sp. and *Pirenella conica*. Moreover, a single specimen of the bivalve *Tellina* sp. and the algae *Rhabdochara* sp. as well as a great many of the ostracod *Cyprideis torosa* were detected within this stratigraphical unit.

Sample MOU 1/21 was taken from the following sand unit showing the highest biodiversity and abundance of species encountered in core MOU 1. The ecological spectrum comprises species typical of shallow marine and littoral environments. Also, several marine gastropod species were identified such as *Alvania* sp*., Rissoa splendida, Rissoa* sp. Furthermore, the euryhaline gastropod *Pirenella conica*, the marine sea snail *Scenea* sp. as well as the aquatic pulmonate gastropod *Planorbis corneus* were found. Besides marine bivalves such as *Neotrigonia lamarcki, Plagiocardium papillosum* and *Spisula substrucata,* a great many of the ostracod *Cyprideis torosa* were encountered, a species that prefers shallow, quiet brackish habitats but also bears freshwater conditions as well as few exemplars of the freshwater algae *Rhabdochara* sp..

Sample MOU 1/20 from the following section of sandy gravel shows a clearly decreased microfossil record but still contained many saltwater-borne species such as *Ammonia beccarii, Ammonia* sp*., Elphidum crispum, Quinqueloculina* sp*., Rosalina* sp*., Alvania* sp*., Pirenella conica, Rissoa* sp*., Cyprideis torosa* and shell debris.

Sample MOU 1/18 again reflects high abundance and biodiversity of marine macro- and microfaunal species. For instance, we detected *Adelosina laevigata, Adelosina mediterranensis, Adelosina* sp*., Ammonia beccarii, Ammonia parkinsonia, Ammonia* sp*., Ammonia tepida, Cycloforina* sp*., Elphidium crispum, Nonion* sp*., Quninqueloculina costata, Quinqueloculina laevigata, Quinqueloculina seminula, Quinqueloculina* sp*., Rosalina* sp*.,* and *Spiroloculina* sp. Moreover, a great many of the gastropod *Pirenella conica*, the bivalve *Macoma cumana* and a single specimen of *Tricolia* sp., as well as many specimens of the ostracod *Cyprideis torosa* were found associated with abundant shell debris.

Samples MOU 1/16, MOU 1/14 and MOU 1/13, taken from layers out of sandy gravel, again show a clearly decreased biodiversity. In addition, the abundance of encountered species is lower. However, we found species that usually live in brackish-lagoonal, shallow marine and littoral environments, such as *Ammonia beccarii, Ammonia tepida, Elphidium* sp*., Haynesina depressula*, *Bittum* sp*., Cerithium* sp*., Mangelia paciniana, Pirenella conica, Rissoa* sp*., Tricolia* sp. as well as *Cyprideis torosa*.

Samples MOU 1/11 and MOU 1/9 originate from the homogeneous grey fine-grained sedimentary unit between 2.58 and 1.17 m b.s.l. and show a very thin microfossil record including, for example, *Ammonia* sp. and *Haynesina* sp. and a great many of *Cyprideis torosa* as well as shell debris.

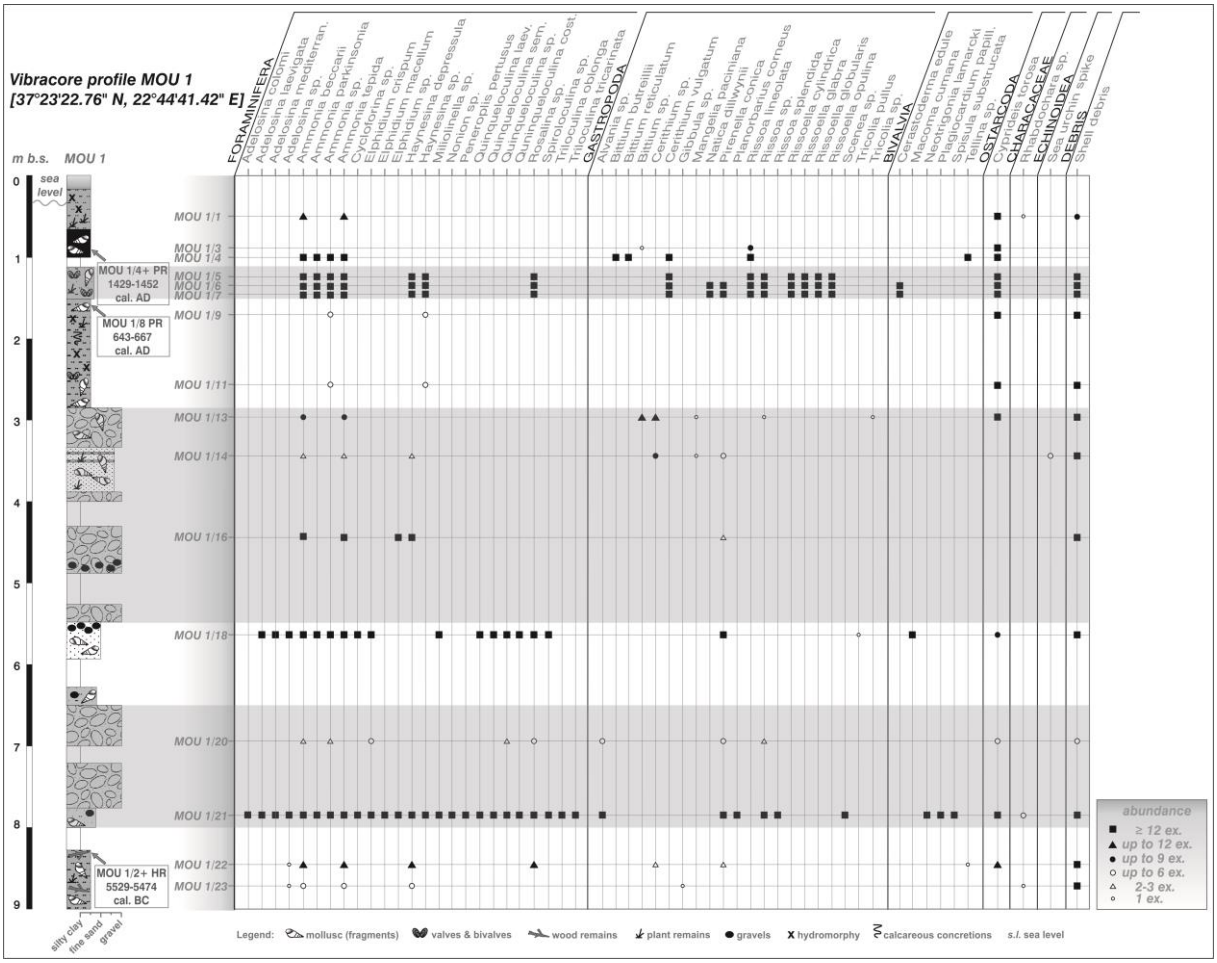

Figure 53: Summarized results of macro- and micropalaeontological analyses of selected samples from vibracore MOU 1 (source: own data and illustration 2013).

Samples MOU 1/7, MOU 1/6, MOU 1/5 and MOU 1/4 were taken from the dark grey fine sandy silt. It is characterized by an abrupt increase of abundance and biodiversity of saltwater-borne species and shows the broadest gastropod spectrum of the entire core. We found marine gastropods such as *Bittium butreillii, Bittium reticulatum, Cerithium vulgatum, Natica dillwynii, Rissoa lineolata, Rissoa* sp.*, Rissoella cylindrica, Rissoella glabra, Rissoella globularis*, *Rissoella opulina* and the lagoonal species *Pirenella conica*. We also encountered the gastropod *Natica dillwynii* that usually lives between the intertidal zone down to several thousand meters depth and prefers sandy substrate or debris (HUELSKEN et al. 2008, VILLA 1986a, 1986b). In samples MOU 1/7, MOU 1/6 and MOU 1/4, we found a great many of the marine bivalves *Cerastoderma glaucum and Tellina* sp., respectively. These samples furthermore contained a great many of the brackish ostracod *Cyprideis torosa* and the foraminifers *Ammonia beccarii, Ammonia parkinsonia, Ammonia tepida, Ammonia* sp.*, Haynesina depressula, Haynesina* sp. and *Rosalina* sp., again documenting a shallow marine and brackish-lagoonal origin of the sedimentary material.

In the following peat layer (sample MOU 1/3) we found no foraminifera tests but a single specimen of *Bittium* sp. and few specimens of *Rissoa lineolata* as well as a great many of *Cyprideis torosa*. The

uppermost sample MOU 1/1 is characterized by many specimens of *Ammonia beccarii*, *Ammonia tepida* and *Cyprideis torosa*, all of them typical of lagoonal conditions.

7.4.3 Radiocarbon dating results

Three samples from vibracore MOU 1 were dated using the ^{14}C-AMS dating method in order to establish a local geochronostratigraphy. We selected plant material and charcoal to avoid a potential marine reservoir effect which is common for marine samples.

Sample name (Lab. No.)	Depth (m b.s.)	Depth (m b.s.l.)	Sample Description	Δ^{13} C (in ‰)	^{14}C age (BP)	1σ max; min (cal BC/AD)
MOU 1/4 PR (UCI 111475)	0.98	0.69	plant remains	-25.6±0.1	450±15	1429 - 1452 cal AD
MOU 1/8 PR (UCI 111476)	1.50	1.21	plant remains	-26.3±0.1	1375±15	643 - 667 cal AD
MOU 1/21+ HR (UCI 111477)	8.33	8.04	char coal	-27.5±0.1	6535±20	5529 - 5474 cal BC

Table 4: Radiocarbon dates of samples from vibracore MOU 1 drilled in the western environs of Limnothalassa Moustou (Argolis Gulf, Peloponnese – Greece). (Lab. No.) – laboratory number Keck Carbon Cycle AMS Facility, Department of Earth System Science, University of California, Irvine (USA); m b.s. – meter below surface; m b.s.l. – meter below sea level; 1σ max; min (cal BC/AD) – calibrated ages, 1σ-range; Calibration is based on the software Calib 6.0 (REIMER et al. 2009).

Sample MOU 1/4 PR was taken from the peat, found in the upper part of the core. It yielded a calibrated age interval of 1429 – 1452 cal AD (Table 4) and thus represents a *terminus post quem* for the deposition of allochthonous fine sandy silt, rich in shells which we found directly underneath the peat unit. On the contrary, sample MOU 1/8 PR, retrieved from the top of autochthonous limnic-lagoonal sedimentary unit yielded a calibrated age interval of 643 – 667 cal AD representing a *terminus ante quem* for the deposition of the fine sandy silt. The latter was thus accumulated between 643 – 667 cal AD and 1429 – 1452 cal AD.

Sample MOU 1/21+ HR was taken from fine-grained deposits found right underneath a thick section of sand and gravel at the base of the core. It yielded a calibrated age interval of 5529 – 5474 cal BC which represents a *terminus ante quem* for the deposition of the overlying coarse-grained deposits.

7.5 Discussion

From a stratigraphical point of view, vibracores MOU 1, MOU 1A and MOU 3 are characterized by significant discrepancies between fine-grained, silt-dominated sediments accumulated under autochthonous quiescent low-energy conditions in quiescent water bodies on the one hand, and dislocated allochthonous coarse-grained sand and gravel originating from marine environments which were deposited by high-energy sedimentary processes on the other hand (Fig. 54).

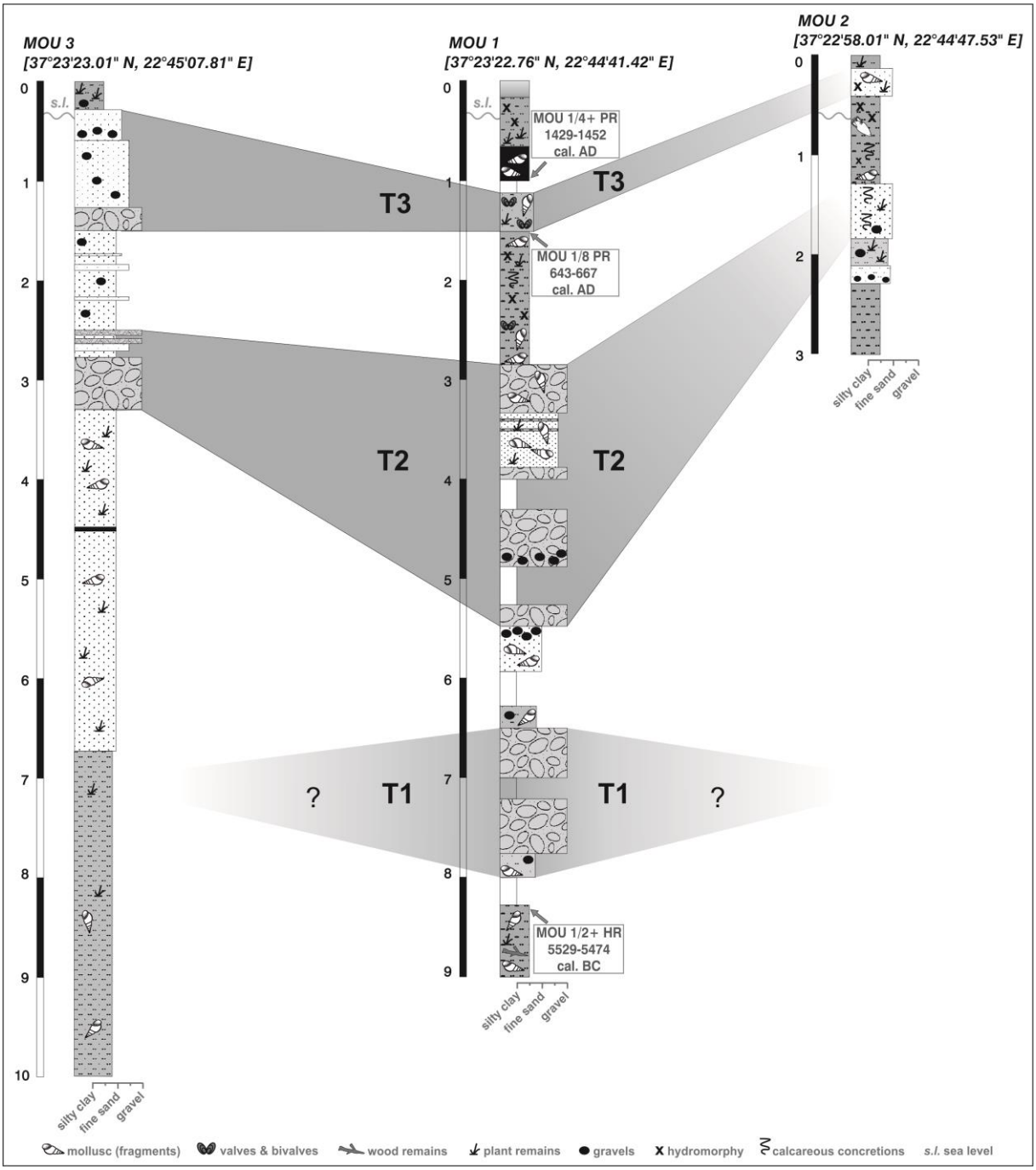

Figure 54: Stratigraphies along the Limnothalassa Moustou vibracoring transect. Coarse grained intercalations (T2 and T3) can be correlated in all cores (source: own data and illustration 2014).

The two upper allochthonous coarse-grained high-energy layers were found in consistent stratigraphical positions in vibracores MOU 1, MOU 1A and MOU 3 over a distance of more than 600 meters. These layers most probably also correspond to the two sandy intercalations encountered in vibracore MOU 2. Our data also indicate that low-energy autochthonous conditions in the environs of Limnothalassa Moustou re-established soon after the high-energy disturbances.

We found the following sedimentary and geochemical features of high-energy wave impact in the environs of Limnothalassa Moustou: (i) basal erosional discordances, (ii) a fining upward in grain size

distribution, (iii) a large landward extent, several hundreds of meters long, with a thinning landward tendency, (iv) high peaks of the Ca/Fe-ratio (GELFENBAUM & JAFFE 2003, TUTTLE et al. 2004, DOMINEY-HOWES et al. 2006, DAWSON & STEWART 2007, KORTEKAAS & DAWSON 2007, MORTON et al. 2007, WILLERSHÄUSER et al. 2013, VÖTT et al. 2011a, 2011b). The allochthonous coarse-grained deposits encountered thus represent the remains of extreme wave events from the sea side. Although similar sedimentary features were found associated to extreme storm events in several parts of the world (i.e. GELFENBAUM & JAFFE 2003, GOFF et al. 2004, DOMINEY-HOWES et al. 2006, NOTT 2006, MORTON et al. 2007, HAWKES et al. 2007, SUGAWARA et al. 2008, HORTON et al. 2009, WILLIAMS 2009, among others), storms in the Mediterranean cannot produce wave lengths and surges required for extensive coastal inundation such as reflected by the stratigraphical and multi proxy findings in our study area. In opposition to storms, there are many historical accounts that document repeated tsunami events in the eastern Mediterranean. Moreover, the annual significant wave height for the Gulf of Argolis is lower than 0.8 m and the probability that the coast is hit by outstanding wave heights of > 4.0 m tends to zero (MEDATLAS GROUP 2004, p. A.26 & A.27). The study area is thus characterized by a low to only moderate wave climate. We thus argue that the stratigraphical and multi-proxy traces of high-energy marine inundation found in the Limnothalassa Moustou sedimentary record are due to repeated tsunami influence.

Regarding the coarse-grained layers, the presence of abundant fragments of marine molluscs together with bio-erosional features associated to individual pieces of gravel which are typical of the coastal zone, clearly document a marine origin of these deposits. Although the study site is located right in between the nearby fluvial systems of Tanos Potamos and Rema Vrasiatis (Section 2), aerial photos demonstrate that Limnothalassa Moustou currently does not underlie fluvial influence such as the formation of a fan delta. The river channels run directly towards the east into the Gulf of Argolis and leave the area around Limnothalassa Moustou untouched (Fig. 50).

Results from geochemical analyses indicate that coarse-grained intersections encountered in core MOU 1 (Fig. 52) are due to high-energy impact from the marine side. These layers show both increased values of the grain size ratios and high peaks of the Ca/Ti- and Ca/Fe-ratios whereas, at the same time, the concentration of K is strongly reduced. This pattern clearly reflects repeated interruptions of autochthonous conditions in the prevailing coastal environments. In coastal Akarnania and the northwestern Peloponnese, VÖTT et al. (2011a, 2011b) correlated high peaks of the Ca/Fe-ratio to the high-energy input of biogenically produced marine carbonate. The same pattern is described by WILLERSHÄUSER et al. (2013) for palaeotsunami deposits found in back-beach archives on Cefalonia Island. Moreover, macro- and micropalaeontological studies of samples from core MOU 1 show that each of the coarse-grained layers is associated to marine indicators. Especially the lowermost and the uppermost intersections found at site MOU 1 are characterized by a distinct

mixture of faunal remains from different habitats documenting an abrupt high-energy inundation in the environs of Limnothalassa Moustou from the seaside. Concerning the high-energy layer from the base of core MOU 1, we interpret the sandy unit as inflow and the subsequent gravel-dominated section as backflow deposit reflecting the re-activation of coarse gravel deposited in fluvial archives. Also, the sand and gravel layer found in mid-core position is characterized by many marine indicators; our studies, however show that subsequent to the first high-energy impact, the area opened up to a shallow marine environment (Figs. 53 and 54). Therefore, it has to be assumed that the site was under water when it was hit by the event which left the mid-core high-energy deposits. The allochthonous material, predominantly sand and gravel with its diluted marine microfossil fingerprint (Fig. 53), thus seems to represent rather backflow than inflow dynamics during inundation from the marine side when also fluvial deposits of the adjacent rivers were re-mobilized (cf. BAHLBURG & SPISKE 2012).

According to our micropalaeontological findings, autochthonous mud was deposited under brackish conditions after the second marine inundation with a microfaunal assemblage clearly reduced in abundance and biodiversity in contrast to the previous shallow marine units. It is thus suggested that considerable coastline changes were associated to the high-energy inundation which led to the separation of a lagoon-type environment from the open sea.

Considering the layer out of fine sandy silt found intersecting limnic-lagoonal silt in the upper part of core MOU 1, a marine origin is clearly attested by the presence of 21 different foraminiferal species occurring in high abundance and typical of different habitats (Fig. 53). The fact, however, that allochthonous gravels are missing and the intersecting layer is much thinner than the older ones recorded in core MOU 1, indicate that the associated event was of a smaller dimension and did not lead to the re-mobilization of fluvial deposits. Most probably, this can also be explained by a longer distance between the site and the coastline due to a seaward shift of the coastline until that time.

Our results show that the area around Limnothalassa Moustou was thus affected three times by tsunami impact. The oldest event occurred during prehistoric times, namely after 5529 – 5474 cal BC. The event deposits found in mid-core position at site MOU 1 could not be dated because adequate dating material was missing. The youngest event layer, however, was sandwich-dated to the time between 643 – 667 cal AD and 1429 – 1452 cal AD. It possibly refers to the well-known event that affected wide parts of the eastern Mediterranean, especially the Peloponnese (AMBRASEYS 2009) in 1303 AD. SCHEFFERS et al. (2008) report on boulders and shell debris which were, most probably, dislocated by this tsunami to the northwest of Cape Pounta in nearby Lakonia. Further tsunamite-candidates of the 1303 AD event were found in near-coast sedimentary archives in central and southeast Lakonia (*Chapters 5* and *6,* this thesis). In the vicinity of Limnothalassa Moustou, the

environment soon recovered after this tsunami landfall and quiescent low-energy marshy conditions were re-established.

7.6 Conclusions

We carried out detailed geomorphological and sedimentological investigations based on vibracorings combined with the multi proxy-based analysis of sediments from near-coast geological archives in the surroundings of Limnothalassa Moustou. The following conclusions can be made.

(i) Vibracore data document that autochthonous sedimentary environments, mostly silt-dominated, were repeatedly affected by the sporadic input of allochthonous deposits, namely sand and gravel including marine shell debris.

(ii) Sedimentary features of intersecting allochthonous layers indicate high-energy inundation. Macro- and micropalaeontological studies revealed clear marine fingerprints of the high-energy deposits. High-energy deposits were found inland in consistent stratigraphical positions over a distance of up to 800 m. These characteristics, compared to the overall low- to mediate wind-generated wave climate of the Gulf of Argolis, lead us to the conclusion that these allochthonous layers are related to repeated tsunami landfall.

(iii) Altogether, three different tsunami events were recognized. The two older ones show distinct traces of complex backflow dynamics during which material from older fluvial archives were re-mobilized.

(iv) Based on ^{14}C-AMS dating of plant material, the oldest event occurred during prehistoric times after 5529 – 5474 cal BC. The second event layer could not be dated whereas the youngest event layer was most probably associated to the 1303 AD tsunami event.

(v) Finally, our results attest that the palaeogeographical evolution of the study area was strongly influenced by tsunami landfalls. After the last tsunami impact, the marsh environment at site MOU 1 recovered so that low-energy conditions have prevailed largely undisturbed during the last centuries.

Chapter 8 – Results from the inner Gulf of Argolis – Asinis Beach and the eastern Argive Plain

8.1 The inner Gulf of Argolis and its adjacent bays

Situated in close vicinity of both the Hellenic Volcanic Arc and the subduction zone of the Hellenic Trench the Argolis Gulf is exposed to the risk of earthquakes and submarine mass movements and thus to seismo-tectonically induced tsunamis. Literature compilations document tsunami events for the (eastern) Peloponnese. The 1303 AD event for instance, is listed by ANTONOPOULOS (1979), GUIDOBONI & COMASTRI (2005), AMBRASEYS (2009), SOLOVIEV et al. (2009), HADLER et al. (2011), among others. Against the background that geomorphological and sedimentological traces of past tsunami activity were successfully detected along several coastal areas of the Peloponnese and other parts of Greece, it is has to be assumed that historic events have left signs along the coasts of the Argolis Gulf. But so far, geoscientific data on past extreme wave action are still missing for the region. Geomorphological and sedimentological studies were carried out in the Argolis and adjacent regions using different sedimentological methods in order to search for traces of past extreme wave inundation.

The back-beach area of Asinis Beach near Drepano and the eastern part of the Argive Plain, both located in the inner northern part of the Argolis Gulf, were investigated by means of sedimentological, geophysical, geochemical and micropaleontological methods. Where possible, suitable dating material were taken from the cores and dated by means of the ^{14}C-AMS technique in order to make statements about the local geochronostratigraphy.

8.2 Palaeotsunami studies around Asinis Beach

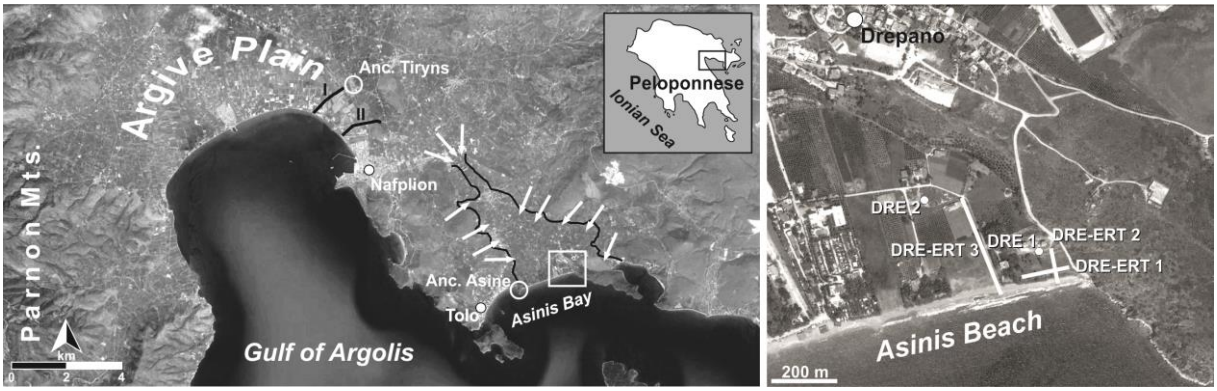

Figure 55: The aerial photos show the investigation area Asinis Beach, located in the northeastern section of the Argolis Gulf (source: own illustration, maps based Bing and Google Earth images/data, access May 2013).

In the northeastern section of the Argolis Golf, within the so called Bay of Tolo, Asinis Beach is situated. The small promontory of Cape Kastraki, located in the bays central part, is separating the town of Tolo in the west from Asinis Beach in the east. On top of Cape Kastraki the ruins of ancient

Asine are situated (Fig. 55). Asine was already named in the second book of HOMER's Iliad, as one of the towns who sent their fleet to the Trojan War (HOMER (B): Illiad: 2nd book, 531-573). Asinis beach itself marks the boundary between the Argolis Gulf and an eastern furcation of the Argive Plain (FINKE 1988: Fig. 9, VAN ANDEL et al. 1990: Fig. 4). The linear shaped beach mainly constitutes of sand and fine gravel. Prominent beachrock complexes are attending the shoreline. In the back-beach area two vibracores DRE 1 (N 37°32'00.71'', E 22°53'52.10'') and DRE 2 (N 37°32'04.15'', E 22°53'41.97'') were drilled and additionally three ERT measurements were conducted (Fig. 55).

8.2.1 Vibracores DRE 1 and DRE 2 from the back-beach area at Asinis Beach

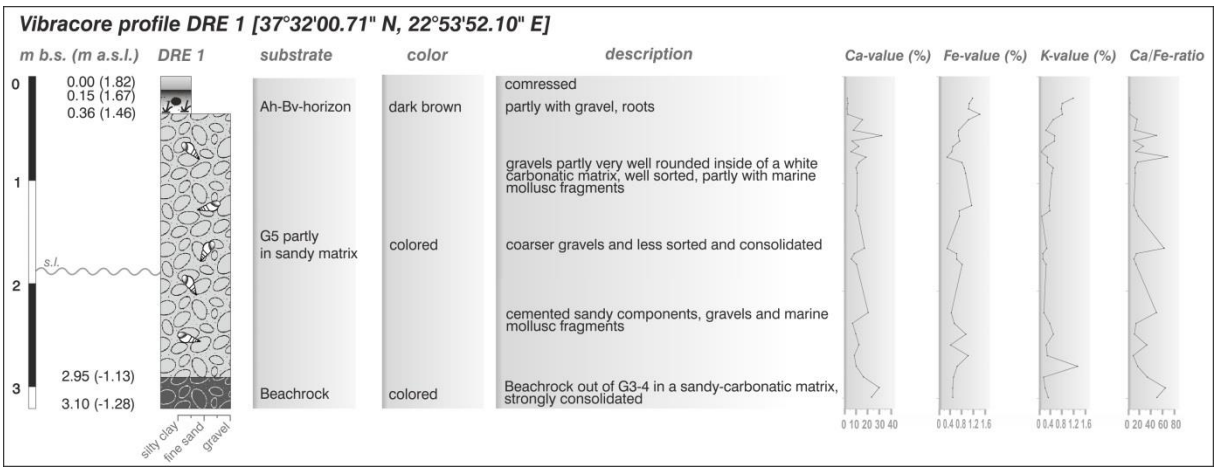

Figure 56: Stratigraphy and results of the accomplished geochemical analyses of vibracore DRE 1 encountered on meadow in the eastern back-beach area of Asinis Beach south of village Drepano (source: own data and illustration 2013).

Vibracore DRE 1 (Fig. 56) begins with consolidated beachrock. Between 1.13 m b.s.l. and 1.46 m a.s.l., the core is characterized by gravel embedded in a sandy matrix and including marine mollusc fragments. Partly the sandy matrix comes along with cementation features. The top of the core (1.46-1.67 m a.s.l.) is represented by dark-brown silt.

The basal section of vibracore DRE 2 (6.97-5.65 m b.s.l.) is also characterized by beachrock (Fig. 57). Cemented mollusc fragments point on a marine-littoral origin of the deposit. Subsequently, a unit out of red brown sand with gravel and charcoal remains was encountered. The following unit out of thick clayey silt includes numerous freshwater gastropods indicating a limnic environment. The top of the core (0.60-0.68 m b.s.l.) is an anthropogenic infill.

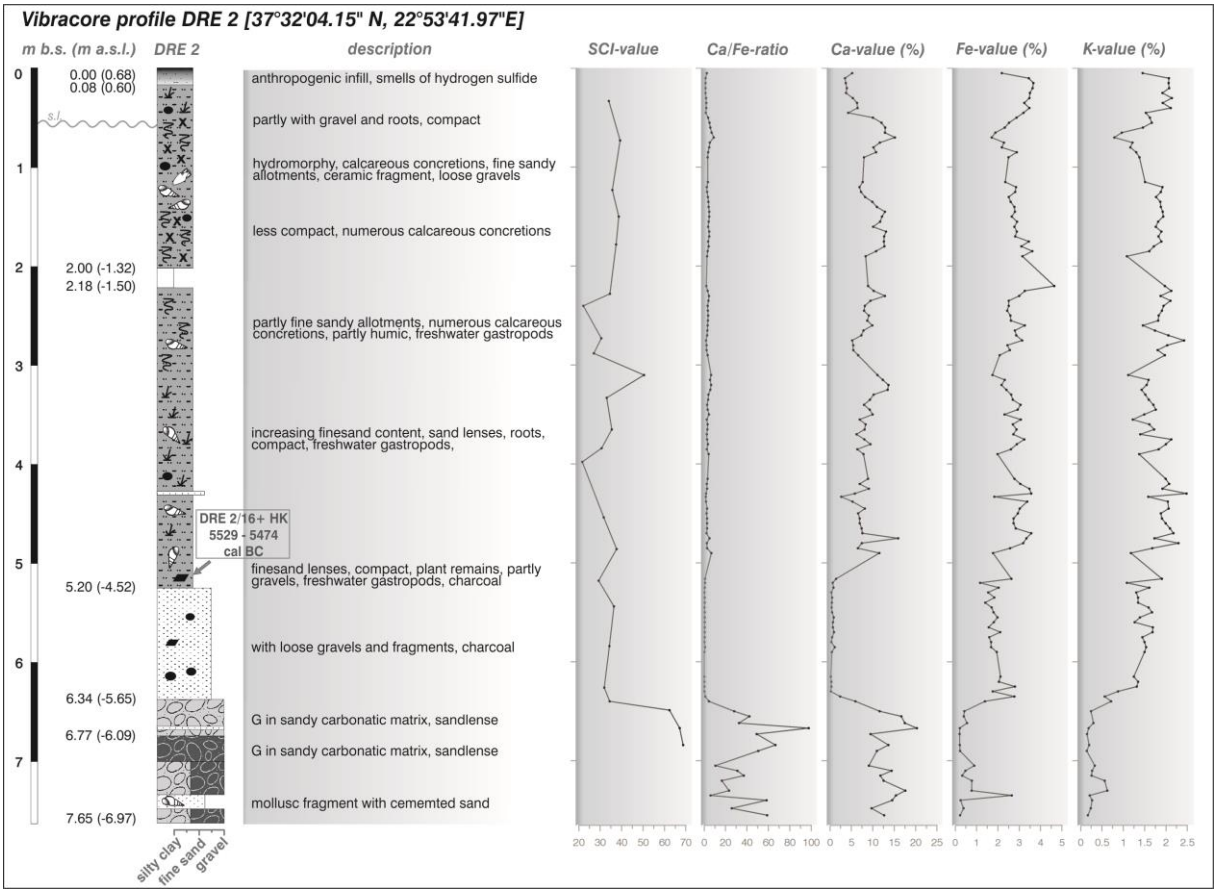

Figure 57: Stratigraphy and results of the accomplished geochemical analyses of vibracore DRE 2 encountered in the eastern back-beach area of Asinis Beach south of village Drepano (source: own data and illustration 2013).

8.2.2 Spectroscopic and XRF measurements

Color data of core DRE 2 show good correlation with main sedimentological facies changes (Fig. 57). Facies changes can also be derived from XRF data. Regarding the geochemical data the basal beachrock comes along with high Ca-values and low Fe- and K-values. In contrast, the overlying sand is almost completely decalcified whereas the concentrations of Fe and K are high. However, the overlying fine grained alluvial sequence is again characterized by increased Ca-values and slightly increased potassium and iron values.

Also at site DRE 1, the basal beachrock comes along with a high Ca-content. The transition towards the overlying less consolidated gravel sequence is marked by a descending Ca-curve. In contrast the curves of the Fe- and K-values rise. The curve shapes largely fluctuate in the height of the dominating partly consolidated gravel sequence. However, Ca-, Fe- and K-contents remain on a similar level, attesting nearly consistent conditions for the entire unit.

8.2.3 Microfaunal studies on core DRE 2

Altogether 12 sediment samples from different sedimentary units of core DRE 2 were analyzed in search of microfaunal contents. However, the core contained almost no microfossils. Only in sample DRE 2/16, extracted from the clayey alluvial unit in between 4.14 and 4.22 m b.s.l., specimens of *Cyprideis torosa* and *Ammonia tepida* were detected indicating a brackish near-coast environment.

8.2.4 Earth resistivity tomography measurements in the back area of Asinis beach

Figure 58: General topographical and geomorphological setting at vibracoring position DRE 1 in the back-beach area of Asinis Beach south of village Drepano. On top of the hill in the background ancient Asine is situated. Detailed views of the outcropping beachrock formations are presented in the two smaller pictures to the left (source: own photos taken in March 2010 and own illustration 2014).

Along two transects earth resistivity measurements were carried out in the area close to vibracoring position DRE 1 (for location of the transects see Figs. 55 and 58).

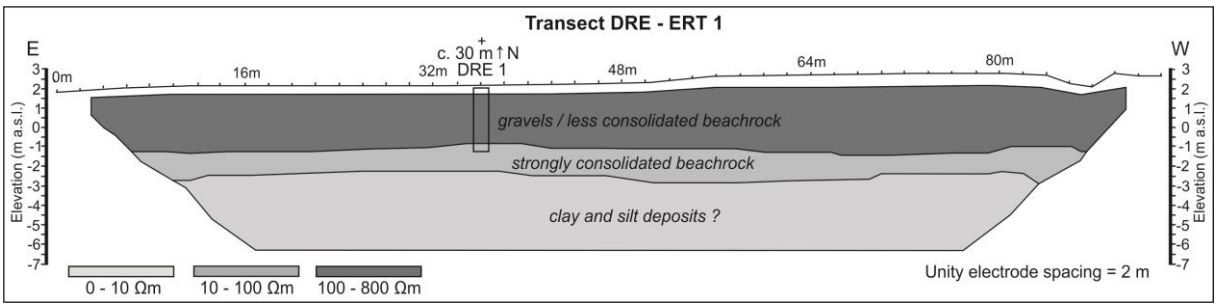

Figure 59: Interpretation of the east-west running ERT transect DRE ERT 1 measured ~30 m south of at vibracoring position DRE 1. The cross "+" marks the crossing point with transect DRE ERT 2. A Wenner-Schlumberger array with 48 electrodes was applied for transect DRE ERT 1 and an electrode spacing of 2 m was chosen (source: own data and illustration 2013).

Comparing the DRE ERT 1 data (Fig. 59) with the stratigraphy of core DRE 1 (Fig. 56), drilled approximately 30 m northwards, a good correlation is visible. The uppermost unit with resistivity values up to 800 Ωm reflects gravel and less consolidated beachrock encountered in core DRE 1 between 1.13 m b.s.l. and 1.46 m a.s.l. The second unit with values between 10 and 100 Ωm

represents strongly consolidated beachrock. The basal conductive unit may represent clay- and silt-dominated sediments underneath.

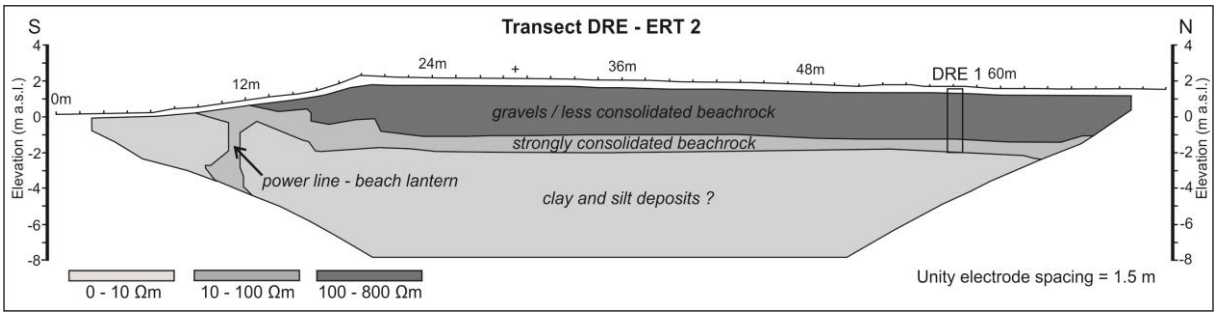

Figure 60: Interpretation of the south-north running ERT transect DRE ERT 2 measured at vibracoring position DRE 1. The cross "+" marks the crossing point with transect DRE ERT 1. Again a Wenner-Schlumberger array with 48 electrodes was applied for this transect but here an electrode spacing of 2 m was chosen (source: own data and illustration 2013).

A similar trisection is identifiable also when regarding the transect DRE ERT 2 (Figs. 60) and additionally the landward extension of the beachrock is documented.

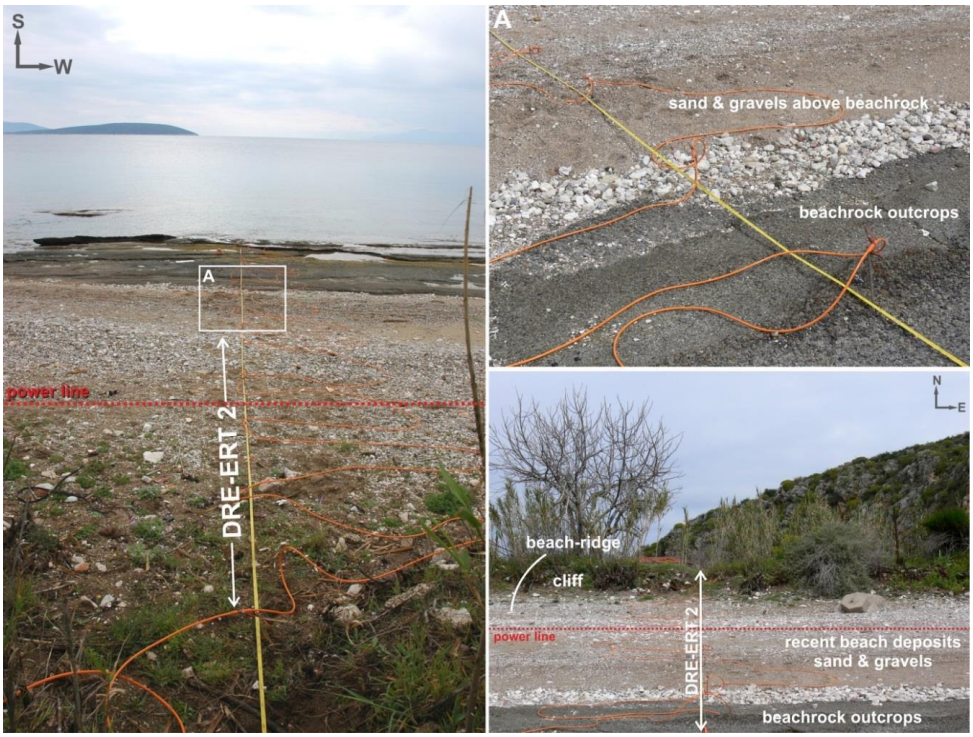

Figure 61: Geomorphological constellation in the eastern corner of Asinis Beach. ERT transect DRE ERT 2 starts on the beachrock outcrops and moves in northern direction towards vibracoring site DRE 1 while crossing the gravelly beach, the small beach-ridge and a subterranean power line (source: own photos taken in March 2010 and own illustrations 2014).

Transect DRE ERT 3 starts on the beachrock outcrops and moves to the north over the gravel beach towards the hinterland and vibracoring site DRE 2. The model resistivity section (Fig. 62) indicates that most of the transect is characterized by resistivity values lower than 5 Ωm. This is most probably attributed to silt and clay deposits encountered in core DRE 2. The southern part of the section however shows values up to 1000 Ωm, representing the gravel beach and beachrock formations. Gravel and beachrock encountered at site DRE 2 below 5.65 m b.s.l. (Fig. 57) are not depicted in the northern section of transect DRE ERT 3.

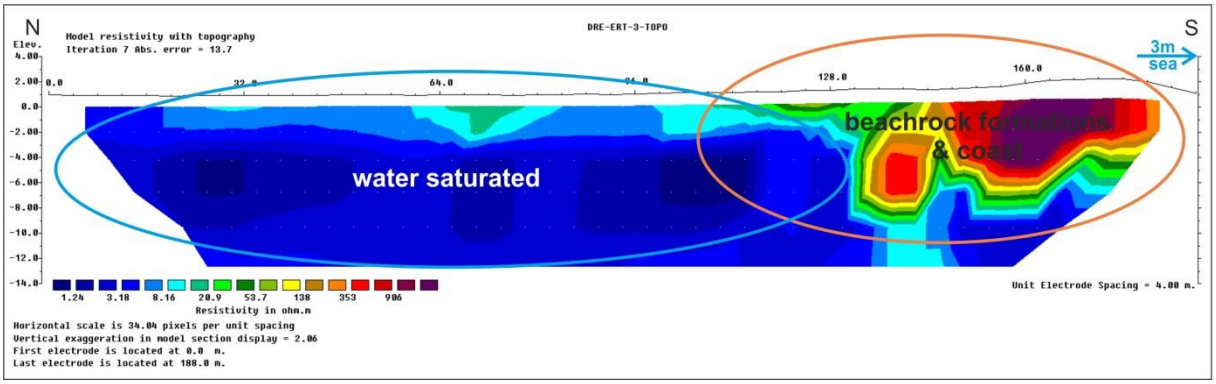

Figure 62: Results of the earth resistivity tomography measurements for transect DRE ERT 3 at Asinis Beach. Here also a Wenner-Schlumberger array with 48 electrodes was accomplished by choosing an electrode spacing of 4 m (source: own data and illustration 2014).

8.2.5 Geochronological dating result

Table 5 summarizes the results of the ^{14}C-dating approach undertaken for sample DRE 2/16+ HK, extracted from core DRE 2. The calibrated age interval of 5478; 5380 cal BC represents a *terminus ante quem* for the deposition of the material which, later, was transformed into beachrock.

Sample name (Lab. No.)	Depth (m b.s.)	Depth (m b.s.l.)	Sample description	δ^{13} C (in ‰)	^{14}C age (BP)	1σ max; min (cal BC/AD)
DRE 2/16+ HK (KIA 45978)[a]	5.16	4.48	charcoal	-26.12 ± 0.38	6465 ± 35	5478; 5380 cal BC

Table 5: Radiocarbon dates of sample DRE 2/16+ HK extracted from vibracore DRE 2, encountered in the back-beach area of Asinis Beach south of village Drepano (Argolis Gulf, Peloponnese – Greece). Note: Sample name – sample name chosen while field work; (Lab. No.) – laboratory number given by the laboratory; [a] – Leibniz Laboratory for Radiometric Dating and Isotope Research, Christian-Albrechts-Universität zu Kiel (Germany); m b.s. – meter below surface; m b.s.l. – meter below sea level; (a) δ^{13}C-value – shows incorporation of C4 plants or aquatic material and indicates a potential reservoir effect; (b) δ^{13}C-value – indicates purely atmospheric C3 photosynthesis without contamination by old carbon; 1σ max; min (cal BC/AD) – calibrated ages, 1σ-range; ";" – semicolon is used in cases where several age intervals because of multiple intersections with the calibration curve are possible**;** oldest and youngest age depicted; Calibration is based on the software Calib 6.0 (REIMER et al. 2009).

8.2.6 Discussing the results of Asinis Beach

In search of past tsunami fingerprints within the stratigraphical record of near-coast geological archives, the eastern back-beach area of Asinis Beach was investigated. Based on the stratigraphical data of two vibracorings, combined with geochemical and microfaunal analyses applied on samples of these cores, besides additional geophysical explorations, no obvious traces of past extreme wave activity were found.

The age 5478; 5380 cal BC obtained for the charcoal fragment of sample DRE 2/16+ HK represents a *terminus ante quem* for the formation of the beachrock at vibracoring site DRE 2. Later, nearly 5 m thick and relatively homogenous back-beach mud was accumulated in the area.

Beachrock is defined as a hard coastal sedimentary formation out of beach material rapidly cemented by aragonitic or calcitic carbonate precipitation (BRICKER 1972, SHORT 2005, TURNER 2005, VOUSDOUKAS et al. 2007, BIRD 2008). Although the formation processes are still unclear for most of the global beachrock outcrops, beachrock is used as an indicator of littoral processes and to reconstruct the sea level evolution (KELLETAT 2006, 2007, KNIGHT 2007). However, in recent times VÖTT et al. (2010, 2011a) detected sedimentary and geomorphological features within beachrock formations along coastal sections of western Greece, that are consistent with characteristics of sub-recent and recent tsunami deposits. Thus, in these cases, beachrock represents cemented high-energy tsunami deposits. Beachrock was also found to be related to palaeotsunami impact at Lechaion, the ancient harbour of Corinth (HADLER et al. 2013).

However, the here presented results from Asinis Beach do not allow to classify the local beachrock as palaeotsunamiite. Further fieldwork is required to better report on the origin and formation of the beachrock complex at Asinis Beach.

8.3 Palaeoevent layers in the stratigraphical record of the Argive Plain

In order to check coastal stratigraphies for sudden marine inundation altogether ten vibracorings were retrieved from the eastern part of the arable Argive Plain arranged in the form of two vibracore transects – both running from the coast towards inland (Fig. 63).

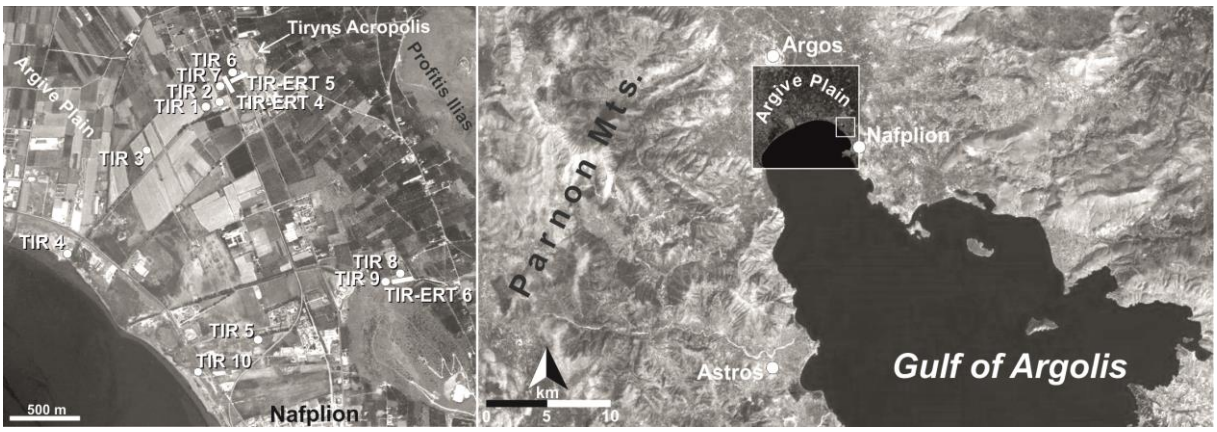

Figure 63: In the Argive Plain a total of 10 vibracorings were drilled along two SW-NE trending transects, both starting at the coast. Additionally, earth resistivity tomography measurements (ERT) were accomplished at selected locations (source: own illustration, maps based Bing and Google Earth images/data, access May 2013).

8.3.1 Vibracore transects I & II in the eastern Argive Plain

Argive Plain vibracore transect I (vibracores TIR 4, 3, 1, 2, 7 and 6)

The locations of the 6 vibracores drilled along the first southwest-northeast running Argive Plain vibracore transect I are depicted in Figure 63.

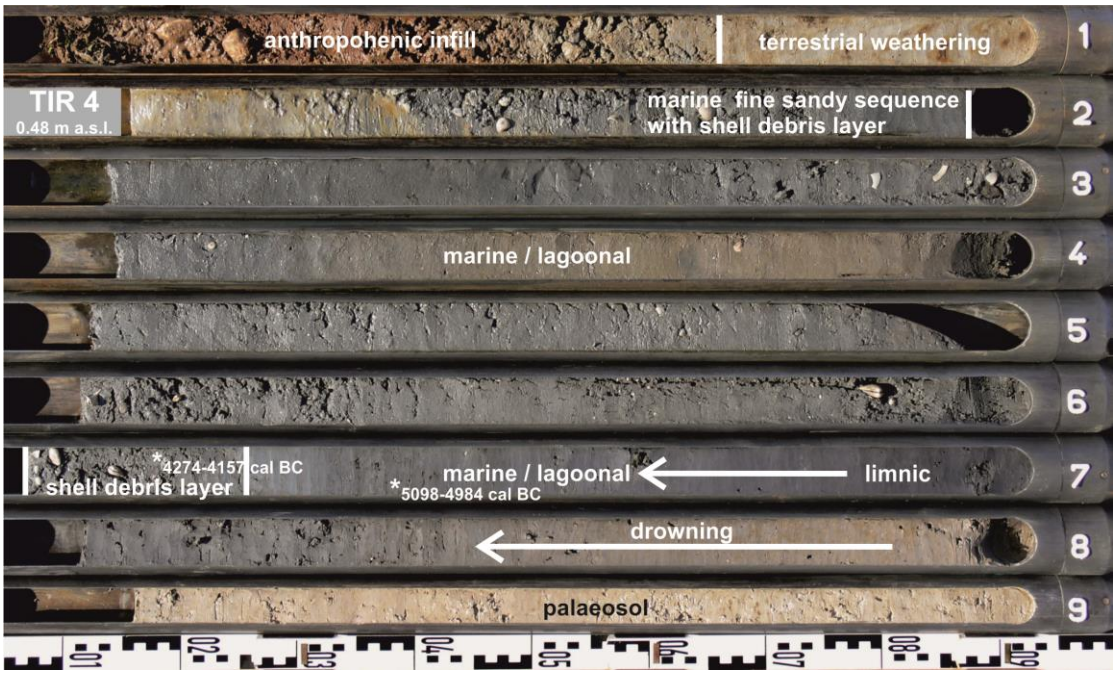

Figure 64: Photo and simplified facies profile of sediment core TIR 4 drilled on the coast 3 km west of Nafplion (source: photo taken by T. Willershäuser in March 2010, own illustration 2014).

Vibracore TIR 4 (N 37°35'15.68'', E 22°47'09.09'') (Fig. 64), drilled in a marshy environment close to the recent shoreline, starts with a unit out of clayey silt that exhibits a rusty coloring in its lower part whereas the upper part is dominated by greyish color shades. Besides the coloring plant remains and hydromorphy remarks, ferric and calcareous concretions speak for a palaeosol that was drowned during time, most possibly due to a rising sea level. This palaoesol turns over at 6.15 m b.s.l. into homogeneous grey limnic-lagoonal mud. And at 5.78 m b.s.l., a 19 cm thick heterogeneous shell debris layer, embedded in a silty-sandy matrix, was encountered. Thereby the valve, bivalve and gastropod fragments are sharp-edged. The subsequent grey sequence is mainly silt dominated in its lower part whereas the upper part also shows sandy intersections (from 3.22 m b.s.l. upwards). At 1.42 m b.s.l., a fine sandy sequence introduces a grey marine fine sandy sequence that shows another shell debris layer in its middle part. From 0.85 m b.s.l. upwards, the color of this sequence turns over to rusty color shades, probably referring to subaerial weathering processes. The top of the core is characterized by an anthropogenic infill.

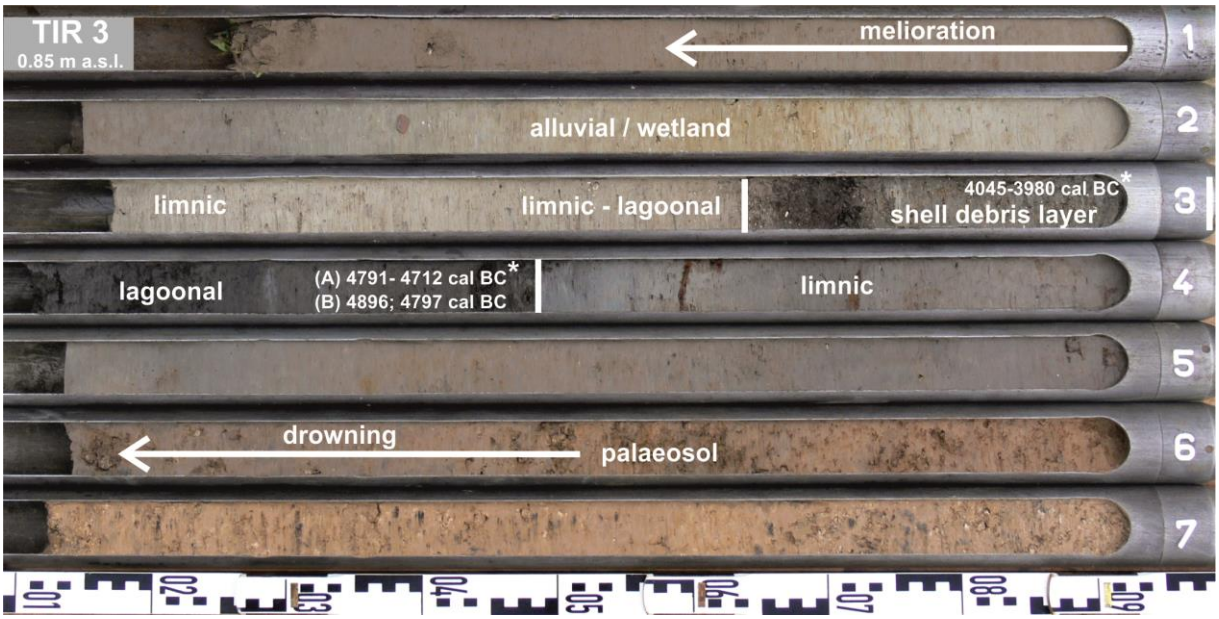

Figure 65: Photo and simplified facies profile of sediment core TIR 3 encountered on an agricultural used area between the coast and ancient Tiryns in the arable Argive Plain (source: photo taken by T. Willershäuser in March 2010, own illustration 2014).

Vibracore TIR 3 (N 37°35'36.81'', E 22°47'30.74'') (Fig. 65), drilled in approximately 850 m distance to the present coastline within an utilized agricultural area, starts with a palaeosol out of clayey silt. At 2.63 m b.s.l. a transition towards a dark grey sequence is to register that contains peat layers, abundant freshwater gastropods and fragments of those. The sedimentary characteristics speak for a progressive silting up of the area, thus referring to a local ingression and the establishment of a marine influenced most probably limnic-lagoonal environment at coring site TIR 4. However, at 2.15 m b.s.l. a discordance leads over to sequence out of clayey silt that contains fine sandy allotments besides numerous mollusc fragments and plant remains. This unit passes seamless over

into a shell debris layer (1.88 and 1.76 m b.s.l.) that was found embedded in a matrix out of organic silt and peat. Again the shell fragments are characterized by sharp edges. These sediments are covered by deposits out of homogenous clay and silt.

The stratigraphical sequence of core TIR 1 (N 37°35'46.11'', E 22°47'47.97'') starts with a palaeosol. This palaeosol is covered at 3.10 m b.s.l. by rust-colored clayey silt. Further upcore the color becomes greyish and freshwater gastropods document limnic conditions. Between 0.26 and 0.15 m b.s.l. a smooth transition leads over to a fine sandy sequence, containing mollusc and charcoal fragments as well as calcareous nodules. From 0.48 m b.s.l. towards the top, the grain size again becomes finer towards clayey silt showing a grey-brown coloring.

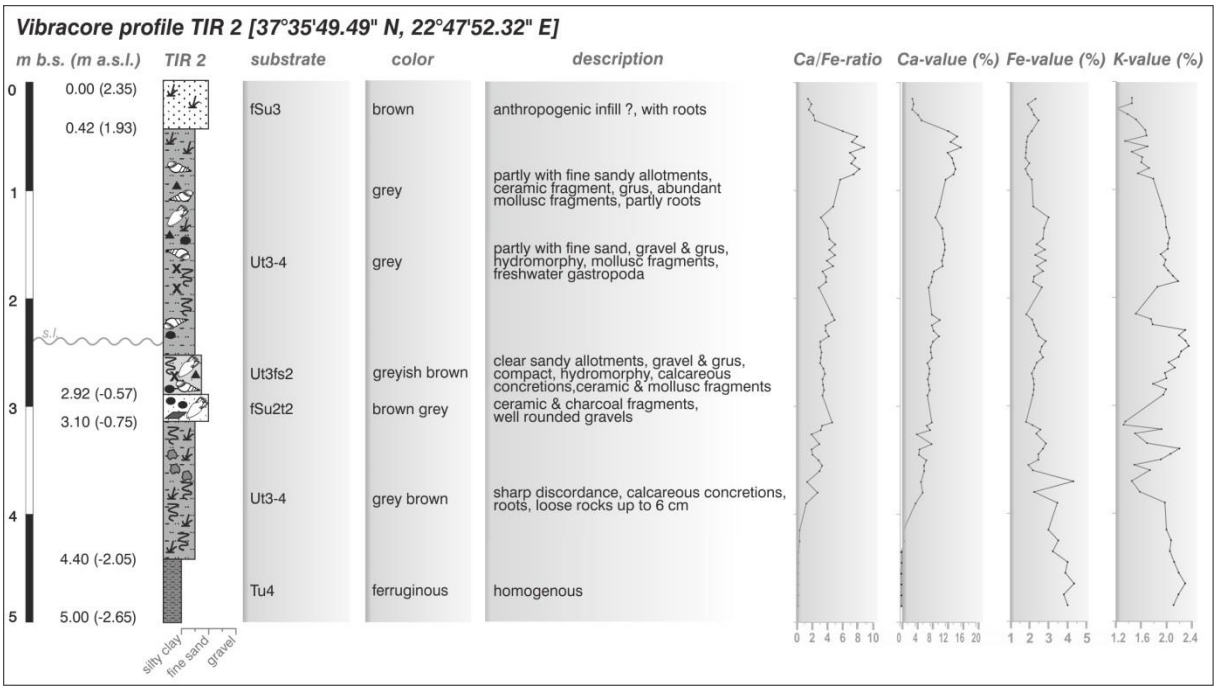

Figure 66: Stratigraphy and results of the conducted geochemical analyses of core TIR 2 (source: own data and illustration 2013).

The stratigraphy of core TIR 2 (N 37°35'49.49'', E 22°47'52.32'') (Fig. 66) is similar to the one of core TIR 1. A palaeosol is covered at 2.05 m b.s.l. by an alluvial deposit. Between 0.75 and 0.57 m b.s.l., fine sand was encountered including ceramic and charcoal fragments besides well rounded pieces of gravel. The upper part of the core is characterized by grey clayey silt. The top of the core is an anthropogenic infill.

The stratigraphy of core TIR 7 (N 37°35'52.11'', E 22°47'52.48'') (Fig. 80) shows a red palaeosol covered by clayey silt. Between 0.66 and 0.35 m b.s.l. a layer of fine sand was found. Upwards the sequence is again dominated by clayey silt representing most probably alluvial and or colluvial deposits. The stratigraphy of the easternmost vibracore TIR 6 (N 37°35'53.82'', E 22°47'54.27'') (Fig. 82) is similar to core TIR 7.

In general, the stratigraphical data of the six cores of transect I indicate that the eastern Argive Plain experienced a local ingression. This resulted in the gradually drowning of Pleistocene palaeosols and alluvial deposits. Marine deposits were deposited close to the recent shore. However, during time a local regression occured in the eastern Argive Plain. Thick fine-grained alluvial deposits were found especially in the cores located in the hinterland, covering marine and/or limnic-lagoonal deposits and palaeosols. However, the stratigraphical data further refers to temporal environmental interferences, at least for the seaward cores, shown by conspicuous shell debris layers and sandy intersections in quiescent low-energetic dominated environments.

Argive Plain vibracore transect II (vibracores TIR 10, 5, 9 and 8)

The locations of the 4 vibracores encountered along the second southwest-northeast running Argive Plain vibracore transect II are depicted in Figure 63.

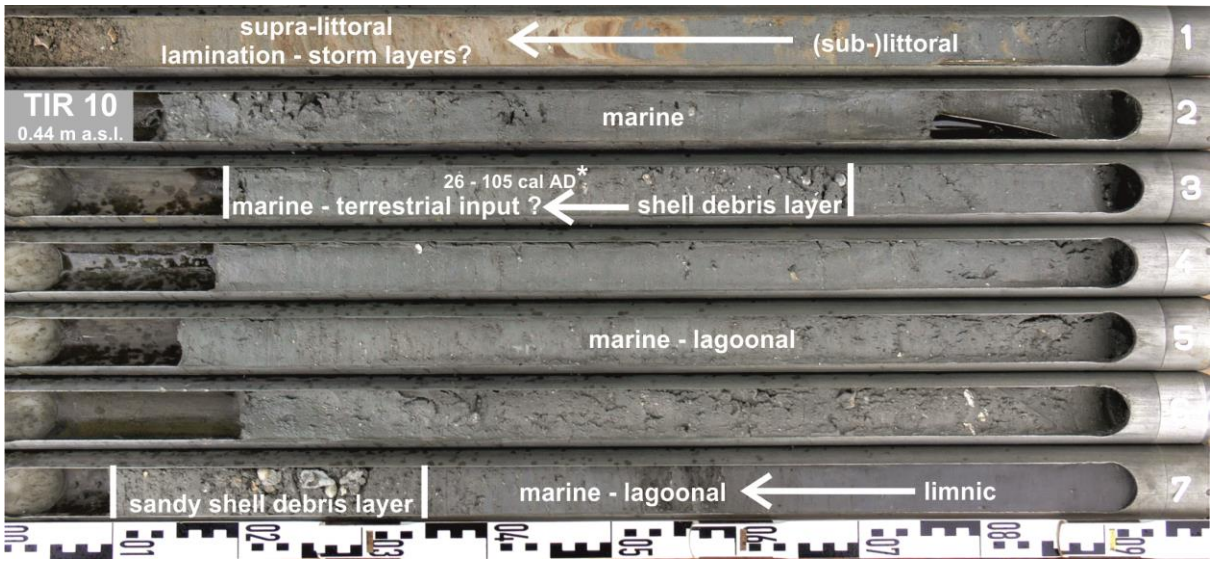

Figure 67: Photo and simplified facies profile of sediment core TIR 10 drilled on the coast close to Nafplion (source: photo taken by T. Willershäuser in March 2010, own illustration 2014).

Vibracore TIR 10 (N 37°34'50.07'', E 22°47'44.80'') (Fig. 67) starts with grey clayey silt referring to former limnic-lagoonal conditions. Upwards the cores stratigraphy is mainly characterized by marine grey fine sandy to clayey silt and partly silty fine sand. A coarse and heterogeneous shell debris layer with incorporated coral fragments abruptly intersects the sequence between 5.86 and 5.66 m b.s.l. Between 2.49 and 2.05 m b.s.l. a second shell debris layer, showing sharp-edged shell fragments, was to encounter which passes seamless over into a unit out of fine sandy silt containing numerous plant remains and incorporated mollusc fragments. Afterwards, marine-lagoonal fine sand and fine sandy silt follows. The fine sandy top of the core is characterized by several alternating laminae.

Vibracore TIR 5 (N 37°34'56.89'', E 22°48'00.40'') (Fig. 68) starts with beige clayey silt that contains numerous carbonate nodules. The following silty clay document a quiescent low-energy

environment. At 4.91 m b.s.l. a seamless transition is to register towards a grey marine sequence which is dominated by alternating units out of fine sand and fine sandy silt. Between 4.02 and 3.92 m b.s.l. a coarse shell debris layer was found including numerous marine mollusc fragments with sharp edges, valves and bivalves as well as coarse and fine coral fragments. Between 2.04 and 1.94 m b.s.l another shell debris layer embedded in a sand silty matrix also including coral fragments was to encounter. Upwards sediments again become finer and more homogeneous. From 1.11 m b.s.l. towards the top, clayey silt deposited in a marsh environment was found.

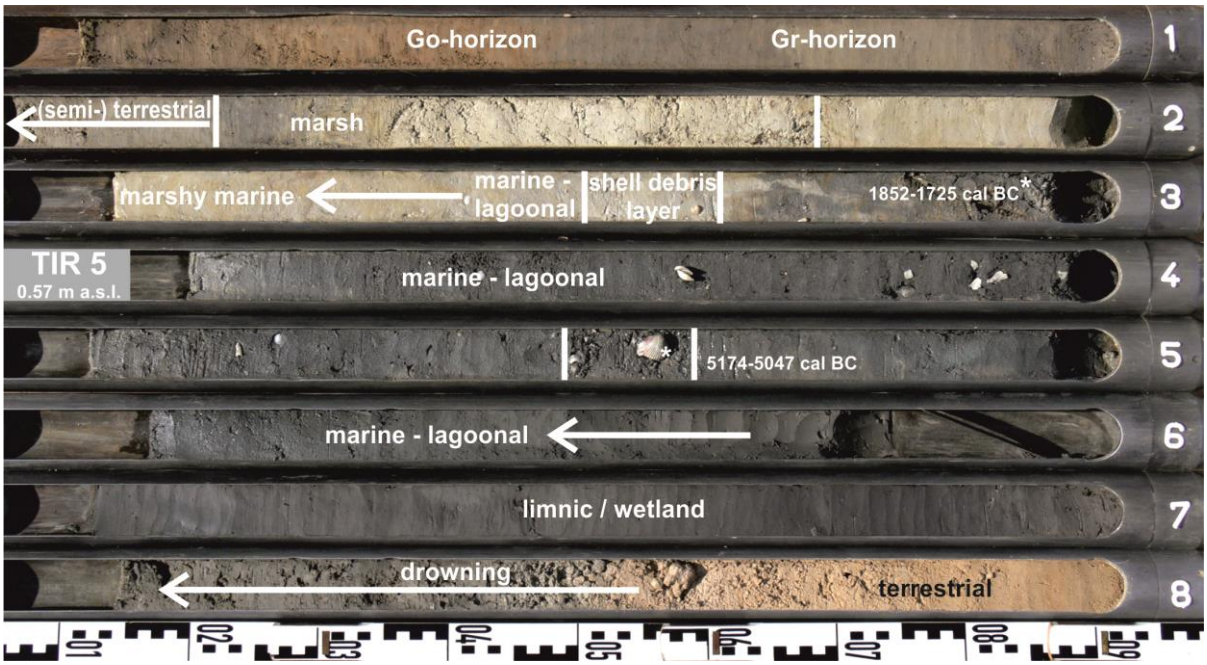

Figure 68: Photo and simplified facies profile of sediment core TIR 5 encountered in the eastern Argive in between the coast close to Nafplion and the small Profitis Ilias hill (source: photo taken by T. Willershäuser in March 2010, own illustration 2014).

At the base of vibracore TIR 9 (N 37°35'09.15'', E 22°48'35.35'') (Fig. 69), the local bedrock was reached which is covered by clayey silt including gravels and grus. Between 7.53 and 8.04 m a.s.l., gravels within a silty fine sand matrix were encountered. Subsequently, silty to sandy deposits which were better sorted although they partly contained pieces of gravel were detected. The top of the core is made out of well sorted material partly containing sandy laminae.

At vibracoring site TIR 8 (N 37°35'10.42'', E 22°48'38.55'') (Fig. 69) the basal unit out of brown alluvial clayey silt is covered at 8.82 m a.s.l. by a 0.97 m thick deposit out of well-rounded gravel. Subsequently, clayey fine sand covered by another gravel layer was found. The top of the core is made out of silty-clayey sand that partly contains gravel and grus.

The sedimentological results of the Argive Plain vibracore transect II document a local marine ingression at sites TIR 10 and TIR 5. However, during the younger geologic past, the area experienced a regression. Again allochthonous shell debris layers were detected in cores TIR 10 and TIR 5, intersecting autochthonous environments probably referring to sporadic environmental

interferences. In contrast, vibracores TIR 9 and TIR 8 mainly reflect alluvial and colluvial processes in the hinterland.

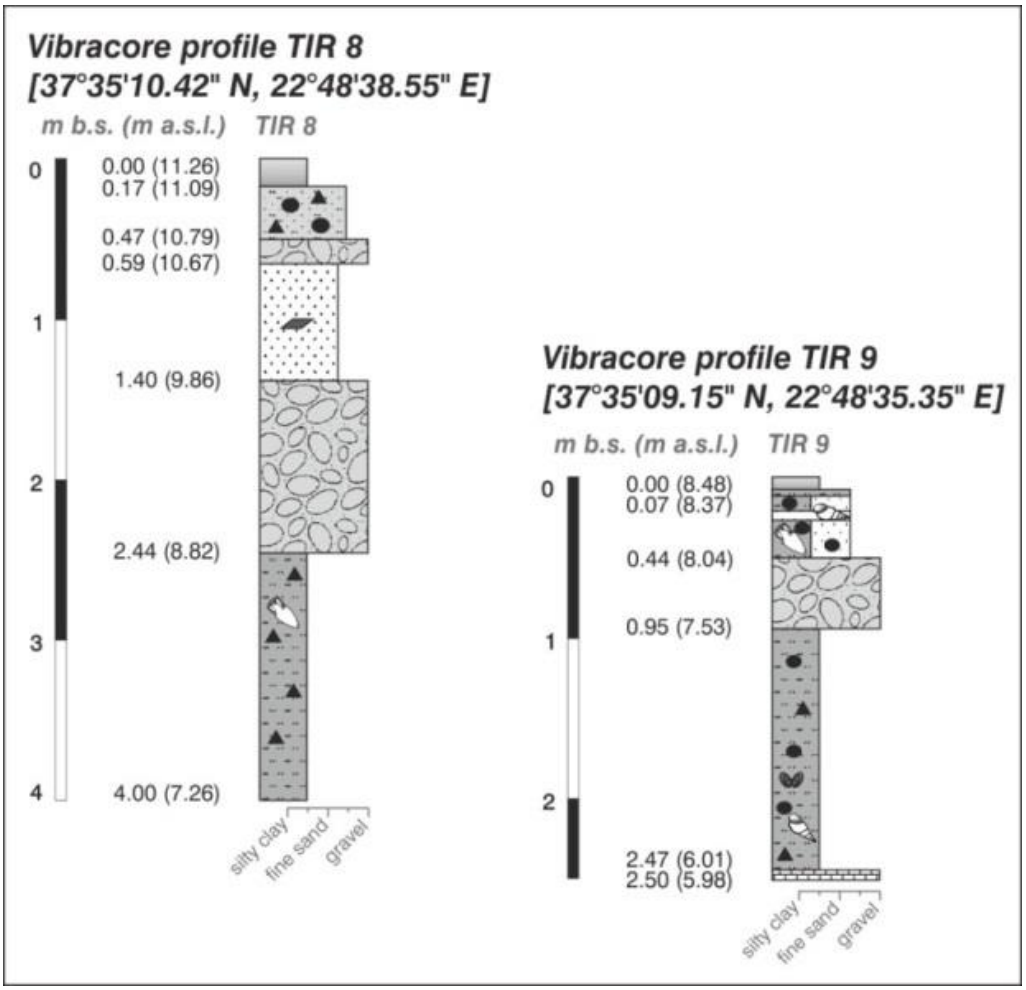

Figure 69: Stratigraphies of cores TIR 8 and TIR 9 encountered on grazing land at the northern foot of the small Profitis Ilias hill close to Nafplion and ancient Tiryns (source: own data and illustration 2013).

8.3.2 Grain size data, magnetic susceptibility and XRF measurements

Laboratory data for the Argive Plain vibracore transect I

In core TIR 4 (Fig. 70) the lower palaeosol unit is characterized by high Fe- and K-values and low Ca-values. The beginning ingressive phase (from 6.15 m b.s.l. upwards) comes along with increasing Ca-values and descending Fe- and K-values. The ingression is also visible when regarding the magnetic susceptibility. Moreover, it is accompanied by a higher input of silty material in contrast to the clay dominated lower unit. Between 5.78 and 2.47 m b.s.l., lagoonal deposits are also characterized by low Fe- and K-values and higher Ca-values. Besides a slightly increased Ca/Fe-ratio and a peak in the magnetic susceptibility curve the shell debris layer also shows a higher content of sand, referring to temporary higher energetic conditions. The fine sandy sequence, encountered between 1.42 and

0.19 m b.s.l. with its incorporated shell debris layer (1.27-0.85 m b.s.l.), is associated with a strong Ca/Fe-peak. This shell debris layer also comes along with strongly reduced magnetic susceptibility values.

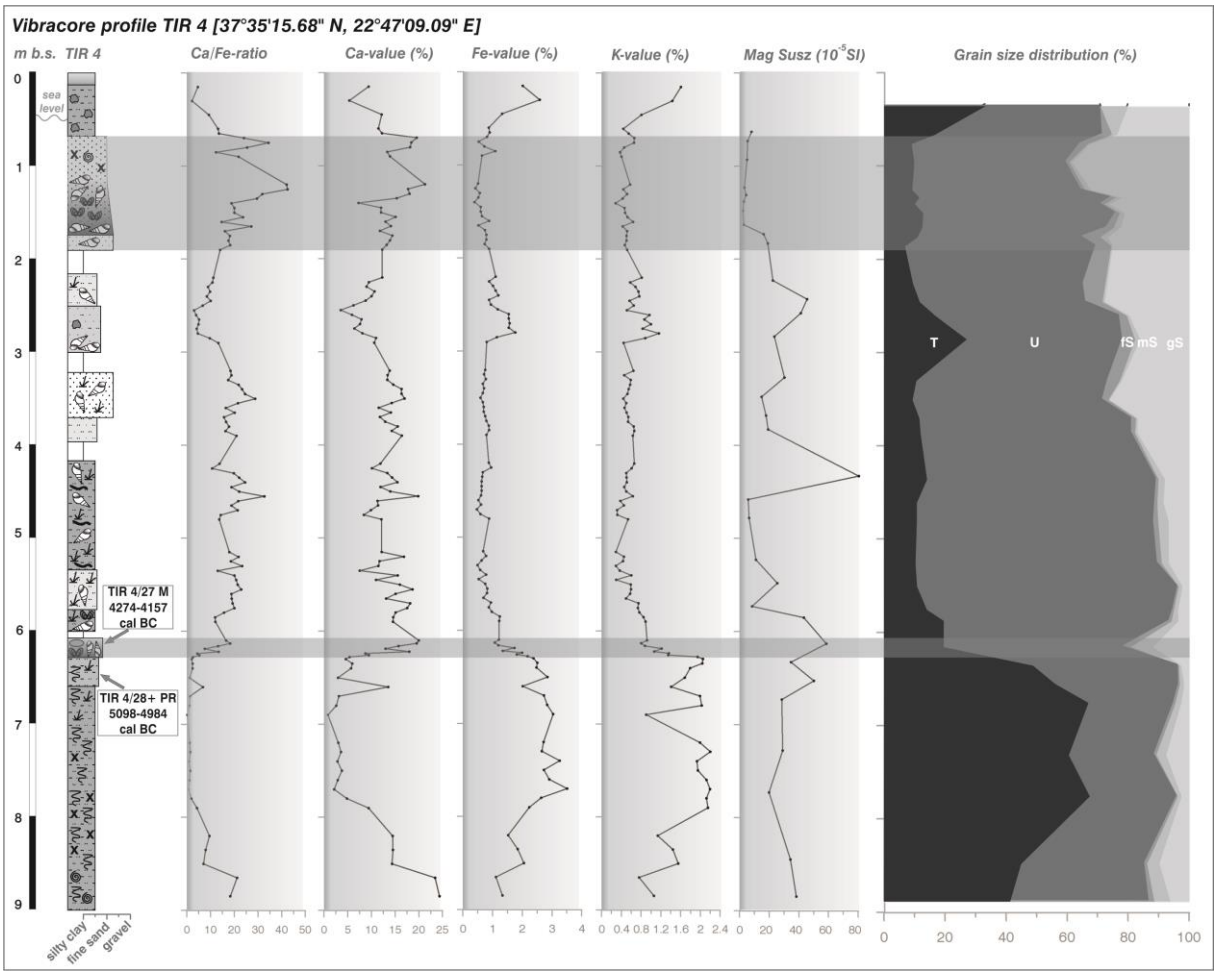

Figure 70: Stratigraphy, grain size data and results of the conducted geochemical analyses of core TIR 4 (source: own data and illustration 2013).

Considering vibracore TIR 3 (Fig. 71) the basal palaeosol sequence is characterized by relatively high Fe- and K-values whereas the Ca-curve shows low values. Similar to core TIR 4 the ingression comes along with increasing Ca-values. And regarding the curve of the magnetic susceptibility the beginning of the ingression at c. 2.63 m b.s.l. is also marked by a strong peak. The highest peak of the Ca/Fe-ratio was found for the shell debris layer, similar as in the case of the upper shell debris layer found in core TIR 4.

The geochemical dataset of the more landward cores TIR1, TIR 2, TIR 7 and TIR 6 shows that the basal units are decalcified but feature high Fe- and K- values. The subsequent upper alluvial units are characterized by slightly increased Ca-values and fluctuating Fe- and K-concentrations. As for vibracore TIR 2, the sandy intercalation shows slightly increased Ca/Fe-values whereas there is a decrease of the K-content.

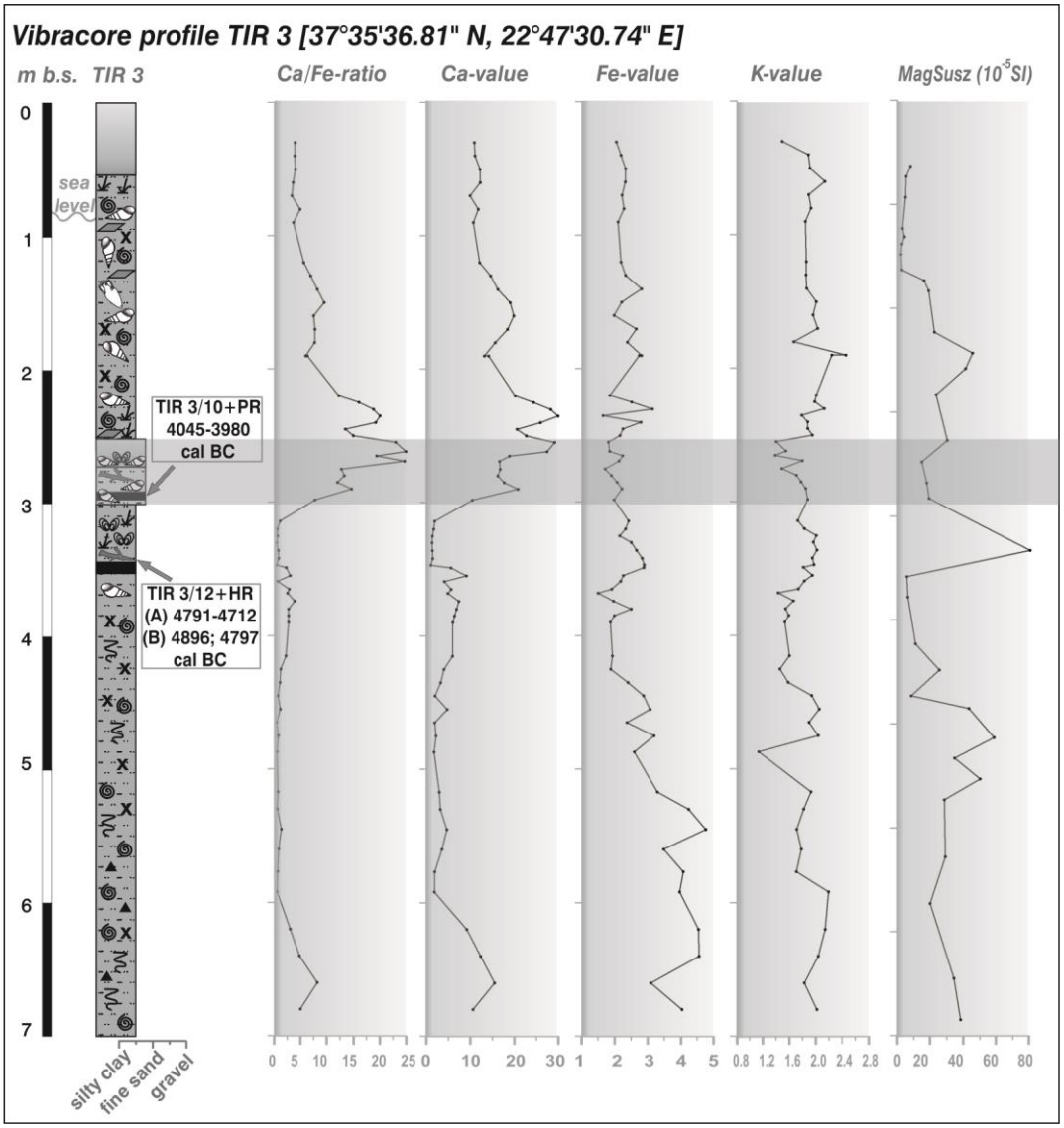

Figure 71: Stratigraphy and results of the conducted geochemical analyses of core TIR 3 (source: own data and illustration 2013).

Laboratory data for the Argive Plain vibracore transect II

The basal part of core TRI 10 (Fig. 72) is characterized by increased Fe- and K-values in contrast to low Ca-values that even tend to nil. The local ingression at 6.31 m b.s.l. comes along with increased Ca-values and decreased K- and Fe-values. The lower shell debris shows a clear peak in the Ca/Fe-curve similar as described for the shell debris layers of transect I. Simultaneously the Fe- and K-curve decrease. This is also true for the upper shell debris layer whereas the subsequent fine sandy silt unit is accompanied by clearly increasing Fe- and K-values and decreasing Ca-values, probably referring to an input of terrigenous material.

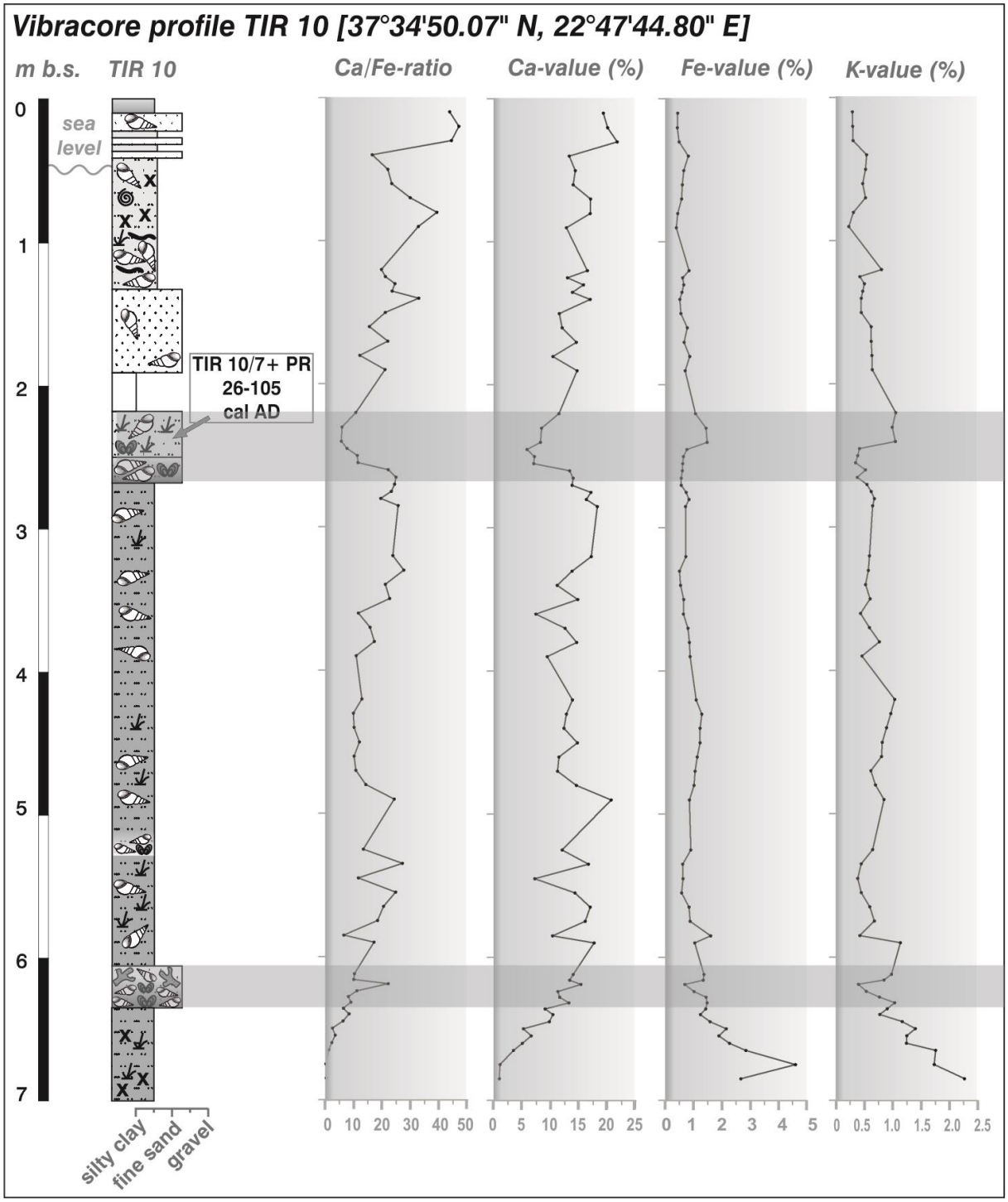

Figure 72: Stratigraphy and results of the conducted geochemical analyses of core TIR 10 (source: own data and illustration 2013).

The basal fine grained sequence of vibracore TIR 5 (Fig. 73) is characterized by high Ca-values and low K- and Fe-values. The drowning of the basal palaeosol sequence, most probably linked to a rising sea level, is expressed from 6.88 m b.s.l. upwards by clearly descending Ca-values and coevally ascending K- and Fe-values. A bend in the magnetic susceptibility curve is also to register at this height. From 4.91 m b.s.l. upwards Ca-concentrations raise constantly whereas the K- and Fe-values decrease referring to marine conditions. Subsequently, marine conditions were replaced by (semi-)terrestrial ones shown by rising K- and Fe-values and falling Ca-values. It is obvious that the Ca/Fe-ratio of the

upper shell debris layer between 2.04-1.94 m b.s.l. stands out significantly from the over- and underlying core sections and is associated to abrupt environmental changes.

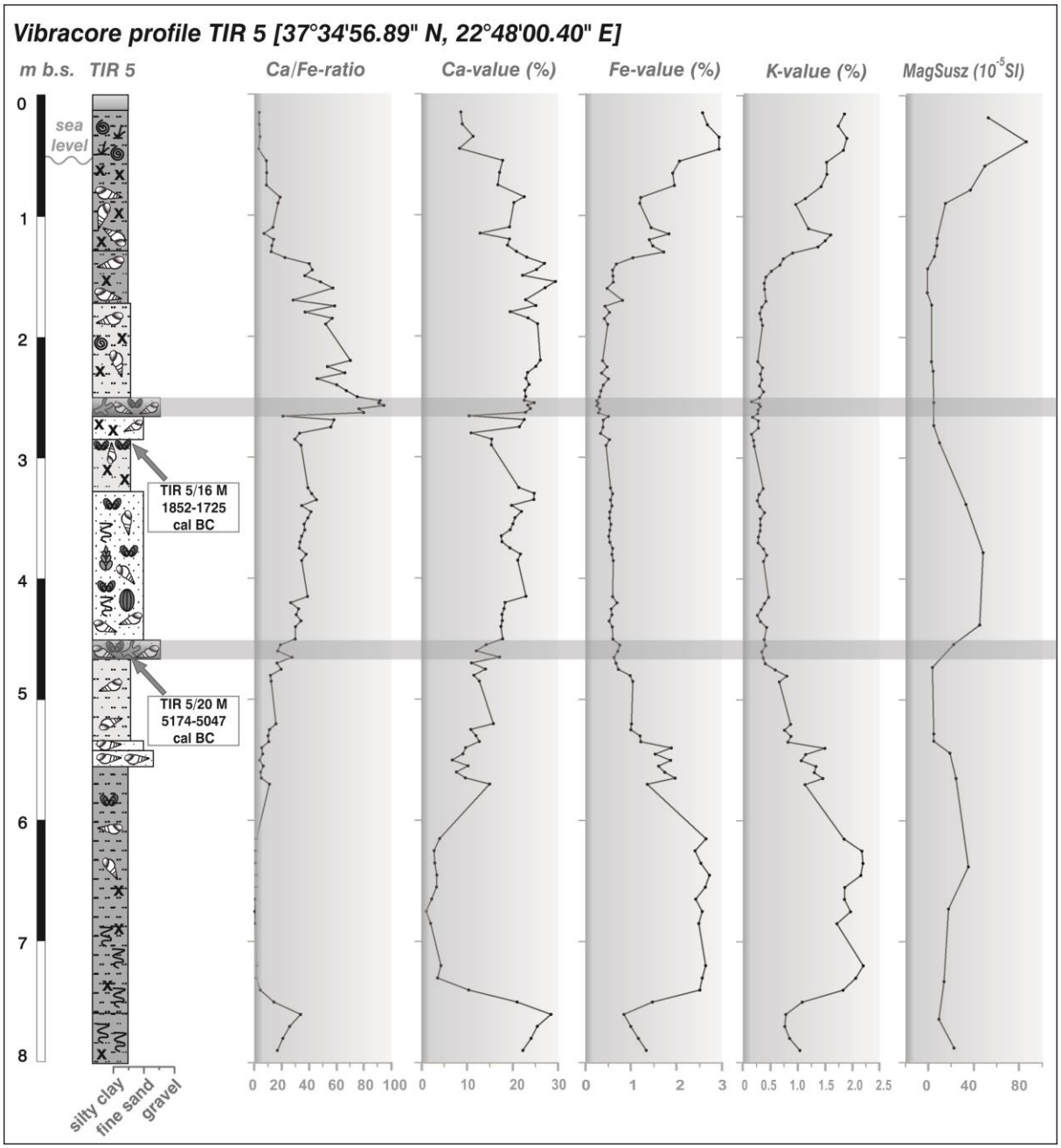

Figure 73: Stratigraphy and results of the conducted geochemical analyses of core TIR 5 (source: own data and illustration 2013).

Regarding the geochemical data of vibracore TIR 8 (Fig. 74) the coarse gravel intersections come along with high Ca-values due to integrated local limestone bedrock material.

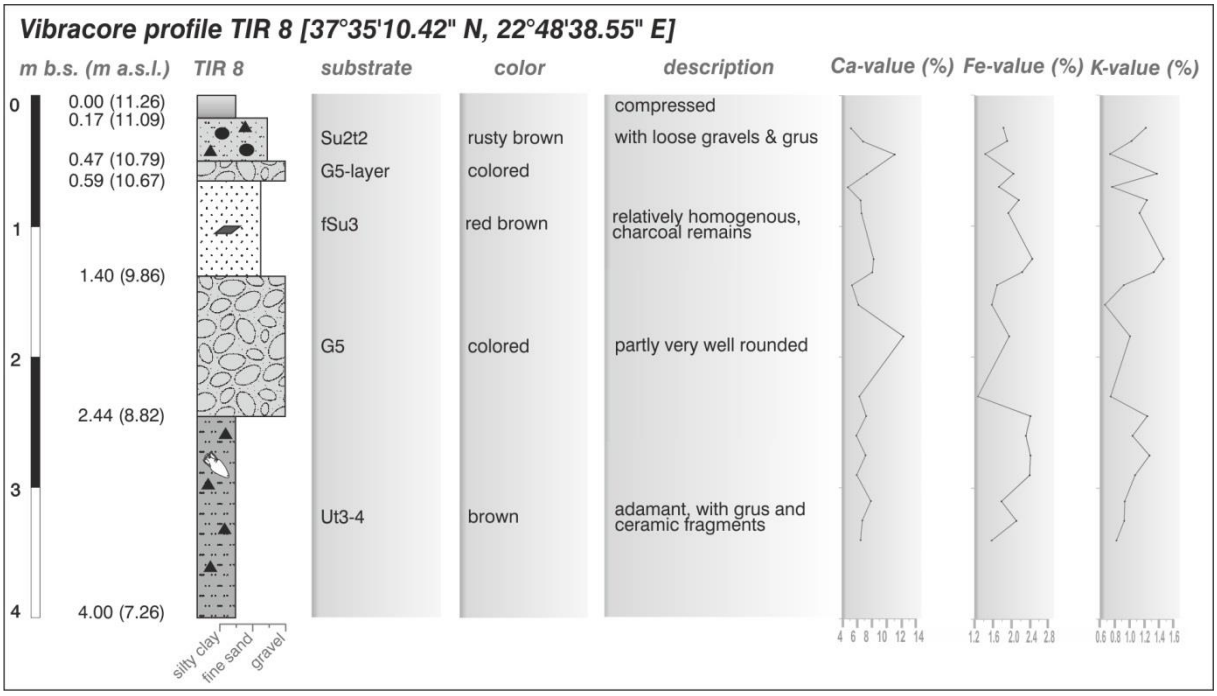

Figure 74: Stratigraphy and results of the conducted geochemical analyses of core TIR 8 (source: own data and illustration 2013).

8.3.3 Microfossil analyses

Micro- and macrofossil analyses were carried out of samples from selected vibracores. Results of microfaunal studies are summarized in Figures 75, 76, 77 and 78.

Microfaunal analyses of samples from vibracores TIR 4 and TIR 6 of transect I

Regarding the microfossil record of vibracore TIR 4 sample TIR 4/32 from the basal unit contained no fossils. Sample TIR 4/29 shows a thin microfaunal record. Species like *Ammonia beccarii* and *Ammonia tepida* as well as *Elphidium crispum*, *Eponides concammeratus*, *Haynesina depressula* and *Nonion* sp. in combination with the brackish ostracod *Cyprideis torosa* document marine influences. The subsequent sample TIR 4/27 taken out of the heterogeneous sandy shell debris layer comes along with 21 different foraminiferal species besides marine gastropods and bivales as well as the ostracod *Cyprideis torosa,* thus showing the broadest spectrum of detected species within the whole profile. The spectrum of foraminfera comprises a great many benthic specimens out of the order of the Rotaliida, such as *Ammonia beccarii*, *Ammonia tepida*, *Elphidium advenum*, *Elphidium crispum*, *Elphidium* sp., *Haynesina depressula*, *Haynesina* sp. and many of *Rosalina* sp. (HAYWARD 2013, GROSS 2001). Moreover, within this sample a great many Miliolida were identified. Miliolida are an order of protists that comprise benthic foraminifera with calcareous and porcelacous tests (LOEBLICH & TAPPAN 1964). According to HAYNES (1981) Miliolida are *"secrete imperforate shells of high magnesium calcite, which are most easily produced in warm, shallow, hypersaline waters saturated with $CaCO_3$"*. Within sample TIR 4/27 the spectrum of Miliolida, that typically occur in lagoonal environments,

comprises the species *Adelosina laevigata, Adelosina* sp., *Cycloforina* sp., *Miliolinella* sp., *Miliolinella subrotunda*, *Quinqueloculina laevigata*, *Quinqueloculina siminula*, *Quinqueloculina costata*, *Quinqueloculina* sp., *Spiroloculina* sp. and *Triloculina* sp. Additionally, the sample contained an example of *Bolivina* sp. (order of Buliminida) and one of *Globorotalia* sp. (order of Globorotaliida) (CIMERMANN & LANGER 1991, LOEBLICH & TAPPAN 1964). Regarding the favored habitat of the detected species association the microfossil content comprises specimens that occur in shallow-marine, littoral and brackish environments (RÖNNFELD 2008, MURRAY 1991, GROSS 2001, CIMERMANN & LANGER 1991). Moreover, within this shell debris layer numerous specimens of the marine bivales *Acanthocardia paucicostata*, *Macoma cumana* and *Parvicardium minimum* and the marine gastropods *Corbula gibba, Cerithium vulgatum* and *Rissoa* sp. were found (DANCE 1977, DELAMOTTE & VARDALA-THEODOROU 2001, GOFAS et al. 2001).

The subsequent samples TIR 4/24, TIR 4/23 and TIR 4/21, taken out of the grey fine-grained unit, again show a microfossil assemblage typical of lagoonal conditions. Thereafter, the samples are mainly dominated by benthic foraminifera of the order of Rotaliida, whereas the abundance Milliolida decreased in contrast to sample TIR 4/27. Also the spectrum of gastropods and bivalves underlines lagoonal character of the sequence as well as the presence of a great many of the ostracod *Cyprideis torosa* and the algae *Rhabdochara* sp.

Sample TIR 4/17, taken out of the upper coarser part of the marine-lagoonal section, shows a microfaunal record dominated by Rotaliida, such as *Ammonia beccarii, Ammonia tepida, Elphidium crispum, Haynesina depressula, Rosalina* sp.*,* and Miliolida such as *Adelosina laevigata, Adelosina* sp., *Cycloforina* sp. *Miliolinella* sp., *Quinqueloculina laevigata, Quinqueloculina seminula, Quinqueloculina costata, Quinqueloculina.* And a single specimen of *Fursenkoina* sp. out of the order of the Buliminida was found (LOEBLICH & TAPPAN 1964, CIMERMANN & LANGER 1991, GROSS 2001, MURRAY 1991, HAYWARD & GROSS 2011, HAYWARD 2013). Also, many brackish *Cyprideis torosa* ostracods were identified. Moreover, fairly many species of the marine snail *Cerithium submamillatum* and few species of *Cerithium vulgatum* were found besides fairly many specimens of the marine bivalve *Parvicardium minimum* and rare specimens of the bivalve *Tricolia tenuis* (DANCE 1977, DELAMOTTE & VARDALA-THEODOROU 2001, GOFAS et al. 2001).

The following sample TIR 4/14 shows a clearly reduced micro- and macrofossil record. Accordingly, foraminifera were detectable only in the form of *Ammonia beccarii* and *Ammonia tepida*, few specimens of *Elphidium advenum*, a single specimen of the planktonic foraminifera *Globigerina* sp. and a few specimens of *Quinqueloculina laevigata.* Abundant *Cyprideis torosa* were also to identify. The spectrum of gastropods is reduced to *Cerithium submamillatum* and *Cerithium vulagtum.* Bivalves were not identified within this sample.

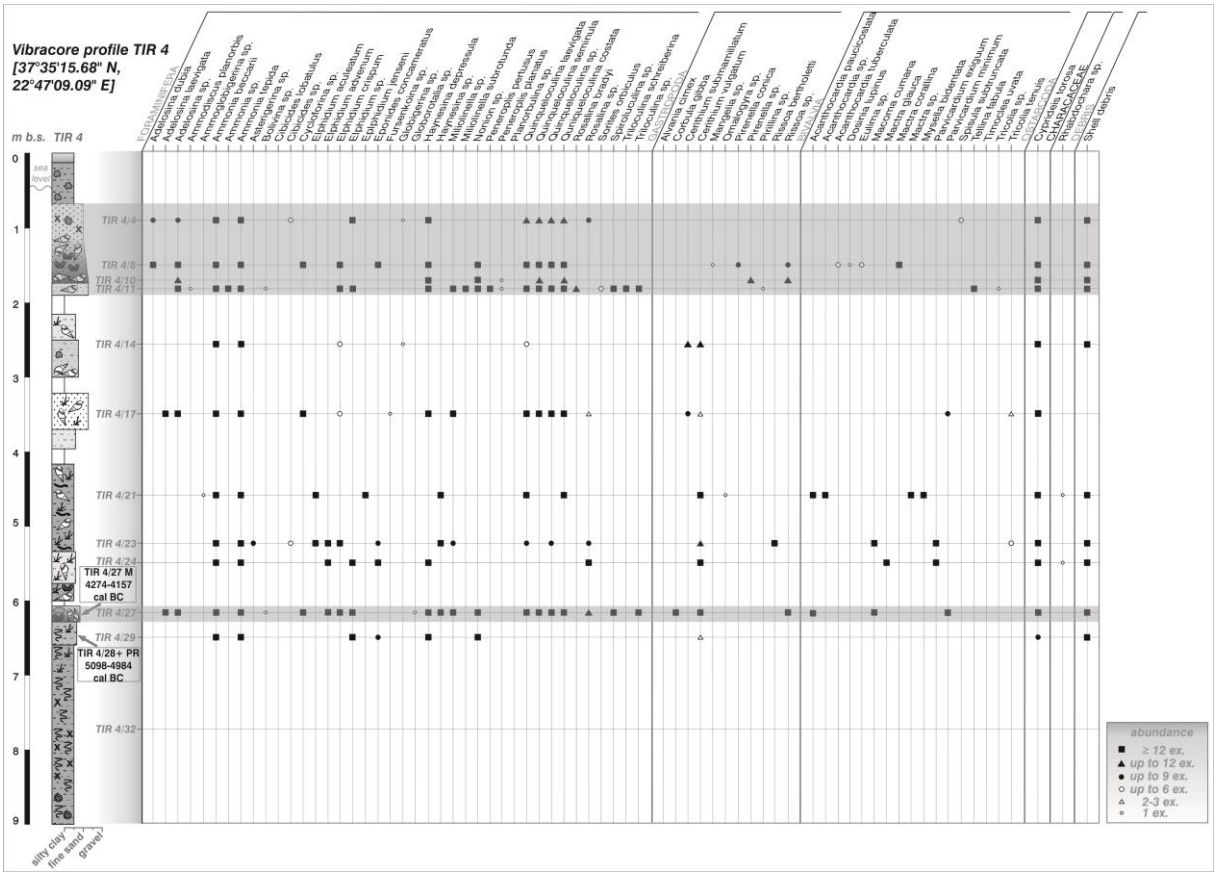

Figure 75: Summarized results of the micro- and macrofossil analyses on samples form vibracore TIR 4 (source: own data and illustration 2013).

In contrast, the subsequent sample TIR 4/11, extracted from the basal part of the fine sandy sequence, showing a fining upward tendency, comes along with a significantly extended micro- and macrofossil record, in terms of diversity and abundance of the detected species. This is also true for the two following samples TIR 4/10 and TIR 4/8 taken out of the shell debris layer located in the basal and middle part of sequence. The faunal record is characterized by a great many of benthic foraminifera of the order of Rotaliida (such as *Ammonia beccarii, Ammonia tepida, Ammonia* sp.*, Cibicides* sp.*, Elphidium crispum, Elphidium* sp.*, Eponides concameratus, Haynesina depressula, Nonion* sp.*, Rosalina bradyi) and* Miliolida, (such as *Adelosina dubia, Adelosina* sp.*, Cycloforina* sp.*, Miliolinella subrotunda, Miliolinella* sp.*, Peneroplis pertusus, Quinqueloculina laevigata*, *Quinqueloculina siminula*, *Quinqueloculina costata*, *Quinqueloculina* sp., *Sorites orbiculus*, *Spiroloculina* sp.*, Triloculina schreiberina, Triloculina* sp.) as well as a single specimen of *Peneroplis planatus.*

Sample TIR 4/11 revealed a single specimen of *Ammodiscus planorbis* from the order of the Spirillinida (GROSS 2001) and a single specimen of *Bolivina sp.* from the order of the Buliminida. Also, numerous brackish ostracods *Cyprideis torosa* were identified as well as many marine gastropods (*Mangelia* sp., *Pirenella conica*, *Pirenella* sp., *Pirillina* sp., *Rissoa* sp. (DANCE 1977, DELAMOTTE & VARDALA-THEODOROU 2001) and marine bivalves (*Dosinia lupinus* and *Tricolia* sp., *Acanthocardia*

tuberculata and *Eulima* sp., *Mactra coralline, Tellina fabula* (DANCE 1977, AMLER et al. 2000, DELAMOTTE & VARDALA-THEODOROU 2001, GOFAS et al. 2001). Regarding the favored habitat of the species found in samples TIR 4/11, TIR 4/10 and TIR 4/8, a mixture of different environments – (shallow) marine, (sub-)littoral, brackish and marshy – is represented. The sequence also contained benthic species that also occur in deep sea regions such as *Ammodiscus planorbis* (PFLUM & FRERICHS 1976).

Sample TIR 4/4 was taken out of the upper part of the sandy sequence and comes along with a reduced micro- and macrofossil content. Thus, mainly benthic foraminifera of the orders of Rotaliida and Miliolida were detected (*Ammonia beccarii, Ammonia tepida, Elphidium* sp., *Haynesina depressula, Quinqueloculina laevigata*, *Quinqueloculina siminula*, *Quinqueloculina costata*, *Quinqueloculina* sp., *Adelosina dubia, Adelosina* sp., *Rosalina sp., Cibicides* sp.*).* Moreover, a specimen of the pelagic and planktonic species *Globigerina sp.* was encountered (CIMERMANN & LANGER 1991, GROSS 2001). This sample again contained a great many of the ostracod *Cyprideis torosa*. Besides abundant undeterminable shell debris, fragments of the marine bivalve *Spisula subtruncata* were found which is common along coastal banks (DEGRAER et al. 2007). Intact gastropods could not be identified within this sample. Again, the mircofossil record of this sample comprises species from different habitats, such as shallow marine, open marine, coastal or marshy environments.

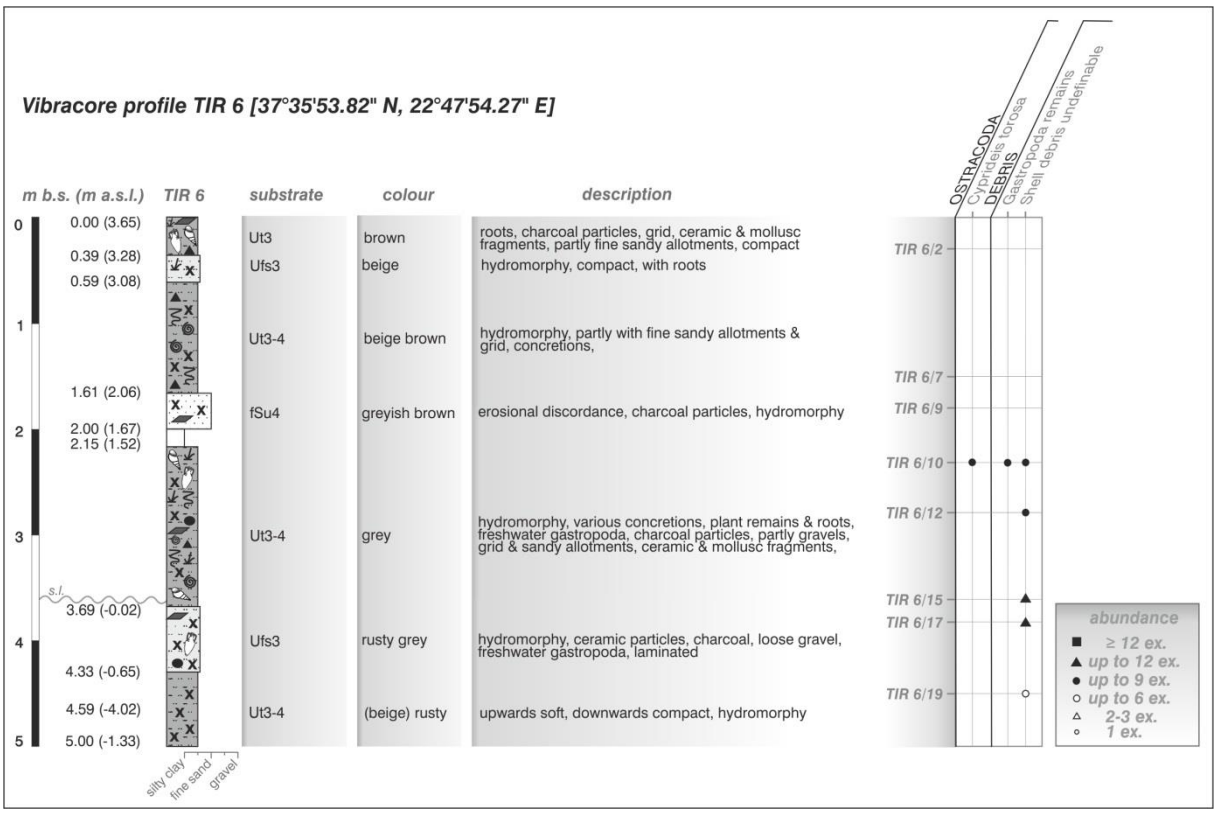

Figure 76: Summarized results of the micro- and macrofaunal analyses on samples form vibracore TIR 6 (source: own data and illustration 2013).

Vibracore TIR 6 comprised only fairly many exemplars of the brackish ostracod *Cyprideis torosa* found in sample TIR 6/10. Besides that the core contained only undefinable shell debris and gastropod remains in its lower and middle part. The cores upper part contained neither shell debris nor microfossils.

Microfaunal analyses of samples from vibracores TIR 10 and TIR 5 of transect II

At vibracoring site TIR 10 environmental conditions influenced by saltwater have been predominant during the younger geologic past (Fig. 77). However, sample TIR 10/7, taken from the fin sandy silt unit overlying the shell debris layer, shows in contrast to samples taken from over- and underlying layers, a thin microfossil record.

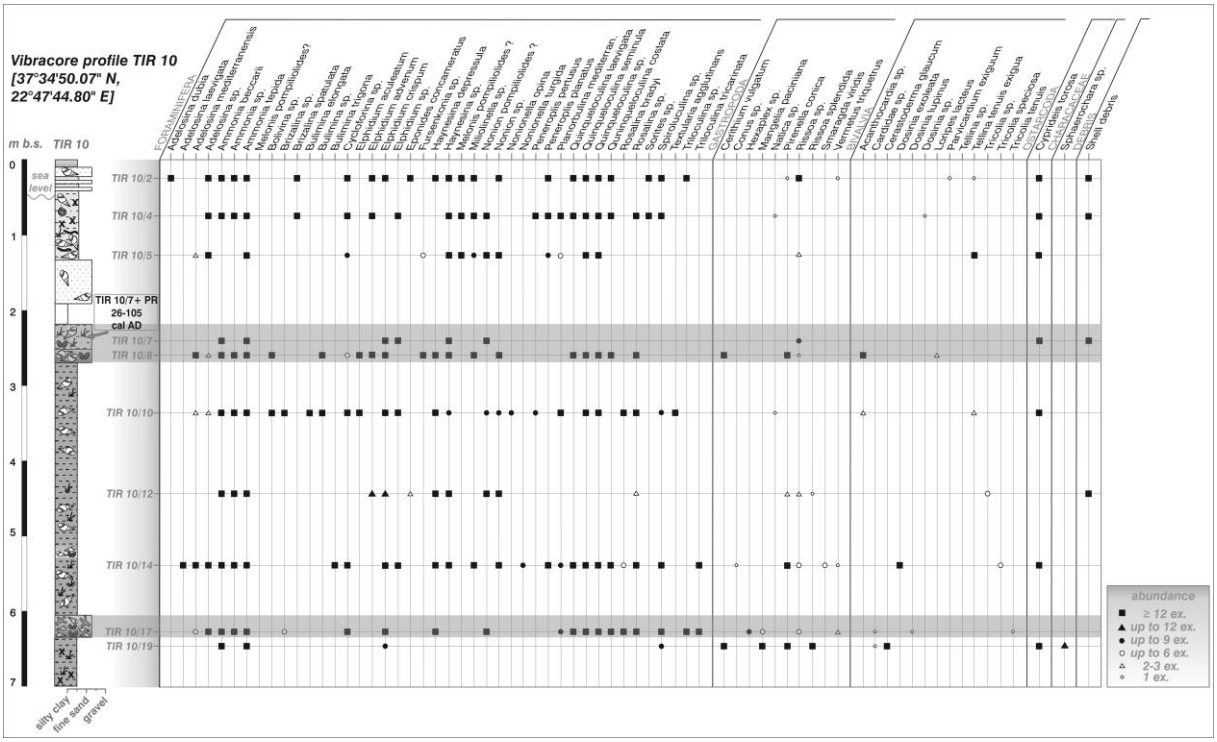

Figure 77: Summarized results of the micro- and macrofossil analyses on samples form vibracore TIR 10 (source: own data and illustration 2013).

The microfossil record of core TIR 5 documents a temporary ingression (Fig. 78). Sample TIR 5/29 contains no micro- or macrofossils. However, the subsequent sample TIR 5/26 shows shell debris and abundant specimens of the ostracod *Cyprideis torosa* thus referring to brackish conditions. Sample TIR 5/23, extracted from medium sand, contains benthic foraminifera from the order of Rotaliida (*Ammonia beccarii, Ammonia tepida, Elphidium* sp., *Haynesina* sp., *Nonion* sp.) and Miliolida (*Adelosina* sp., *Quniqueloculina costata, Quniqueloculina laevigata, Quniqueloculina seminula, Quniqueloculina* sp., *Spiroculina* sp.) that preferably live in shallow-marine, coastal and lagoonal environments (LOEBLICH & TAPPAN 1964, CIMERMANN & LANGER 1991, GROSS 2001, MURRAY 1991, HAYWARD & GROSS 2011, HAYWARD 2013). The microfaunal content of samples TIR 5/21, TIR 5/20, TIR 5/16, TIR 5/14 and TIR 5/13 mirrors an even wider range of marine foraminifera, gastropods and

bivalves from an even increased variety of environments. Only sample TIR 5/18 documents a thinner faunal record reflecting marine conditions.

Diversity and abundance of micro- and macrofossils decrease from 1.11 m b.s.l. towards the top of the core – most probably reflecting a regressive trend at vibracoring position TIR 5.

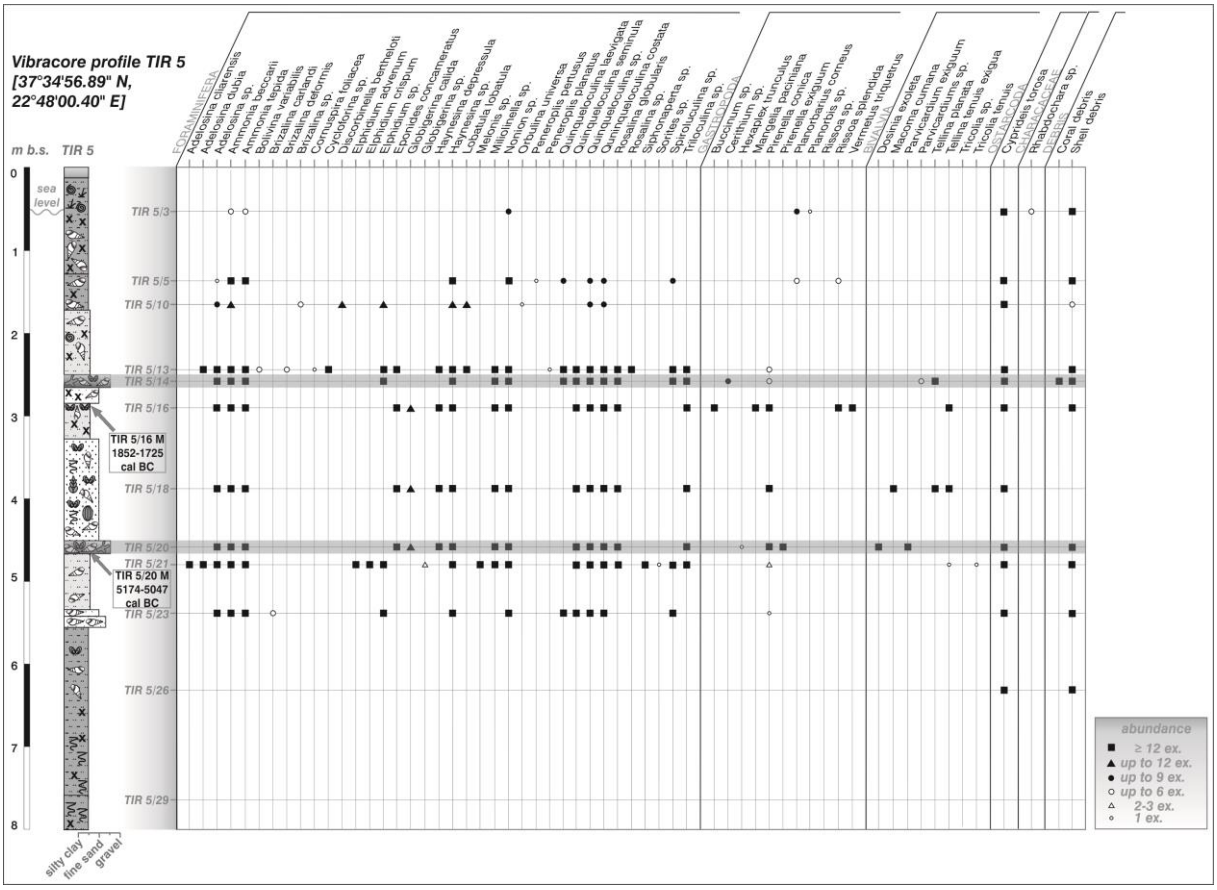

Figure 78: Summarized results of the micro- and macrofossil analyses on samples form vibracore TIR 5 (source: own data and illustration 2013).

8.3.4 Earth resistivity tomography measurements in the eastern Argive Plain

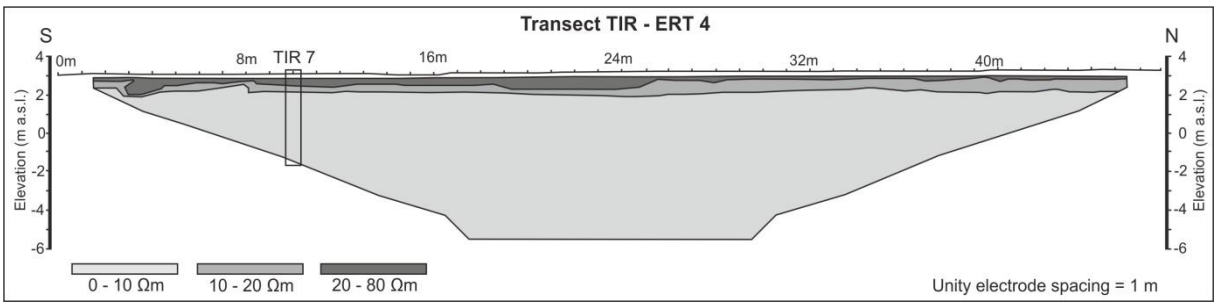

Figure 79: Interpretation of the south-north running ERT transect TIR ERT 4 measured at vibracoring position TIR 7 in an orange grove on private property. In this case a Wenner-Schlumberger array with 48 electrodes and an electrode spacing of 1 m was applied. With the aims of the RES2Dinv software pseudosection models were computed. The south-north trending ERT transect pseudosection model was based on the 7th iteration with an absolute error of 0.71 % (source: own data and illustration 2013).

The locations of the ERT transects are depicted in Figure 63. For methodological information see Chapter 4.1 (Fieldwork methods). Results of the computed pseudosection models are illustrated in the form of interpreted and simplified diagrams (Fig. 79, 81 and 83).

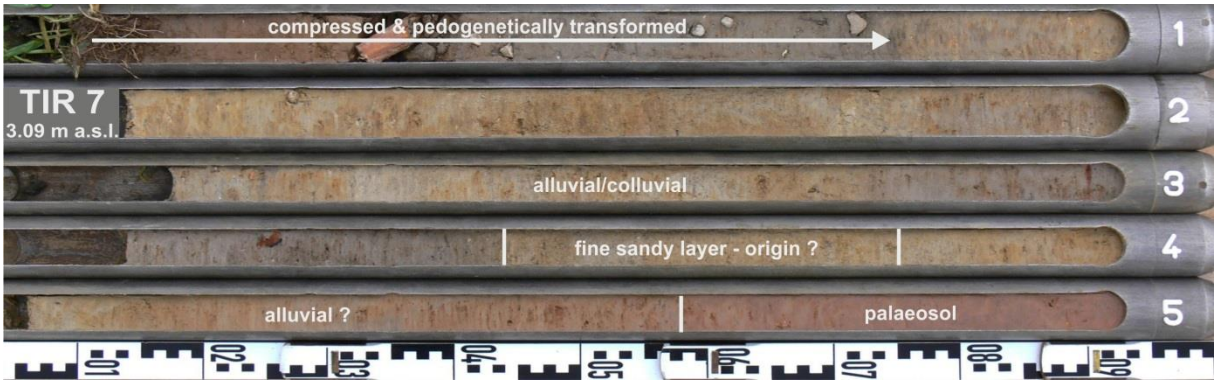

Figure 80: Photo and simplified facies profile of sediment core TIR 7 encountered on private property in an orange grove in front of ancient Tiryns (source: photo taken by T. Willershäuser in March 2010, own illustration 2014).

Interpreting the inverse model resistivity results of transect TIR ERT 4 (Fig. 79) three subsurface units can be identified. Based on the comparison of the ERT data with the sedimentary sequence of vibracore TIR 7 (Fig. 80), drilled at meter 10 of the ERT profile, these units represent the compressed, weathered and pedogenetically transformed upper part of the fine-grained alluvial and/or colluvial sediments. The lower unit is characterized by resistivity values between 4 to 10 Ωm. As documented in vibracore TIR 7 this unit stands for the fine sandy layer and clayey unit.

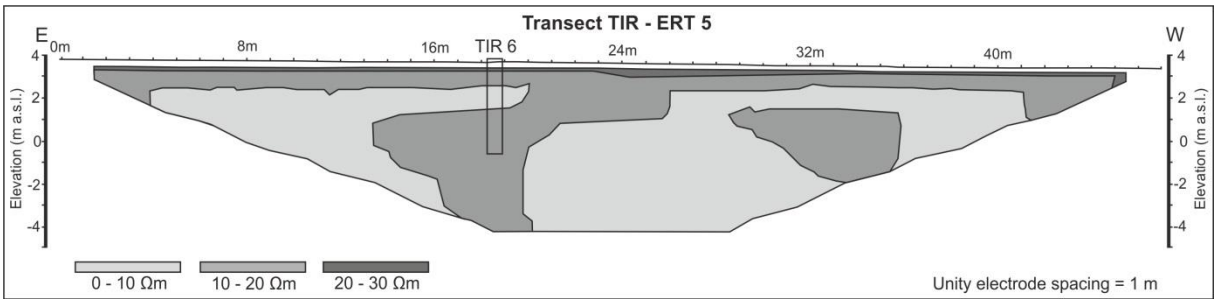

Figure 81: Interpretation of the east-west running ERT transect TIR-ERT 5 measured at vibracoring position TIR 6 in an orange grove on private property. Here also a Wenner-Schlumberger array with 48 electrodes and an electrode spacing of 1 m was applied. With the aims of the RES2Dinv software pseudosection models were computed. This east-west running ERT transect pseudosection model was based on the 7th iteration with an absolute error of 0.79 % (source: own data and illustration 2013).

Regarding transect TIR ERT 5 again three main resistivity units can be separated (Fig. 81). The uppermost unit with values of 20 to 30 Ωm represents the near-surface layer. Thereafter, lower resistivity values between 10 and 20 Ωm were measured which – according to sedimentological data of vibracore TIR 6 (Fig. 82), drilled between meter 18 and 19 of the transect – represents fine-grained alluvial and colluvial material. The third unit, comprising resistivity values between 0 and 10 Ωm, represents clay-dominated sediments.

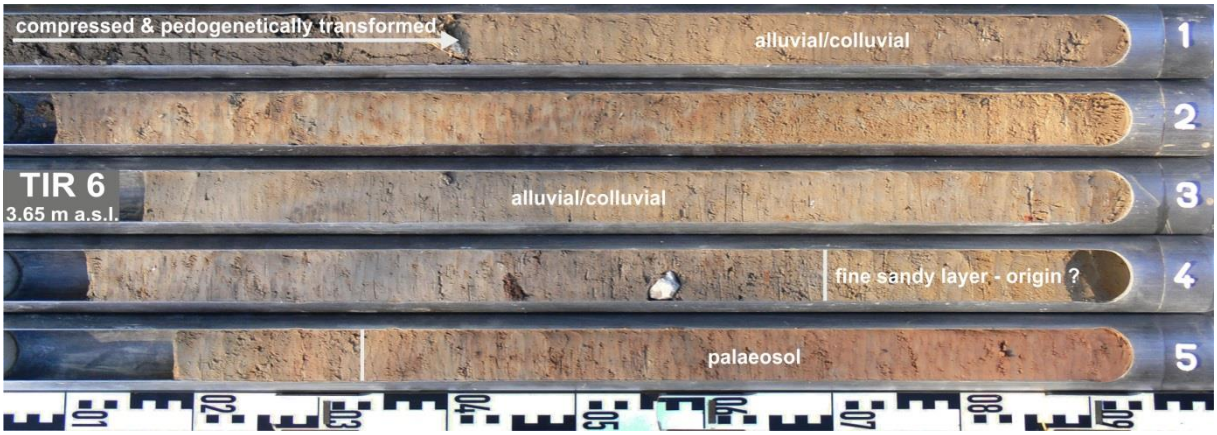

Figure 82: Photo and simplified facies profile of sediment core TIR 6 encountered on private property in an orange grove in front of ancient Tiryns (source: photo taken by T. Willershäuser in March 2010, own illustration 2014).

Comparing TIR ERT 6 (Fig. 83) with the stratigraphical data from vibracore TIR 8 (Fig. 69), drilled at meter 8 of the transect, a good correlation is to register. Gravel, which was found on the surface to the northeast of meter 66 shows high resistivity values up to 200 Ωm. This is also true for the encountered gravel layer in the middle and upper section of core TIR 8 possibly forming palaeochannels. The basal fine-grained deposits of core TIR 8 low resistivity values around 25 Ωm whereas the upper fluvial-colluvial sandy and gravelly unit is characterized by values between 50 and 100 Ωm.

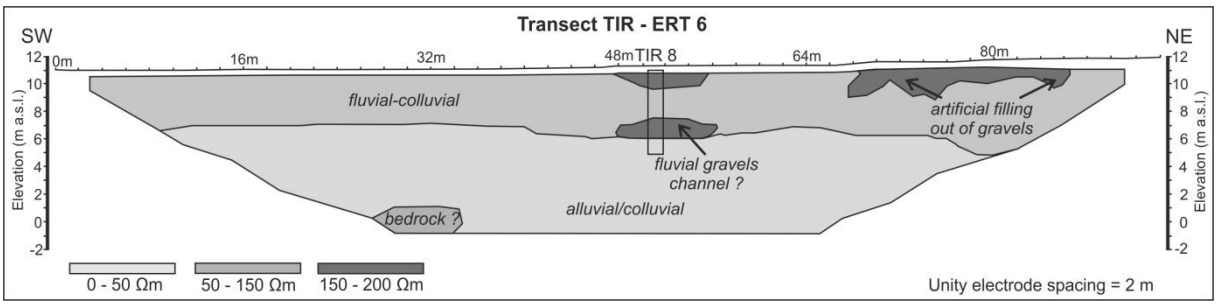

Figure 83: Interpretation of the southwest-northeast running ERT transect TIR-ERT 6 measured at vibracoring position TIR 8 on grazing land at the northern foot of the small Profitis Ilias hill. For this 94 meter long southwest-northeast trending transect a Wenner-Schlumberger array with 48 electrodes and an electrode spacing of 2 m was chosen. Pseudosection models were again computed by using the RES2Dinv software. The calculated pseudosection model was based on the 7th iteration with an absolute error of 1.1 % (source: own data and illustration 2013).

In general, the results indicate that the geophysical data shows good correlation with the encountered main sedimentary units.

8.3.5 Geochronological dating results

Altogether seven samples were chosen from selected vibracores from both Argive Plain transects for the purpose of radiocarbon dating. The laboratory analyses were accomplished by the Leibniz Laboratory for Radiometric Dating and Isotope Research of the Christian-Albrechts-Universität zu Kiel (Germany). The results are summarized in Table 6.

Sample name (Lab. No.)	Depth (m b.s.)	Depth (m b.s.l.)	Sample Description	δ^{13}C (in ‰)	^{14}C age (BP)	1σ max; min (cal BC/AD)
TIR 3/10+ PR (KIA 46020) [a]	2.99	2.14	unidentified plant remains	-23.85±0.20	5994; 5929	4045; 3980 cal BC
(A) TIR 3/12+ HR (KIA 46021) [a]	3.43	2.58	wood fragment	-26.52±0.16	6740 - 6661	4791 - 4712 cal BC
(B) TIR 3/12+ HR (KIA 46021) [a]	3.43	2.58	wood fragment	-28.67±0.16	6845; 6746	4896; 4797 cal BC
TIR 4/27 M (KIA 46022) [a]	6.13	5.65	unidentified marine bivalve	2.97±0.09	6223 - 6106	4274 - 4157 cal BC
TIR 4/28+ PR (KIA 46023) [a]	6.37	5.89	unidentified plant remains	-17.35±0.25	7047 - 6933	5098 - 4984 cal BC
TIR 5/16 M (KIA 46024) [a]	2.87	2.30	articulated specimen *Dosinia exoleta*	3.83±0.24	3801 - 3674	1852 - 1725 cal BC
TIR 5/20 M (KIA 46025) [a]	4.57	4.00	unidentified marine bivalve	0.96±0.10	7123 - 6996	5174 - 5047 cal BC
TIR 10/7+ PR (KIA 46026) [a]	2.46	2.02	unidentified plant remains	-7.35±0.19	1924 - 1845	26 - 105 cal AD

Table 6: Radiocarbon dates of samples from vibracores TIR 3, TIR 4, TIR 5 and TIR 10 drilled in the eastern part of the Argive Plain in the central part of the Argolis Gulf (Peloponnese – Greece). Note: Sample name – sample name chosen while field work; (Lab. No.) – laboratory number given by the laboratory; [a] – Leibniz Laboratory for Radiometric Dating and Isotope Research, Christian-Albrechts-Universität zu Kiel (Germany); m b.s. – meter below surface; m b.s.l. – meter below sea level; (a) δ^{13}C-value – shows incorporation of C4 plants or aquatic material and indicates a potential reservoir effect; (b) δ^{13}C-value – indicates purely atmospheric C3 photosynthesis without contamination by old carbon; 1σ max; min (cal BC/AD) – calibrated ages, 1σ-range; ";" – semicolon is used in cases where several age intervals because of multiple intersections with the calibration curve are possible**;** oldest and youngest age depicted; Calibration is based on the software Calib 6.0 (REIMER et al. 2009).

Sample TIR 4/28+ PR, taken from the lower part of the limnic-lagoonal mud overlying a drowned palaeosol, represents a *terminus post quem* for the beginning of the associated local ingression at vibracoring position TIR 4. Sample TIR 4/27 M from the midst of the heterogeneous shell debris layer, yielded a *terminus ad* respectively a *terminus post quem* for the deposition of the shell debris layer/ingression.

For samples, TIR 3/10+ PR (plant remains) and TIR 3/12+ HR (wood fragment) δ^{13}C values were found typical of C3 plants so that a marine reservoir effect can be excluded. However, the wood fragment of sample TIR 3/12+ HR was dated two times by the laboratory. The sample material was extracted with 1 % HCl, 1 % NaOH at 60 °C and then again with 1 % HCl (lye residue). In order to improve the control always two portions of the treated sample material, in this case the lye residue, were burned to CO_2 and finally measured. Accordingly, the dating approach of this two times measured wood fragment yielded two similar age intervals of 4791 - 4712 cal BC and 4896; 4797 cal BC. The wood fragment was taken right above the transition between fine grained wetland deposits and lagoonal sediments. Hence, these age intervals mark the beginning of the documented ingression at vibracoring position TIR 3. And taken right below the discordance at 2.15 m b.s.l. represents a

terminus ad quem respectively *terminus post quem* for the deposition of this layer that passes over into a shell debris unit.

The age interval of 5174 - 5047 cal BC for sample TIR 5/20 M, taken directly below the shell debris layer represents a *terminus ante quem* for the deposition of the overlying shell debris layer.

And sample TIR 5/16 M yielded an age interval of 1852 - 1725 cal BC thus representing a *terminus ante quem* for the deposition of the overlying shell debris layer that was found in the upper section of the marine sequence.

The revealed age interval of 26 - 105 cal AD of sample TIR 10/7+ PR represents a *terminus post quem* for the deposition of the underlying shell debris layer. However, in the case that the overlying unit, form which sample TIR 10/7+ PR was taken from, belongs to the underlying shell debris unit the age interval would represent a *terminus ad quem* respectively *terminus post quem* for the deposition of the deposit.

8.3.6 Interpreting the sedimentological results of the Argive Plain vibracore transects

The conducted multidisciplinary approach has brought to light that with regard to the palaeogeographical evolution of the eastern Argive Plain the stratigraphical sequences of vibracore transect I and II nearly resemble those presented by ZANNGER (1993) (transect IV: cores AP-28 respectively AP-35, AP-31, AP-40, AP-72 and transect V: cores AP-22, AP-16).

Thus, a local ingressive trend caused the drowning of terrestrial sediments and palaeosols at around 5000 BC. In the spatial context marine influenced conditions prevailed in the area from the recent beach up to ~1 km landwards. This is best documented, besides the sedimentological characteristics, by the different laboratory studies that were performed on the retrieved vibracores. Thereafter, the geochemical parameters such as high potassium and iron values and coevally low calcium values attest terrestrial conditions whereas the marine sequences show a nearly opposite trend. Marine sediments were further identified by the micropalaeontological analyses. However, during time a local regression occurred in the eastern Argive Plain. This is identifiable by thick fine-grained alluvial deposits that were encountered especially in the landward cores of transect I, covering marine and/or limnic-lagoonal sediments and palaeosols.

However, ZANGGER (1993) did not provide any clear indications about extreme wave events or their related deposits in his comprehensive work. But from today's perspective and against the background of the here presented results some of ZANGGER's (1993) remarks leads one to speculate whether the described findings are possibly linked to past extreme wave activity. Probably the following text passages may refer to this, for instance: i) related to the plains western section *"…the presence of some rare marine Ostracods towards the top of the lake sediments appears to be due to severe winter storm floods…(p. 61)"*,ii) in relation to the plains central part *"…indicating the*

interfingering of marine and freshwater conditions … a postmortem mixing of freshwater and marine organisms cannot be excluded (p. 60)" and iii) the text passage that refers to some landward cores of ZANGGER's (1993) central cross-section III *"…early alluvium which is covered by marine gravelly mud in holes 5, [AP-D], and 4…(p. 29)"*. Similar references and striking features can be found also in the study of JAHNS (1993). JAHNS (1993) reconstructed the Holocene vegetation history by using palynological methods based on a 706 cm long core which was drilled/recovered by E. ZANGGER in the southwestern part of the Argive plain about 150 m distant from the beach. The stratigraphy of the core is dominated by silt and loam typical of a limnic environment (JAHNS 1993: p. 191). However, between 39 and 121 cm below surface, clayey to silty loam was found mixed "*with pebbles and mollusc shells"*, thus documenting at least one temporary high-energetic (marine?) geomorphodynamic impact on the low-energy environment.

With regard to the here presented results the stratigraphical data attest conspicuous layers that point on repeated high-energy wave dynamics repeatedly affecting the Argive Plain during the younger geological past.

Thereafter, cores TIR 4 and TIR 3 of transect I as well as cores TIR 10 and TIR 5 of transect II all exhibit heterogeneous and allochthonous shell debris layers that significantly stand out from to the over- and underlying autochthonous low-energetic limnic-lagoonal sections.

Moreover, cores TIR 4 (transect I), TIR 10 and TIR 5 (transect II) show shell debris layers, embedded in a fine sandy matrix, in comparable stratigraphical positions. And regarding the geochronological dating approach a correlation with the shell debris layer of core TIR 3 is also given within this context. Accordingly, these intercalations seem to correspond to each other, all of them reflecting temporary environmental interferences. The geochemical data further attests that the shell debris layers all show strongly increased Ca/Fe-ratios. And the sharp edged mollusc and gastropod fragments, the coarse composition of these sedimentary units, the presence of sandy material, the poorly sorting and basal erosional discordance further refer to high-energy dynamics associated to the deposition of the shell debris layers that intersect low-energetic environments. Thereafter, a spatial correlation between these intersections is given between both transects over a distance of about 1.5 km besides a great landward extend of more than 800 m.

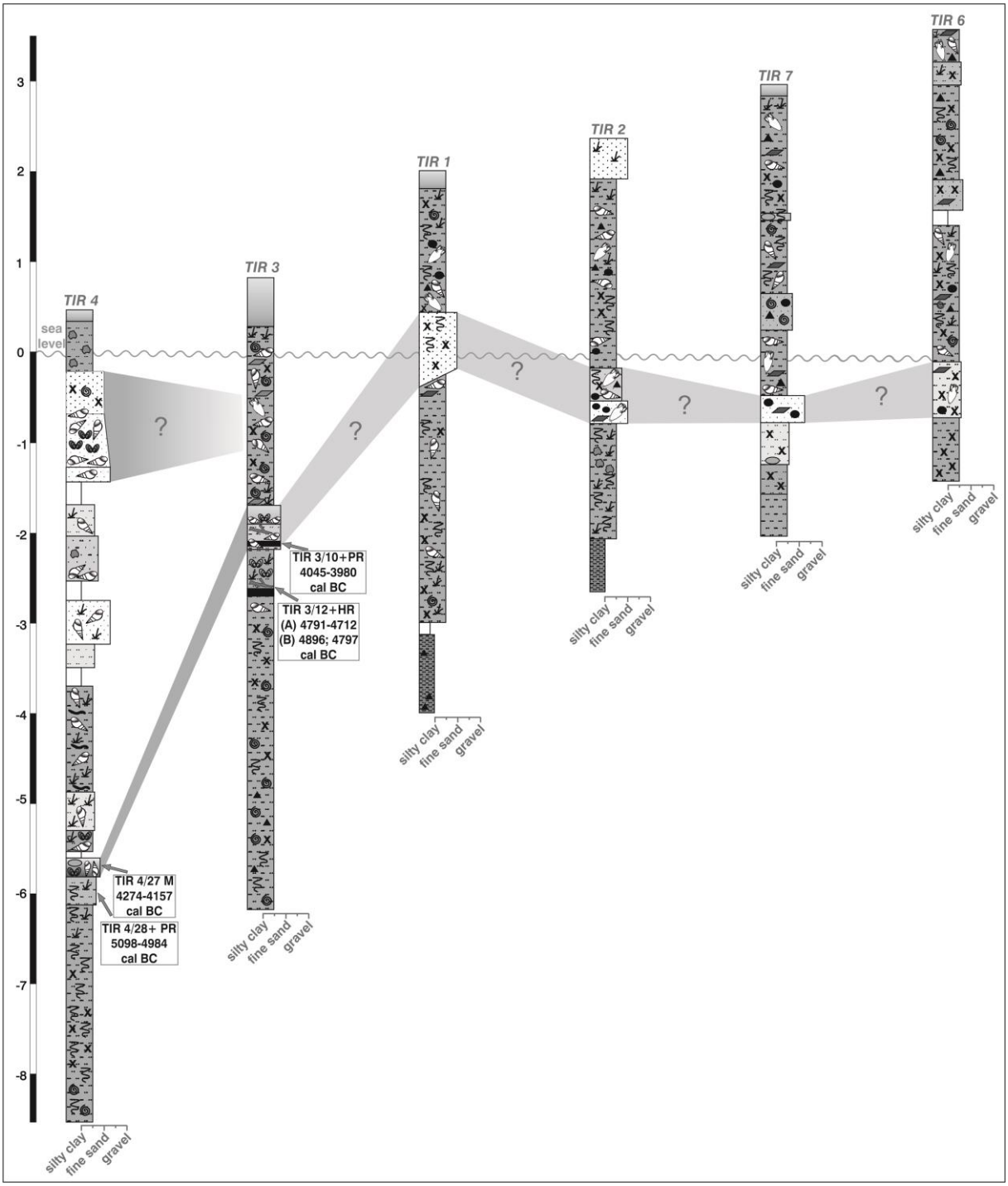

Figure 84: Simplified stratigraphies of the six cores of the SW-NE trending vibracore transect I conducted in the Argive Plain's eastern section (source: own data and illustration 2014).

In his study ZANNGER (1993) interprets sandy deposits, found in landward situated cores of his transect IV, as beach deposits. Sandy layers were also encountered in some of the vibracores of transect I (Fig. 84) but, from a sedimentological and micropalaeontological view, must not be interpreted as beach deposits. Regarding the stratigraphical data of transect I it is thus apparent that the sandy layers of the landward cores are to be found in similar stratigraphical positions as the shell debris layers of the seaward cores – and by this probably corresponding to each other.

Additionally, the most seaward core of transect I TIR 4 shows signatures of a second younger high-energy layer in its upper part, namely a grey marine fine sandy sequence, introduced by an erosional discordance, featuring a fining upward tendency and an incorporated shell debris layer. Regarding the microfaunal analyses this sequence shows in contrast to the underlying sedimentary units a clearly increased microfossil record, comprising species form different environments – (shallow) marine, (sub-)littoral, brackish and marshy besides open marine taxa.

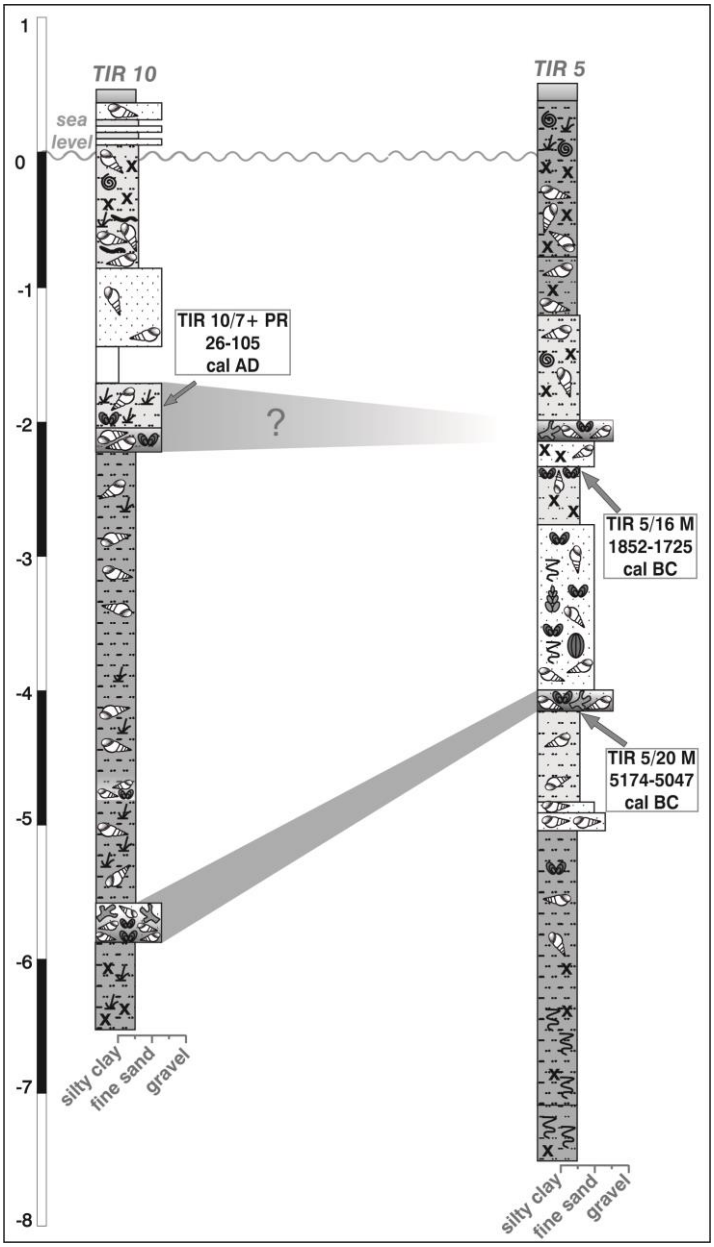

Figure 85: Simplified stratigraphies of cores TIR 10 and TIR 5 of the SW-NE trending vibracore transect II conducted in the Argive Plain's eastern section (source: own data and illustration 2014).

Signs for a second younger high-energy layer are to be found further in the upper parts of cores TIR 10 and TIR 5 of transect II (Fig. 85). Here again shell debris layers are to be found in consistent stratigraphical positions, intersecting marine-lagoonal mud. Additionally, a thinning landward tendency is to register when comparing these upper allochthonous high-energy layers of transect II.

Regarding the stratigraphical data of the seaward core TIR 10 it is obvious that the upper section of the younger event deposit features characteristics that speak for a mixture of marine and terrestrial material, like numerous plant remains in which mollusc fragments are incorporated. A mixture of marine and terrestrial material is also attested by the geochemical data. Thereafter, the basal shell debris layer shows typical marine characteristics in the form of a high Ca/Fe-peak, high Ca-values and simultaneously low Fe- and K-values, whereas the sections upper part is characterized by increased K- and Fe-values and decreased Ca-values, the latter ones referring to terrestrial influences. With regard to the detection of palaeotsunami deposits in near coast stratigraphies the basal shell debris layer could thus represent an inflow deposits whereas the upper section characterizes a deposits of a backwash flow. This refers once more to terrestrial influences respectively a mixing of terrigenous and marine material due to backwash flow dynamics because of extreme wave activity.

Based on the above, the sedimentological inventory of the allochthonous high-energy layers comprises features that are common for past tsunamigenic activity, namely i) basal erosional contacts (DOMINEY-HOWES et al. 2006), ii) a bad/poor sorting (BABU et al. 2007), iii) a great landward extent of allochthonous high-energy deposits (TUTTLE et al. 2004) (in the case that that the sandy layers of cores TIR 1, TIR 2, TIR 7, TIR 6 likewise correspond to the shell debris layer of cores TIR 3 and the lower one of TIR 4 of about 1.7 km), iv) fining upward tendencies (GELFENBAUM & JAFFE 2003) (at least in the case of the younger event deposit of core TIR 10), iv) high Ca/Fe values of allochthonous high-energy deposits (VÖTT et al. 2011a, 2011c, WILLERSHÄUSER et al. 2013), v) allochthonous marine micro fauna (KORTEKAAS & DAWSON 2007) and iii) findings of backwash flow deposits (BAHLBURG et al. 2010) (in the case of the upper part of the younger event deposit found in core TIR 10).

Furthermore, the upper and thus youngest event deposit encountered in core TIR 4 shows traces of subaerial weathering. VÖTT et al. (2011c) and WILLERSHÄUSER (2013) also found terrestrial weathering traces within fine-grained onshore tsunami sediments that were deposited above the local sea level and thus underwent post-sedimentary weathering.

Indeed, literature comparing storm related deposits with tsunami related ones, based on findings from regions all over the world with different local storm regimes, indicate that some of the sedimentological features can also be linked to severe storm surge activity.

During winter, the windiest season in Greece, the mean annual wind speed around the Argive Plain measures about 2.0-3.0 m/sec (CHRONOPOULOU et al. 2010). Within the Argolis Gulf the prevailing winds and thus wind-generated waves show northern directions, reaching only mean wave heights lower than 0.8 m (MEDATLAS GROUP 2004), but at the entrance of the Argolis Gulf winds from southeastern directions dominate (CHRONOPOULOU et al. 2010). For the development of storm surges, onshore winds are necessary in order to push the water directly towards the coast. The shelf offshore the Argive plain is with 3-5 km very wide, measuring water depths less than 100 m along

wide parts (GAKI-PAPANASTASSIOU 2010). Bathymetric maps indicate maximum water depths off the investigated area close to Nafplion of 22 m (MITROPOULOS & ZANANIRI 2010). And along gradually ascending shores, like the Argolis Gulf, the waves break mainly as spilling breakers in sufficient distance to the shoreline while dissipating their energy slowly (KALLENRODE 2003). It is thus believed that the study area exhibits a low to only moderate wave climate and thus low vulnerability for storm wave driven littoral dynamic processes. And as storm related event deposits generally extend less than 300 m form the coast towards the hinterland (MORTON et al. 2007) especially the great landward extend (800 – 1700 m) of the detected event deposits rather speak for tsunamigenic flooding. Moreover, literature research was unsatisfactory with regard to reports or compilations on disastrous extreme storm events within the eastern Mediterranean that had comparable effects like tsunamis – probably because such compilations or reports seemingly do not exist.

Based on the above and because multiple tsunami traces were successfully detected by different authors along several coastal regions of the Peloponnese and within the Aegean Sea, and as literature reports about tsunami events affecting the Argolis Gulf (e.g. SOLOVIEV et al. 2000) and as the Argolis Gulf is directly situated in between the highly active Hellenic Trench and the Hellenic Volcanic Arc a tsunamigenic origin for the event deposits is thus concluded.

Regarding the geochronological dating approach the data refers, together with the sedimentological findings to two most probably also to three events that affected the Argive Plain during the last 7000 years. Thereafter, the first event (event generation I) occurred sometimes after 4791 – 4712 cal BC and at the earliest at 4045 – 3980 cal BC. On a local scale this event probably corresponds to event generation I detected within the Limnothalassa Moustou geo-archive. Within a supra-regional context this event shows parallels to palaeotsunami event deposits that were detected in the northwestern Peloponnese at Pheia by VÖTT et al. (2011c) and that were dated at around 4300 ± 200 cal BC. And traces for an event that hit the Palairos Coastal Plain in Akarnania (NW-Greece) at around 4400 cal BC were detected also by VÖTT et al. (2011a) and would thus also represent a correlation candidate.

With regard to the upper and thus younger event deposit, stratigraphical correlation is given between core TIR 10 and TIR 5. But the geochronological data attest a very wide time span for the event (event generation II ?) that must thus have happened sometimes after 1852 – 1725 cal BC and at the earliest at 26 – 105 cal BC.

But against the background that the upper event deposit of core TIR 4 cannot be correlated with any layer in the more landward cores this event layer probably only corresponds to the upper shell debris layer found in the seaward core of transect II TIR 10. Thereafter, the derived age interval of 26 – 105 cal BC would represent a *terminus ad* respectively a *terminus post quem* for the deposition of the upper associated shell debris layer of core TIR 10. It is thus thinkable that this event (event

generation III) did not have had the same extend as the former one so that the associated event left its signal only in seaward position.

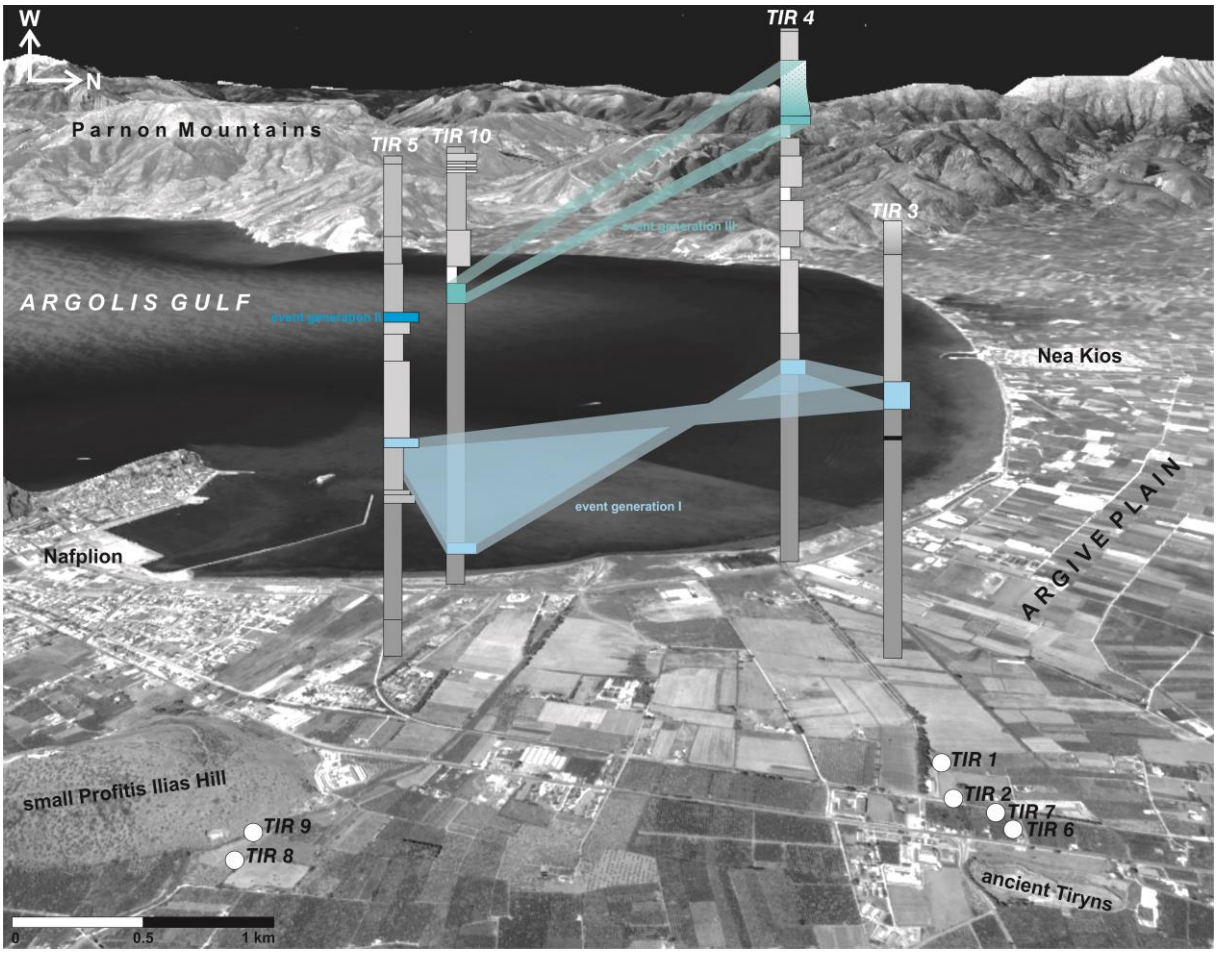

Figure 86: Conceivable spatial distribution of the corresponding event layers found in the stratigraphies of cores TIR 4 & TIR 10 and in cores TIR 3 & TIR 5 drilled in the near-coast eastern section of the Argive Plain. The stratigraphical findings refer to at least three tsunami events (event generations I, II & III) that affected the Argive plain during the last 7000 years (source: own data and illustration, map based on Google Earth images/data, access July 2014).

Accordingly the upper shell debris layer of core TIR 5, that must have been deposited soon after 1852 – 1725 cal BC, would thus represent a good correlation candidate for the Late Bronze Age Santorini event (ca. 1630 – 1550 BC after GOODMAN-TCHERNOV et al. (2009)) that affected wide parts of the whole eastern Mediterranean. Anyway, in this case another stratigraphical correlation layer for this event layer (event generation II) is missing in both transects. But this seems likely as especially the stratigraphical sequences of the seaward cores, located in a marshy littoral environment, must have been subjected to coastal erosional processes during time yielding in an incomplete stratigraphy, so that the probable correlation layers were eroded respectively masked.

All in all the sedimentological, geochemical and microfaunal analyses give evidence for up to three high-energy events, implicating complex backflow dynamics, that refer to repeated tsunamigenic flooding of the Argive Plain during the last 7000 years.

8.4 Conclusions for the investigations in the study areas around the Argolis Gulf

Detailed sedimentological investigation based on vibracorings combined with various geochemical methods, microfaunal analyses, geochronological dating approaches besides geophysical explorations at two selected low-lying coastal areas of the northern Argolis Gulf (Peloponnese) yielded in the following conclusions:

(i) Within the eastern back-area of Asinis Beach valid proofs for past tsunamigenic activity could not be provided. But the presented results and the general geological and geomorphological setting however, deliver promising grounds for further studies, especially against the background of geoarchaeological and palaeogeographical investigations. Accordingly, above all the beachrock formations require further explorations, as they are currently subject of scientific discussion and possibly linked to past tsunami activity.

(ii) However, within the eastern Argive Plain traces of repeated past tsunamigenic activity were detected. Thereafter, the data refers to at least two most probably three palaeotsunamis layers that correspond over a distance of more than 1.5 km.

(iii) The oldest event generation I must have hit the Argive Plain during the middle – late 5th Millennium cal BC and thus corresponding most probably to the oldest event detected in the nearby Limnothalassa Moustou geo-archive. Correlations for this event are given also within a (supra-)regional context such as the event that affected ancient Pheia around 4300 ± 200 cal BC or the Palairos Coastal Plain in Akarnania around 4400 cal BC. Event generation II refers to the well know and frequently described Late Bronze Age Santorini event. And the youngest event generation III was dated to around the beginning of the Common Era, but probably referring to the well-studied 365 AD event, that devastated wide coastal parts of the Mediterranean from Egypt up to Croatia.

Chapter 9 – Synopsis

The main focus of the present study was to search for palaeotsunami deposits in near-coast geological archives of the southeastern, the southern-central and eastern Peloponnese. As discussed in the literature review of *Chapter 2.2* the identification of past extreme wave processes is complex with regard to the associated sedimentary characteristic. In this study the identification of event deposits was based on a multidisciplinary research approach – comprising sedimentological, geochemical and microfaunal analyses – which has proven to be helpful for that purpose.

This final chapter summarizes the presented findings of the investigated study regions (*Chapters 5, 6, 7* and *8*). Based on the defined general objectives of this study (see *Chapter 1*), this chapter also regards the described findings within a regional and supra-regional view as well as in a synoptic geochronological context. Finally, general perspectives as well as those for coastal management and decision makers will be presented.

9.1 Extreme wave event deposits in coastal Lakonia and Argolida

The stratigraphical data derived from differing near-coastal environments of the investigated areas document repeated past tsunamigenic impact. This was shown by allochthonous, mostly coarse-grained deposits associated with high-energy dynamics, intersecting autochthonous low-energetic environments. In southeastern Lakonia traces for at least three palaeotsunami events were detected. Also for the northern central part of the Lakonian Gulf the findings attest three events. And with exception of Asinis Beach, the findings from the Argolis Gulf further indicate up to four events.

In general, the summarized sedimentary and geomorphological inventory of the studied areas comprised features that are associated to marine high-energy wave dynamics – all of them emphasizing the tsunamigenic origin of the associated geomorphodynamic driving forces. These are:

i) coarse-grained high-energy deposits intersecting respectively overlying autochthonous fine-grained sediments;
ii) basal erosional contacts respectively discordances;
iii) badly sorted shell debris layers;
iv) fining upward trends in grain size distribution;
v) laminations;
vi) partly the event deposits end with mud caps;
vii) sometimes the deposits contain rip-up clasts out of footwall material;
viii) bad respectively poor sorting and thus multimodal grain size distribution;

ix) the input of allochthonous marine micro- and macrofauna respectively a mixture of species from different habitats;

x) great landward extents of the sediment body;

xi) thinning landward tendencies of the event deposits;

xii) mixing of marine and terrestrial material due to backwash flow dynamics;

xiii) distinct geochemical patterns;

xiv) dislocated boulders, partly arranged as imbrication trains;

xv) as well as washover structures.

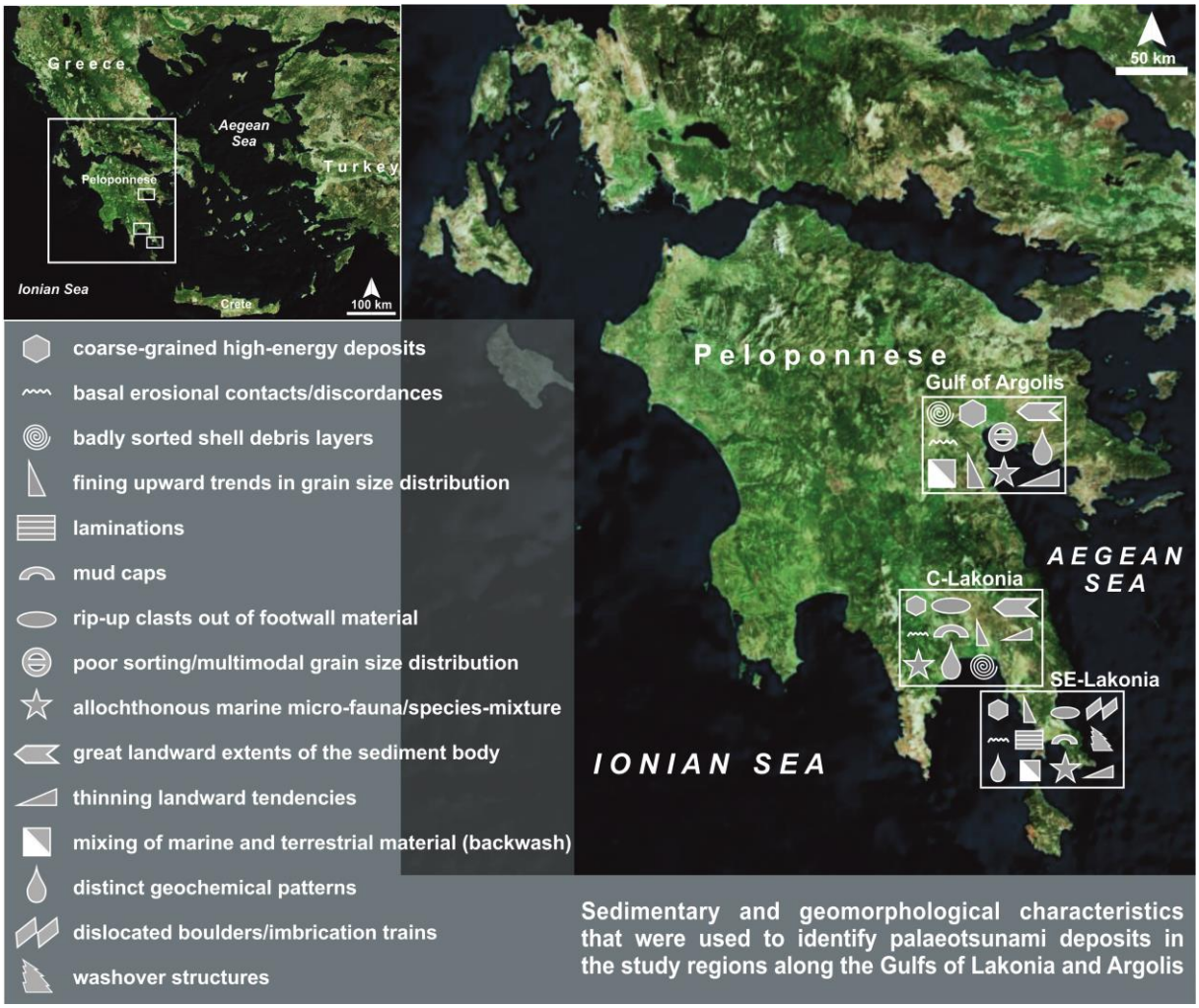

Figure 87: The figure summarizes the sedimentary and geomorphological identification criteria that were used to determine palaeotsunami imprints in the geological record of the study regions in southeastern Lakonia, in northern-central Lakonia and in the Argolis Gulf (source: own data and illustration, maps based on Bing aerial images/data, access July 2014).

However, comparing the presented sedimentary palaeotsunami findings of the investigated areas several similarities are to register but also differences. This is because not every event leaves the same kind of traces and the quality of local geo-archives differs from region to region, which has to be attended when comparing tsunami findings from different locations. Moreover, the preservation of past tsunami imprints in near-coast geological archives is varying in time and space – partly even

on a local scale – and is therefore depending on many factors, such as the pre-event topographical setting, post-event geomorphodynamic processes (especially the erosion, the reworking or masking of event layers), the sediment supply during the event, wave physics or post-event environmental changes respectively interferences. Hence, each study area, respectively geo-archive, is characterized by an individual sedimentological and geomorphological palaeotsunami fingerprint. The detected tsunami fingerprints in each studied area are summarized in Figure 87.

With regard to the studies along the coasts of the Lakonian Gulf palaeotsunami event deposits generally are characterized by erosional discordances introducing fining upward sequences intersecting autochthonous environments. Moreover, these sequences feature allochthonous marine microfauna respectively a mixture of species form different environments. Nearly the same also applies to the findings from the Limnothalassa Moustou geo-archive. Additionally, there the event deposits feature thick coarse-grained gravelly units representing backwash deposits associate to tsunamigenic flooding. In contrast, the identified event layers in the eastern Argive Plain indeed show some of the before named typical sedimentological event features but are mainly characterized by distinct allochthonous shell debris layers, showing abundant sharp-edged broken valves and gastropod remains and additionally containing a mixture of microfaunal species from different habitats. Moreover, these shell debris layers, intersecting autochthonous quiescent limnic-lagoonal environments, show a characteristically geochemical pattern in the form that the layers come along with high peaks in the curves of the Ca/Fe-ratio.

Moreover, by the here used multidisciplinary research approach it was further possible to differentiate between channel-like flood deposits of a fluvial system and high-energy deposits from the marine side encountered from dry-valley bottoms in southeastern Lakonia. Thereby, especially the accomplished microfaunal analyses yielded in the distinction between fluvial and marine high-energy facies.

Summarized it can be concluded that distinct traces of repeated palaeotsunami activity were identified in 8 of the 9 studied near-coast geo-archives. It is thus evident that these archives are able to preserve sedimentological remains of palaeotsunami events. Moreover, a local and even (supra-) regional correlation between findings from the different locations is given.

9.2 The tsunami event chronology for the Gulfs of Lakonia and Argolis in a supra-regional context

In a summary view, for this study the geochronological data attest repeated tsunamigenic activity at least since the mid to late 5th millennium BC. In the following the geochronologically classified palaeotsunami events that were detected in the studied areas, are compared to each other and to

events whose traces were already identified in other regions of the eastern Mediterranean. The timeslots for the associated events detected in the three study regions are summarized in Table 7.

SE-Lakonia	C-Lakonia	Argolis Gulf
	after 4456; 4370 cal BC	after 5529 – 5474 cal BC respectively between 4791-4712 and 4045-3980 cal BC
		soon after 1852-1725 cal BC
	between 1313-1210 and 972; 850 cal BC	
at or after 134-380 cal AD*		after 26-105 cal AD
	between 19-85 and 1422-1460 cal AD	
around 1300 cal AD*		between 643-667 and 1429; 1452 cal AD
at or after 1467; 1618 cal AD		
after 1618 cal AD ?		

Table 7: Summarized timeslots for detected event deposits in the different study regions (source: own data 2014, *data from SCHEFFERS et al. 2008)

The results of this study, together with those from SCHEFFERS et al. (2008), attest at least three palaeotsunamis whose deposits are still detectable along the shores of southeastern Lakonia. These are most probably (i) the remains of the 365 AD tsunami triggered by the well-studied earthquake off Crete, (ii) the deposits of the 1303 AD tsunami generated by a great earthquake in the area south of Rhodes Island and (iii) the until now not detected and described remains of an event that occurred during or after the Renaissance period more precisely sometimes at or after 1467; 1618 cal AD. And regarding the fact that the stratigraphical sequences of cores ELA 6A and BOZ 1 refer to a further potential younger tsunami layer in their upper parts, a (iv) fourth event has to be taken into consideration for the studied region that probably happened after 1618 cal AD.

The Elos Plain was hit at least three times by tsunamis during the mid- and younger Holocene. Accordingly, tsunami landfall for the northern-central Lakonian Gulf was dated (i) to the second half of the 5th millennium cal BC, to (ii) the beginning of the 1st millennium cal BC and (iii) the youngest one most probably occurred not much before 1422 – 1460 cal AD and thus referring to the well-known 1303 AD event.

Regarding the results from the Argolis Gulf the Limnothalassa Moustou geo-archive shows traces of at least three tsunami events. Two of the three event layers could chronologically be classified. Thereafter, the oldest event hit the area after 5529 – 5474 cal BC and the youngest event occurred sometimes between 643 – 667 and 1429; 1452 cal AD, probably also referring to the medieval 1303 AD tsunami. Also the Argive Plain shows traces of at least three events that were dated to (i) an event that took place after 4791 – 4712 cal BC and at the earliest at 4045 – 3980 cal BC, most probably this event can be correlated with the oldest detected event in the nearby geo-archive of Limnothalassa Moustou and with the oldest event generation found in the Elos Plain, to (ii) an event

that hit the plain soon after 1852 – 1725 cal BC and thus referring to the Late Bronze Age Santorini tsunami dated at around 1600 BC and to (iii) an event that occurred after 26 – 105 cal AD, once more referring to the 365 AD Crete earthquake and associated tsunami. Thereafter, the studies along the Argolis Gulf totally refer to up to four past tsunami events.

Accordingly, temporal correlation between some events is given not only on a local scale, as shown in Chapters 5, 6, 7 and 8, but also on (supra-) regional one, as illustrated in Figure 88.

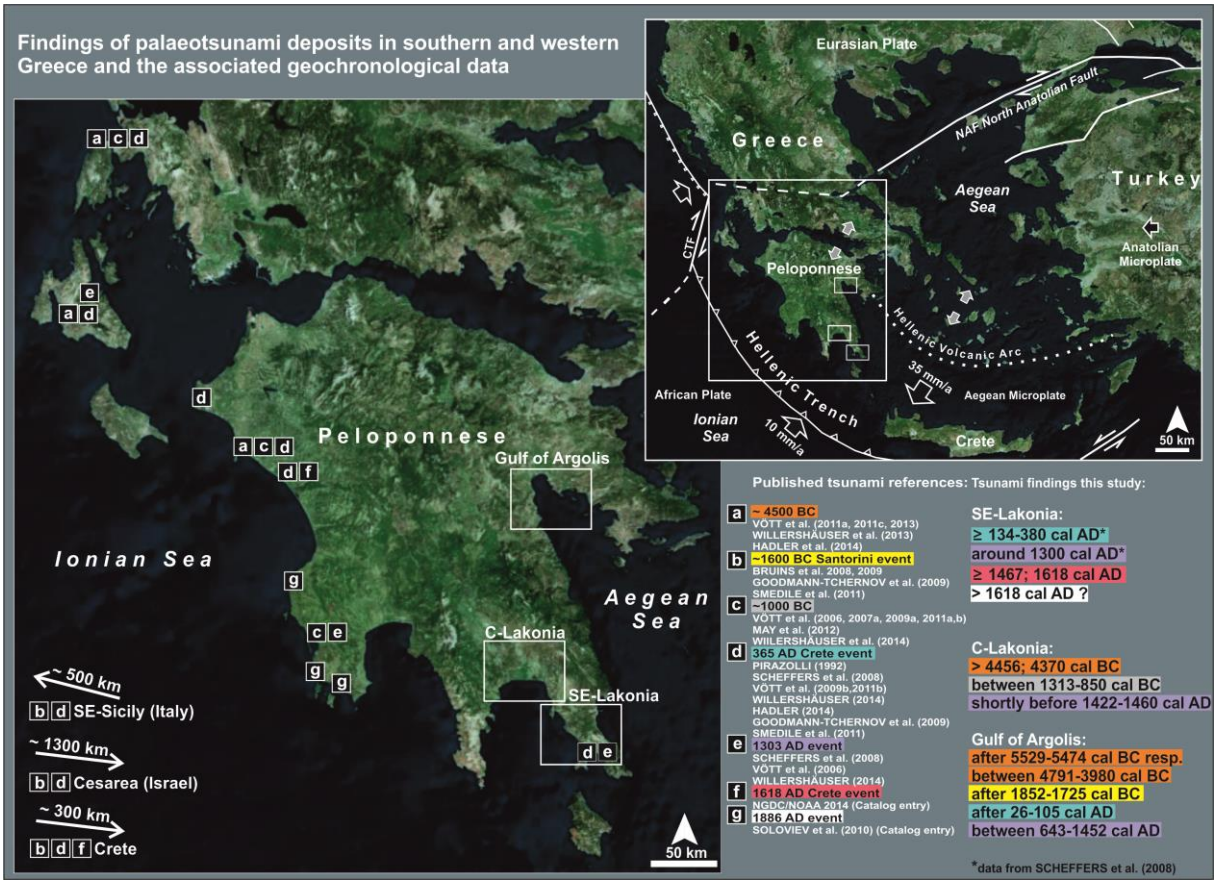

Figure 88: Synoptic view of the geochronological dating results and sedimentary palaeo-tsunami findings within the Greek eastern Mediterranean Sea. The coloring of the references should depict the parallels between already published findings and those of this study (source: own data and illustration, maps based on Bing aerial images/data, access July 2014).

As presented in the beginning, during the last years numerous tsunamiite findings were detected along several coastal areas of the eastern Mediterranean, especially along the Greek coasts (see *Chapter 2.1*). And with respect to the dating accuracies parallels can be drawn also on a supra-regional scale between some of the here described events and already published tsunamiite findings.

The oldest identified event in this study, whose traces are to be found in the records of the Elos Plain, of Limnothalassa Moustou and the Argive Plain, refer to an incident that took place during the mid to late 5th Millennium cal BC. Potential correlation candidates for this Neolithic event are described for coastal Akarnania in northwestern Greece by VÖTT et al. (2011a) [~4400 cal BC], for the ancient harbor of Krane by VÖTT et al. (2013) and HADLER (2014) [~4150 cal BC], for the bay of Lixouri by

WILLERSHÄUSER et al. (2013) [~4250 cal BC], all located on the Ionian Island of Cefalonia, as well as for Pheia the ancient harbor of Olympia situated in the western part of the Peloponnese by VÖTT et al. (2011c) [~4300 cal BC]. However, comparable traces of this event were not found in southeastern Lakonia.

Soon after 1852 – 1725 cal BC another event must have left its signal in the eastern section of the Argive Plain. This timespan refers to the tsunami which was triggered after the collapsing of the Thera volcano (Santorini Island) during the Late Bronze Age between 1627 – 1600 BC (FRIEDRICH et al. 2006). From literature it is well known that the volcanic eruption and the generated tsunami were to register in wide parts of the Mediterranean Sea (FRIEDRICH 2009, FRIEDRICH et al. 2013). Geoarchaeological tsunami deposits of this Santorini event were identified in the northeastern part of Crete in Palaiokastro by BRUINS et al. (2008, 2009). Offshore deposits of this event were detected and described by GOODMAN-TCHERNOV et al. (2009) for Cesarea (Israel) and offshore findings in the Augusta Bay in eastern Sicily (Italy) probably also refer to this event (SMEDILE et al. 2011).

The second tsunami event generation, detected in the Elos Plain archive, refers to an event at around 1000 cal BC. This timespan falls in the line with an incident that occurred at the beginning of the 1st millennium cal BC. Examples pointing on this event are presented for the northwestern Peloponnese around ancient Pheia in Elis (VÖTT et al. 2011b) as well as for coastal northwestern Greece around the Island of Lefkada, the Ambrakian Gulf, the Bay of Palairos-Pogonia and the Voulkaria Lake (VÖTT et al. 2006, 2007a, 2009a, 2009b, 2011a, MAY et al. 2012). Correlations can be drawn also to tsunami event deposits that were detected in the Gialova Lagoon (SW-Peloponnese) and that were dated to around 1100 cal BC by WILLERSHÄUSER (2014).

Regarding the frequently and precisely described 365 AD Crete earthquake and associated tsunami (GALANOPOULOS 1960, PAPADOPOULOS & CHALKIS 1984, AMBRASEYS 2009, SOLOVIEV et al. 2010), traces of this event are to be found most probably in southeastern Lakonia. The derived *terminus post quem* of 26 - 105 cal AD for the youngest event deposit identified within the Argive Plain transect II probably also correlates with the 365 AD event. Tsunami imprints in the ancient harbor of Phalasarna in western Crete (PIRAZOLLI 1992), in the ancient harbor site of Pheia (NW-Peloponnese) (VÖTT et al. 2011b), in coastal Akarnania (VÖTT et al. 2009 b), in the former Mouria Lagoon (SW-Peloponnese) (WILLERSHÄUSER 2014) and probably in the ancient harbor site of Kyllini (NW-Peloponnese) (HADLER 2014) also point to correlations with the 365 AD event. And offshore deposits found in the Augusta Bay (eastern Sicily) by SMEDILE et al. (2011) possibly even refer to this event. Accordingly, a supra-regional correlation for this event is also given.

Considering the well-known 1303 AD southeast Aegean tsunami (GUIDOBONI 1994, ANTONOPOULOS 1980, PAPADOPOULOS & CHALKIS 1984, PAPAZACHOS & PAPAZACHOU 1994, AMBRASEYS 2009, SOLOVIEV et al. 2010), traces of that event are to be found in northern-central Lakonia and under certain

circumstances also within the Limnothalassa Moustou geo-archive. Considering the youngest event deposits found in the Elos Plain a *terminus ante quem* of 1422 – 1460 cal AD and *terminus post quem* of 19 – 85 cal AD was determined. The time span thus includes the devastating 365 AD and 1303 AD tsunami events. But because of the sharp basal erosional discordance a considerable hiatus due to tsunami erosion has to be assumed so that this event most probably took place not much before 1422 – 1460 cal AD. Accordingly, the youngest event-generation found in the Elos Plain, in northern-central Lakonia, is a reasonable candidate for the historically well-known 1303 AD event. In southeast Lakonia, near Neapolis, SCHEFFERS et al. (2008) also found signatures of this event in the form of dislocated mega-clasts. Within a supra-regional view possible correlations can be drawn to event deposits from the Gialova Lagoon (SW-Peloponnese) that are dated to around 1300 cal AD (WILLERSHÄUSER 2014) thus also referring to the 1303 AD event. Moreover, VÖTT et al. (2006) report about an event that hit the Ionian Island of Lefkada sometimes between 1000 and 1400 cal AD. And at around 1300 cal AD an event must have struck also the Bay of Livadi on Cefalonia Island according to the results presented by WILLERSHÄUSER (2014). Consequently, all mentioned events fall in the period of the 1303 AD earthquake and associated tsunami, so that a correlation on a supra-regional scale is given once more.

Regarding the event-stratigraphical record for SE-Lakonia a further incident left its traces at or after 1467; 1618 cal AD. Comparing this time interval with the *NGDC/NOAA Historical Tsunami Database*, the November 8th, 1612 AD Crete island earthquake and associated tsunami represent a potential and serious candidate for this Renaissance period event, as it is listed, with regard to the tsunami event validity, as "*definite tsunami"* (for further details see NGDC/NOAA 2014).

Whether a further later event affected the area around Neapolis after 1618 cal AD is speculative but not inconceivable since event compilations also catalogue several events for that timespan (e.g. NGDC/NOAA 2014). Tsunami compilations for instance indicate that the August 27th, 1886 event was to register at Methoni, Gialova, Filiatra and Kyparissia (GALANOPOULOS 1960, PAPADOPOULOS & CHALKIS 1984, PAPADOPOULOS & FOKAEFS 2005, AMBRASEYS 2009, AMBRASEYS & SYNOLAKIS 2010, SOLOVIEV et al. 2010), all located in Messenia (SW-Peloponnese) the regional unit neighboring Lakonia to the west. It is thus possibly, that this event represents a correlation candidate for the post 1618 cal AD layer identified in southeastern Lakonia.

In a summary view, it can be concluded that during the last 7 millennia up to 8 palaeotsunami events affected the coasts of the studied areas around the Gulf of Lakonia and Gulf of Argolis – from which most of them can be correlated with already described events on a supra-regional scale. By this a significant tsunami frequency is attested for the regions. However, the younger events that left their imprints in the geological records around Neapolis in southeastern Lakonia probably only had local effects.

9.3 General perspectives

The results of this study were supposed to make a contribution to detect past tsunami events and thereby to complement and support already existing datasets and event-compilations with new suitable information. And as the key to the future lies in the past, the detection of past extreme events should thus help to better understand recent and future events as a general contribution for the purpose of modern risk assessment.

In everyday life of Greek people the vulnerability to earthquakes is aware. However, the risk by tsunamis is not intrinsically perceived. Rather a tsunami is perceived by the public as "exotic" and as "something what happens only far away from the Mediterranean". Even though, as especially with broad participation of Greek researchers, detailed tsunami and earthquake compilations were published during the last few decades, indicating repeated tsunamigenic activity during historic times for the (eastern) Mediterranean. The here presented findings have brought to light that the coasts along the Gulfs of Lakonia and Argolis where repeatedly affected by tsunami events during historic times.

In younger times, especially the hazard of submarine slides as triggering mechanism for tsunamis have been investigated (e.g. EBELING et al. 2012, POLONIA et al. 2013, see also *Chapter 2.2*). With regard to the studied areas in the southeastern Peloponnese, above all the Kythera Ridge represents substantial danger for SE-Lakonia. Since the ridge is located along the southwestern segment of the outer Hellenic Arc, connecting the southeastern most tip of the Peloponnese with Crete, by separating the 3000 - 4000 m deep Hellenic Trench to the southwest from the 1500 m deep Maleas Basin to the northeast and since the ridges surface layers were affected by various mass movements and since metastable conditions are to identify (FERENTINOS 1992). Thereafter, a high vulnerability towards tsunamis generated by submarine slides is given in particular for coastal Lakonia and northwestern Crete. And as stated also by EBELING et al. (2013) submarine landslides must thus be considered a significant source of regional hazard, so that decision-makers and the local populations must be educated about them.

Against the background that Greece exhibits a coastline with a total length of 13.676 km (source: CIA - THE WORLD FACTBOOK 2014) a very vulnerable situation is given especially for the low-lying and often densely settled coastal areas. In response to the tragic tsunami on December 26th, 2004 "*The Intergovernmental Coordination Group for the Tsunami Early Warning and Mitigation System in the North-eastern Atlantic, the Mediterranean and connected seas (ICG/NEAMTWS)"* was formed by the UNESCO and the IOC-International Oceanographic Commission, in order to establish an early tsunami warning system in the associated regions (see: http://neamtic.ioc-unesco.org/). The Greek National Tsunami Warning Centre (NTWC) is the National Observatory of Athens (NOA), acting as Tsunami

Watch Provider (TWP) for the NEAM region. These Tsunami Watch Providers are those NTWCs willing and able to provide tsunami alert information outside their Member State at designated Forecast Points (NEAMTIC 2014). Further TWPs are to be found in Turkey, Italy, France and Portugal. Fortunately governments and decision makers have recognized the high risk of tsunami hazard within the Mediterranean region and took the necessary steps into the right direction. But due to short travel/wave propagation times for tsunamis especially public education for self-evacuation is imperative (SYNOLAKIS & BERNARD 2006, MITSOUDIS et al. 2012).

Literature

AD-HOC-ARBEITSGRUPPE BODEN DER STAATLICHEN GEOLOGISCHEN DIENSTE UND DER BUNDESANSTALT FÜR GEOWISSENSCHAFTEN UND ROHSTOFFE (eds.) (2005): Bodenkundliche Kartieranleitung.- Stuttgart, 438 pp.

ALTINOK, Y., TINTI, S., ALPAR., B., YALÇINCER, A.C., ERSOY, Ş., BORTOLUCCI, E. & ARMIGLIATO, A. (2001): The tsunami of August 17, 1999 in Izmit Bay, Turkey.- Natural Hazards, 24: 133-146.

ALVAREZ-ZARIKIAN, C.A., SOTER, S. & KATSOPOULOU, D. (2008): Recurrent Submergence and Uplift in the Area of Ancient Helike, Gulf of Corinth, Greece: Microfaunal and Archaeological Evidence.- Journal of Coastal Research, 24 (1A): 110-125.

AMBRASEYS, N. N. (1960): The seismic sea wave of July 9, 1956 in the Greek Archipelago.- Journal of Geophysical Research, 65 (4): 1257-1265.

AMBRASEYS, N. (2009): Earthquakes in the Mediterranean and Middle East. A multidisciplinary study of seismicity up to 1900.- Cambridge, 968 pp.

AMBRASEYS, N. & C. SYNOLAKIS (2010): Tsunami Catalogs for the Eastern Mediterranean, Revisited.- Journal of Earthquake Engineering, 14 (3): 309-330.

AMLER, M., FISCHER, R. & ROGALLA, N. (2000): Muscheln.- Stuttgart, 214pp.

ANDRADE, C. (1992): Tsunami Generated Forms in the Algarve Barrier Islands (South Portugal).- Science of Tsunami Hazards, 10 (1): 21-34.

ANGELIER, J., LYBERIS, N., LE PICHON, X., BARRIER, E. & HUCHON, P. (1982): The tectonic development of the Hellenic arc and the Sea of Crete: a synthesis.- Tectonophysics, 86: 159-196.

ANTONOPOULOS, J. (1979): Catalogue of tsunamis in the Eastern Mediterranean from Antiquity to present times.- Annali di Geofisica, 32: 113-130.

ANTONOPOULOS, J. (1992): The tsunami of 426 in the Maliakos Gulf, eastern Greece.- Natural Hazards, 5: 83-93.

ATWATER B.F. (1987): Evidence for great Holocene earthquakes along the outer coast of Washington State.- Science, 236: 942-944.

BABU, N., SURESH BABU, D.S. & MOHAN DAS, P.N. (2007): Impact of tsunami on texture and mineralogy of a major placer deposit in southwest coast of India.- Environmental Geology, 52: 71-80.

BACHMANN, G.H. & RISCH, H. (1979): Die geologische Entstehung der Argolis-Halbinsel (Peloponnes, Griechenland).- Geologisches Jahrbuch, 32: 1-177.

BAHLBURG, H. & SPISKE, M. (2012): Sedimentology of tsunami inflow and backflow deposits: key differences revealed in a modern example.- Sedimentology, 59: 1063-1086

BAHLBURG, H., SPISKE, M. & WEISS, R. (2010): Comment on “Sedimentary features of tsunami backwash deposits in a shallow marine Miocene setting, Mejillones Peninsula, northern Chile” by G. Cantalamessa and C. Di Celma.- Sedimentary Geology, 178: 259-273.

BARSCH, H., BILLWITZ, K. & BORK, H.-R. (eds.) (2000): Arbeitsmethoden in Physiogeographie und Geoökologie.- Gotha, Stuttgart, 612 pp.

BASILI, R., TIBERTI, M.M., KASTELIC, V., ROMANO, F., PIATANESI, A., SELVA, J. & LORITO, S. (2013): Integrating geologic fault data into tsunami hazard studies.- Natural Hazards and Earth System Sciences, 13: 1025-1050.

BECK, R., BURGER, D. & PFEFFER, K.-H. (1995): Laborskript.- Kleinere Arbeiten aus dem Geographischen Institut der Universität Tübingen, 11.

BECKER-HEIDMANN, P., REICHERTER, K. & SILVA, P.G. (2007): ^{14}C dated charcoal and sediment drilling cores as first evidence of holocene tsunami at the southern Spanish coast. Proceedings of the 19th International Radiocarbon Conference.- Radiocarbon, 49 (2): 827-835.

BENNER, R., BROWNE, T., BRÜCKNER, H., KELLETAT, D. & SCHEFFERS, A. (2010): Boulder Transport by Waves: Progress in Physical Modelling.- Zeitschrift für Geomorphologie N.F., Suppl. Vol. 54 (39): 127-146.

BENNER, R., BROWNE, T., BRÜCKNER, H., KELLETAT, D., SCHEFFERS, A. (2010): Boulder Transport by Waves: Progress in Physical Modeling.- Zeitschrift für Geomorphologie, 54 (3): 127-146.

BERCKHEMER, H. (1997): Grundlagen der Geophysik.- Darmstadt, 201 pp.

BERNARD, E.N., & VASTANO, A.C. (1977): Numerical computation of tsunami response for island systems.- Journal of Physical Oceanography, 7: 389-395.

BERNARD, E.N., MOFJELD, H.O., TITOV, V., SYNOLAKIS, C.E. & GONZÁLEZ, F.I. (2006): Tsunami: scientific frontiers, mitigation, forecasting and policy implications.- Philosophical Transactions of the Royal Society A, 364: 1989-2007.

BESONEN, M.R. (1997): The Middle and Late Holocene Geology and landscape Evolution of the Lower Acheron River Valley, Epirus, Greece.- Thesis submitted to the faculty of the Graduate School of the University of Minnesota.- Minneapolis, 140 pp.

BILLI, A., FUNICIELLO, R., MINELLI, L., FACCENNA, C., NERI, G., ORECCHIO, B. & PRESTI, D. (2008): On the cause of the 1908 Messina tsunami, Southern Italy.- Geophysical Research Letters, 35 (6): DOI: 10.1029/2008GL033251.

BIRD, E. (2008): Coastal Geomorphology.- 2nd edition, Wiley.- Chichester, 436 pp.

BLOOM, A.L. (1983): Seal Level and Coastal Change.- In: WRIGHT, H.E. & PORTER, S.C. (eds.): Late Quaternary Environments of the United States.- The Holocene, 2: 42-51.

BLUME, H.-P., STAHR, K. & LEINWEBER, P. (2011): Bodenkundliches Praktikum. Eine Einführung in pedologisches Arbeiten für Ökologen, insbesondere Land- und Forstwirte, und für Geowissenschaftler.- 3rd edition, Spektrum Akademischer Verlag.- Heidelberg, 255 pp.

BONDEVIK, S., MANGERUD, J., DAWSON, S., DAWSON, A. & LOHNE, Ø. (2005): Evidence for three North Sea tsunamis at the Shetland Islands between 8000 and 1500 years ago.- Quaternary Science Reviews, 24: 1757-1775.

BOURGEOIS, J. & MACINNES, B. (2010): Tsunami boulder transport and other dramatic effects of the 15 November 2006 central Kuril Islands tsunami on the island of Matua.- Zeitschrift für Geomorphologie N.F., 54 (3): 175-195.

BOURGEOIS, J., PINEGINA, T., PONOMAREVA, V. & ZARETSKAIA, N. (2006): Holocene tsunamis in the southwestern Bering Sea, Russian Far East, and their tectonic implications.- Geological Society of America Bulletin, March/April issue, 118: 449-463.

BORNOVAS, J. & RONDOGIANNI-TSIAMBAOU, T. (1983): Geological map of Greece 1:500.000.- Institute of Geology and Mineral Exploration (IGME).- Athens

BRANDÃO, S. & HORNE, D. (2013): *Cyprideis torosa* (Jones, 1850).- In: BRANDÃO, S. N., ANGEL, M. V. & KARANOVIC, I. (2013): World Ostracoda Database. Accessed through: World Register of Marine Species at http://www.marinespecies.org/aphia.php?p=taxdetails&id=127986 on 2013-10-07

BRICKER, O.P. (1971): Introduction: beachrock and intertidal cement.- In: BRICKER, O.P. (Ed.): Carbonate cements.- 1-13. Johns Hopkins Press, Baltimore.

BRILL, D. (2012): The tsunami history of southwest Thailand - Recurrence, magnitude and impact of palaeotsunamis inferred from onshore deposits.- PhD Thesis, Universität zu Köln, Cologne, 213pp.

BRILL, D., KLASEN, N., BRÜCKNER, H., JANKEAW, K., KELLETAT, D., SCHEFFERS, A. & SCHEFFERS, S. (2012): Local inundation distances and regional tsunami recurrence in the Indian Ocean inferred from luminescence dating of sandy deposits in Thailand.- Natural Hazards and Earth System Sciences, 12: 2177-2192.

BRILL, D., KLASEN, N., BRÜCKNER, H., JANKEAW, K., KELLETAT, D., SCHEFFERS, A. & SCHEFFERS, S. (2011): Potential predecessors of the 2004 Indian Ocean Tsunami – sedimentary evidence of extreme wave events at Ban Bang Sak, SW Thailand.- Sedimentary Geology: 239, 146-161.

BRILL, D., KLASEN, N., BRÜCKNER, H., JANKEAW, K., SCHEFFERS, A., KELLETAT, D. & SCHEFFERS, S. (2012): OSL dating of tsunami deposits from Phra Thong Island, Thailand.- Quaternary Geochronology, 10: 224-229.

BROCKMÜLLER, S., VÖTT, A., BRÜCKNER, H., FLOTH, U., MAY, S.M., LANG, F. (2012): The Holocene evolution of the Sound of Lefkada (NW Greece) – sedimentological, archaeological and historical issues.- In: OLSHAUSEN, E. & SAUER, V. (eds.): Die Schätze der Erde – Natürliche Ressourcen in der antiken Welt. Stuttgarter Kolloquium zur Historischen Geographie des Altertums 10, 2008.- Geographica Historica, 28: 49-66.

BRÜCKNER , H. KELTERBAUM, D., MARUNCHAK, O, POROTOV, A. &VÖTT, A. (2010): The Holocene sea level story since 7500 BP – Lessons from the Eastern Mediterranean, the black and Azov Seas.- Quaternary International, 225 (2): 160-179.

BRÜCKNER, H. & RADTKE, U. (1990): Küstenlinien – Indikatoren für Neotektonik und Eustasie.- Geographische Rundschau, 42 (12): 654-661.

BRÜCKNER, H. (1997): Geoarchäologische Forschungen in der Westtürkei – das Beispiel Ephesos.- In: Breuer, T. (Hrsg.): Geographische Forschungen im Mittelmeerraum und in der neuen Welt.- Passauer Schriften zur Geographie, 15: 39-51.

BRÜCKNER, H. (2003): Delta Evolution and Culture – Aspects of Geoarchaeological Research in Miletos and Priene.- In: WAGNER, G.A., PERNICKA, E. & UERPMANN, H.-P. (eds.): Troia and the Troad. Scientific approaches.- Natural Science in Archaeology: 121-144.

BRUINS, H.J., VAN DER PLICHT, J. & MACGILLIVARY, J.A. (2009): The Minoan Santorini eruption and tsunami deposits in Palaiokastro (Crete): Dating by Geology, Archaeology, ^{14}C, and Egypt Chronology.- Radiocarbon, 51 (2): 397-411.

BRUINS, H.J., MACGILLIVRAY, J.A., SYNOLAKIS, C.E., BENJAMINI, C., KELLER, J., KISCH, H., KLÜGEL, A. VAN DER PLICHT, J. (2008): Geoarchaeological tsunami deposits at Palaikastro (Crete) and the Late Minoan IA eruption of Santorini.- Journal of Archaeological Science, 35: 191-212.

BRYANT, E. (2008): Tsunami: The Underrated Hazard.- Berlin, 330pp.

BRYANT, E.A. & NOTT, J. (2000): Geological indicators of large tsunami in Australia.- Natural Hazards, 24: 231-249.

CHAGUÉ-GOFF, C. (2010): Chemical signatures of palaeotsunamis: A forgotten proxy?- Marine Geology, 271: 67-71.

CHAGUÉ-GOFF, C., SCHNEIDER, J.C., GOFF, J.R., DOMINEY-HOWES, D. & STROTZ, L. (2011).Expanding the proxy toolkit to help identify past events – Lessons from the 2004 Indian Ocean Tsunami and the 2009 South Pacific Tsunami.- Earth Science Reviews, 107: 107-122.

CHAGUÉ-GOFF, C., ANDREW, A., SZCZUCIŃSKI, GOFF, J. & NISHIMURA, Y. (2012): Geochemical signatures up to the maximum inundation of the 2011 Tohoku-oki tsunami — Implications for the 869 AD Jogan and other palaeotsunamis.- Sedimentary Geology, 282, 65-77.

CHRONOPOULOU, S., NASTOS, P.T. & KAMPANIS, N.A. (2010): Estimation of the wind potential in Greece.- Proceedings of 5th International Conference on Deregulated Electricity Market issues in South-Eastern Europe, September 23-24, 2010, Sitia, Greece (full paper available on CD-ROM).

CHOOWONG, M., MURAKOSHI, N., HISADA, K.-I., CHARUSIRI, P., CHAROENTITIRAT, T., CHUTAKOSITKANON; V., JANKEAW, K., KANJANAPAYONT, P. & PHANTUWONGRAJ, S. (2008): 2004 Indian Ocean Tsunami inflow and outflow at Phuket, Thailand.- Marine Geology, 248 (3-4): 179-192.

CIA-CENTRAL INTELLIGENCE AGENCY - THE WORLD FACTBOOK (2014): Greece.- URL: https://www.cia.gov/library/publications/the-world-factbook/geos/gr.html.- last access: February 12th, 2014.

CIMERMANN, F. & LANGER, M.R. (1991): Mediterranean Foraminifera.- Ljubiljana.

CISTERNAS, M. ATWATER, B.F., TORREJON, F. SAWAI, Y., MACHUCA, G., LAGOS, M., EIPERT, A., YOULTON, C., SALGADO, I., KAMATAKI, T., SHISHIKURA, M., RAJENDRAN, C.P., MALIK, J.K., RIZAL, Y., & HUSNI, M. (2005): Predecessors of the giant 1960 Chile earthquake.- Nature, 437: 404-407.

CLAGUE, J.J. & BOBROWSKY, P.T. (1993): Evidence for a large Earthquake and Tsunami 100-400 years ago on Western Vancouver Island, British Columbia.- Quaternary Research, 41: 176-184.

CLAGUE, J.J., BOBROWSKY, P.T. & HUTCHINSON, I.(2000): A review of geological records of large tsunamis at Vancouver Island, British Columbia, and implications for hazard.- Quaternary Science Reviews, 19: 849-863.

CLAGUE, J.J., BOBROWSKY, P.T. & HAMILTON, T.S. (1994): A Sand Sheet deposit by the 1964 Alaska tsunami at Port Alberini, British Columbia.- Estuarine, Coastal and Shelf Science, 38: 413-421.

CLEWS, J.E. (1989): Structural controls on basin evolution: Neogene to quaternary of the Ionian zone, Western Greece.- Journal of Geological Society, 146: 447-457.

COCARD, M., KAHLE, H.-G., PETER, Y., GEIGER, A., VEIS, G., FELEKIS, S., PARADISSIS, D. & BILLIRIS, H. (1999): New constraints on the rapid crustal motion of the Aegean region: recent results inferred from GPS measurements (1993-1998) across the West Hellenic Arc, Greece.- Earth an Planetary Science Letters, 172: 39-47.

CONCHOLOGICAL SOCIETY OF GREAT BRITAIN AND IRELAND (2010): Family: Planorbidae.- Available at: http://www.conchsoc.org/aids_to_id/Planorbis.php.

COSTA, P., ANDRADE, C., FREITAS, M. C., OLIVEIRA, M. A., TABORDA, R. & DA SILVA, C. M. (2008): High energy boulder deposition in Barranco and Furnas lowlands, western Algarve (south Portugal).- In: MASTRONUZZI, G., PIGNATELLI, C., SANSÒ, P., MILELLA, M. & G. SELLERI (eds.): 2nd International Tsunami Field Symposium, 22-27 September 2008, Ostuni - Puglia (Italy) and Lefkada (Ionian Islands, Greece), Abstract Book.- GI2S Coast Research Publication, 6: 19-22.

COSTELLO, M.J., EMBLOW, C. & WHITE, R.J. (2001): European register of marine species: a check-list of the marine species in Europe and a bibliography of guides to their identification. Collection Patrimoines Naturels, 50. Muséum national d'Histoire naturelle: Paris. ISBN 2-85653-538-0. 463 pp.

CRISCIONE, F. & PONDER, W.F. (2013): A phylogenetic analysis of rissooidean and cingulopsoidean families (Gastropoda: Caenogastropoda).- Molecular Phylogenetics and Evolution, 66: 1075-1082.

CUNDY, A.B., KORTEKAAS, S., DEWEZ, T., STEWART, I.S., COLLINS, P.E.F., CROUDACE, I.W., MAROUKIAN, H., PAPANASTASSIOU, D., GAKI-PAPANASTASSIOU, P., PAVLOPOULOS, K. & DAWSON, A. (2000): Coastal wetlands as recorders of earthquake subsidence in the Aegean: a case study of the 1894 Gulf of Atalanti earthquakes, central Greece.- Marine Geology, 170: 3-26.

CUNDY, A.B., SPRAGUE, D., HOPKINSON, L., MAROUKIAN, H., GAKI-PAPANASTASSIOU, K. & FROGLEY, M.R. (2006): Geochemical and stratigraphic indicators of late Holocene coastal evolution in the Gythio area, southern Peloponnese, Greece.- Marine Geology, 230: 161-177.

DANCE, S.P. (1977): Das große Buch der Meeresmuscheln: Schnecken und Muscheln der Weltmeere.- Stuttgart, 304 pp.

DA SILVA C., HINDSON R. & ANDRADE C. (1996): Bioerosion evidence of extreme marine flooding of Algarve region (Southern Portugal) associated with the tsunami of the AD 1755 Lisbon earthquake.- Taphonomic and palaeoecological analysis. Proceed. Taphos '96, II Reunion de Tafonomia y Fosilizacion, Zaragoza: 371-378.

DABRIO, C.J., GOY, J.L. & ZAZO, C. (1998): The record of the tsunami produced by the 1755 Lisbon earthquake in Valdelagrana spit (Golf of Cádiz, southern Spain): Geogaceta, 23: 31-34.

DAS GUPTA, S.P (2006): The Indian Ocean Mega-Tsunami of 2004.- Geographical Review of India, 68 (2): 113-160.

DAWSON, A.G. (1999): Linking tsunami deposits, submarine slides and offshore earthquakes.- Quaternary International, 60: 119-26.

DAWSON, A.G. (2005): Tsunamis.- In: SCHWARTZ, M.L. (ed.): Encyclopedia of Coastal Science.- Dordrecht, 1017-1021.

DAWSON A.G., LONG D. & SMITH D.E. (1988): The Storegga slides: evidence from eastern Scotland for a possible tsunami.- Marine Geology, 82: 271-276.

DAWSON, A.G., HINDSON, R., ANDRADE, C., FREITAS, C., PARISH, R. & BATEMAN, M. (1995): Tsunami sedimentation associated with the Lisbon earthquake of 1 November AD 1755: Boca do Rio, Algarve, Portugal.- The Holocene, 5 (2): 209-215.

DAWSON, A.G & SHI, S. (2000): Tsunami deposits.- Pure and Applied Geophysics, **157**: 875-897.

DAWSON, A.G. & STEWART, I. (2007): Tsunami deposits in the geological record.- Sedimentary Geology, 200 (3-4): 166-183.

DAWSON, S. (2007): Diatom biostratigraphy of tsunami deposits: Examples from the 1998 Papua New Guinea tsunami.- Sedimentary Geology, 200: 328-335.

DE MARTINI, P.M., BURRATO, P., PANTOSTI, D., MARAMAI, A., GRAZIANI, L. & ABRAMSON, H. (2003): Identification of liquefaction features and tsunami deposits in the Gargano area (Italy): paleoseismological implication.- Annals of Geophysics, 46 (5): 883-902.

DEARING, J.A. (1999): Environmental Magnetic Susceptibility – Using the Bartington MS2 System.- Kenilworth, 54 pp.

DEGG, M.R. (1990): A Database of Historical Earthquake Activity in the Middle East.- Transactions of the Institute of British Geographers, New Series, 15 (3): 294-307.

DEGRAER, S., MEIRE, P. & VINCX, M. (2007): Spatial distribution, population dynamics and productivity of *Spisula subtruncata*: implications for *Spisula* fisheries in seaduck wintering areas.- Marine Biology, 152: 863-875.

DELAMOTTE, M. & VARDALA-THEODOROU, E. (2001): Shells from the Greek seas.- In: THE GOULANDRIS NATURAL HISTORY MUSEUM (Ed.).- Athens, 323 pp.

DOMINEY-HOWES, D.T.M. (2002): Documentary and geological records of tsunamis in the Aegean Sea region of Greece and their potential value to risk assessment and disaster management.- Natural Hazards, 25: 195–224.

DOMINEY-HOWES, D.T.M., HUMPHREYS, G.S. & HESSE, P.P. (2006): Tsunami and palaeotsunami depositional signatures and their potential value in understanding the late-Holocene tsunami record.- The Holocene, 16 (8): 1095-1107.

DONATO, S.V., REINHARDT, E.G., BOYCE, J.I., PILARCYK, J.E. & JUPP, B.P. (2009): Particle-size distribution of inferred tsunami deposits in Sur Lagoon, Sultanate of Oman.- Marine Geology, 257: 54-64.

DONATO, S.V., REINHARDT, E.G., BOYCE, J.I., ROTHAUS, R. & VOSMER, T. (2008): Identifying tsunami deposits using bivalve shell taphonomy.- Geology, 36 (3): 199-202.

DONNELLY, C., KRAUS, N. & LARSON, M. (2006): State of Knowledge on Measurement and Modelling of coastal Overwash.- Journal of Coastal Research, 22 (4): 965-991.

DOUTSOS, T. & KOKKALAS, S. (2001): Stress and deformation patterns in the Aegean region.- Journal of Structural Geology, 23: 455-472.

EBELING, C.W., OKAL, E.A., KALLIGERIS, N. & SYNOLAKIS, C.E. (2012): Modern seismological reassessment and tsunami simulation of historical Hellenic Arc earthquakes.- Tectonophysics, 530-531: 225-239.

ENGEL, M. (2012): The chronology of prehistoric high-energy wave events (tropical cyclones, tsunamis) in the southern Caribbean and their impact on coastal geo-ecosystems – a case study from Bonaire (Leeward Antilles).- PhD Thesis, Universität zu Köln, Cologne, 182 pp.

ENGEL, M., BOLTEN, A., BRÜCKNER, H., DAUT, G., KELLETAT, D., SCHÄBITZ, F., SCHEFFERS, A., SCHEFFERS, S.R., VÖTT, A., WILLE, M. & WILLERSHÄUSER, T. (2009a): Reading the chapter of extreme wave events in nearshore geo-bio-archives of Bonaire (Netherlands Antilles) – initial results from Lagun and Boka Bartol.- Marburger Geographische Schriften, 145: 157-178.

ENGEL, M., KNIPPING, M., BRÜCKNER, H., KIDERLEN, M. & KRAFT, J.C. (2009b): Reconstructing Middle to Late Holocene palaeogeographies of the lower Messinian Plain (Southwestern Peloponnese, Greece): Coastline Migration, Vegetation History and Sea Level Change.- Palaeogeography, Palaeoclimatology, Palaeoecology, 284 (3-4): 257-270.

ENGEL, M., BRÜCKNER, H., MESSENZEHL, K., FRENZEL, P., WENNRICH, V., MAY, S.M., DAUT, G., WILLERSHÄUSER, T., SCHEFFERS, A., SCHEFFERS, S., VÖTT, A. & KELLETAT, D. (2010a): Palaeotsunami in the southern Caribbean: clarity through new geological archives?- Eos Transactions AGU, Fall Meeting Suppl., Abstract OS31D-1452.

ENGEL, M., BRÜCKNER, H., WENNRICH, V., SCHEFFERS, A., KELLETAT, D., VÖTT, A., SCHÄBITZ, F., DAUT, G., WILLERSHÄUSER, T. & MAY, S.M. (2010b): Coastal stratigraphies of eastern Bonaire (Netherlands Antilles): new insights into the palaeotsunami history of the southern Caribbean.- Sedimentary Geology, 231: 14-30.

ENGEL, M. & BRÜCKNER, H. (2011): The identification of palaeo-tsunami deposits – a major challenge in coastal sedimentary research.- In: KARIUS, V., HADLER, H., DEICKE, M., VON EYNATTEN, H., BRÜCKNER, H. & VÖTT, A. (eds.): Dynamische Küsten – Grundlagen, Zusammenhänge und Auswirkungen im Spiegel angewandter Küsten-forschung.- Coastline Reports, 17: 65-80.

ENGEL, M. & MAY, S.M. (2012): Bonaire's boulder fields revisited: Evidence for Holocene tsunami impact on the Leeward Antilles.- Quaternary Science Reviews, doi: 0.1016/j.quascirev. 2011.12.011.

ETIENNE, S., BUCKLEY, M., PARIS, R., NANDASENA, A.K., CLARK, K., STROTZ, L., CHAGUÉ-GOFF, C., GOFF, J. & RICHMOND, B. (2011): The use of boulders for characterizing past tsunamis: Lessons from the 2004 Indian Ocean and 2009 South Pacific tsunamis.- Earth-Science Reviews, 107: 76-90.

EVANS, M.E. & HELLER, F. (2003): Environmental magnetism - principles and applications of enviromagnetics.- Amsterdam, Boston, 299 pp.

FAHRBACH, E. (2002): Meeresspiegelschwankungen.- In: MARTIN, C & EIBLMAIER, M. (eds.): Lexikon der Geowissenschaften.- Heidelberg, CD-ROM.

FAIRBANKS, R.G. (1989): A 17.000-year glacio-eustatic sea level record: influence of glacial melting rates on the younger Dryas event and deep-ocean circulation.- Nature, 342: 637-642.

FAZZITO, S. Y., RAPALINI, A. E., CORTES, J. M. & TERRIZZANO, C. M. (2009): Characterization of Quaternary faults by electric resistivity tomography in the Andean Precordillera of Western Argentina.- Journal of South American Earth Sciences, 28(3): 217-228.

FECHTER, R. & FALKNER, G. (1990): Steinbachs Naturführer - Weichtiere. Europäische Meeres- und Binnenmollusken.- München.

FEDERICI, P.R., RODOLFI, G. & STOCKER, E. (2002): Geomorphological mapping and relief evolution of the Dokali River catchment near Demonià (South-western Lakonia, Greece).- Géomorphologie, 3: 23-238.

FEDERICI, P.R. & RODOLFI, G. (2008): Traces of an ancient tsunami event on the Archangelos coast (Southern Peloponnese, Lakonia, Greece).- In: MASTRONUZZI, G., PIGNATELLI, C., SANSÒ, P., MILELLA, M. & G. SELLERI (eds.): 2nd International Tsunami Field Symposium, 22-27 September 2008, Ostuni - Puglia (Italy) and Lefkada (Ionian Islands, Greece), Abstract Book.- GI^{2}S Coast Research Publication, 6: 37-38.

FINLEY, M.I. (1969): Back to Atlantis.- The New York Review of Books, 13 (10). URL: http://www.nybooks.com/articles/archives/1969/dec/04/back-to-atlantis/, last access: May 20th, 2014.

FINKE, E. (1988): Landscape Evolution of the Argive Plain, Greece: Paleoecology, Holocene Depositional History and Coastline Changes.- Ph.D. dissertation. Stanford University, CA. Ann Arbor, University Microfilms.

FITA, L., ROMERO, R., LUQUE, A., EMANUEL, K. & RAMIS, C. (2007): Analysis of the environment of seven Mediterranean tropical-like storms using and axi-symmetric. Nonhydrostatic, cloud reolving model.- Natural Hazards and Earth Sytem Sciences, 7: 41-56.

FLEMMING, N.C. (1973): Archaeological evidence for eustatic and tectonic components of relative sea level change in the south Aegean.- In: BLACKMANN, D.J. (ed.): Marine Archaeology.- London, Butterworth, 1-66.

FLOTH, U., VÖTT, A., MAY, S.M., BRÜCKNER, H. & BROCKMÜLLER, S. (2010): Estimating tsunami hazards between Lefkada and Preveza, NW Greece, by means of computer modeling.- Coastline Reports, 16: 11-14.

FONT, E., NASCIMENTO, C., BAPTISTA, M.A. & SILVA, P.F. (2010): Identification of tsunami-induced deposits using numerical modelling and rock magnetism techniques: A study case of the 1755 Lisbon tsunami in Algarve, Portugal.- Physics of the Earth and Planets Interiors, 182: 187-198.

FRIEDRICH, W.L. (2013): The Minoan eruption of Santorini around 1613 B.C. and its consequences.- In: MELLER, H., BERTEMS, F., BORK, H.R. & RISCH, R. (eds.): 1600 – Kultureller Umbruch im Schatten des Thera-Ausbruchs?.- Tagungen des Landesmuseums für Vorgeschichte Halle, 9: 37-48.

FRIEDRICH, W.L. (2009): Santorini - Volcano, Natural History, Mythology.- Aarhus University Press, Aarhus, 312pp.

FRIEDRICH, W.L., KROMER, B., FRIEDRICH, M., HEINEMEIER, J., PFEIFFER, T., & TALAMO, S. (2006): Santorini eruption radicarbon dated to 1627-1600 BC.- Science, 312 (5773): 548.

FRITZ, H.F., PETROFF, C.M., CATALÁN, P.A., CIENFUEGOS, R., WINCKLER, P., KALLIGERIS, N., WEISS, R., BARRIENTOS, S.E., MENESES, G., VALDERAS-BERMEJO, C., EBELING, C., PAPADOPOULOS, A., CONTRERAS, M., ALMAR, R., DOMINGUEZ, J.C. & SYNOLAKIS, C. (2011): Field survey of 27 February 2010 Chile Tsunami.- Pure Applied Geophysics, 168: 1989-2000.

FROHLICH, C., HORNBACH, M.J., TAYLOR, F.W., SHEN, C.-C., MOALA, 'A., MORTON, A.E. & KRUGER, J. (2009): Huge erratic boulders in Tonga deposited by a prehistoric tsunami.- Geology 37: 131-134.

FUJIWARA, O. (2008): Bedforms and sedimentary structures characterizing tsunami deposits.- In: SHIKI, T., TSUJI, Y., YAMAZAKI, T. & MINOURA, K. (eds.): Tsunamiites – Features and Implications.- Elsevier, Amsterdam, Oxford: 51-62.

FUJIWARA, O., MASUDA, F., SAKAI, T., IRIZUKI, T. & FUSE, K. (2000): Tsunami deposits in Holocene bay mud in southern Kanto region, Pacific coast of central Japan.- Sedimentary Geology, 135: 219-230.

GAFFNEY, C. & GATER, J. (2011): Revealing the Buried Past: Geophysics for Archaeologists.- Stroud, 192 pp.

GAKI-PAPANASTASSIOU, K., MAROUKIAN, H., PAPANASTASSIOU, D., PALYVOS, N. & LEMEILLE, F., (2001): Geomorphological study in the Lokrian coast of northern Evoikos Gulf (central Greece) and evidence of palaeoseismic destructions.- Rapports et Procès-verbaux des Réunions, Commission Internationale pour l'Exploration Scientifique de la Mer Méditerranée, 36**:** 25.

GAKI-PAPANASTASSIOU, K., KARYMBALIS, E., POULOS, S. E., SENI, A. & ZOUVA, C. (2010): Coastal vulnerability assessment to sea-level rise based on geomorphological and oceanographical parameters: the case of Argolikos Gulf, Peloponnese, Greece.- Hellenic Journal of Geosciences, 24: 109-122.

GALANOPOULOS, A.G. (1957): The seismic sea wave of July 9, 1956.- Prakt. Acad. Athens, 32: 90- 101.

GALANOPOULOS, A. G. (1960): Tsunamis Observed on the coasts of Greece from Antiquity to present times.- Annali di Geofisica, 13 (3-4): 369-386.

GALANOPOULOS, A.G & BACON, E. (1969): Atlantis: the truth behind the legend.- Nelson, 216 pp.

GALANOPOULOS, A.G. (1970): The End of Atlantis – A.G. Galanopoulos, reply by M.I. Finley.- In response to: *Back to Atlantis* from the December 4, 1969 issue.- The New York Review of Books (1970), 14, (5).- URL: http://www.nybooks.com/articles/archives/1970/mar/12/the-end-of-atlantis/, last access: November 29th, 2013.

GELFENBAUM G. & JAFFE B. (2003): Erosion and sedimentation from the 17 July 1998 Papua New Guinea tsunami.- Pure and Applied Geophysics, 160 (10-11): 1969-1999.

GEYH, M.A. (2005): ^{14}C dating – still a challenge for users?.- Zeitschrift für Geomorphologie N.F., Suppl. 139: 63-86.

GGU – GESELLSCHAFT FÜR GEOPHYSIKALISCHE UNTERSUCHUNGEN MBH (2003): Die Widerstandsgeoelektrik (Gleichstromelektrik).- URL: http://www.ggukarlsruhe.de/Messverfahren_Geophysik_zersto/Geoelektrik_1_Widerstandsgeoel/hauptteil_geoelektrik_1_widerstandsgeoel.html.- last access: January 20th, 2014.

GIANFREDA, F., MASTRONUZZI, G. & SANSÒ, P. (2001): Impact of historical tsunamis on a sandy coastal barrier: an example from northern Gargano coast, southern Italy.- Natural Hazard and Earth System Science, 1: 213-219.

GOFAS, S., LE RENARD, J. & BOUCHET, P. (2001): Mollusca.- In: COSTELLO, M.J., EMBLOW, C. & WHITE, R.J. (Eds.) (2001): European register of marine species: a check-list of the marine species in Europe and a bibliography of guides to their identification.- Collection Patrimoines Naturels, 50: 180-213.

GOFF, J., CHAGUÉ-GOFF, C. & NICHOL, S. (2001): Palaeotsunami depoists: a New Zealand perspective.- Sedimentary Geology, 143: 1-6.

GOFF, J.R., LANE, E. & ARNOLD, J. (2009): The tsunami geomorphology of coastal dunes.- Natural Hazards and Earth System Sciences, 9 (3): 847-854.

GOODMANN-TCHERNOV, B., DEY, H., REINHARDT, E., MCCOY, F. & MART, Y. (2009): Tsunami waves generated by the Santorini eruption reached eastern Mediterranean shores.- Geology, 37: 943-946.

GOTO, K., CHAVANICH, S.A., IMAMURA, F., KUNTHASAP, P., MATSUI, T., MINOURA, K., SUGAWARA, D. & YANAGISAWA, H. (2007): Distribution, origin and transport process of boulders deposited by the 2004 Indian Ocean tsunami at Pakarang Cape, Thailand.- Sedimentary Geology, 202 (4): 821-837.

GOTO, K., OKADA, K. & IMAMURA., F. (2009): Characteristics and hydrodynamics of boulders transported by storm waves at Kudaka Island, Japan.- Marine Geology, 262: 14-24.

GOTO, K., KAWANA, T. & IMAMURA, F. (2010): Historical and geological evidence of boulders deposited by tsunamis, southern Ryukyu Islands, Japan.- Earth-Science Reviews, 102: 77-99.

GOTO, K., CHAGUÉ-GOFF, C., FUJINO, S., GOFF, J., JAFFE, B., NISHIMURA, Y., RICHMOND, B., SUGAWARA, D., SZCZUCIŃSKI, W., TAPPIN, D.R., WITTER, R.C. & YULIANTO, E. (2011): New insights of tsunami hazard from the 2011 Tohoku-oki event.- Marine Geology, 290: 46-50.

GRAZIANI, L., MARAMAI, A., TINTI, S. & BRIZUELA, B. (2008): Four tsunami events in the Euro-Mediterranean region: analysis and reconstruction of the effects.- In: MASTRONUZZI, G., PIGNATELLI, C., SANSÒ, P., MILELLA, M. & G. SELLERI (eds.): 2nd International Tsunami Field Symposium, 22-27 September 2008, Ostuni - Puglia (Italy) and Lefkada (Ionian Islands, Greece), Abstract Book.- GI^{2}S Coast Research Publication, 6: 49-50.

GREINWALD, S. & THIERBACH, R. (1997): Elektrische Eigenschafteen der Gesteine.- In: BEBLO, M. (eds.): Umweltgeophysik. Berlin: 89 – 96.

GROSS, O. (2001): Foraminifera.- In: COSTELLO, M.J., EMBLOW, C. & WHITE, R.J. (eds.): European register of marine species: a check-list of the marine species in Europe and a bibliography of guides to their identification.- Collection Patrimoines Naturels, 50: 60-75.

GROSS, O. (2013): *Ammonia tepida* (Cushman, 1926).- In: HAYWARD, B.W., CEDHAGEN, T., KAMINSKI, M. & GROSS, O. (2013): World Foraminifera Database. Accessed through: World Register of Marine Species at http://www.marinespecies.org/aphia.php?p=taxdetails&id=112857 on 2014-01-18

GUIDOBONI, E., COMASTRI, A. & TRAINA, G. (1994): Catalogue of Ancient Earthquakes in the Mediterranean Area up to the 10th Century.- Bologna, 504 pp.

GUIDOBONI, E. & COMASTRI, A. (1997): The large earthquake of 8 August 1303 in Crete: seismic scenario and tsunami in the Mediterranean.- Journal of Seismology, 1: 55-72.

GUIDOBONI, E. & COMASTRI, A. (2005): Catalogue of Earthquakes and Tsunamis in the Mediterranean Area from the 11th to the 15th Century.- Bologna, 1037 pp.

HADJIDAKI, E. & LIANOS, N. (1985): A preliminary report on an underwater survey at Plitra, South Laconia, Greece: 1980.- The International Journal of Nautical Archaeology and Underwater Exploration, 14 (3): 227-236.

HADLER, H., VÖTT, A., BRÜCKNER, H., BARETH, G., NTAGERETZIS, K., WARNECKE, H. & WILLERSHÄUSER, T. (2011a): The harbour of ancient Krane, Kutavos Bay (Cefalonia, Greece) – an excellent geo-archive for palaeo-tsunami research. In: KARIUS, V., H. HADLER, M. DEICKE, H. VON EYNATTEN, H. BRÜCKNER & A. VÖTT (eds.): Dynamische Küsten – Grundlagen, Zusammenhänge und Auswirkungen im Spiegel angewandter Küstenforschung.- Coastline Reports, 17: 111-122.

HADLER, H., VÖTT, A., KOSTER, B., MATHES-SCHMIDT, M. MATTERN, T., NTAGERETZIS, K., REICHERTER, K., SAKELLARIOU, D. & T. WILLERSHÄUSER (2011b): Lechaion, the ancient harbour of Corinth (Peloponnese, Greece) destroyed by tsunamigenic impact.- In: GRÜTZNER, C., PÉREZ-LÓPEZ, R., FERNÁNDEZ STEEGER, T., PAPANIKOLAOU,I., REICHERTER, K., SILVA, P.G. & VÖTT, A. (eds.): Earthquake Geology and Archaeology. Science, Society and Critical Facilities.- Proceedings Vol. 2, 2nd INQUA-IGCP 567 International Workshop on Active Tectonics, Earthquake Geology, Archaeology and Engineering, 19.-24.09.2011, Corinth (Greece): 70-73.

HADLER, H., WILLERSHÄUSER, T., NTAGERETZIS, K., HENNING, P. & VÖTT, A. (2012a): Comparing palaeotsunami traces with historical and catalogue data from western Greece – review and implications.- 36. Hauptversammlung der Deutschen Quartärvereinigung DEUQUA, Umwelt, Mensch, Georisiken im

Quartär, Universität Bayreuth, 16.-20. September 2012, Tagungsband.- Bayreuther Forum Ökologie, 117: 89.

HADLER, H., WILLERSHÄUSER, T., NTAGERETZIS, K., HENNING, P.& VÖTT, A. (2012b)**:** Catalogue entries and non-entries of earthquake and tsunami events in the Ionian Sea and the Gulf of Corinth (eastern Mediterranean, Greece) and their interpretation with regard to palaeotsunami research.- In: VÖTT, A. & VENZKE, J.-F. (eds.): Beiträge der 29. Jahrestagung des Arbeitskreises „Geographie der Meere und Küsten", 28. bis 30. April 2011 in Bremen.- Bremer Beiträge zur Geographie und Raumplanung, 44: 1-15.

HADLER, H., VÖTT A., KOSTER, B., MATHES-SCHMIDT, M., MATTERN, T., NTAGERETZIS, K., REICHERTER, K., & WILLERSHÄUSER, T. (2013): Multiple late-Holocene tsunami landfall in the eastern Gulf of Corinth recorded in the palaeotsunami geo-archive at Lechaion, harbour of ancient Corinth (Peloponnes, Greece).- Zeitschrift für Geomorphologie, 57 (Suppl. 4): 139-180.

HADLER, H. (2014): Ancient Greek harbours used as geo-archives for palaeotsunami research – case studies from Krane (Cefalonia), Lechaion (Gulf of Corinth) and Kyllini (Peloponnese).- PhD Thesis, Johannes Gutenberg-University Mainz, Mainz, 140pp.

HASLINGER, F., KISSLING, E., ANSORGE, J., HATZFELD, D., PAPADIMITRIOU, E., KARAKOSTAS, V., MARKOPOULOS, K., KAHLE, H.-G. & PETER, Y. (1999): 3D crustal structure from local earthquake tomography around the Gulf of Arta (Ionian region, NW Greece).- Tectonophysics, 304 (3): 201-218.

HAWKES, A.D., BIRD, M., COWIE, S., GRUNDY-WARR, C., HORTON, B.P., HWAI, A.T.S., LAW, L., MC GREGOR, C., NOTT, J., ONG, J.E., RIGG, J., ROBINSON, R., TAN-MULLINS, M., SA, T.T., YASIN, Z. & AIK, L.W. (2007): Sediments deposited by the 2004 Indian Ocean Tsunami along the Malaysia-Thailand Peninsula.- Marine Geology, 242: 169-190.

HAYNES, J. R. (1981): Foraminifera.- London, 433 pp.

HAYWARD, B.W., BUZAS, M.A., BUZAS-STEPHENS, P. & HOLZMANN, M. (2003): The lost types of *Rotalia beccarii var tepida* Cushman, 1926.- Journal of Foraminiferal Research, 33: 352-354.

HAYWARD, B. & GROSS, O. (2011): Neoglobuquadrina dutertrei (d'Orbigny 1839).- In: HAYWARD, B.W., CEDHAGEN, T., KAMINSKI, M. & GROSS, O. (2011): World Modern Foraminifera Database.- IN: COSTELLO, M.J., BOUCHET, P., BOXSHALL, G., ARVANTIDIS, C. & APPELTANS, W. (2012): European Register of Marine Species, accessed through PESI at http://www.eu-nomen.eu/portal/taxon.php?GUID=urn:lisd:marinespecies.org:taxname:113473

HAYWARD, B. (2013): Rotaliida.- In: HAYWARD, B.W., CEDHAGEN, T., KAMINSKI, M. & GROSS, O. (2013): World Modern Foraminifera Database. Accessed through: HAYWARD, B.W., CEDHAGEN, T., KAMINSKI, M. & GROSS, O. (2013): World Modern Foraminifera Database at http://www.marinespecies.org/foraminifera/aphia.php?p=taxdetails&id=163158 on 2013-10-21

HECHT, S. (2007): Sedimenttomographie für die Archäologie - Geoelektrische und refraktionsseismische Erkundungen für on-site und off-site studies.- In: WAGNER, G. (ed.): Einführung in die Archäometrie.- Heidelberg: 95 – 112.

HEIP, C. (1976): The life-cycle of *Cyprideis torosa* (Curstacea, Ostracoda).- Oecologia, 24: 229-245.

HENDERSON, J. C., GALLOU, C., FLEMMING, N. & SPONDYLIS, E., 2011: The Pavlopetri underwater archaeology project; investigating an ancient submerged town.- In: BENJAMIN, J., BONSALL, C., PICKARD, C. & FISCHER, A. (eds): Underwater archaeology and the submerged prehistory of Europe Oxbow Books: 207-218.

HERMAN, P.M.J. & HEIP, C. (1982): Growth and Respiration of *Cyprideis torosa* Jones 1850 (Crustacea Ostarcoda).- Oecologica, 54: 300-303.

HIEKE, W. & WERNER, F. (2000): The Augias megaturbidite in the central Ionian Sea (central Mediterranean) and its relation to the Holocene Santorini event.- Sedimentary Geology, 135: 205-218.

HIGMAN, B. & BOURGEOIS, J. (2008): Deposits of the 1992 Nicaragua tsunami.- In: Shiki, T., Tsuji, Y., Yamazaki, T. & Minoura, K. (eds.): Tsunamiites – Features and Implications.- Elsevier, Amsterdam, Oxford: 81-103.

HINDSON, R. A., ANDRADE, C. & DAWSON, A. G. (1996): Sedimentary processes associated with the tsunami generated by the 1755 Lisbon earthquake on the Algarve coast, Portugal.- Physical and Chemistry of Earth, 21 (12): 57-63.

HINDSON, R. A. & ANDRADE, C. (1999): Sedimentation and hydrodynamic processes associated with the tsunami generated by the 1755 Lisbon earthquake.- Quaternary International, 56: 27-38.

HNMS – HELLENIC NATIONAL METEOROLOGICAL SERVICE / ΕΘΝΙΚΗ ΜΕΤΕΩΡΟΛΟΓΙΚΗ ΥΠΗΡΕΣΙΑ (2013): The climate of Greece.- URL: http://www.hnms.gr/hnms/english/meteorology/full_story_html?dr_url=%2Fhnms%2Fdocrep%2Fdocs%2Fmisc%2FClimateOfGreece, last access: 15th June, 2013.

HOFFMEISTER, D., NTAGERETZIS, K., AASEN, H., CURDT, C., HADLER, H., WILLERSHÄUSER, T., BARETH, G., BRÜCKNER, H. & VÖTT, A. (2013a): 3D model-based estimations of volume and mass of high-energy dislocated boulders in coastal areas of Greece by terrestrial laser scanning.- Zeitschrift für Geomorphologie N.F., Supplementary issue (in print).

HOFFMEISTER, D., TILLY, N., CURDT, C. NTAGERETZIS, K. BARETH, G. & VÖTT, A. (2013b): Monitoring annual changes of coastal sedimentary budget in western Greece by terrestrial laser scanning.- Zeitschrift für Geomorphologie, 57 (Suppl. 4): 47-67.

HOLLENSTEIN, C., MÜLLER, M.D., GEIGER, A. & KAHLE, H.G. (2008): Crustal motion and deformation in Greece from a decade of GPS measurements, 1993–2003.- Tectonophysics, 449: 17-40.

HOMER (A): Illiad.- W.H.D. Rouse, Translation, 1954 (New American Library).- New York.

HOMER (B): Klassische Sagen – Ilias.- Übersetzung von Johann Heinrich Voß (1751-1826).- Mundus Verlag Germany (2000).

HORTON, B.P., SAWAI, Y., HAWKES, A.D. & WITTER, R.C. (2011): Sedimentology and paleontology of a tsunami deposit accompanying the great Chilean earthquake of February 2010.- Marine Micropaleontology, 79 (3-4): 132-138.

HUELSKEN, T., MAREK, C., SCHREIBER, S., SCHMIDT, I. & HOLLMANN, M. (2008): The Naticidae (Mollusca: Gastropoda) of Giglio Island (Tuscany, Italy): Shell characters, live animals, and a molecular analysis of egg masses.- Zootaxa, 1770: 1–40.

IMAMURA, F., KAZUHISA, G. & OHKUBO, S. (2008): A numerical model for the transport of a boulder by tsunami.- Journal of Geophysical Research, 113: 1008-1029.

INSTITUTE OF GEOLOGY AND MINERAL EXPLORATION (IGME 1989): Geological map of Greece, 1:50.000, Gythion Sheet.- Athens.

INSTITUTE OF GEOLOGY AND MINERAL EXPLORATION (IGME 2002): Geological map of Greece, 1: 50.000, Pappadhianika-Potamos Sheet.- Athens.

INSTITUTE OF GEOLOGY AND SUBSURFACE RESEARCH (IGSR 1970a): Geological map of Greece, 1:50.000, Argos Sheet.- Athens.

INSTITUTE OF GEOLOGY AND SUBSURFACE RESEARCH (IGSR 1970b): Geological map of Greece, 1:50.000, Astros Sheet.- Athens.

INSTITUTE OF GEOLOGY AND SUBSURFACE RESEARCH (IGSR 1970c): Geological map of Greece, 1:50.000, Paralion Astros Sheet.- Athens.

INSTITUTE OF GEOLOGY AND SUBSURFACE RESEARCH (IGSR 1970d): Geological map of Greece, 1:50.000, Nafplion Sheet.- Athens.

JACKSON, J. & MC KENZIE, D. (1984): Active tectonics of the Alpine- Himalayan Belt between western Turkey and Pakistan.- Geophysical Journal - Royal Astronomical Society, 77 (1): 185-264.

JACOBSHAGEN, V. (1986): Geologie von Griechenland – Beiträge zur regionalen Geologie der Erde.- Berlin, Stuttgart, 363 pp.

JACOBSHAGEN, V., RISCH, H. & ROEDER, D. (1976): Die echellenische Phase, Definition and Interpretation.- Zeitschrift der deutschen geologischen Gesellschaft, 127: 133-145.

JAFFE, B. E., BORRERO, J. C., PRASETYA, G. S., DENGLER, L.,GELFENBAUM, G., HIDAYAT, R., HIGMAN B., KINGSLEY, E., LUKIYANTO MCADOO, B., MOORE, A., MORTON, R., PETERS, R., RUGGIERO, P., TITOV, V., KONGKO, W. & YULIANTO, E. (2006): The December 26, 2004 Indian Ocean Tsunami in Northwest Sumatra and Offshore Islands.- Earthquake Spectra, 22 (3): 105-136.

JAFFE, B.E. & GELFENBAUM, G. (2007): A simple model for calculating tsunami flow speed from tsunami deposits.- Sedimentary Geology, 200: 347-361.

JAHNS, S. (1993): On the Holocene vegetation history of the Argive Plain (Peloponnese, southern Greece).- Vegetation History and Archaeobotany, 2: 187-203.

JANKAEW, K., ATWATER, B.F., SAWAI, Y., CHOOWONG, M., CHAROENTITIRAT, T., MARTIN M.E. & PRENDERGAST, A. (2008): Medieval forewarning of the 2004 Indian Ocean tsunami in Thailand.- Nature, 455: 1228-1231.

JORDAN, D. (2009): How effective is geophysical survey? A regional review.- Archaeological Prospection, 16 (2): 77-90.

KAHLE, H., COCARD, M., PETER, Y., GEIGER, A., REILINGER, R., BARKA, A. & VEIS, G. (2000): GPS-derived strain rate field with the boundary zones of the Eurasian, African and Arabian Plates.- Journal of Geophysical Research, 105 (B10): 23353-23370.

KAHLE, H., STRAUB, H., REILINGER, CH., MCCLUSKY, S., KING, R., HURST, K., VEIS, G., KASTENS, K. & CROSS, P. (1998): The strain rate field in the eastern Mediterranean region, estimated by repeated GPS measurements.- Tectonophysics, 294: 237-252.

KALLENRODE, M.-B. (2003): Ozeane und Küsten.- Vorlesungsskript Sommersemster 2003, Fachbereich Physik, Universität Osnabrück.- Osnabrück, 256 pp.

KARAGIOZI, E., FOUNTOULIS, I, KONSTANTINIDIS, A., ANDREADAKIS, E. & NTOUROS, K. (2011): Flood hazard assessment based on geomorphological analysis with GIS tool – the case of Laconia (Peloponnesus, Greece): Proceedings, Symposium GIS Ostrava 201, 24-26 January 2011: 11p.

KARAKAISIS, G. F. & PAPAZACHOS, C. B., (2002). Seismology in Greece: a report.- In: LEE, W. H. K., KANAMORI, H., JENNINGS, P. C. & KISSLINGER, C. (Eds.): IASPEI – International Handbook of Earthquake and Engineering Seismology: 1-21.

KEAREY, P., BROOKS, M. & HILL, I. (2006): An Introduction to Geophysical Exploration.- Oxford, 296 pp.

KELLETAT, D. (1974): Beiträge zur regionalen Küstenmorphologie des Mittelmeerraumes. Gargano/Italien und Peloponnes/Griechenland.- Zeitschrift für Geomorpholgie N.F., Suppl. 19: 161 pp.

KELLETAT, D. (1990): Meeresspiegelanstieg und Küstengefährdung.- Geographische Rundschau, 42 (12): 648-652.

KELLETAT, D.(1999): Physische Geographie der Meere und Küsten.- Stuttgart, 258 pp.

KELLETAT, D.(2002a): Meeresspiegelindikatoren.- In: BRUNOTTE, E., GEBHARDT, H., MEURER, M., MEUSBURGER, P. & NIPPER, J. (eds): Lexikon der Geographie, Zweiter Band.- Darmstadt: 364-365.

KELLETAT, D.(2002b): Meeresspiegelschwankungen.- In: BRUNOTTE, E., GEBHARDT, H., MEURER, M., MEUSBURGER, P. & NIPPER, J. (eds): Lexikon der Geographie, Zweiter Band.- Darmstadt: 365-367.

KELLETAT, D. (2005): Neue Beobachtungen zu Paläo-Tsunami im Mittelmeergebiet: Mallorca und Bucht von Alanya, türkische Südküste.- In: BECK, N. (eds.): Neue Ergebnisse der Meeres- und Küstenforschung. Beiträge der 23. Jahrestagung des Arbeitskreises ''Geographie der Meere und Küsten'' (AMK), Koblenz, 28–30 April 2005.- Schriften des Arbeitskreises Landes- und Volkskunde Koblenz (ALV), 4, 1–14.

KELLETAT, D. (2006): Beachrock as sea-level indicator? Remarks from a geomorphological point of view.- Journal of Coastal Research, 22 (6): 1558-1564.

KELLETAT, D. (2007): Reply to KNIGHT, J. (2007): Beachrock reconsidered. – Discussion of: KELLETAT, D. (2006): Beachrock as sea-level indicator? Remarks from a geomorphological point of view.- Journal of Coastal Research, 22 (6): 1558-1564.- Journal of Coastal Research, 23 (6): 1605-1606.

KELLETAT, D. (2008): Comments to Dawson, A.G. and Stewart, I. (2007), Tsunami deposits in the geological record.- Sedimentary Geology, 211: 87-91.

KELLETAT, D. & GASSERT, D. (1975): Quartärmorphologische Untersuchungen im Küstenraum der Mani-Halbinsel, Peloponnes.- Zeitschrift für Geomorphologie N.F., 22: 8-56.

KELLETAT, D. & SCHEFFERS, A. (2003): Sedimentologische und geomorphologische Tsunamispuren an den Küsten der Erde.- In: EITEL, B., GAMERITH, W., SCHWAN, T., SACHS, K. & WALTER, A. (eds.): Naturrisiken und Naturkatastrophen. Lateinamerika.- HGG-Journal, 18: 11-2.

KELLETAT, D. & SCHEFFERS, A. (2004): Tsunami im Atlantischen Ozean.- Geographische Rundschau, 56 (6): 4-12.

KELLETAT, D., SCHEFFERS, A. & SCHEFFERS, S. (2004): Holocene tsunami deposits on the Bahaman islands of Long Island and Eleuthera.- Zeitschrift für Geomorphologie, 48 (4): 519-540.

KELLETAT, D., SCHEFFERS A. & SCHEFFERS, S. (2007): Field signatures of the SE-Asian mega-tsunami along the west coast of Thailand compared to Holocene palaeo-tsunami from the Atlantic region.- Pure and Applied Geophysics, 164: 413-431.

KELLETAT, D. & SCHELLMANN, G. (2001): Sedimentologische und geomorphologische Belege starker Tsunami-Ereignisse jung-historischer Zeitstellung im Westen und Südosten Zyperns.- Essener Geographische Arbeiten, 32: 1–74.

KELLETAT, D. & SCHELLMANN, G. (2002): Tsunamis on Cyprus: Field evidences and ^{14}C dating results.- Zeitschrift für Geomorphologie, 137: 19–34.

KILFEATHER, A.A., BLACKFORD, J.J. & VAN DER MEER, J.J.M. (2007): Micromorphological analysis of coastal sediments from Willapa Bay, Washington, USA: A technique for analysing inferred tsunami deposits.- Pure and Applied Geophysics, 164: 509-525.

KNEISEL, C. (2003): Electrical resistivity tomography as a tool for geomorphological investigations – some case studies.- Zeitschrift für Geomorphologie, 132: 37-49.

KNEISEL, C. (2006): Assessment of subsurface lithology in mountain environments using 2D resistivity imaging.- Geomorphology, 80: 32 – 44.

KNIGHT, J. (2007): Beachrock reconsidered. – Discussion of: KELLETAT, D. (2006): Beachrock as sea-level indicator? Remarks from a geomorphological point of view.- Journal of Coastal Research, 22 (6): 1558-1564.- Journal of Coastal Research, 23 (4): 1074-1078.

KÖHN, M. (1928): Bemerkungen zur mechanischen Bodenanalyse. III. Ein neuer Pipettierapparat.- Journal of Plant Nutrition and Soil Science, 11 (1): 50-54.

KONICA MINOLTA SENSING, INC. (2003): Precise Color Communication.- URL: http://www2.konicaminolta.eu/eu/Measuring/pcc/en/part3/index.html.- last access: 03rd November, 2013.

KONTOPOULOS, N. & AVRAMIDIS, P. (2003): A late Holocene record of environmental changes from the Aliki lagoon, Egion, North Peloponnesus, Greece.- Quaternary International, 111: 75–90.

KÖPPEN, W. (1931): Grundriß der Klimakunde.- Leipzig, 388 pp.

KORTEKAAS, S. & DAWSON, A.G. (2007): Distinguishing tsunami and storm deposits: An example from Martinhal, SW Portugal.- Sedimentary Geology, 200: 208–221.

KORTEKAAS, S., PAPADOPOULOS, G.A., GANAS, A., CUNDY A.B. & DIAKANTONI, A. (2011): Geological identification of historical tsunamis in the Gulf of Corinth, Central Greece.- Natural Hazards and Earth System Sciences, 11 (7): 2029-2041.

KOUSOULIS, A.A., CHATZIGEORGIOU, K-S., DANIS, K., TSOUCALAS, G., VAKALIS, N., BONOVAS, S. & TSIODRAS, S. (2013): Malaria in Laconia, Greece, then and now: a 2500-year-old-pattern.- International Journal of Infectious Diseases, 17: e8-e11.

KOWALCZYK, G., WINTER, K.-P., STEINICH, G. & REISCH, L. (1992): Jungpleistozäne Strandterrassen in Südost-Lakonien (Peloponnes, Griechenland).- Schriftenreihe für Geowissenschaften, 1: 72 pp.- Berlin.

KRAFT, J.C. (1972): A reconnaissance of the geology of the sandy coastal areas of Eastern Greece and the Peloponnese, with speculations on Middle–Late Helladic paleogeography (3000–4000 years before present).- Technical Report, No. 9. Newark, DE: College of Marine Studies, University of Delaware.

KRAFT, J.C., ASCHENBRENNER, S.E. & RAPP, G. (1977): Palaeogeographic reconstructions of coastal Aegean archaeological sites.- Science, 195: 941-947.

KRAFT, J.C., KAYAN İ. & ASCHENBRENNER, S.E. (1985): Geological Studies of Coastal Change Applied to Archaeological Settings.- In: RAPP, G. & GIFFORD, J.A. (eds.): Archaeological Geology: 57-84, New Haven, London.

KRAFT, J.C., RAPP, G.R., GIFFORD, J.A. & ASCHENBRENNER, S.E. (2005): Coastal Change and Archaeological Settings in Ellis.- Hesperia, 74 (1): 1-39.

KRAFT, J.C., BRÜCKNER, H., KAYAN, I. & ENGELMANN, H. (2007): The geographies of ancient Ephesus and the Artemision in Anatolia.- Geoarchaeology: An International Journal, 22 (1): 121-149.

KRAUS, N.C. (2003): Analytical model of incipient breaching of coastal barriers.- Coastal Engineering Journal, 45 (4): 511–531.

KURAN, U. & YALÇINER, A.C. (1993): Crack propagations, earthquakes and tsunamis in the vicinity of Anatolia.- In: TINTI, S. (Ed.): Tsunamis in the World.- pp. 159-175.

LAGIOS, E., SAKKAS, V., PAPADIMITRIOU, P., PARCHARIDIS, I., DAMIATA, B.N., CHOUSIANITIS, K. & VASSILOPOUIOU, S. (2007): Crustal deformation in the central Ionian Islands (Greece): Results from DGPS and DInSAR analyses (1995-2006).- Tectonophysics 444 (1-4): 119–145.

LAGOUVARDOS, K., KOTRONI, V., NICKOVIC, S., JOVIC, D., KALLOS, G. & TREMBECK, C.J. (1991): Observations and model simulations of a winter sub-synoptic vortex over the central Mediterranean.- Meteorological Applications, 6: 371-383.

LAMBECK, K. (1996): Sea-level change and shore-line evolution in Aegean Greece since Upper Palaeolithic time.- Antiquity, 70: 588-611.

LOEBLICH, A.R. JR. & TAPPAN, H. (1964): Sarcodina, chiefly "Thecamoebians" and Foraminiferida.- In: MOORE, R.C. (ed.): Treatise on Invertebrate Paleontology.- Part C, Protista 2, Vol. 1: C436–C510. The Geological Society of America and the University of Kansas Press.

LOKE, M. & BARKER, R. (1996): Rapid least-squares inversion of apparent resistivity pseudosections by a quasi-Newton method.- Geophysical Prospecting, 44: 131-152.

LOKE, M. H. & DAHLIN, T. (2002): A comparison of the Gauss-Newton and quasi-Newton methods in resistivity imaging inversion.- Journal of Applied Geophysics, 49 (3): 149-162.

LOKE, M.H., ACWORTH, I. & DAHLIN, T. (2003): A comparison of smooth and blocky inversion methods in 2D electrical imaging surveys.- Exploration Geophysics, 34: 182-187.

LORITO, S., TIBERTI, M.M., BASILI, R., PIATANESI, A. & VALENSISE, G. (2008): Earthquake-generated tsunamis in the Mediterranean Sea: Scenarios of potential threats to Southern Italy.- Journal of Geophysical Research, 113: B01301.

LOY, W.G. (1967): The Land of Nestor. A physical geography of the southwest Peloponnese.- Office of Naval Research Report, 34: 1-139.

LUQUE, L., LARIO, J., CIVIS, J., SILVA, P.G., ZAZO, C., GOY, J.L. & DABRIO, C.J. (2002): Sedimentary record of a tsunami during Roman times, Bay of Cadiz, Spain.- Journal of Quaternary Science, 17 (5-6): 623-631.

MAMO, B., STROTZ, L. & DOMINEY-HOWES, D. (2009): Tsunami sediments and their foraminiferal assemblages. Earth-Science Reviews 96, 263-278.

MAOUCHE, S., MORHANGE, C. & MEGHRAOUI, M. (2009): Large boulder accumulation on the Algerian coast evidence tsunami events in the western Mediterranean.- Marine Geology, 262: 96-104.

MARRINER, N., MORHANGE, C. & SKRIMSHIRE, S. (2010): Geoscience meets the four horsemen?: Tracking the rise of neocatastrophism.- Global and Planetary Change, 74 (1): 43-48.

MARTORANA, R., FIANDACA, G., CASAS PONASTI, A. & COSENTINO, P.L. (2009): Comparative tests on different multi-electrode arrays using models in near-surface geophysics.- Journal of Geophysics and Engineering, 6 (1): 1-20.

MASTRONUZZI, G. & PIGNATELLI, C. (2012): The boulder berm of Punta Saguerra (Taranto, Italy): a morphological imprint of the Rossano Calabro tsunami of April 24, 1836?.- Earth Planets and Space, 64 (10): 829-842.

MASTRONUZZI, G. & SANSÒ, P. (2000): Boulders transport by catastrophic waves along the Ionian coast of Apulia (Southern Italy).- Marine Geology, 170: 93-103.

MASTRONUZZI, G. & SANSÒ, P. (2004): Large Boulder Accumulations by Extreme Waves along the Adriatic Coast of southern Apulia (Italy).- Quaternary International, 120: 173-184.

MASTRONUZZI, G., PIGNATELLI, C. & SANSÒ, P. (2006): Boulder fields: a valuable morphological indicator of paleotsunami in the Mediterranean Sea.- Zeitschrift für Geomorphologie, 146: 173-194.

MASTRONUZZI, G., PIGNATELLI, C., SANSÒ, P. & SELLERI, G. (2007): Boulder accumulation produced by the 20th of February, 1743 tsunami along the coast of southeastern Salento (Apulia region, Italy).- Marine Geology, 242: 191-205.

MATHES-SCHMIDT, M., SCHWARZBAUER, J., PAPANIKOLAOU, I., SYBERBERG, F., THIELE, A., WITTKOPP, F. & REICHERTER, K. (2013): Geochemical and micropaleontological investigations of tsunamigenic layers along the Thracian Coast (North-Aegean Sea, Greece).- Zeitschrift für Geomorphologie, 57 (Suppl. 4): 5-27.

MATTIOLI, G.S., VOIGHT, B., LINDE, A.T., SACKS, I.S., WATTS, P., WIDIWIJAYANTI, C., YOUNG, S.R., HIDAYAT, D., ELSWORTH, D., MALIN, P.E., SHALEV, E., VAN BOSKIRK, E., JOHNSTON, W., SPARKS, R.S.J., NEUBERG, J., BASS, V., DUNKLEY, P., HERD, R., SYERS, T., WILLIAMS, P. & WILLIAMS, D. (2007): Unique and remarkable dilatometer measurements of pyroclastic flow-generated tsunamis.- Geology 35: 25-28.

MAY, S.M. (2010): Sedimentological, geomorphological and geochronological studies on Holocene tsunamis in the Lefkada – Preveza area (NW Greece) and their implications for coastal evolution.- PhD Thesis, Universität zu Köln, Cologne, 167 pp.

MAY, S. M., VÖTT, A., BRÜCKNER, H & BROCKMÜLLER, S. (2007): Evidence of tsunamigenic impact on Actio headland near Preveza, NW Greece.- Coastline Reports, 9: 115-125.

MAY, S.M., VÖTT, A., BRÜCKNER, H., GRAPMAYER, R., HANDL, M. & WENNRICH, V. (2011): The Lefkada barrier and beachrock system (NW Greece) - controls on coastal evolution and the significance of extreme wave events.- Geomorphology, 139-140: 330–347.

MAY, S.M., A. VÖTT, H. BRÜCKNER & A. SMEDILE (2012): The Gyra washover fan in the Lefkada Lagoon, NW Greece – possible evidence of the 365 AD Crete earthquake and tsunami.- Earth, Planets and Space, 64 (10): 859-874.

MCCLUSKY, S., BALASSANIAN, S., BARKA, A., DEMIR, C., ERGINTAV, S., GEORGIEV, I., GURKAN, O., HAMBURGER, M., HURST, K., KAHLE, H., KASTENS, K., KEKELIDZE, G., KING, R., KOTZEV, V., LENK, O., MAHMOUD, S., MISHIN, A., NADARIYA, M., OUZOUNIS, A., PARADISSIS, D., PETER, Y., PRILEPIN, M., REILINGER, R., SANLI, I., SEEGER, H., TEALAB, A., TOKSOZ, M.N. & VEIS. G. (2000): Global Positioning System constraints on plate kinematics and dynamics in the eastern Mediterranean and Caucasus.- Journal of Geophysical Research: Solid Earth, 105 (B3): 5695-5719.

MCCOY, F.W. & HEIKEN, G. (2000): Tsunami Generated by the Late Bronze Age Eruption of Thera (Santorini), Greece.- Pure Applied Geophysics, 157 (6-8): 1227-1256.

MEDATLAS GROUP (2004): Wind and Wave atlas of the Mediterranean Sea.- Paris, Athens.

MILLER, D.J. (1960): The Alaska Earthquake of July 10, 1958: Giant wave in Lituya Bay.- Bulletin of the Seismological Society of America, 50: 253-266.

MINOURA, K. & NAKATA, T. (1994): Discovery of an ancient tsunami deposit in coastal sequences of southwest Japan: Verification of a large historic tsunami.- Island Arc, 3: 66-72.

MINOURA, K., IMAMURA, F., KURAN, U., NAKAMURA, T., PAPADOPOULOS, G.A., TAKAHASHI, T. & YALCINER, A.C. (2000): Discovery of Minoan tsunami deposits.- Geology, **28** (1): 59–62.

MISCHKE, S., SCHUDACK, U., BERTRAND, S. & LEROY, S.A.G. (2012): Ostracods from a Marmara Sea Lagoon (Turkey) as tsunami indicators.- Quaternary International, 261: 156-161.

MITROPOULOS, D. & ZANANIRI, I. (2010): Upper Quaternary evolution of the northern Argolis Gulf, Nafplion Area.- Bulletin of the Geological Society of Greece, 2010, Proceedings of the 12th International Congress, Patras, May 2010.- Ψηφιακή Βιβλιοθήκη Θεόφραστος - Τμήμα Γεωλογίας. Α.Π.Θ., XLIII (3): 1474-1485.

MITSOUDIS, D.A., FLOURI, E.T., CHRYSOULAKIS, N., KAMARIANAKIS, Y., OKAL, E.A. & SYNOLAKIS, C.E. (2012): Tsunami hazard in the southeast Aegean Sea.- Coastal Engineering, 60: 136-148.

MOORE, A., NISHIMURA Y., GELFENBAUM G., KAMATAKI, T. & TRIYONO R. (2006): Sedimentary deposits of the 26 December 2004 tsunami on the northwest coast of Aceh, Indonesia.- Earth, Planets and Space, 58: 253-258.

MORHANGE, C., MARRINER, N. & PIRAZZOLI, P.A. (2006): Evidence of Late-Holocene Tsunami Events in Lebanon.- Zeitschrift für Geomorphologie N.F., Suppl. Vol., 146: 81-95.

MORTON, R.A., GELFENBAUM, G. & JAFFE, B.E. (2007): Physical criteria for distinguishing sandy tsunami and storm deposits using modern examples.- Sedimentary Geology, 200: 184–207.

MORTON, R.A., RICHMOND, B.M., JAFFE, B.E. & GELFENBAUM, G. (2008a): Coarse-clast ridge complexes of the Caribbean: A preliminary basis for distinguishing tsunami and storm-wave origins.- Journal of Sedimentary Research, 78 (9-10): 624-637.

MORTON, R.A., GOFF, J.R. & NICHOL, S.L. (2008b): Hydrodynamic implications of textural trends in sand deposits of the 2004 tsunami in Sri Lanka.- Sedimentary Geology, 207 (1-4): 56-64.

MORTON, R.A., GELFENBAUM, G., BUCKLEY, M.L. & RICHMOND, B. (2011): Geological effects and implications of the 2010 tsunami along the central coast of Chile.- Sedimentary Geology, 242 (1-4): 34-51.

MOSCATELLO, A., MIGLIETTA, M.M. & ROTUNNO, R. (2008): Observational analysis of a Mediterranean 'hurricane' over south-eastern Italy.- Weather, 63 (10): 306-311.

MUHR, B. (2007): Klimadiagramm für Athen – Griechenland.- URL: http://www.klimadiagramme.de/Europa/griechenland.html, last access May 20th, 2014.

MURRAY, J.W. (1991): Ecology and paleoecology of benthic foraminifera.- NewYork, 408 pp.

MURRAY, R. W. & LEINEN, M. (1996): Scavenged excess aluminum and its relationship to bulk titanium in biogenic sediment from the central equatorial Pacific Ocean.- Geochimica et Cosmochimica Acta, 60: 3869–3878.

NANAYAMA, F. (2008): Sedimentary Characteristics and Depositional Processes of Onshore Tsunami Deposits: An Example of Sedimentation Associated with the 12 July 1993 Hokkaido-Nansei-oki Earthquake Tsunami.- In: SHIKI, T., TSUJI, Y., YAMAZAKI, T. & MINOURA, K. (eds.): Tsunamiites – Features and Implications.- Elsevier, Amsterdam, Oxford: 63-80.

NANAYAMA, F., SHIGENO, K., SATAKE, K., SHIMOKAWA, K., KOITABASHI, S., MIYASAKA, S. & ISHII, M. (2000): Sedimentary differences between the 1993 Hokkaido-nansei-oki tsunami and the 1959 Miyakojima typhoon at Taisei, southwestern Hokkaido, northern Japan.- Sedimentary Geology, 135 (1-4): 255-264.

NANAYAMA, F., FURUKAWA, R., SHIGENO, K., MAKINO, A., SOEDA, Y. & IGARASHI, Y. (2007): Nine unusually large tsunami deposits from the past 4000 years at Kiritappu marsh along the southern Kuril Trench.- Sedimentary Geology, 200: 275-294.

NANDASENA, N.A.K., PARIS, R. & TANAKA, N. (2011): Reassessment of hydrodynamic equations: Minimum flow velocity to initiate boulder transport by high energy events (storms, tsunamis).- Marine Geology, 28: 70-84.

NASTOS, P.T., PHILANDRAS, C.M. & REPAPIS, C.C. (2002): Application of canonical analysis to air temperature and precipitation regimes over Greece.- Fresenius Environmental Bulletin, 11 (8): 488-493.

NATIONAL GEOPHYSICAL DATA CENTER/NATIONAL OCEANIC AND ATMOSPHERIC ADMINISTRATION (NGDC/NOAA) (2013): Natural Hazards – Tsunami data and Information.- URL: http://www.ngdc.noaa.gov/hazard/tsu.shtml, last access: June 18th, 2013.

NEAMTIC (2014): North-Eastern Atlantic and Mediterranean Tsunami Information Centre.- URL: http://neamtic.ioc-unesco.org/, last access: June 17th, 2014.

NGDC/NOAA – NATIONAL GEOPHYSICAL DATA CENTER/NATIONAL OCEANIC AND ATMOSPHERIC ADMINISTRATION (2014): Tsunami
Event Search.- URL: http://www.ngdc.noaa.gov/nndc/struts/results?bt_0=&st_0=&type_8=EXACT&query_8=50&op_14=eq&v_14=&st_1=&bt_2=&st_2=&bt_1=&bt_10=&st_10=&ge_9=&le_9=&bt_3=&st_3=&type_19=EXACT&query_19=None+Selected&op_17=eq&v_17=&bt_20=&st_20=&bt_13=&st_13=&bt_16=&st_16=&bt_6=&st_6=&bt_11=&st_11=&d=7&t=101650&s=70, last access: February 10th, 2014.

NATURA 2000 – STANDARD DATA FORM (2013): Site GR2520003, Site name Limnothalassa Moustou.- URL: http://natura2000.eea.europa.eu/Natura2000/SDFPublic.aspx?site=GR2520003, last access: May 23rd, 2013.

NEUBAUER, N.P., BRILL, D., BRÜCKNER, H., KELLETAT, D., SCHEFFERS, S. & VÖTT, A. (2011): 5000 Jahre Tsunami-Geschichte am Kap Pakarang (Thailand).- In: KARIUS, V., HADLER, H., DEICKE, M., VON EYNATTEN, H., BRÜCKNER, H. & VÖTT, A. (eds.): Dynamische Küsten – Grundlagen, Zusammenhänge und Auswirkungen im Spiegel angewandter Küsten-forschung.- Coastline Reports, 17: 81-98.

NEWIG, J. & KELLETAT, D. (2011): The North Sea Tsunami of 1858.- Journal of Coastal Research, 27 (5): 931-941.

NEWIG, J. (2013): Merkmale eines historischen Tsunamis in der Nordsee.- Mainzer Geographische Studien, 55: 95-110.

NISHIMURA, Y. & MIYAJI, N. (1995): Tsunami deposits from the 1993 Southwest Hokkaido earthquake and the 1640 Hokkaido Komagatake eruption, northern Japan.- Pure and Applied Geophysics, 114: 525-536.

NOMANBHOY, N. & SATAKE, K. (1995): Generation mechanism from the 1883 Krakatau eruption.- Geophysical Research Letters, 22: 509-512.

NOMIKOU, P., ALEXANDRI, M., LYKOUSIS, V., SAKELLARIOU, D. & BALLAS, D. (2011): Swath bathymetry and morphological slope analysis of the Corinth Gulf.- In: GRÜTZNER, C., PÉREZ-LÓPEZ, R., FERNÁNDEZ STEEGER, T., PAPANIKOLAOU,I., REICHERTER, K., SILVA, P.G. & VÖTT, A. (eds.): Earthquake Geology and Archaeology. Science, Society and Critical Facilities.- Proceedings Vol. 2, 2nd INQUA-IGCP 567 International Workshop on Active Tectonics, Earthquake Geology, Archaeology and Engineering, 19.-24.09.2011, Corinth (Greece): 218-221.

NOORMETS, R., CROOK, K.A.W. & FELTON, E.A. (2004): Sedimentology of rocky shorelines: 3. Hydrodynamics of megaclast emplacement and transport on a shore platform, Oahu, Hawaii.- Sedimentary Geology, 172: 41-65.

NOTT, J. (1997): Extremely high-energy wave deposits inside Great Barrier Reef, Australia: determining the cause – tsunami or tropical cyclone.- Marine Geology, 141: 193-207.

NOTT, J. (2003): Waves, coastal boulder deposits and the importance of the pre-transport setting.-Earth and Planetary Science Letters, 210: 269-276.

NOTT, J. (2006): Tropical cyclones and the evolution of the sedimentary coast of northern Australia.- Journal of Coastal Research, 2: 49-62.

NOVIKOVA, T., PAPADOPOULOS, G.A. & MCCOY, F.W. (2011): Modelling of tsunami by the giant Late Bronze Age eruption of Thera, South Aegean Sea, Greece.- Geophysical Journal International, 186: 665-680.

NTAGERETZIS, K. (2009): Geomorphologische und sedimentologische Untersuchungen zu holozänen Extremereignissen im Golf von Lakonien (Peloponnes) und auf Kephallonia (Ionische Inseln), Griechenland.- Unpublished Diploma-Thesis, Universität zu Köln, Köln, 189 pp.

NTAGERETZIS, K., HOFFMEISTER, D., VÖTT, A., BRÜCKNER, H., HADLER, H. & WILLERSHÄUSER, T. (2011): High-resolution 3D laser scanning measurements of dislocated boulders on the coasts of the Lakonian Gulf and on Cefalonia Island (Greece).- Abstract volume of the 29th annual meeting of the German working group on "Geography of Oceans and Coasts", Bremen, 28-30 April 2011: 22-23.

NTAGERETZIS, K., VÖTT, A., HADLER, H., HENNING, P., & WILLERSHÄUSER, T. (2012): In search of tsunami fingerprints in geo-archives of southeastern Lakonia (southern Peloponnese, Greece). In: VÖTT, A., VENZKE, J.-F. (eds.): Beiträge der 29. Jahrestagung des Arbeitskreises „Geographie der Meere und Küsten", 28. bis 30. April 2011 in Bremen.- Bremer Beiträge zur Geographie und Raumplanung, 44: 16-26.

OKAL, E.A., FRITZ, H.M., SYNOLAKIS, C.E., BORRERO, J.C., WEISS, R., LYNETT, P.J., TITOV, V.V., FOTEINIS, S., JAFFE, B.E., LIU, P.L.F. & CHAN, I. (2010): Field Survey of the Samoa Tsunami of 29 September 2009.- Seismological Research Letters, 81: 577-591.

OKAL, E.A., SYNOLAKIS, C.E., USLU, B., KALLIGERIS, N. & VOUKOUVALAS, E. (2009): The 1956 Earthquake and Tsunami in Amorgos, Greece.- Geophysical Journal International, 178 (3): 1533-1554.

PANTOSTI, D., BARBANO, M.S., SMEDILE, A., DE MARTINI, P.M., GERARDI, F. & PIRROTTA C. (2008): Geological evidence of paleotsunamis at Torre degli Inglesi (northeastern Sicily).- In: MASTRONUZZI, G., PIGNATELLI, C., SANSÒ, P., MILELLA, M. & G. SELLERI (eds.): 2nd International Tsunami Field Symposium, 22-27 September 2008, Ostuni - Puglia (Italy) and Lefkada (Ionian Islands, Greece), Abstract Book.- GI^{2}S Coast Research Publication, 6: 89-92.

PAPADOPOULOS, G.A. (2002): Tsunamis in the East Mediterranean: A catalogue for the area of Greece and adjacent seas.- Proc. Workshop Tsunami Risk Assessment Beyond 2000: Theory, Practice and Plans, Moscow, June 14-16, 2003: 34-42.

PAPADOPOULOS, G.A. (2011): A seismic history of Crete: earthquakes and tsunamis 2000 B.C.-2011 A.D.- Athens, 415pp.

PAPADOPOULOS, G.A. & CHALKIS, B.J. (1984): Tsunamis observed in Greece and the adjacent seas.- Institute of Geodynamics, National Observatory of Athens, Publication Number 8, 17pp.

PAPADOPOULOS, G.A. & FOKAEFS, A. (2005): Strong Tsunamis in the Mediterranean Sea: a Re-evaluation.- ISET – Journal of Earthquake Technology, 463 (42/4): 159-170.

PAPADOPOULOS, G.A., DASKALAKI, E., FOKAEFS, A. & GIRALEAS, N. (2007): Tsunami Hazards in the Eastern Mediterranean: Strong Earthquakes and Tsunamis in the East Hellenic Arc and Trench System. – Natural Hazards and Earth System Sciences, 7 (1): 57-64.

PAPADOPOULOS, G.A., DASKALAKI, E., FOKAEFS, A. & NOVIKOVA, T. (2013): Tsunamigenic potential of local and distant tsunami sources threatening SW Peloponnese.- Bollettino di Geofisica Teorica ed Applicata.- DOI 10.4430/bgta0097.

PAPADOPOULOS, G.A. & PAPAGEORGIOU, A. (2014): Large earthquakes and tsunamis in the Mediterranean region and its connected areas.- In: ISMAIL-ZADEH, A., FUCUGAUCHI, J. U., KIJKO, A., TAKEUCHI, K. & ZALIAPIN, I. (eds.): Extreme natural hazards, disaster risks and social implications: 252-266.

PAPAIOANNOU, I., PAPADOPOULOS, G.A., PAVLIDES, S. (2004): The Earthquake of 426 BC in N. Evoikos Gulf revisited: amalgamation of two different strong earthquake events?- In: Proceedings of the 10th International Congress, Thessaloniki (April 2004).- Bulletin of the Geological Society of Greece, Vol. 36: 1477–1481

PAPANIKOLAOU, D., LYKOUSSIS, V., CHRONIS, G. & PAVLAKIS, P. (1988): A comparative study of neotectonic basins across the Hellenic arc: the Messiniakos, Argolikos, Saronikos and southern Evoikos Gulfs.- Basin research, 1 (3): 167-176.

PAPANIKOLAOU, I.D., ROBERTS, G., DELIGIANNAKIS G., SAKELLARIOU, A. & VASSILAKIS E. (2013): The Sparta Fault, Southern Greece: From segmentation and tectonic geomorphology to seismic hazard mapping and time dependent probabilities.- Tectonophysics, 597-598: 85-105.

PAPAZACHOS, B.C. (1990): Seismicity of the Aegean and surrounding area.- Tectonophysics, 178: 287-308.

PAPAZACHOS, B.C. & DELIBASIS, N.D. (1969): Tectonic stress field and seismic faulting in the area of Greece.- Tectonophysics, 7:231-255.

PAPAZACHOS, B.C. & COMNINAKIS, P.E. (1970): Geophysical features of the Greek Island Arc and the Eastern Mediterranean Ridge.- Com. Ren. Des Seances de la Conference Reunie a Madrid 1969, 16: 74-75.

PAPAZACHOS, B.C. & COMNINAKIS, P.E. (1971): Geophysical and tectonic features of the Aegean arc.- Journal of Geophysical Research, 76: 8517-8533.

PAPAZACHOS, B. C., KOUTITAS, CH., HATZIDIMITROU, P. M., KARAKOSTAS, B. C. & PAPAIOANNOU, CH. A. (1986): Tsunami hazard in Greece and the surrounding area.- Annales Geophysicae, 4B (1): 79–90.

PAPAZACHOS, B.C. & DIMITRIU, P. P. (1991): Tsunamis in and near Greece and their relation to the earthquake focal mechanism. – In: BERNARD, E.N. (ed.): Tsunami hazard. A practical guide for tsunami hazard reduction.- Nat. Hazards, 4 (2-3): 161-170.

PAPAZACHOS, B.C. & KIRATZI, A.A. (1996): A detailed study of the active crustal deformation in the Aegean and surrounding area.- Tectonophysics, 253: 129-153.

PAPAZACHOS, B.C. &. PAPAZACHOU, C. B (1997): The earthquakes of Greece.- Thessaloniki.

PARARAS-CARAYANNIS, G. (2011): The earthquake and tsunami of July 21, 365 AD in the eastern Mediterranean Sea – Review of impact on the ancient world – assessment of recurrence and future impact.- Science of Tsunami Hazards, 30 (4): 253-292.

PARIS, R., LAVIGNE, F., WASSMER, P. & SARTOHADI, J. (2007): Coastal sedimentation associated with the December 26, 2004 in Lhok Nga, west Banda Aceh (Sumatra, Indonesia).- Marine Geology, 238: 93-106.

PARIS, R., WASSMER, P., SARTOHADI, J., LAVIGNE, F., BARTHOMEUF, B., DESGAGES, E., GRANCHER, D., BAUMERT, P., VAUTIER, F., BRUNSTEIN, D. & GOMEZ, C. (2009): Tsunamis as geomorphic crises: Lessons from the December 26, 2004 tsunami in Lhok Nga, West Banda Aceh (Sumatra, Indonesia).- Geomorphology, 104: 59-72.

PARIS, R., FOURNIER, J., POIZOT, E., ETIENNE, S., MORIN, J., LAVIGNE, F. & WASSMER, P. (2010): Boulder and fine sediment transport and deposition by the 2004 tsunami in Lhok Nga (western Banda Aceh, Sumatra, Indonesia): A coupled offshore-onshore model.- Marine Geology, 268: 43-54.

PERISSORATIS, C. & CONISPOLIATIS, N. (2003): The impacts of sea-level changes during latest Pleistocene and Holocene times on the morphology of the Ionian and Aegean Seas (SE Alpine Europe).- Marine Geology, 196: 145-156.

PERRONE, A., IANNUZZI, A., LAPENNA, V., LORENZO, P., PISCITELLI, S., RIZZO, E. & SDAO, F. (2004): High-resolution electrical imaging of the Varco d'Izzo earthflow (southern Italy).- Journal of Applied Geophysics, 56 (1): 17-29.

PETERS, R. & JAFFE, B.E. (2010a): Identification of Tsunami Deposits in the Geological Record: Developing Criteria Using Recent Tsunami Deposits.- USGS Open-File Report, 2010-1239: 39 pp.

PETERS, R. & JAFFE, B.E. (2010b): Recent tsunami deposit database.- USGS Open-File Report: 2010-1172.

PETTERSSEN, S. (1956): Weather analysis and forecasting.- 2nd Ed., McGraw-Hill.- New York, 288 pp.

PFLUM, C.E. & FRERICHS, W.E. (1976): Gulf of Mexico deep-water foraminifers.- In: SLITER, W.V. (ed.): Cushman Foundation for Foraminiferal Research, Special Publication, No. 14: 125 pp.

PIGNATELLI, C., SANSÒ, P. MASTRONUZZI, G. (2009): Evaluation of tsunami flooding using geomorphologic evidence.- Marine Geology, 260 (1-4): 6-18.

PILARCZYK, J.E., HORTON, B.P., WITTER, R.C., VANE, C.H., CHAGUÉ-GOFF, C. & GOFF, J. (2012): Sedimentary and foraminiferal evidence of the 2011 Tōhoku-oki tsunami on the Sendai coastal plain, Japan.- Sedimentary Geology, 282: 78-89.

PILARCZYK, J.E. & REINHARDT, E.G. (2012): Testing foraminiferal taphonomy as a tsunami indicator in a shallow arid system lagoon: Sur (Sultanate of Oman).- Marine Geology, 295-298: 128-136.

PINEGINA, T.K. & BOURGEOIS, J. (2001): Historical and paleo-tsunami deposits on Kamchatka, Russia: long-term chronologies and long-distance correlations.- Natural Hazards and Earth System Sciences, 1: 177-185.

PIRAZOLLI, P.A., THOMMERET, J., THOMMERET, Y., LABOREL, J. & MONTAGIONNI, L. (1982): Crustal block movements from Holocene shorelines: Crete and Antikythira (Greece).- Tectonophysics, 68: 27-43.

PIRAZOLLI, P.A., AUSSEIL-BADIE, J., GIRESSE, P., HADJIDAKI, E. & ARNOLD, M. (1992): Historical environmental changes at Phalasarna harbour, West Crete.- Geoarchaeology, 7 (4): 371-392.

PIRAZZOLI, P.A., STIROS, S., ARNOLD, M., LABOREL, J. & LABOREL-DEGUEN, F. (1999): Late Holocene coseismic vertical displacements and Tsunami deposits near Kynos, Gulf of Euboa, central Greece.- Phys. Chem. Earth, 24 (4): 361-367.

POLONIA, A., BONATTI, E., CAMERLENGHI, A., LUCCHI, R.G., PANIERI, G.& GASPERINI, L. (2013): Mediterranean megaturbidite triggered by the AD 365 cretan earthquake and tsunami.- Scientific Reports, 3, 1285; DOI:10.1038/srep01285 (2013).

POMONI-PAPAIOANNOU, F. (2008): Facies analysis of Lofer cycles (Upper Triassic), in the Argolis Peninsula (Greece).- Sedimentary Geology, 208: 79-87.

PONSERO, A., DABOUINEAU, L. & ALLAIN, J. (2009): Modelling of the Common European Cockle (*Cerastoderma edule* L.) fishing grounds aimed at sustainable management of traditional harvesting.- Fisheries Science, 75 (4): 839-850.

POPE, R.J.J., WILKINSON, K.N. & MILLINGTON, A.C. (2003): Human and climatic impact on Late Quaternary deposition in the Sparta Basin Piedmont: evidence from alluvial fan systems.- Geoarchaeology: An International Journal, 18 (7): 685-724.

PYTHAROULIS, I., CRAIG, G.C. & PALLARD, S.P. (2000): The hurricane-like Mediterranean cyclone if January 1995.- Meteorological Applications, 7: 261-279.

REGNAULD, H., OSZWALD, J., PLANCHON, O., PIGNATELLI, C., PISCITELLI, A., MASTRONUZZI, G. & AUDEVARD, A. (2010): Polygenetic (tsunami and storm) deposits? A case study from Ushant Island, western France.- Zeitschrift für Geomorphologie, 54 (3): 197-217.

REICHERTER, K. & BECKER-HEIDMANN, P. (2009). Tsunami Deposits in the Western Mediterranean: Remains of the 1522 Almería Earthquake?- In: REICHERTER, K., MICHETTI, A.M. & SILVA, P.G. (eds.): Paleoseismology: Historical and prehistorical records of earthquake ground effects for seismic hazard assessment.- Journal of the Geological Society of London, Special Publication, 316: 217-235.

REICHERTER, K., VONBERG, D., KOSTER B., FERNÁNDEZ-STEEGER T., GRÜTZNER C., MATHES-SCHMIDT, M. (2010a): The sedimentary inventory of the 1755 Lisbon tsunami along the southern Gulf of Cádiz (southwestern Spain).- Zeitschrift für Geomorphologie, 54 (3): 147-173.

REICHERTER, K., PAPANIKOLAOU, I., ROGER, J., MATHES-SCHMIDT, M., PAPANIKOLAOU, D., RÖSSLER, S., GRÜTZNER, C., STAMATIS, G. (2010b): Holocene tsunamigenic sediments and tsunami modelling in the Thermaikos Gulf area (northern Greece).- Zeitschrift für Geomorphologie, 54 (3): 99-126.

REIMER, P.J, BAILLIE, M.G.L., BARD, E., BAYLISS, A., BECK, J.W., BLACKWELL, P.G., BRONK RAMSEY, C., BUCK, C.E., BURR, G.S., EDWARDS, R.L., FRIEDRICH, M., GROOTES, P.M., GUILDERSON, T.P., HAJDAS, I., HEATON, T.J., HOGG, A.G., HUGHEN, K.A., KAISER, K.F., KROMER, B., MCCORMAC, F.G., MANNING, S.W., REIMER, R.W., RICHARDS, D.A., SOUTHON, J.R., TALAMO, S., TURNEY, C.S.M., VAN DER PLICHT, J. & WEYHENMEYER, C.E. (2009): IntCal09 and Marine09 Radiocarbon Age Calibration Curves, 0 - 50,000 Years cal BP.- Radiocarbon, 51: 1111-1150.

REIMER, P.J. & MCCORMAC, F.G. (2002): Marine Radiocarbon Reservoir Corrections for the Mediterranean and Aegean Seas.- Radiocarbon, 44 (1): 159–166.

REINHARDT, E.G., GOODMANN, B.N., BOYCE, J.I., LOPEZ, G., VAN HENGSTUM, P. RINK, W.J. & RABAN , A. (2006): The tsunami of 13 December A.D. 115 and the destruction of Herod the Great's harbor at Caesarea Maritima, Israel.- Geology, 34: 1061-1064.

REYNOLDS, J.M. (1997): An Introduction to Applied and Environmental Geophysics.- Chichester, 778 pp.

RICHMOND, B., SZCZUCIŃSKI, W., CHAGUÉ-GOFF, C., GOTO, K, SUGAWARA, D., WITTER, R., TAPPIN, D.R., JAFFE, B., FUJINO, S., NISHIMURA, Y. & GOFF, J. (2012): Erosion, deposition and landscape change on the Sendai coastal plain, Japan, resulting from the March 11, 2011 Tohoku-oki tsunami.- Sedimentary Geology, 282: 27-39.

RIXHON, G., BRÜCKNER, H., ENGEL, M., MAY, S.M. & DUNAI, T. (2012): Dating tsunami-induced transport of coral reef megaclasts on Bonaire (Leeward Antilles): a cosmogenic nuclide dating approach (^{36}Cl).- Abstract for the International Geographical Congress, Cologne, 26-30 August 2012.

ROBERTSON, A.H.F., CLIFT, P.D., DEGNAN, P.J. & JONES, G. (1991): Palaeogeographic and Palaeotectonic evolution of the eastern Mediterranean Neotethys.- Palaeogeography, Palaeoclimatology, Palaeoecology, 87: 289-343.

RÖBKE, B.R., SCHÜTTRUMPF, H., WÖFFLER, T., HADLER, H., WILLERSHÄUSER, T. & VÖTT, A. (2012): Tsunamis in the Gulf of Kyparissia (western Peloponnese, Greece) – risk assessment based on numeric simulation and field evidence.- In: SCHÜTTRUMPF, H. & TOMASICCHIO (eds., 2012): Proceedings of the 5th International Short Conference on Applied Coastal Research, 6th to 9th June, 2011, RWTH Aachen University, Germany: 560-569.

RÖBKE, B.R., SCHÜTTRUMPF, H., FLER, T.W., FISCHER, P., HADLER, H., NTAGERETZIS, K., WILLERSHÄUSER, T. & VÖTT, A. (2013): Tsunami inundation scenarios for the Gulf of Kyparissia (western Peloponnese, Greece) derived from numerical simulations and geoscientific field evidence.- Zeitschrift für Geomorphologie, 57 (Suppl. 4): 69-104.

RODRÍGUEZ-VIDAL, J., CÁCERES, L.M., ABAD, M., RUIZ, F., GONZÁLEZ-REGALADO, M.L., FINLAYSON, C., FINLAYSON, G. FA, D., RODRÍGUEZ-LLANES, J.M. & BAILEY, G. (2011): The recorded evidence of AD 1755 Atlantic tsunami on the Gibraltar coast.- Journal of Iberian Geology, 37 (2): 177-193.

RÖNNFELD, W. (2008): Foraminiferen. Ein Katalog typischer Formen.- Tübingen, 146pp.

RÖSSLER, S., REICHERTER, K. PAPANIKOLAOU, I., ROGER, J., MATHES-SCHMIDT, M. & GRÜTZNER, C. (2008): In search of the 479 BC Tsunami and its sediments in the Thermaikos Gulf area (northern Greece).- In: MASTRONUZZI, G., PIGNATELLI, C., SANSÒ, P., MILELLA, M. & G. SELLERI (Hrsg.): 2nd International Tsunami Field Symposium, 22-27 September 2008, Ostuni - Puglia (Italy) and Lefkada (Ionian Islands, Greece), Abstract Book.- GI^{2}S Coast Research Publication, 6: 143-146.

RUIZ, F., ABAD, M., CÁCERES, L.M., RODRÍGUEZ VIDAL, J., CARRETERO, M.I., POZO, M. & GONZÁLEZ-RGEALADO, M.L. (2010): Ostracods as tsunami tracers in Holocene sequences.- Quaternary Research, 73 (1): 130-135.

SAKELLARIOU, D., LYKOUSSIS, V. & ROUSAKIS, G. (2011): Holocene seafloor faulting in the Gulf of Corinth: The potential for underwater paleoseismology.- In: GRÜTZNER, C., PÉREZ-LÓPEZ, R., FERNÁNDEZ STEEGER, T., PAPANIKOLAOU,I., REICHERTER, K., SILVA, P.G. & VÖTT, A. (eds.): Earthquake Geology and Archaeology. Science, Society and Critical Facilities.- Proceedings Vol. 2, 2nd INQUA-IGCP 567 International Workshop on Active Tectonics, Earthquake Geology, Archaeology and Engineering, 19.-24.09.2011, Corinth (Greece): 218-221.

SALMINEN, R., PLANT, J. & REEDER, S. (eds.) (2006): Geochemical atlas of Europe. Part 1, Background information, methodology and maps (electronic version).- Geological Survey of Finland.- Espoo, Finland, 526 pp.

SASS, O. (2003): Moisture distribution in rockwalls derived from 2D-resistivity measurements. In: Geophysical applications in geomorphology.- Zeitschrift für Geomorphologie, Suppl. Vol., 132: 51- 69.

SATO, H., SHIMAMOTO, T., TSUTSUMI, A. & KAWAMOTO, E. (1995): Onshore tsunami deposits caused by the 1993 southwest Hokkaido and 1983 Japan Sea Earthquakes.- Pire and Applied Geophysics (PAGEOPH), 144 (3/4): 693-717.

SAUERWEIN, F. (1996): Das Klima Griechenlands unter besonderer Berücksichtigung der Gebirgszone.- In: OLSHAUSEN, E. & SONNABEND, H. (eds.): Stuttgarter Kolloquium zur Historischen Geographie des Altertums 5, 1993, Gebirgsland als Lebensraum.- Geographica Historica, 8**:** 143-149.

SCHEFFERS, A. (2002): Paleotsunami in the Caribbean: field evidences and datings from Aruba, Curaçao and Bonaire.- Essener Geographische Arbeiten, 33.

SCHEFFERS, A. (2004): Tsunami imprints on the Leeward Netherlands Antilles (Aruba, Curaçao, Bonaire) and their relation to other coastal problems.- Quaternary International, 120: 163-172.

SCHEFFERS, A. (2006a): Coastal transformation during and after a sudden neotectonic uplift in western Crete (Greece).- Zeitschrift für Geomorphologie, 146: 97–124.

SCHEFFERS, A. (2006b): Argumente und Methoden zur Unterscheidung von Sturm- und Tsunamischutt und das Problem der Datierung von Paläo-Tsunami.- Die Erde, Variaheft 4: 1-36.

SCHEFFERS, A. & KELLETAT, D. (2001): Hurricanes and Tsunamis - Dynamik und küstengestaltende Wirkungen.- Bamberger Geographische Schriften, 20: 29-53.

SCHEFFERS, A. & KELLETAT, D. (2003): Sedimentologic and geomorphologic tsunami imprints worldwide - a review.- Earth-Science Reviews, 63: 83-92.

SCHEFFERS, A., SCHEFFERS, S. & KELLETAT, D. (2005): Paleo-tsunami relics on the southern and central Antillean Island Arc.- Journal of Coastal Research, 21: 263-273.

SCHEFFERS, A. & SCHEFFERS, S. (2007): First significant tsunami evidence from historical times in western Crete (Greece).- Earth and Planetary Science Letters, 259 (3-4): 613-624.

SCHEFFERS, A., KELLETAT, D., VÖTT, A., MAY, S.M. & SCHEFFERS, S. (2008): Late Holocene tsunami traces on the western and southern coastlines of the Peloponnesus (Greece).- Earth and Planetary Science Letters, 269: 271-279.

SCHEFFERS, A., KELLETAT D. & ENGEL, M. (2009): Die Entwicklung der Tsunamiforschung nach der Katastrophe vom 26. Dezember 2004.- Geographische Rundschau, 61 (12): 12-18.

SCHIELEIN, P., ZSCHAU, J., WOITH, H. & SCHELLMANN, G. (2007): Tsunamigefährdung im Mittelmeer - Eine Analyse geomorphologischer und historischer Zeugnisse.- Bamberger Geographische Schriften, 22: 153-199.

SCHLICHTING, E., BLUME, H. P. & STAHR, K. (1995): Bodenkundliches Praktikum. Eine Einführung in pedologisches Arbeiten für Ökologe, insbesondere Land- und Forstwirte, und für Geowissenschaftler.- Berlin, Wien, 295 pp.

SCHÖNENBERG, R. & NEUGEBAUER, J. (1997): Einführung in die Geologie Europas.- Freiburg, 294 pp.

SCHROTT, L. & SASS, O. (2008): Application of field geophysics in geomorphology: Advances and limitations exemplified by case studies.- Geomorphology, 93 (1-2): 55-73.

SCICCHITANO, G., MONACO, C. & TORTORICI, L. (2007): Large boulder deposits by tsunami waves along the Ionian coast of south-eastern Sicily (Italy).- Marine Geology, 238(1-4): 75-91.

SCICCHITANO, G., COSTA, B., DI STEFANO, A., LONGHITANO, S. & MONACO, C. (2008): Tsunami deposits in the Siracusa coastal area (south-eastern Sicily).- In: MASTRONUZZI, G., PIGNATELLI, C., SANSÒ, P., MILELLA, M. & G. SELLERI (eds.): 2nd International Tsunami Field Symposium, 22-27 September 2008, Ostuni - Puglia (Italy) and Lefkada (Ionian Islands, Greece), Abstract Book.- GI^{2}S Coast Research Publication, **6**: 155-156.

SCICCHITANO, G., PIGNATELLI, C., SPAMPINATO, C.R., PISCITELLI, A., MILELLA, M., MONACO, C. & MASTRONUZZI, G. (2012): Terrestrial Laser Scanner techniques in the assessment of tsunami impact on the Maddalena Peninsula (south-eastern Sicily, Italy).- Earth Planets and Space, 64 (10): 889-903.

SEDDON, M. & VAN DAMME, D. (2012): *Planorbis planorbis*.- In: IUCN – INTERNATIONAL UNION FOR CONSERVATION OF NATURE (2013): IUCN Red List of Threatened Species. Version 2013.1. <www.iucnredlist.org>. Downloaded on 08 October 2013.

SENOWBARI-DARYAN, B., MATARANGAS, D. & VARTIS-MATARANGAS, M. (1996): Norian-Rhaetian Reefs in Argolis Peninsula, Greece.- Facies, 34: 77-82.

SHAW, B., AMBRASEYS, N.N., ENGLAND, P.C., FLOYD, M.A., GORMAN, G.J., HIGHMAN, T.F.G., JACKSON, J.A., NOCQUET, J.-M., PAIN, C.C. & PIGGOTT, M.D. (2008): Eastern Mediterranean tectonics and tsunami hazard inferred from the AD 365 earthquake.- Nature Geoscience: 1 (4): 268-276.

SHORT, A.D. (2008): Carbonate sandy beaches.- In: SCHWARTZ, M.L. (ed.): Encyclopedia of coastal science.- Dordrecht: 218-221.

SHIKI, T. &CITA, M.B. (2008): Tsunami-related sedimentary properties of Mediterranean Homogenites as an example of deep-sea tsunamite.- In: SHIKI, T., TSUJI, Y., YAMAZAKI, T. & MINOURA, K. (eds.): Tsunamiites – Features and Implications.- Elsevier, Amsterdam, Oxford: 203-215.

SHIKI, T., TSUJI, Y., YAMAZAKI, T. & MINOURA, K. (2008): Tsunamiites – Tsunamiites – Features and Implications.- Elsevier, Amsterdam, Oxford: 411 pp.

SMEDILE, A., DE MARTINI, P.M., PANTOSTI, D., BELLUCCI, L., DEL CARLO, P., GASPERINI, L., PIRROTTA, C., POLONIA, A. & BOSCHI, E. (2011): Possible tsunami signatures from an integrated study in the Augusta Bay offshore (Eastern Sicily, Italy).- Marine Geology, 281: 1-13.

SMID, T.C. (1970): Tsunamis in Greek Literature.- Greece and Rome, 17 (1): 100-104.

SOLOVIEV, S. L. (1990): Tsunamigenic zones in the Mediterranean Sea.- Natural Hazards, 3: 183-202.

SOLOVIEV, S.L., SOLOVIEVA, O.N., GO, C.N., KIM, K.S. & SHCHETNIKOV, N.A. (2000): Tsunamis in the Mediterranean Sea 2000 B.C. – 2000 A.D.- Dordrecht: 237 pp.

SPISKE, M. & BAHLBURG, H. (2011): A quasi-experimental setting of coarse clast transport by the 2010 Chile tsunami (Bucalemu, Central Chile).- Marine Geology, 289 (1-4): 72-85.

SPISKE, M., BÖRÖCZ, Z. & BAHLBURG, H. (2008): The role of porosity in discriminating between tsunami and hurricane emplacement of boulders – A case study from the Lesser Antilles, southern Caribbean. Earth and Planetary Science Letters, 268 (3-4): 384-396.

SPISKE, M., WEISS, R., BAHLBURG, H., ROSKOSCH, J. & AMIJAYA, H. (2010): The TsuSedMod inversion model applied to the deposits of the 2004 Sumatra and 2006 Java tsunami and implications for estimating flow parameters of palaeo-tsunami.- Sedimentary, 224: 29-37.

STATE AGENCY FOR GEODESY AND CARTOGRAPHY AT THE COUNCIL OF MINISTERS OF THE USSR (1988): Soviet ordnance map of the Peloponnese (Greece) on a scale 1: 500.000, sheet 500--j34-4.- Moscow.- URL: http://poehali.org/maps, last access: 15th June, 2011.

STIROS, S.C. (2009): The 8.5+ magnitude, AD365 earthquake in Crete: coastal uplift, topography changes, archaeological and historical signature.- Quaternary International, 216: 1-10.

SUGAWARA, D., MINOURA, K. & IMAMURA, F. (2008): Tsunamis and Tsunami Sedimentology.- In: SHIKI, T., TSUJI, Y., YAMAZAKI, T. & MINOURA, K. (eds.): Tsunamiites – Features and Implications.- Elsevier, Amsterdam, Oxford: 9-49.

SUGAWARA, D. & GOTO, K. (2012): Numerical modeling of the 2011 Tohoku-oki tsunami in the offshore and onshore of Sendai Plain, Japan.- Sedimentary Geology, 282: 110-123.

SURESH GANDHI, M., SOLAI, A. & MOHAN, S.P. (2007): Benthic foraminiferal and its environmental degradation studies between the tsunamigenic sediments of Mandapam and Tuticorin, south east coast of India.- Science of Tsunami Hazards, 26 (2): 115-139.

SWITZER, A.D., PUCILLO, K., HAREDY, R.A., JONES, B.G. & BRYANT, E.A. (2005): Sea Level, Storm, or Tsunami: Enigmatic Sand Sheet Deposits in a Sheltered Coastal Embayment from Southeastern New South Wales, Australia.- Journal of Coastal Research, 21(4), 655–663.

SWITZER, A.D. & JONES, B.G. (2008a): Large-scale washover sedimentation in a freshwater lagoon from the southeast Australian coast: sea-level change, tsunami or exceptionally large storm?- The Holocene, 18 (5): 787-803.

SWITZER, A.D. & JONES, B.G. (2008b): Setup, Deposition, and Sedimentary Characteristics of Two Storm Overwash Deposits, Abrahams Bosom Beach, Southeastern Australia.- Journal of Coastal Research, 24 (1A): 189-200.

SWITZER, A.D. & BURSTON, J.M. (2010): Competing mechanisms for boulder deposition on the southeast Australian coast.- Geomorphology, 114: 42-54.

SYMONDS, G.L., JUDD, J.J., STRACHEY, R., WHARTON, W.J.L., EVANS, F., RUSSELL, F.A.R., ARCHIBALD, D., WHIPPLE, D. & WHIPPLE, G.M. (1888): The eruption of Krakatoa and subsequent phenomena.- London.

SZCZUCIŃSKI, W., KOKOCIŃSKI, M., RZESZEWSKI, M., CHAGUÉ-GOFF, C., CACHÃO, M., GOTO, K. & SUGAWARA, D. (2012): Sediment sources and sedimentation processes of 2011 Tohoku-oki tsunami deposits on the Sendai Plain, Japan — Insights from diatoms, nannoliths and grain size distribution.- Sedimentary Geology, 282: 40-56.

SZCZUCIŃSKI, W., NIEDZIELSKI, P., RACHLEWICZ, G., SOBCZYNSKI, T., ZIONA, A., KOWALSKI, A., LORENC, S. & SIEPAK, J. (2006): Contamination of tsunami sediments in a coastal zone inundated by the 26 December 2004 tsunami in Thailand.- Environmental Geology, 49 (2): 321-331.

TARASCHEWSKI, H. & PAPERNA, I. (1981): Distribution of the Snail *Pirenella conica* in Sinai and Israel and its Infection by Heterophydae and Other Trematodes.- Marine Ecology – Progress Series, 5: 193-205.

THERMO FISHER SCIENTIFIC (2010): Thermo Scientific Niton XL3t GOLDD+ XRF Analyzer.- URL: http://www.niton.com/docs/literature/Niton_XL3t_GOLDD_Spec_Sheet.pdf, last access: 11th, December 2013.

THOMPSON, R. & OLDFIELD, F. (1986): Environmental magnetism.- London: 227pp.

TINTI, S. & MARAMAI, A. (1999): Large tsunamis and tsunami hazard from the New Italian Tsunami Catalog.- Physics and Chemistry of the Earth, 24a: 151-156.

TINTI, S., MARAMAI, A. & GRAZIANI, L. (2001): A new version of the European tsunami catalogue: updating and revision.- Natural Hazards and Earth System Sciences, 1: 255-262.

TINTI, S., MARAMAI, A. & GRAZIANI, L. (2004): The New Catalogue of Italian Tsunamis.- Natural Hazards, 33: 439-465.

TINTI, S., ARMIGLIATO, A., PAGNONI, G. & ZANIBONI, F. (2005a): Scenarios of giant tsunamis of tectonic origin in the Mediterranean.- ISET – Journal of Earthquake Technology.- 42 (464): 171-188.

TINTI, S., MANUCCI, A., PAGNONI, G., ARMIGLIATO, A.& ZANIBONI, F. (2005b): The 30 December 2002 landslide induced tsunamis in Stromboli: sequence of the events reconstructed from eyewitness accounts.- Natural Hazards and Earth System Sciences, 5: 763-775.

TOLLNER, H. (1976): Zum Klima Griechenlands.- In: RIEDL, H. (ed.): Arbeiten aus dem Geographischen Institut der Universität Salzburg, Salzburg, **6**: 265-284.

TOUGIANNIDIS, N. (2009): Karbonat- und Lignitzyklen im Ptolemais-Becken: Orbitale Steuerung und suborbitale Variabilität (Spätneogen, NW-Griechenland). Sedimentologische Fallstudie unter Berücksichtigung gesteinsmagnetischer Eigenschaften.- PhD Thesis, Universität zu Köln, Cologne, 122 pp.

TSELENTIS, G.-A., G. STAVRAKAKIS, E. SOKOS, F. GKIKA & A. SERPETSIDAKI (2010): Tsunami hazard assessment in the Ionian Sea due to potential tsunamigenic sources – results from numerical simulations.- Natural Hazards and Earth System Sciences, 10: 1-10.

TSIMPLIS, M.N., & SHAW, A.G.P. (2010): Seasonal seal level extremes in the Mediterranean Sea and the Atlantic European coasts.- Natural Hazards and Earth System Sciences, 10: 1457-1475.

TURNER, R.J. (2005): Beachrock.- In: SCHWARTZ, M.L. (ed.): Encyclopedia of coastal science.- Dordrecht: 24-25.

TUTTLE, M.P., RUFFMAN, A., ANDERSON, T. & JETER, H. (2004): Distinguishing Tsunami from Storm Deposits in Eastern North America: The 1929 Grand Banks Tsunami versus the 1991 Halloween Storm.- Seismological Research Letters, 75 (1): 117-131.

USGS – UNITED STATES GEOLOGICAL SURVEY (2013): The Flandrian Transgression.- URL: http://3dparks.wr.usgs.gov/nyc/moraines/flandrian.htm, last access: 24th June, 2013.

VAN ANDEL, T.H., ZANGGER, E. & DEMITRACK, A. (1990): Land use and soil erosion in prehistorcal and historical Greece.- Journal of Field Archaeology, 17: 379-396.

VAN DER SPOEL, S., NEWMAN, L.& ESTEP, K.W. (1997): Pelagic Molluscs of the World.- World Biodiversity Database CD-ROM Series. Version 1.0. ETI, University of Amsterdam, Amsterdam.

VESPER, B. (1972): Zur Morphologie und Ökologie von *Cyprideis torosa* Jones 1850 (Crustacea, Ostracoda, Cytheridae) unter besonderer Berücksichtigung seiner Biometrie.- Mitt. Ham. Zool. Mus. Inst., 68: 21-77.

VILLA, R. (1986a): La famiglia Naticidae Forbes, 1838 nel Mar Mediterraneo - Part II.- Argonauta (Roma), 2 (1-2): 134-136.

VILLA, R. (1986b): La famiglia Naticidae Forbes, 1838 nel Mar Mediterraneo - Part III.- Argonauta (Roma), 2 (3–4): 179-182.

VÖTT, A. (2007a): Relative sea level changes and regional tectonic evolution of seven coastal areas in NW Greece since the mid-Holocene.- Quaternary Science Reviews, 26: 894-919.

VÖTT, A. (2007b): Silting up Oiniadai's harbours (Acheloos River delta, NW Greece). Geoarchaeological implications of the late Holocene landscape changes.- Géomorphologie: relief, processus, environment, 1: 19-36.

VÖTT A., HANDL M. & BRÜCKNER, H. (2002): Rekonstruktion holozäner Umweltbedingungen in Akarnanien (Nordwestgriechenland) mittels Diskriminanzanalyse von geochemischen Daten.- Geologica et Palaeontologica, 36: 123-147.

VÖTT, A., BRÜCKNER, H., SCHRIEVER, A., BESONEN, M., VAN DER BORG, K. & HANDL, M. (2003): Landschaftsveränderungen im Mündungsgebiet des Acheloos (Nordwestgriechenland) während des Holozäns.- In: KELLETAT, D. (ed.): Neue Ergebnisse der Küsten- und Meeresforschung.- Essener Geographische Arbeiten, 35: 115-136.

VÖTT, A., MAY, M., BRÜCKNER, H. & BROCKMÜLLER, S. (2006): Sedimentary evidence of Late Holocene Tsunami Events near Lefkada Island (NW Greece).- Zeitschrift für Geomorphologie, 146: 139–172.

VÖTT, A., BRÜCKNER, H., MAY, S.M., LANG, F. & BROCKMÜLLER, S. (2007): Late Holocene tsunami imprint on Actio headland at the entrance to the Ambrakian Gulf.- Méditerranée, revue géographique des pays méditerranées, 108: 43-57.

VÖTT, A., BRÜCKNER, H., BROCKMÜLLER, S., MAY, M., FOUNTOULIS, I., GAKI-PAPANASTASSIOU, K., HERD, R., LANG, F., MAROUKIAN, H., PAPANASTASSIOU, D. & SAKELLARIOU, D. (2008a): Tsunami impacts on the Lefkada coastal zone during the past millennia and their palaeogeographical implications.- In: PAPADATOU-GIANNOPOULOU, H. (Hrsg.): Proceedings of the International Conference Honouring Wilhelm Dörpfeld, August 6-9, 2006, Lefkada: 419-438.- Patras.

VÖTT, A., MAY, S.M., MASBERG, P., KLASEN, N., GRAPMAYER, R., BRÜCKNER, H., BARETH, G., SAKELLARIOU, D., FOUNTOULIS, I. & LANG, F. (2008b): Tsunamite findings along the shores of the Eastern Ionian Sea – the Cefalonia case study (NW Greece).- In: MASTRONUZZI, G., PIGNATELLI, C., SANSÒ, P., MILELLA, M. & SELLERI, G. (Hrsg.): 2nd International Tsunami Field Symposium, 22-27 September 2008, Ostuni - Puglia (Italy) and Lefkada (Ionian Islands, Greece), Abstract Book.- GI^{2}S Coast Research Publication, 6: 167-170.

VÖTT, A., BRÜCKNER, H., MAY, M., LANG, F., HERD, R. & BROCKMÜLLER, S. (2008c): Strong tsunami impact on the Bay of Aghios Nikolaos and its environs (NW Greece) during Classical–Hellenistic times.- Quaternary International, 181: 105-122.

VÖTT, A. & MAY, S.M. (2009): Auf den Spuren von Tsunamis im östlichen Mittelmeer.- Geographische Rundschau, 12: 42-48.

VÖTT, A., BRÜCKNER, H., BROCKMÜLLER, S., HANDL, M., MAY, S.M., GAKI-PAPANASTASSIOU, K., HERD, R., LANG, F., MAROUKIAN, H., NELLE, O. & PAPANASTASSIOU, D. (2009a): Traces of Holocene tsunamis across the Sound of Lefkada, NW Greece.- Global and Planetary Change, 66 (1-2): 112-128.

VÖTT, A., BRÜCKNER, H., MAY, S.M., SAKELLARIOU, D., NELLE, O., LANG, F., KAPSIMALIS, V., JAHNS, S., HERD, R., HANDL, M. & FOUNTOULIS, I. (2009b): The Lake Voulkaria (Akarnania, NW Greece) palaeoenvironmental archive - a sediment trap for multiple tsunami impact since the mid-Holocene.- Zeitschrift für Geomorphologie N.F., 53 (1): 1-37.

VÖTT, A., BARETH, G., BRÜCKNER, H., CURDT, C., FOUNTOULIS, I., GRAPMAYER, R., HADLER, H., HOFFMEISTER, D., KLASEN, N., LANG, F., MASBERG, P., MAY, S.M., NTAGERETZIS, K., SAKELLARIOU, D. & WILLERSHÄUSER, T. (2010): Beachrock-type calcarenitic tsunamites along the shores of the eastern Ionian Sea (western Greece) – case studies from Akarnania, the Ionian Islands and the western Peloponnese.- Zeitschrift für Geomorphologie, 54 (3): 1-50.

VÖTT, A. (2011): Die Olympia-Tsunami-Hypothese – neue sedimentologische und geoarchäologische Befunde zur Verschüttung Olympias (Peloponnes, Westgriechenland). Antike Welt 5: 4. VÖTT, A. (2011): Tsunamis – Entstehung, Dynamik, Ausmaß und Überlieferung.- In: GEBHARDT, H., GLASER, R., RADTKE, U., REUBER, P. (eds.): Geographie. Physische Geographie und Humangeographie. 2nd edition. Spektrum Akademischer Verlag, Berlin, Heidelberg: 1134-1137.

VÖTT, A., LANG, F., BRÜCKNER, H., GAKI-PAPANASTASSIOU, K., MAROUKIAN, H., PAPANASTASSIOU, D., GIANNIKOS, A., HADLER, H., HANDL, M., NTAGERETZIS, K. WILLERSHÄUSER, T. & ZANDER, A. (2011a): Sedimentological and geoarchaeological evidence of multiple tsunamigenic imprint on the Bay of Palairos-Pogonia (Akarnania, NW Greece).- Quaternary International, 242 (1): 213-239.

VÖTT, A., FISCHER, P., HADLER, H., HANDL, M., LANG, F., NTAGERETZIS, K., WILLERSHÄUSER, T. (2011b): Sedimentary burial of ancient Olympia (Peloponnese, Greece) by high-energy flood deposits – the Olympia Tsunami Hypothesis.- IN: GRÜTZNER, C., PÉREZ-LOPEZ, R., FERNÁNDEZ STEEGER, T., PAPANIKOLAOU, I., REICHERTER, K., SILVA, P.G., VÖTT, A. (eds.): Earthquake Geology and Archaeology: Science, Society and Critical facilities.- Proceedings of the 2nd INQUA-IGCP 567 International Workshop on Active Tectonics, Earthquake Geology, Archaeology and Engineering, 19-24 September 2011, Corinth (Greece): 259-262.

VÖTT, A., BARETH, G., BRÜCKNER, H., LANG, F., SAKELLARIOU, D., HADLER, H., NTAGERETZIS, K. & WILLERSHÄUSER, T. (2011c): Olympia's harbour site Pheia (Elis, western Peloponnese, Greece) destroyed by tsunami impact.- Die Erde, 142 (3): 259-288.

VÖTT, A., FISCHER, P., HADLER, H., HANDL, M., HENNING, P., LANG, F., NTAGERETZIS, K., RÖBKE, B. & WILLERSHÄUSER, T. (2012): Testing the Olympia Tsunami Hypothesis (OTH) – new results from tsunami modeling and palaeotsunami studies in the lower Alpheios River valley (Peloponnese, Greece). 36. Hauptversammlung der Deutschen Quartärvereinigung DEUQUA, Umwelt, Mensch, Georisiken im Quartär, Universität Bayreuth, 16.-20. September 2012, Tagungsband.- Bayreuther Forum Ökologie, 117: 119-120.

VÖTT, A., HADLER, H., WILLERSHÄUSER, T., NTAGERETZIS, K., BRÜCKNER, H., WARNECKE, H., GROOTES, P.M., LANG, F., NELLE, O. & SAKELLARIOU, D. (2013): Ancient harbours used as tsunami sediment traps – the case study of Krane (Cefalonia Island, Greece).- In: PIRSON, F., LADSTÄTTER, S., SCHMIDTS, T. (eds.): Häfen und Hafenstädte im östlichen Mittelmeerraum von der Antike bis in byzantinische Zeit. Aktuelle Entdeckungen und neue Forschungsansätze. Byzas, Istanbul (accepted).

VÖTT, A. (2014): Personal communication.- Institute for Geography, Johannes Gutenberg-University Mainz, Germany.

VOUSDOUKAS, M.I., VELEGRAKIS, A.F. & PLOMARITIS, T.A. (2007): Beachrock occurrence, characteristics, formations mechanisms and impacts.- Earth Science Reviews, 85: 23-46

VRIELYNCK, B. (1981/82): Evolution paleogeographique et strucurale de la presqe isle de Argolise (Grece).- Revue de Géologie Dynamique et de Géographie Physique, 23 (4): 227-288.

WALKER, M. (2005): Quaternary dating methods.- West Sussex, 286 pp.

WASSMER P., BAUMERT PH., LAVIGNE F., PARIS R. & SARTOHADI J. (2007): Sedimentary facies and transfer associated with the December 26, 2004 tsunami on the north eastern littoral of Banda Aceh (Sumatra, Indonesia).- Géomorphologie, 4: 335-346.

WEISCHET, W. & ENDLICHER, W. (2000): Regionale Klimatologie Teil 2 – Die Alte Welt: Europa – Afrika – Asien.- Stuttgart, 625 pp.

WHELAN, F. & KELLETAT, D. (2002): Geomorphic evidence and relative and absolute dating results for tsunami events on Cyprus.- Science of Tsunami Hazards, 20 (1): 3–18.

WILLERSHÄUSER, T., VÖTT, A., BRÜCKNER, H., BARETH, G., HADLER, H. & K. NTAGERETZIS (2011a). New insights in the Holocene evolution of the Livadi coastal plain, Gulf of Argostoli (Cefalonia, Greece).- In: KARIUS, V., HADLER, H., DEICKE, M., VON EYNATTEN, H., BRÜCKNER, H. & VÖTT, A. (eds.): Dynamische Küsten – Grundlagen, Zusammenhänge und Auswirkungen im Spiegel angewandter Küstenforschung.- Coastline Reports, 17: 99-110.

WILLERSHÄUSER, T., VÖTT, A., BARETH, G., BRÜCKNER, H., HADLER, H., NTAGERETZIS, K. (2011b): Sedimentary evidence of Holocene tsunami impacts at the Gialova Lagoon (southwestern Peloponnese, Greece).- In: GRÜTZNER, C., PÉREZ-LOPEZ, R., FERNÁNDEZ STEEGER, T., PAPANIKOLAOU, I., REICHERTER, K., SILVA, P.G., VÖTT, A. (eds.): Earthquake Geology and Archaeology: Science, Society and Critical facilities. Proceedings of the 2nd INQUA- IGCP 567 International Workshop on Active Tectonics, Earthquake Geology, Archaeology and Engineering, 19-24 September 2011, Corinth (Greece), pp. 283-285. ISBN: 978-960-466-093-3.

WILLERSHÄUSER, T., VÖTT, A., HADLER, H., HENNING, P. & NTAGERETZIS, K. (2012a): Tracing palaeotsunami sediments near Kato Samiko, Gulf of Kyparissia (western Peloponnese, Greece) by combining earth resistivity measurements and vibacoring.- 36. Hauptversammlung der Deutschen Quartär-vereinigung DEUQUA, Umwelt, Mensch, Georisiken im Quartär, Universität Bayreuth, 16.-20. September 2012, Tagungsband.- Bayreuther Forum Ökologie, 117: 91-92.

WILLERSHÄUSER, T., VÖTT, A., HADLER, H., HENNING, P., NTAGERETZIS, K. (2012b): Evidence of high-energy impact near Kato Samiko, Gulf of Kyparissia (western Peloponnese, Greece), during history. In: Vött, A., Venzke, J.-F. (eds.): Beiträge der 29. Jahrestagung des Arbeitskreises „Geographie der Meere und Küsten“, 28. bis 30. April 2011 in Bremen.- Bremer Beiträge zur Geographie und Raumplanung, 44: 26-36.

WILLERSHÄUSER, T., VÖTT, A., BRÜCKNER, H., BARETH, G., NELLE, O., NADEAU, M.-J., HADLER, H. & NTAGERETZIS, K. (2013): Holocene tsunami landfall along the shores of the inner Gulf of Argostoli (Cefalonia Island, Greece).- Zeitschrift für Geomorphologie, 57 (Suppl. 4): 105-138.

WILLERSHÄUSER, T. (2014): Holocene tsunami events in the eastern Ionian Sea – geoscientific evidence from Cefalonia and the western Peloponnese (Greece).- PhD Thesis, Johannes Gutenberg-University Mainz, Mainz, 132pp.

WILLIAMS, H.F.L. (2009): Stratigraphy, sedimentology and microfossil content of Hurricane Rita storm surge deposits on southwest Louisiana.- Journal of Coastal Research, 25: 1041-1051.

WWW.PARNONAS.GR (2014): Internet-site of the project co-funded by the European Agricultural Guidance and Guarantee Fund – Guidance Section (EAGGF-G) and the Hellenic Ministry of Rural Development and Food within the framework of the local programme C.I. LEADER+ of Parnonas L.A.G. – URL: http://www.parnonas.org/, last access: 23nd September 2013.

YULIANTO, E., PRENDERGAST, A.L., JANKAEW, K., EIPERT, A.A., ATWATER, B.F., CISTERNAS, M., FERNANDO, S. & TEJAKUSUMA, I. (2007): Tsunami scour-fan deposits in south-central Chile.- XVII INQUA Congress Abstract 0955, Quaternary International, 469: 167–168.

ZANGGER, E. (1993): The geoarchaeology of the Argolid – Argolis II (Deutsches Archäologisches Institut Athen).- Gebr. Mann.- Berlin, 149pp.

ZEEH, S. (1989): Fazies und Diagenese triassischer/jurassischer Plattformkarbonate der Tripolitza-Serie (SE-Lakonien/Peloponnes).- Geologisch-Paläontologische Mitteilungen Innsbruck, 16: 130-132.

Stratigraphical legend

 bedrock fragments

 calcareous nodules

 ceramic fragments

 charcoal

 coral fragments

 ferric concretions

 fir cone

 gravel

 grus

 hydromorphic spots

 mollusc (fragments)

 plant remains

 pumice

 rip up clast

s.l. sea level

 sea weed

 seed vessel

 valves & bivalves

 wood remains